



**Universidad**  
Zaragoza

**UNIVERSITÀ DEGLI STUDI DI TRIESTE**  
**UNIVERSIDAD DE ZARAGOZA**  
– Tesi in Cotutela –

**XXXVI CICLO DEL DOTTORATO DI RICERCA IN**  
INGEGNERIA INDUSTRIALE E DELL'INFORMAZIONE

**PROGRAMA DE DOCTORADO EN**  
INGENIERÍA MECÁNICA

**Optimal Synthesis, Operation, and Thermo-economic  
Analysis of Distributed Polygeneration Systems for  
Energy Communities**

Settore scientifico-disciplinare: **ING-IND/09**

DOTTORANDO  
**Ronelly José De Souza**

COORDINATORE  
**PROF. Fulvio Babich**

SUPERVISORE DI TESI  
**PROF. Mauro Reini**

SUPERVISORE DI TESI  
**PROF. Luis María Serra de Renobales**

**ANNO ACCADEMICO 2022/2023**





UNIVERSITÀ  
DEGLI STUDI  
DI TRIESTE



Universidad  
Zaragoza

**UNIVERSITÀ DEGLI STUDI DI TRIESTE**  
**UNIVERSIDAD DE ZARAGOZA**  
– Tesi in Cotutela –

**XXXVI CICLO DEL DOTTORATO DI RICERCA IN**  
INGEGNERIA INDUSTRIALE E DELL'INFORMAZIONE

**PROGRAMA DE DOCTORADO EN**  
INGENIERÍA MECÁNICA

**Optimal Synthesis, Operation, and Thermo-economic  
Analysis of Distributed Polygeneration Systems for  
Energy Communities**

Settore scientifico-disciplinare: **ING-IND/09**

DOTTORANDO  
**Ronelly José De Souza**

COORDINATORE  
**PROF. Fulvio Babich**

SUPERVISORE DI TESI  
**PROF. Mauro Reini**

SUPERVISORE DI TESI  
**PROF. Luis María Serra de Renobales**

**ANNO ACCADEMICO 2022/2023**



## Acknowledgments

As I sit down to write these acknowledgments, the journey of my PhD unfolds in my mind not just as an academic endeavor, but as a personal journey, one that has been as much about self-discovery as it has been about research. Starting this journey in the middle of a pandemic was not the best scenario at all, as you can imagine, especially when you should move from your home country and start a new life far from family, friends, and (of course) my loved regional Brazilian dishes (from the Northeast more specifically, I should add!). As I moved to Italy, this last “difficulty” has been easily overcome, as you might guess.

Despite the unfavorable scenario of my first year of PhD (due to the pandemic), I have been fortunate to be surrounded by amazing people along the way, starting from my supervisors. Mauro, I would like to express my heartfelt gratitude for having met you and for having had the opportunity to work with you. Thank you very much for welcoming me to Italy and for helping me on both the personal and professional levels. And Luis, thank you very much for welcoming me to Zaragoza with wide arms open and for helping me in the further development of the work. I really feel that it brought a substantial improvement to the quality of my thesis.

During my first months at the University of Trieste, I also had the pleasure to meet Emanuele and Melchiorre who also helped a lot during this time. Emanuele, thank you very much for our frequent and long meetings through which you have provided me with substantial and very important help on my work and, of course, with substantial and interesting knowledge about Star Wars! And Melchiorre, thank you very much for our interesting talks about the details of the Italian energy market. *Sei un vero e proprio cultore della materia!*

I also would like to thank all the professors and colleagues from the GITSE group at the University of Zaragoza. You are like a family! And during my stay, I felt like part of this family. *Un mogollón de gracias* for the friendships, the conversations, the coffee breaks, the lunches, and the chocolates!

And...last but not least...Cinthia and Lavynia, *meus amores!* You were always there supporting me at any moment, as always. Love you!



## Abstract

The sector of energy use in buildings accounts for a substantial portion of global energy consumption and greenhouse gas (GHG) emissions, representing a large potential for energy savings and emissions reduction. In this sense, the energy community (EC) concept has become gradually more attractive due to the potential to reduce energy consumption and GHG emissions. In such a scenario, polygeneration systems emerge as advantageous energy supply systems. They can efficiently meet the energy demands of buildings by producing multiple energy services from a single energy resource and be supported by renewable energy sources (RES). However, defining an optimal configuration and operational strategy for polygeneration systems is a multifaceted task which becomes even more complex when considering the integration of the buildings into an EC. The reasons for this include the several types of considered technologies, their interrelations, and the intrinsic dynamic behavior of buildings. In addition, the question remains of defining the best operational approach for these complex systems when variations in demand for energy services occur. Based on this framework, this thesis aims to develop a mathematical model for defining the optimal synthesis and operation of polygeneration systems integrated into ECs and based on a mixed integer linear programming (MILP) algorithm. The work rests on three main pillars: (i) the multi-objective optimization of an EC powered by polygeneration systems and sharing electricity, heating, and cooling among the buildings, (ii) the proposal of a thermoeconomic analysis (through marginal costs) to evaluate the best operational strategy according to variations on the energy services demand, and (iii) evaluation of the role of such ECs in the economic and environmental aspects of a future Italian national energy system (NES) scenario by using a local optimization approach. The results from an EC case study show the possibility of reducing (i) CO<sub>2</sub>eq emissions by around 20% (about 1.5 kt CO<sub>2</sub>eq/year), (ii) costs by approximately 24% (about 1.1 M€/year), and (iii) the total annual Italian NES cost by 6% (representing 6.6 billion€/year). Regarding the thermoeconomic analysis, the results provide specific and well-defined marginal paths representing the operational strategy which will have the lowest effect in the defined objective function. The work developed within this research can be easily adapted to different case studies, such as in the residential-commercial buildings and industrial sectors. Therefore, the model resulting from this work constitutes an effective tool to optimally design and operate polygeneration systems integrated into ECs.





## Sommario

Il settore dell'utilizzo dell'energia negli edifici rappresenta una parte sostanziale del consumo globale di energia e delle emissioni di gas serra (GS), rappresentando un grande potenziale per il risparmio energetico e la riduzione delle emissioni. In questo senso, il concetto di comunità energetica (CE) è diventato gradualmente più attraente a causa del potenziale di riduzione del consumo energetico e delle emissioni di GS. In tale scenario, i sistemi di poligenerazione emergono come sistemi di fornitura di energia vantaggiosi. Possono soddisfare in modo efficiente le domande energetiche degli edifici producendo più servizi energetici da una singola risorsa energetica e essere supportati da fonti di energia rinnovabile. Tuttavia, definire una configurazione ottimale e una strategia operativa per i sistemi di poligenerazione è un compito multifaccettato che diventa ancora più complesso quando si considera l'integrazione degli edifici in una CE. I motivi includono i vari tipi di tecnologie considerate, le loro interrelazioni e il comportamento dinamico intrinseco degli edifici. Inoltre, rimane la questione di definire il miglior approccio operativo per questi sistemi complessi quando si verificano variazioni nella domanda di servizi energetici. Basandosi su questo quadro, questa tesi mira a sviluppare un modello matematico per definire la sintesi ottimale e il funzionamento dei sistemi di poligenerazione integrati nelle CE e basato su un algoritmo di programmazione lineare intera mista (MILP). Il lavoro si basa su tre pilastri principali: (i) l'ottimizzazione multi-obiettivo di una CE alimentata da sistemi di poligenerazione e che condivide elettricità, riscaldamento e raffreddamento tra gli edifici, (ii) la proposta di un'analisi termoeconomica (attraverso costi marginali) per valutare la migliore strategia operativa secondo le variazioni sulla domanda di servizi energetici, e (iii) valutazione del ruolo di tali CE negli aspetti economici e ambientali di uno scenario futuro del sistema energetico nazionale italiano (NES) utilizzando un approccio di ottimizzazione locale. I risultati di uno studio di caso su una CE mostrano la possibilità di ridurre (i) le emissioni di CO<sub>2</sub>eq di circa il 20% (circa 1,5 kt CO<sub>2</sub>eq/anno), (ii) i costi di circa il 24% (circa 1,1 M€/anno), e (iii) il costo annuale totale del NES del 6% (rappresentando 6,6 miliardi di €/anno). Riguardo all'analisi termoeconomica, i risultati forniscono percorsi marginali specifici e ben definiti che rappresentano la strategia operativa che avrà l'effetto minore nella funzione obiettivo definita. Il lavoro sviluppato all'interno di questa ricerca può essere adattato a diversi casi di studio, come nei settori degli edifici residenziali-commerciali e industriali.



## Resumen

El sector del uso de energía en los edificios representa una parte sustancial del consumo global de energía y de las emisiones de gases de efecto invernadero (GEI), representando un gran potencial para el ahorro de energía y la reducción de emisiones. En este sentido, el concepto de comunidad energética (CE) se ha vuelto gradualmente más atractivo debido al potencial para reducir el consumo de energía y las emisiones de GEI. En tal escenario, los sistemas de poligeneración emergen como sistemas de suministro de energía ventajosos. Pueden satisfacer eficientemente las demandas energéticas de los edificios produciendo múltiples servicios energéticos a partir de una única fuente de energía y ser apoyados por fuentes de energía renovable (FER). Sin embargo, definir una configuración óptima y una estrategia operacional para los sistemas de poligeneración es una tarea multifacética que se vuelve aún más compleja al considerar la integración de los edificios en una CE. Además, queda la cuestión de definir el mejor enfoque operacional para estos sistemas complejos cuando ocurren variaciones en la demanda de servicios energéticos. Basándose en este marco, esta tesis tiene como objetivo desarrollar un modelo matemático para definir la síntesis óptima y la operación de sistemas de poligeneración integrados en CEs y basado en un algoritmo de programación lineal entera mixta (PLEM). El trabajo se apoya en tres pilares principales: (i) la optimización multiobjetivo de una CE alimentada por sistemas de poligeneración y compartiendo electricidad, calefacción y refrigeración entre los edificios, (ii) la propuesta de un análisis termoeconómico (a través de costes marginales) para evaluar la mejor estrategia operacional según las variaciones en la demanda de servicios energéticos, y (iii) la evaluación del papel de tales CEs en los aspectos económicos y ambientales de un futuro escenario del sistema energético nacional (SEN) italiano utilizando un enfoque de optimización local. Los resultados de un caso de estudio de una CE muestran la posibilidad de reducir (i) las emisiones de CO<sub>2</sub>eq en alrededor del 20% (aproximadamente 1,5 kt CO<sub>2</sub>eq/año), (ii) los costes en aproximadamente el 24% (alrededor de 1,1 M€/año), y (iii) el coste anual total del SEN italiano en un 6% (representando 6,6 mil millones de €/año). En cuanto al análisis termoeconómico, los resultados proporcionan caminos marginales específicos y bien definidos que representan la estrategia operacional que tendrá el menor efecto en la función objetivo definida. El trabajo desarrollado dentro de esta investigación puede ser fácilmente adaptado a diferentes casos de estudio, como en los sectores de edificios residenciales-comerciales e industriales.



## Resumo

O setor de uso de energia em edifícios responde por uma parcela substancial do consumo global de energia e das emissões de gases de efeito estufa (GEE), representando um grande potencial para economia de energia e redução de emissões. Nesse sentido, o conceito de comunidade energética (CE) tornou-se gradativamente mais atraente devido ao potencial para reduzir o consumo de energia e as emissões de GEE. Em tal cenário, sistemas de poligeração emergem como vantajosos sistemas de fornecimento de energia. Eles podem atender eficientemente às demandas energéticas dos edifícios produzindo múltiplos serviços de energia a partir de um único recurso energético e serem alimentados por fontes de energia renovável. No entanto, definir uma configuração ótima e estratégias operacionais para tais sistemas é uma tarefa multifacetada que se torna ainda mais complexa ao considerar a integração de edifícios em uma CE. Os motivos para isso incluem os vários tipos de tecnologias consideradas, suas inter-relações e o comportamento dinâmico intrínseco dos edifícios. Além disso, permanece a questão de definir a melhor abordagem operacional para esses sistemas complexos quando ocorrem variações na demanda por serviços de energia. Com base nessa fundamentação, esta tese visa desenvolver um modelo matemático para definir a síntese e operação ótimas de sistemas de poligeração integrados em CEs, baseando-se em um algoritmo de programação linear inteira mista (PLIM). O trabalho se apoia em três pilares principais: (i) a otimização multiobjetivo de uma CE alimentada por sistemas de poligeração e compartilhando eletricidade, aquecimento e resfriamento entre os edifícios, (ii) a proposta de uma análise termoeconômica (por meio de custos marginais) para avaliar a melhor estratégia operacional de acordo com variações na demanda por serviços de energia, e (iii) avaliação do papel de tais CEs nos aspectos econômicos e ambientais de um futuro cenário do sistema energético nacional (SEN) italiano usando uma abordagem de otimização local. Os resultados de um estudo de caso de uma CE mostram a possibilidade de reduzir (i) as emissões de CO<sub>2</sub>eq em cerca de 20% (aproximadamente 1,5 kt CO<sub>2</sub>eq/ano), (ii) custos em aproximadamente 24% (cerca de 1,1 M€/ano), e (iii) o custo anual total do SEN italiano em 6% (representando 6,6 bilhões de €/ano). Quanto à análise termoeconômica, os resultados fornecem trajetórias marginais específicos e bem definidos representando a estratégia operacional que terá o menor efeito na função objetivo definida. O trabalho desenvolvido nesta pesquisa pode ser adaptado para diferentes estudos de caso, como nos setores de edificações residenciais-comerciais e industriais.



# Table of Contents

<b>Acknowledgments</b> .....	<b>v</b>
<b>Abstract</b> .....	<b>vii</b>
<b>Sommario</b> .....	<b>ix</b>
<b>Resumen</b> .....	<b>xi</b>
<b>Resumo</b> .....	<b>xiii</b>
<b>List of figures</b> .....	<b>xxi</b>
<b>List of tables</b> .....	<b>xxvi</b>
<b>List of acronyms</b> .....	<b>xxx</b>
<b>List of publications</b> .....	<b>xxxiii</b>
<b>CHAPTER 1 – Introduction</b> .....	<b>1</b>
<b>1.1 Background and Context</b> .....	<b>1</b>
1.1.1 Global energy landscape and environmental issues .....	1
1.1.2 Global energy crises: triggers, consequences, and actions .....	3
1.1.3 Approaches by the scientific community.....	5
1.1.3.1 On the environmental issues caused by energy supply systems.....	5
1.1.3.2 On the efficiency improvement of energy supply systems for buildings ..	7
1.1.3.3 On the thermoeconomic analysis of energy supply systems .....	11
<b>1.2 Problem Statement</b> .....	<b>14</b>
1.2.1 Foundational elements.....	14
1.2.2 Identification of the research problem.....	16
<b>1.3 Objectives</b> .....	<b>18</b>
1.3.1 General.....	18
1.3.2 Specific .....	18
<b>1.4 Thesis structure</b> .....	<b>20</b>
<b>CHAPTER 2 – Optimization and Thermoeconomics of Energy Systems</b> .....	<b>25</b>

<b>2.1 Synthesis and Optimization of Energy Systems.....</b>	<b>25</b>
2.1.1 Research framework .....	25
2.1.2 Definition of a superstructure .....	28
2.1.3 Data collection and analysis .....	30
2.1.3.1 Modeling temporal resolution and technology detail level .....	32
2.1.3.2 Use of representative days .....	32
2.1.3.3 Economic and environmental data .....	34
2.1.4 Translation of the superstructure into a mathematical model.....	35
2.1.5 Calculation of an optimal structure .....	38
<b>2.2 Thermoconomics .....</b>	<b>41</b>
2.2.1 Marginal costs.....	42
2.2.2 Local optimization.....	42
<b>2.3 Conclusion .....</b>	<b>43</b>
<b>CHAPTER 3 – Multi-Objective Optimization of Energy Communities.....</b>	<b>47</b>
<b>3.1 Superstructure of the Energy Community .....</b>	<b>50</b>
3.1.1 EC Superstructure.....	50
3.1.2 Superstructure: building and central unit.....	52
<b>3.2 Data gathering.....</b>	<b>56</b>
3.2.1 Buildings description.....	57
3.2.2 Energy demands .....	57
3.2.2.1 Electricity demand.....	59
3.2.2.2 Heating demand .....	61
3.2.2.3 Cooling demand.....	63
3.2.3 Technical related data .....	65
3.2.3.1 Building k superstructure technologies .....	66
3.2.3.2 DHCN technical data.....	69
3.2.4 Economic data .....	70



3.2.4.1	Fixed costs plus maintenance factors .....	70
3.2.4.2	Variable costs .....	72
3.2.4.3	Electricity and gas economic data .....	73
3.2.5	Environmental data .....	76
<b>3.3</b>	<b>Mathematical model .....</b>	<b>78</b>
3.3.1	Objective functions .....	79
3.3.2	Models of the adopted technologies .....	82
3.3.2.1	Buildings .....	83
3.3.2.2	Central unit .....	88
3.3.3	Energy balances .....	90
3.3.4	DHCN pipelines model .....	93
<b>3.4</b>	<b>Conventional solution (reference case) .....</b>	<b>94</b>
<b>3.5</b>	<b>Single-Objective optimization .....</b>	<b>96</b>
3.5.1	Optimal economic solution .....	99
3.5.1.1	Optimal structure for each building .....	99
3.5.1.2	Energy balances for the entire EC .....	108
3.5.2	Optimal environmental solution .....	111
3.5.2.1	Optimal structure of selected buildings .....	111
3.5.2.2	Energy balances for the entire EC .....	114
<b>3.6</b>	<b>Multi-Objective optimization .....</b>	<b>116</b>
<b>3.7</b>	<b>Conclusions .....</b>	<b>124</b>
<b>CHAPTER 4</b>	<b>– Thermo-economic Analysis of Energy Communities .....</b>	<b>129</b>
<b>4.1</b>	<b>Optimal operation of each building .....</b>	<b>131</b>
4.1.1	Energy balance per building .....	133
<b>4.2</b>	<b>Marginal cost analysis: preliminary information .....</b>	<b>147</b>
4.2.1	Energy balances: hourly dual values obtention .....	147
4.2.2	Dual values .....	150

4.2.2.1 Marginal cost values .....	150
4.2.2.2 Marginal cost values associated with technologies .....	154
4.2.3 TES and DHCN pipelines thermal losses .....	158
4.2.3.1 TES: simultaneous, advanced, and delayed production of energy services .....	158
4.2.3.2 DHCN: remote production of energy services .....	159
<b>4.3 Marginal cost analysis and interpretation.....</b>	<b>160</b>
4.3.1 Electricity marginal costs .....	161
4.3.2 Heat marginal costs.....	162
4.3.2.1 Building 1 (Town hall) .....	162
4.3.2.2 Building 2 (Theater) .....	162
4.3.2.3 Building 3 (Library).....	168
4.3.2.4 Building 4 (Primary school) .....	170
4.3.2.5 Building 5 (Retirement home).....	171
4.3.2.6 Building 6 (Museum).....	173
4.3.2.7 Building 7 (Hospital).....	176
4.3.2.8 Building 8 (Secondary school) .....	179
4.3.2.9 Building 9 (Swimming pool).....	181
4.3.3 Cooling marginal costs .....	181
4.3.3.1 Building 7 (Hospital).....	181
<b>4.4 Conclusions.....</b>	<b>183</b>
<b>CHAPTER 5 – On the Role of Energy Communities in the Italian National Energy System: A Local Optimization Approach .....</b>	<b>187</b>
<b>5.1 The local optimization approach .....</b>	<b>188</b>
<b>5.2 The proposed local optimization .....</b>	<b>191</b>
5.2.1 The global system .....	191
5.2.2 The local system .....	193
<b>5.3 Global energy system: an Italian national energy system (NES) model.....</b>	<b>196</b>

5.3.1 Models applied to the Italian NES.....	196
5.3.2 The selected Italian NES model .....	197
5.3.2.1 Procedure to modify energy demand input data .....	199
5.3.2.2 LCOE and electricity price calculation procedure .....	201
<b>5.4 Local energy system model: the energy community (EC) .....</b>	<b>201</b>
<b>5.5 Italian NES and EC: a local optimization .....</b>	<b>202</b>
5.5.1 On the role of ECs in the Italian NES .....	207
<b>5.6 Conclusions.....</b>	<b>209</b>
<b>CHAPTER 6 – Conclusions.....</b>	<b>213</b>
6.1 Synthesis .....	213
6.2 Contributions .....	215
6.3 Future work.....	216
<b>CAPITOLO 6 – Conclusioni.....</b>	<b>219</b>
6.1 Sintesi.....	219
6.2 Contributi.....	221
6.3 Prospettive future .....	223
<b>CAPÍTULO 6 – Conclusiones.....</b>	<b>225</b>
6.1 Síntesis .....	225
6.2 Contribuciones .....	227
6.3 Trabajos futuros.....	229
<b>CAPÍTULO 6 – Conclusões .....</b>	<b>231</b>
6.1 Síntese .....	231
6.2 Contribuições .....	233
6.3 Trabalhos Futuros.....	235
<b>CHAPTER 7 – References.....</b>	<b>239</b>
<b>APPENDIX A – Additional information .....</b>	<b>261</b>
A.1 Energy demand of the buildings.....	261

<b>A.2 Mathematical model (complement)</b> .....	<b>267</b>
<b>A.3 Technical data</b> .....	<b>271</b>
A.3.1 Internal combustion engine (ICE) .....	271
A.3.2 Micro gas turbine (MGT) .....	272
A.3.3 Absorption chiller (ABS).....	274
A.3.4 Heat pump (HP).....	279
A.3.5 Solar technologies.....	280

## List of figures

Figure 1.1 – November global surface temperatures (land and ocean) (NOAA, 2023a).	1
Figure 1.2 – Climate anomalies and events in November 2023 (NOAA, 2023b).	2
Figure 1.3 – Evolution of energy prices: comparison with pre-pandemic levels (IEA, 2022a). Dark blue line (Asian spot LNG): Asian LNG daily market price; Light blue line (European natural gas (TTF month-ahead)): Title Transfer Facility for NG price in the following month; Green line: daily price of the German power; Yellow line: daily price of the EU imported coal.	4
Figure 1.4 – Categories included in the “Fit for 55” EU package (European Council, 2023).	5
Figure 1.5 – Schematic representation of CHP and CCHP systems.	8
Figure 1.6 – Paradigm shift in the energy landscape (Pina, 2019).	10
Figure 2.1– Interactions among polygeneration systems including energy resources, technology types, and demanded energy services for a typical building. Source: own elaboration.	30
Figure 2.2 – Optimization problems classification. Source: own elaboration.	36
Figure 2.3 – Pareto front diagram indicating feasible and infeasible regions, optimal solutions for $g_1$ and $g_2$ functions (left); dominated and non-dominated solutions (right). Source: own elaboration.	40
Figure 3.1 – Multi-objective optimization framework applied to the energy community. Source: own elaboration.	48
Figure 3.2 – Energy community superstructure. Source: own elaboration.	51
Figure 3.3 – Electricity balance management of the distribution substation. Source: own elaboration.	52
Figure 3.4 – DHCN superstructure for nine buildings plus central unit located in Pordenone, Italy. Source: own elaboration.	53
Figure 3.5 – Superstructure of a given building plus the central unit.	55
Figure 3.6 – Annual electricity demand profiles (two 24-hours typical days per month) for the buildings: town hall, theater, library, and primary school.	60
Figure 3.7 – Annual electricity demand profiles (two 24-hours typical days per month) for the buildings: retirement home, museum, hospital, secondary school, and swimming pool.	61

Figure 3.8 – Annual heating demand profiles (two 24-hours typical days per month) for the buildings: town hall, theater, library, and primary school. ....	62
Figure 3.9 – Annual heating demand profiles (two 24-hours typical days per month) for the buildings: retirement home, museum, hospital, secondary school, and swimming pool. ....	63
Figure 3.10 – Annual cooling demand profiles (two 24-hours typical days per month) for the buildings: town hall, theater, library, and primary school. ....	64
Figure 3.11 – Annual cooling demand profiles (two 24-hours typical days per month) for the buildings: retirement home, museum, hospital, secondary school, and swimming pool. ....	65
Figure 3.12 – Hourly CO <sub>2</sub> emissions for two typical days per month (input data to the EC model) and daily CO <sub>2</sub> emissions (reference data). ....	77
Figure 3.13 – Electricity connections for each building in the reference case (left). Structure of each building (right). Source: own elaboration. ....	95
Figure 3.14 – Installed capacities and annual energy flows for building 1 (Town Hall). ....	100
Figure 3.15 – Installed capacities, annual energy flows, and DHCN connections for building 2 (Theater). ....	101
Figure 3.16 – Installed capacities, annual energy flows, and DHCN connections for building 3 (Library). ....	102
Figure 3.17 – Installed capacities, annual energy flows, and DHN connection for building 4 (Primary school). ....	103
Figure 3.18 – Installed capacities, annual energy flows, and DHCN connection for building 5 (Retirement home). ....	103
Figure 3.19 – Installed capacities, annual energy flows, and DHCN connection for building 6 (Museum). ....	104
Figure 3.20 – Installed capacities, annual energy flows, and DHN connection for building 7 (Hospital). ....	105
Figure 3.21 – Installed capacities, annual energy flows, and DHN connection for building 8 (Secondary school). ....	106
Figure 3.22 – Installed capacities, annual energy flows, and DHN connection for building 9 (Swimming pool). ....	108
Figure 3.23 – EC electricity balance for a working day in January (A) and a working day in July (B). ....	109

Figure 3.24 – EC and central unit heat balance for a working day in January (A) and (B) and a working day in July (C) and (D). .....	110
Figure 3.25 – EC cooling balance for a working day in January (A) and a working day in July (B). .....	111
Figure 3.26 – Installed capacities, annual energy flows, and DHCN connections for building 2 (Theater). Optimal environmental solution. ....	112
Figure 3.27 – Installed capacities, annual energy flows, and DHCN connections for building 7 (Hospital). Optimal environmental solution. ....	113
Figure 3.28 – Optimal environmental solution: EC electricity balance for a working day in January (A) and a working day in July (B). .....	114
Figure 3.29 – Optimal environmental solution: EC and central unit heat balances for a working day in January (A) plus (B) and a working day in July (C) plus (D). ....	115
Figure 3.30 – Optimal environmental solution: EC cooling balances for a working day in January (A) and a working day in July (B). .....	116
Figure 3.31 – Single-objective optimization solutions: boundaries of the Pareto front. Total annual costs in the vertical axis and total annual CO2 emissions in the horizontal axis. ....	117
Figure 3.32 – Pareto front for the multi-objective optimization of the EC. ....	118
Figure 3.33 – Groups of buildings: Group I (south) and Group II (north). ....	119
Figure 4.1 – Electricity and heat balances for building 1 (Town hall). The reader may refer to section 4.1 for a better understanding of “DS connection”. ....	134
Figure 4.2 – Electricity and heat balances for building 2 (Theater). The reader may refer to section 4.1 for a better understanding of “DS connection”. ....	135
Figure 4.3 – Electricity and heat balances for building 3 (Library). The reader may refer to section 4.1 for a better understanding of “DS connection”. ....	137
Figure 4.4 – Electricity and heat balances for building 4 (Primary school). The reader may refer to section 4.1 for a better understanding of “DS connection”. ....	138
Figure 4.5 – Electricity and heat balances for building 5 (Retirement home). The reader may refer to section 4.1 for a better understanding of “DS connection”. ....	139
Figure 4.6 – Electricity and heat balances for building 6 (Museum). The reader may refer to section 4.1 for a better understanding of “DS connection”. ....	141
Figure 4.7 – Electricity and heat balances for building 7 (Hospital). The reader may refer to section 4.1 for a better understanding of “DS connection”. ....	143

Figure 4.8 – Electricity and heat balances for building 8 (Secondary school). The reader may refer to section 4.1 for a better understanding of “DS connection”.....	145
Figure 4.9 – Electricity and heat balances for building 9 (Swimming pool). The reader may refer to section 4.1 for a better understanding of “DS connection”.....	146
Figure 4.10 – Central unit heat balance (A) and building 7 (Hospital) cooling balance (B). .....	147
Figure 4.11 – Optimal economic solution: DHN pipeline connections between buildings 2, 3, and 4 (to the north) and 2, 6, and 5 (to the south). ....	163
Figure 4.12 – Optimal economic solution: DHN pipeline connections between buildings 7, 9, 8, and central unit. ....	176
Figure 5.1 – Global system schematic diagram. Part (A) illustrates the starting point for the Italian NES, i.e., buildings of future ECs are connected to the NES in the conventional way (see section 3.4). Part (B) illustrates a future scenario where there is a deployment of ECs throughout the Italian territory. ....	192
Figure 5.2 – (A) Illustration representing the group of 200 ECs implemented over 200 municipalities located in the north and central Italian regions (the indicated locations do not necessarily coincide with the actual locations of the municipalities). (B) Schematic diagram representing the connections between the group of ECs and the NES.....	195
Figure 5.3 – Schematic diagram of the energy flows within the EnergyScopeIT model (Borasio and Moret, 2022). Abbreviations: natural gas (NG), carbon capture and storage (CCS), synthetic natural gas (SNG), geothermal (geoth.) combined cycle gas turbine (CCGT), integrated gasification combined cycle (IGCC), photovoltaic (PV), temperature (T), plug-in hybrid electric vehicle (PHEV), cogeneration of heat and power (CHP), biomass for electricity generation (Bio. Elec), pressure swing adsorption (PSA). ....	198
Figure 5.4 – Step-by-step of the local-global iteration procedure until the convergence of the independent design variables. Abbreviations: (GO) global optimization, (LO) local optimization, (LCOE) levelized cost of electricity, (TPES) total primary energy supply. ....	205
Figure 5.5 – Results from the iterations. Iteration zero regards the initial conditions while iteration 3 regards the conditions of the optimal global solution. The total annual EC cost refers to one EC only. LCOE (levelized cost of electricity), TPES (total primary energy supply). ....	206
Figure A.1 – Internal combustion engine. Vitobloc 200 (EM-50/81) (Viessmann, 2020). .....	271



Figure A.2 – Micro gas turbine Capstone C65 (Capstone, 2009).....	274
Figure A.3 – Water fired Absorption Chiller WFC series (Yazaki, 2018). ....	275
Figure A.4 – Heat pump EWYQ-DAYN (Daikin, 2013). ....	279

## List of tables

Table 3.1 – Total annual energy services demands and peak demand per building. ....	59
Table 3.2 – ICE, MGT, ABS, and HP nominal capacities per building. Values in kW....	66
Table 3.3 – Electric and thermal efficiencies for ICE and MGT at nominal capacity. ....	67
Table 3.4 – COP values for ABS at nominal capacity. ....	67
Table 3.5 – Annual COP values for the HP in heating (H) and cooling (C) modes. ....	67
Table 3.6 – Main technical data regarding BOI, CC, HST and CST. ....	68
Table 3.7 – Main technical data regarding central unit technologies. ....	69
Table 3.8 – Capacity limits for pipelines connecting buildings and for the central unit pipeline. ....	69
Table 3.9 – DHCN pipeline length between buildings allowed to connect. Zero-values means that the model is not allowed to connect the buildings. Values in meters. ....	70
Table 3.10 – Investment costs and maintenance factors for the EC selected technologies. ....	71
Table 3.11 – Variable costs for the EC selected technologies. ....	72
Table 3.12 – Natural gas price. ....	73
Table 3.13 – Monthly average PUN divided into three hour bands (GME, 2019). ....	74
Table 3.14 – Hourly distribution of the time bands (F1, F2, and F3) for purchasing electricity, according to ARERA (2006). ....	74
Table 3.15 – Portion of the final electricity price regarding electricity production cost (per trimester). ....	75
Table 3.16 – Monthly average electricity price divided into three time bands. Values in €/MWh. ....	75
Table 3.17 – Hourly distribution of the time bands (F1, F2, and F3) for selling electricity, according to GSE (2008). ....	75
Table 3.18 – Monthly average electricity selling price divided into three time bands. Values in €/MWh. ....	76
Table 3.19 – CO <sub>2</sub> emission factors for each typical day and for each month. Values in gCO <sub>2</sub> /kWh. ....	78
Table 3.20 – Main results from the reference case. ....	96
Table 3.21 – Main results from the optimal economic solution. ....	97
Table 3.22 – Main results from the optimal environmental solution. ....	98

Table 3.23 – Data regarding installed capacities, costs, and CO2 emissions from the Pareto front solutions. ....	121
Table 4.1 – Hourly marginal costs (in €/kWh) associated with electricity, heat, and cooling demand variations for all buildings plus central unit. Values for a January working day. ....	151
Table 4.2 – Hourly marginal costs (in €/kWh) associated with the hourly heat demand variations ( $\lambda \cdot \mathbf{HeatDemt}, \mathbf{B}$ ) for the nine buildings. Values for a January working day. ....	152
Table 4.3 – Hourly marginal costs (in €/kWh) associated with the hourly cooling demand variations ( $\lambda \cdot \mathbf{CoolDemt}, \mathbf{B}$ ) for the nine buildings. Values for a January working day. ....	153
Table 4.4 – Marginal cost value associated with 1 kWh of heat production from the BOI. ....	155
Table 4.5 – Marginal cost values associated with 1 kWh of heat production from HP. ....	156
Table 4.6 – Marginal cost value associated with 1 kWh of cooling production from the CC. ....	157
Table 4.7 – Marginal cost values associated with 1 kWh of cooling production from HP. ....	157
Table 4.8 – Loss factors ( <i>losspipe</i> ) regarding heat pipelines. ....	160
Table 4.9 – Loss factors ( <i>losspipe</i> ) regarding cooling pipelines. ....	160
Table 4.10 – Marginal costs calculation for building 2, regarding hours 1 to 9 and 11 to 17. Advanced and delayed cases. ....	165
Table 4.11 – Marginal costs for building 2, regarding hours 18 to 20. Cases of delayed and remote production. ....	167
Table 4.12 – Marginal costs for building 3, regarding hours 6 to 17. Cases of advanced, delayed, and remote production. ....	169
Table 4.13 – Marginal costs for building 4, regarding hours 6 to 17. Cases of advanced, delayed, and remote production. ....	171
Table 4.14 – Marginal costs for building 4, regarding hours 21 and 22. Cases of delayed and remote production. ....	171
Table 4.15 – Marginal costs for building 5, regarding hours 1 to 24. Cases of advanced, delayed, and simultaneous production. ....	173
Table 4.16 – Marginal costs for building 6, regarding hours 1 to 24. Cases of advanced, delayed, and remote production. ....	175

Table 4.17 – Marginal costs for buildings 7, 9, 8, and central unit (in this order – see Figure 4.12). Cases of advanced, delayed, simultaneous, and remote production. Blue arrows: marginal path passing through DHN pipeline; red arrows: marginal path passing through the HST of a given building; green arrows: marginal path passing through the HSTc of the central unit; red boxes: cases of simultaneous heat production; red dashed and dotted lines represent specific cases of marginal paths explained throughout the text. ....178

Table 4.18 – Cooling marginal costs regarding building 7. Cases of advanced, delayed, and simultaneous production. ....182

Table 5.1 – Detailed description of two approaches to tackle the problem of the local-global optimization. ....190

Table 5.2 – Review of national energy system models applied to Italy. Selected time range: 2020 onwards.....197

Table 5.3 – EnergyScopeIT: energy demand input divided by type, economic sector, and region (Borasio and Moret, 2022). Values in GWh. Abbreviations: (HT) high temperature, (LTSH) low temperature spacing heat, (LTHW) low temperature hot water, (PRO) process, (SC) spacing cooling, (P) passenger, (FR) freight, (FA) farming.....200

Table A.1 – Electricity demand for each building in a January working day. Values in kW. ....262

Table A.2 – Heat demand for each building in a January working day. Values in kW..263

Table A.3 – Cooling demand for each building in a January working day. Values in kW. ....264

Table A.4 – Electricity demand for each building in a July working day. Values in kW. ....265

Table A.5 – Heat demand for each building in a July working day. Values in kW.....266

Table A.6 – Cooling demand for each building in a July working day. Values in kW. .267

Table A.7 – Lifetime of the adopted technologies. ....269

Table A.8 – Factor to account for a cost reduction when installing more than one from the same technology. ....270

Table A.9 – Technical data regarding the four ICE models from Viessmann (2020)...272

Table A.10 – Linear coefficients for the linearized equations derived from the ICE performance data (Table A.9). ....272

Table A.11 – Technical data regarding the four MGT models from Capstone (2009). .273

Table A.12 – Linear coefficients for the linearized equations derived from the MGT performance data (Table A.11 shows the technical data obtained from the Capstone catalogues of the four MGT models. Then, Table A.12 provides the linear coefficients obtained from the data shown in Table A.11. ....	274
Table A.13 – Technical data from the ABS manufacturer (Yazaki, 2018) for the model WFC-SC10. Nominal cooling capacity: 35.2 kW; Heat input: 50.2 kW. Abbreviations: Heat Medium Inlet Temperature (HMIT), Cooling Capacity Factor (CCF), Heat Input Factor (HIF). ....	276
Table A.14 – Technical data from the ABS manufacturer (Yazaki, 2018) for the model WFC-SC20. Nominal cooling capacity: 70.3 kW; Heat input: 100 kW. Abbreviations: Heat Medium Inlet Temperature (HMIT), Cooling Capacity Factor (CCF), Heat Input Factor (HIF). ....	277
Table A.15 – Technical data from the ABS manufacturer (Yazaki, 2018) for the model WFC-SC30. Nominal cooling capacity: 105.6 kW; Heat input: 151 kW. Abbreviations: Heat Medium Inlet Temperature (HMIT), Cooling Capacity Factor (CCF), Heat Input Factor (HIF). ....	278
Table A.16 – Technical data regarding the three adopted HP models (Daikin, 2013)...	280
Table A.17 – Hourly photovoltaic (PV) specific energy production ( $kPV(t)$ ), in $W/m^2$ . ....	281
Table A.18 – Hourly solar thermal (ST) specific energy production ( $kST(t)$ ), in $W/m^2$ . ....	282
Table A.19 – Main input parameters (to SAM software (NREL, 2023)) to simulate the hourly energy production from PV and ST panels. Abbreviations: Annual average (AA), Collector heat removal factor ( $FR$ ), Transmittance and Absorptance ( $\tau\alpha$ ), Heat loss coefficient ( $UL$ ), Incidence Angle Modifier (IAM).....	283

## List of acronyms

ABS	Absorption chiller
AEEG	Italian electricity and gas authority
AIC	Annual investment cost
AMC	Annual maintenance cost
AOC	Annual operation cost
ARERA	Italian regulatory authority for energy, networks, and environment
BOI	Boiler
BOIc	Boiler central unit
CC	Compression chiller
CCHP	Combined cooling, heat, and power
CHP	Combined heat and power
COP	Coefficient of performance
CST	Chilled water storage
DAIT	Italian Department of Internal and Territorial Affairs
DCN	District cooling network
DES	Distributed energy systems
DHCN	District heating and cooling network
DHN	District heating network
DS	Distribution substation
EC	Energy community
EEA	European environmental agency
EU	European union
GHG	Greenhouse gas
GME	Italian energy market manager
GO	Global optimization
GSE	Italian energy service manager
HP	Heat pump
HST	Hot water storage
HSTc	Hot water storage central unit
IC	Investment cost
ICE	Internal combustion engine
ICEc	Internal combustion engine central unit

IEA	International energy agency
IP	Integer programming
IPCC	Intergovernmental Panel on Climate Change
IPEX	Italian power exchange market
ISPRA	Italian superior institute for environmental protection and research
LCOE	Levelized cost of electricity
LGO	Local-global optimization
LO	Local optimization
LP	Linear programming
mC	Maintenance cost
MGT	Micro gas turbine
MILP	Mixed-integer linear programming
MINLP	Mixed-integer non-linear programming
MIP	Mixed-integer programming
MOO	Multi-objective optimization
NES	National energy system
NG	Natural gas
NLP	Non-linear programming
NOAA	National oceanic and atmospheric administration
NREL	National Renewable Energy Laboratory
OC	Operation cost
OE	Operation emission
PUN	Italian national unique price
PV	Photovoltaic panel
RE	Renewable energy
SAM	System advisor model
SH	Spacing heating
SHW	Sanitary hot water
SOO	Single-objective optimization
ST	Solar thermal panel
STc	Solar thermal panels central unit
TAC	Total annual cost
TAE	Total annual environmental emissions

TAT	Thermally activated technologies
TES	Thermal energy storage
TPES	Total primary energy supply
UNFCCC	United Nations Framework Convention on Climate Change



## List of publications

**De Souza, R.;** Casisi, M.; Micheli, D.; Reini, M. *A Review of Small–Medium Combined Heat and Power (CHP) Technologies and Their Role within the 100% Renewable Energy Systems Scenario*. *Energies* 2021, 14, 5338. <https://doi.org/10.3390/en14175338>

**De Souza, R.;** Nadalon, E.; Casisi, M.; Reini, M. *Optimal Sharing Electricity and Thermal Energy Integration for an Energy Community in the Perspective of 100% RES Scenario*. *Sustainability* 2022, 14(16), 10125. <https://doi.org/10.3390/su141610125>

Emanuele Nadalon, **Ronelly De Souza**, Melchiorre Casisi, and Mauro Reini. *Part-Load Energy Performance Assessment of a Pumped Thermal Energy Storage System for an Energy Community*. *Energies* 2023, 16(15), 5720; <https://doi.org/10.3390/en16155720>

**Ronelly J. De Souza**, Emanuele Nadalon, Melchiorre Casisi, Mauro Reini, Luis M. Serra, Miguel A. Lozano. *Towards a Low Carbon Future: Evaluating Scenarios for an Energy Community through a Multi-Objective Optimisation Approach*. ECOS 2023, 25-30 June 2023, Las Palmas de Gran Canaria, Spain. <https://doi.org/10.52202/069564-0235>

**Ronelly J. De Souza**, Luis M. Serra, Mauro Reini, Miguel A. Lozano, Emanuele Nadalon, Melchiorre Casisi. *Marginal Cost Analysis Applied to Complex Polygeneration Systems: Case Study of an Italian Energy Community*. ECOS 2024, 30 June – 4 July 2024, Rhodes, Greece.



---

*CHAPTER 1 – Introduction*

---



## CHAPTER 1 – Introduction

### 1.1 Background and Context

This section provides the reader with a brief overview regarding the global energy landscape, energy crisis, environmental issues, and some of the responses from the scientific community.

#### 1.1.1 Global energy landscape and environmental issues

The growing demand of the global population as well as the growing level of social and economic development is provoking an increasing demand of primary energy in the world. In fact, a country's economic development is directly connected to its level of primary energy consumption. As stated by Vogel et al. (2021) in a research study that gathered data from 106 countries, economic growth and extractivism activities (which includes fossil fuels) are associated with high levels of energy requirements. Moreover, during the past 50 years, global energy consumption has increased by over 200% (IEA, 2017). Consequently, greenhouse gas (GHG) emissions have also risen, resulting in serious environmental impacts, especially global warming (Waters *et al.*, 2016).

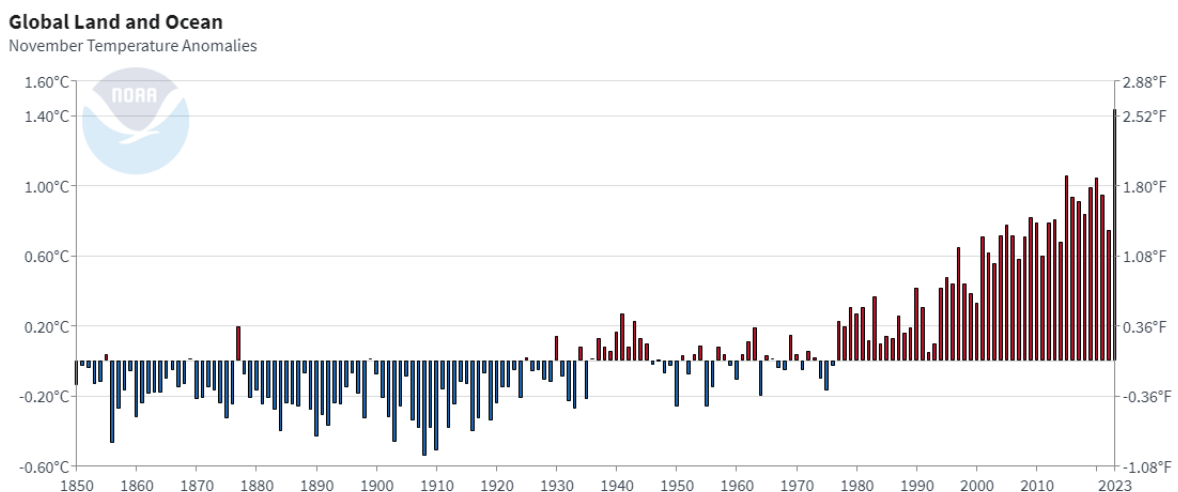


Figure 1.1 – November global surface temperatures (land and ocean) (NOAA, 2023a).

The increase in the year-to-date average global temperature achieved a new record in November 2023, as can be observed in Figure 1.1 (NOAA, 2023a). On top of that,

consumption of fossil fuels has achieved high rates in recent years in all energy sectors (IEA, 2019), and the resulting impacts related to greenhouse gas (GHG) emissions are known for their strong influence on the global warming caused by humankind (Waters *et al.*, 2016). The potential damage that such an issue can cause to the entire world has raised the attention of society and global leaders, recognizing that trends towards a clean-energy economy must keep going and with no way back (Obama, 2017).

## Selected Significant Climate Anomalies and Events: November 2023

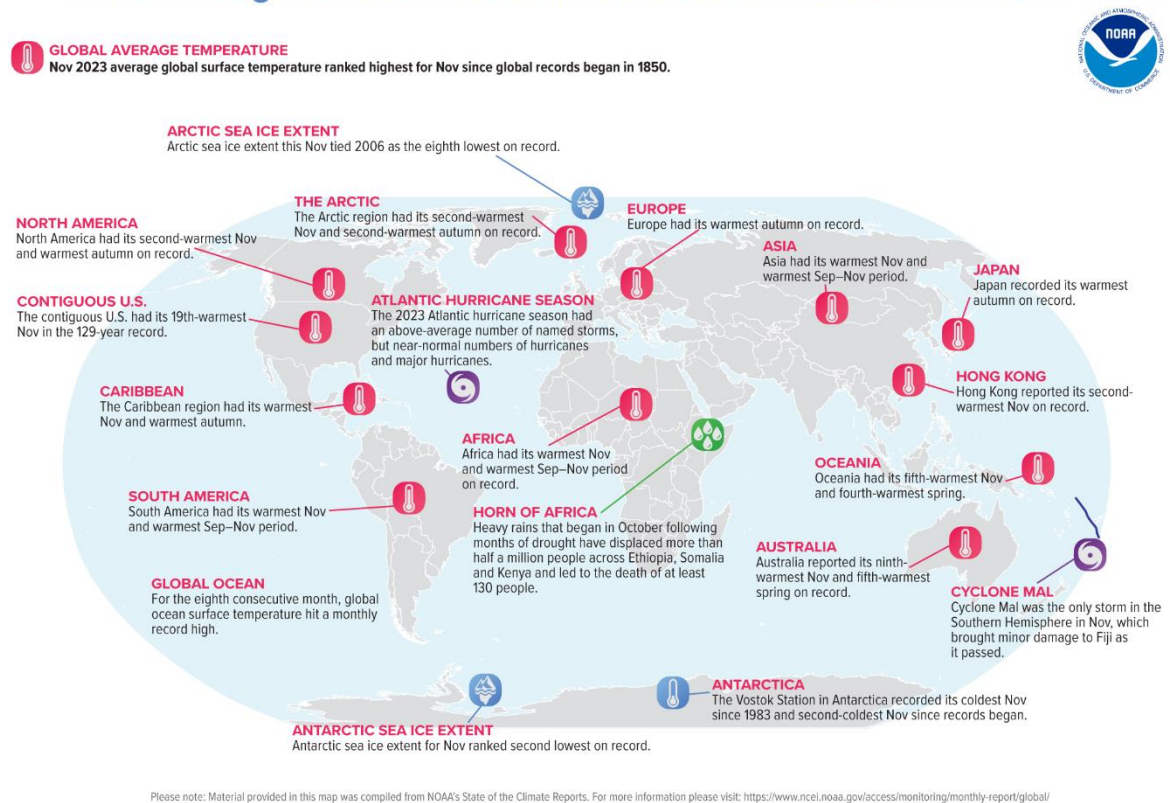


Figure 1.2 – Climate anomalies and events in November 2023 (NOAA, 2023b).

In this sense, the Paris Agreement (UNFCCC, 2015), a historical milestone, was raised as an international treaty on climate change, signed by 196 countries, which has the aim to limit global warming below 2 °C with comparison to pre-industrial levels. However, some countries have faced difficulties in achieving their GHG reduction rates, a fact that might contribute to not achieving the 2 °C goal (Rogelj *et al.*, 2015). In fact, the National Centers for Environmental Information (NOAA, 2023b) have registered significant climate anomalies, such as the highest temperatures ever reported in several regions across the world, the smallest Arctic and Antarctic sea ice extent (Figure 1.2). There is plenty of

evidence regarding climate change effects all around the world as for temperature deviations (Schellnhuber, Rahmstorf and Winkelmann, 2016), impacts on sea and land ecosystems (Hughes *et al.*, 2018; IPCC, 2023), and unusual rainy seasons (Steffen *et al.*, 2018). Therefore, the acknowledgment of the problem by world society, especially by the scientific community, has turned the world attention to renewable energy (RE) sources as a long-term solution, which can also be observed in the special Global Warming 1.5 report from Intergovernmental Panel on Climate Change (IPCC) (IPCC, 2018).

### **1.1.2 Global energy crises: triggers, consequences, and actions**

The 2021/2022 global energy crisis was essentially the consequence of two main worldwide problems regarding primary energy: supply chain and prices. According to a report by IEA (2022b), such problems were triggered by several factors, including the economic recovery that started to take place as the Covid-19 pandemic progressively weakened in 2021 and the beginning of Russia/Ukraine war in February 2022. The result was a brutal energy prices increase in comparison with pre-pandemic levels (IEA, 2022a) (Figure 1.3), followed by a substantial coal consumption growth (IEA, 2021). The European Union (EU), deeply affected by a plunge in Russian's gas supply, released a report (IEA, 2022c) with a set of actions to avoid gas shortages in 2023 such as energy efficiency improvements of industries and public and private buildings, deployment of renewables, and electrification of heat.

In addition to primary energy savings, the EU report (IEA, 2022c) highlights also the importance of deploying renewables. This is a key concern for EU since it has fixed deadlines, through different pieces of legislation, to reach carbon neutrality by 2050. For instance, the EU 2030 target plan (EEA, 2023) aims at a more ambitious and cost-effective direction to reach the carbon neutrality by 2050, without forgetting the encouragement for creating new green jobs and for stimulating international partners to also increase their carbon neutrality ambitious. As a part of the EU 2030 target plan, the so called "Fit for 55" package (European Council, 2023) proposes an ambitious target for decreasing the net greenhouse gas (GHG) emissions by at least 55% (of the 1990 net GHG emissions level) by 2030. According to the EU council, the package aims to create a balanced and coherent framework for attaining the EU's climate goals, while ensuring a just and equitable transition, promoting innovation and competitiveness of EU industry,

and maintaining a level playing field with third country economic operators. Still according to them, to accomplish these goals, member states must implement concrete measures to decarbonize their economies, and the “Fit for 55” package provides legislative proposals and amendments to assist in achieving this objective.

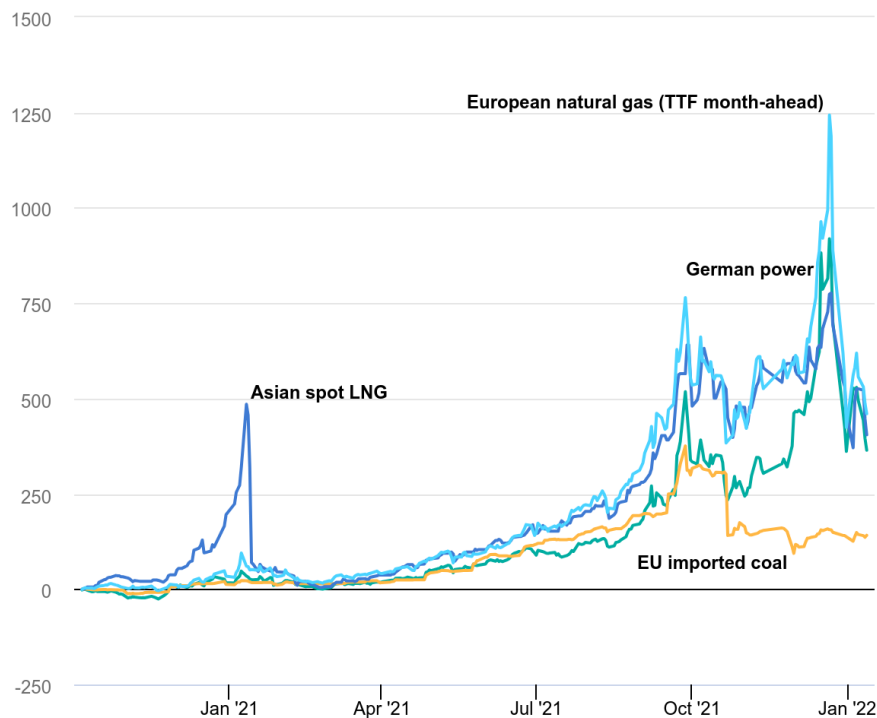


Figure 1.3 – Evolution of energy prices: comparison with pre-pandemic levels (IEA, 2022a).

Dark blue line (Asian spot LNG): Asian LNG daily market price; Light blue line (European natural gas (TTF month-ahead)): Title Transfer Facility for NG price in the following month; Green line: daily price of the German power; Yellow line: daily price of the EU imported coal.

The mentioned package describes also, in detail, how the EU will translate its climate goals into legislation. Specific categories (Figure 1.4) will give directives that include energy taxation, energy-efficient transition, reform to the EU emissions trading system, energy performance of buildings, and boost of renewable energy sources. For instance, the directive regarding energy-efficient transition claims that energy saving is the most cost-effective solution for reaching the climate goals in the energy sector. Indeed, with such a solution it is possible to reduce lots of GHG emissions besides providing more affordable energy. In the same line, the directive for boosting renewable energy sources says that moving towards such energy sources the GHG emissions will be substantially





water–solar energy sources. Their work was based on avoiding 1.5 °C global warming (a more daring goal comparing to Paris Agreement), and the simulation has foreseen societal benefits such as the creation of 24 million net new full-time jobs, reduction in energy costs and air pollution, and increase in the world population with access to energy. In another studies, such as those developed by Pursiheimo, Holttinen and Koljonen (2019) and Breyer et al. (2018), the authors also reported benefits with the 100% RE scenario, claiming that solar photovoltaic (PV) energy source is going to play a key role in the generation of electricity by 2050 due to costs reductions and, consequently, a rapid increase in installations.

Although the feasibility of a 100% RE electricity system has been put in doubt (Heard *et al.*, 2017), other authors claims that such a scenario is not only feasible, but it is also viable (Brown *et al.*, 2018). Over the past two years, further steps have been taken when it comes to the analysis and simulation of a possible 100% RE scenario. The analyses that some authors have performed include detailed energy transition pathways that can take the current world fossil-fuel-based energy system to a completely renewable global energy system (Bogdanov *et al.*, 2019). Obviously, the intrinsic intermittent characteristic of RE sources requires a considerable amount of energy storage capacity. However, if properly managed, storage facilities can enhance the dependability of energy systems and decrease electricity costs (Assembayeva, Zhakiyev and Akhmetbekov, 2017).

It is also possible to find studies, in the literature, that deal with energy transition scenarios applied to specific countries. For instance, the research conducted by Bogdanov et al. (2021) presented a model for the simulation of a complex energy system transition for the power, heat, transport, and industry sectors of Kazakhstan. They claim that, based on their results, the transition towards a 100% RE based system by 2050 is possible, even under some unforeseen conditions, and that (i) the levelized cost of electricity (LCOE) can be reduced by 26%, and (ii) it is possible to achieve, by 2040, a reduction on the CO<sub>2</sub>eq emissions (from the mentioned sectors) of 90%. The paper published by Limpens et al. (2019), presented a model that, according to the authors, can be used “for the strategic energy planning of urban and regional energy systems”. The model was applied to the case of the national energy system of Switzerland and was a bit less optimistic since they evaluated a 50% RE scenario. Another interesting study is the one developed by Borasio and Moret (2022) in which they have simulated different possible energy transition

scenarios for the Italian energy system. They claimed having developed “the first open-source whole-energy system model of Italy” to simulate decarbonization strategies. The evaluated scenarios demonstrated that emissions can be cut by 79% to 97% thanks to (i) a radical electrification of the energy system, and (ii) a wide deployment of renewable energy and efficient conversion technologies.

In order to make such energy transition happen, studies point out also the types of technologies needed to generate/store electricity and thermal energy as well as the bridging technologies responsible for converting energy from a given sector into products for another sector (Bogdanov *et al.*, 2019, 2021). Among those technologies, there exist the polygeneration systems, which can provide two or more products taking advantage of the same energy source. With their flexibility as for the energy source, polygeneration technologies can be fed from fossil-based or renewable-based sources (Bogdanov *et al.*, 2021).

As reported by Bogdanov *et al.* (2021), polygeneration systems are expected to play an important role in the transition to a scenario highly supported by renewable energy sources. Focusing on large scale systems, the flexibility of such polygeneration systems will support the energy system to keep running already-existing fossil-fuel-based power plants (e.g., operating with CHP technologies) and gradually move towards RE sources (such as biomass and organic waste). When it comes to smaller scale systems, such as building scale polygeneration systems (Buoro, 2013; Casisi *et al.*, 2019; Pina *et al.*, 2020; Pinto, 2021; De Souza *et al.*, 2022), the energy system can be supported by the efficiency improvement derived from the process integration provided by polygeneration systems, i.e., energy demands are covered although less primary energy is needed.

#### *1.1.3.2 On the efficiency improvement of energy supply systems for buildings*

Energy process integration, in the context of polygeneration systems, involves the strategic management and optimization of various energy conversion processes within an interconnected framework. Polygeneration systems aim to simultaneously produce multiple forms of energy, such as electricity, heat, and cooling, often from a common energy source. Such simultaneous production approach focuses on maximizing overall efficiency, minimizing resource use, and enhancing the synergies between different energy streams. By carefully designing and managing the interaction of various

technologies, energy process integration seeks to achieve a more sustainable and economically viable utilization of resources. In this way, the overall performance of the energy supply system can be improved and, hence, the environmental impacts can be reduced.

As mentioned in the last section, polygeneration systems are flexible technologies, in terms of the energy source, and are also capable of generating two or more products from the same energy source (Subramanian *et al.*, 2020). Polygeneration systems are often classified according to their number of products. Cogeneration systems are technologies known by simultaneously generating two products, generally heat and electricity. They are also known as Combined Heat and Power (CHP), as the technology essentially produces shaft power (which is converted into electricity power) and heat employing the same energy source. A further extension of cogeneration is trigeneration, also known as Combined Cooling, Heating, and Power (CCHP), which involves the integrated production of electricity, heat, and cooling. A simplified schematic representation of cogeneration and trigeneration systems are delineated in Figure 1.5.

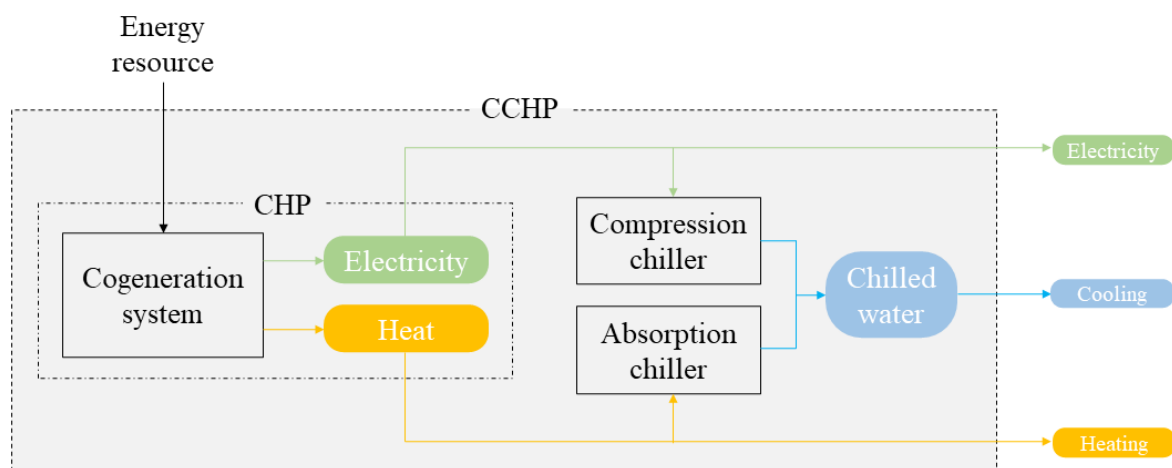


Figure 1.5 – Schematic representation of CHP and CCHP systems.

The prime mover of a cogeneration system can comprise a reciprocating internal combustion engine, Stirling engine, gas turbine, microturbine, or fuel cell. Within its core (the cogeneration module), the chemical energy derived from the fuel undergoes conversion into shaft power, closely linked to both an electricity generator and a heat recovery system. Trigeneration systems takes further advantage of the thermal and/or electrical products of the cogeneration system through the integration of absorption

chillers (thermally activated technology – TAT) and/or mechanical chillers. This design makes trigeneration systems particularly pertinent for applications characterized by seasonal heating requirements and substantial cooling needs, as observed in Mediterranean countries. To ensure a continuous supply and prevent over-dimensioning of the cogeneration module, auxiliary equipment such as steam or hot water boilers and heat pumps is frequently incorporated (Pina, 2019).

Such process integration techniques, through polygeneration systems, is closely related to a paradigm shift in modern energy landscapes (Figure 1.6): Distributed Energy Systems (DES), i.e., decentralized energy generation and storage. Within this framework, the concept of energy community (EC) emerges as a strategic path, particularly relevant in the context of district heating and cooling networks (Buoro, 2013; Casisi *et al.*, 2019; Pinto, Serra and Lázaro, 2022). Energy communities, comprised of interconnected consumers, producers, and prosumers, harness the potential of DES to collectively generating, sharing, and managing energy resources within a local network. By incorporating diverse energy technologies, such as solar thermal collectors, PV panels, CHP/CCHP units, thermal storage systems, and pipelines to thermal energy transport (Buoro *et al.*, 2010; De Souza *et al.*, 2022), energy communities have the potential to contribute to the resilience and sustainability of DES. This collaborative approach not only enhances overall energy efficiency but also fosters community engagement, allowing participants to actively contribute in the transition towards more sustainable and locally integrated energy systems. In this sense, energy communities present an effective pathway for achieving economically viable, resilient, and environmentally conscious urban energy infrastructures.

Therefore, when it comes to the efficiency improvement of energy supply systems, energy communities present the possibility of standing as a (i) way for highly integration of energy systems, (ii) effective method for saving primary energy, and (iii) potential solution to contribute to the transition process to a 100% RE scenario, mentioned on section 1.1.3.1. The intended meaning for energy community (EC), in this thesis, is described by Bauwens *et al.* (2022), i.e., the community as a place where buildings are able to share energy among each other (whether it be electricity, heat, and/or cooling) with the aim to pursue economic and environmental benefits.

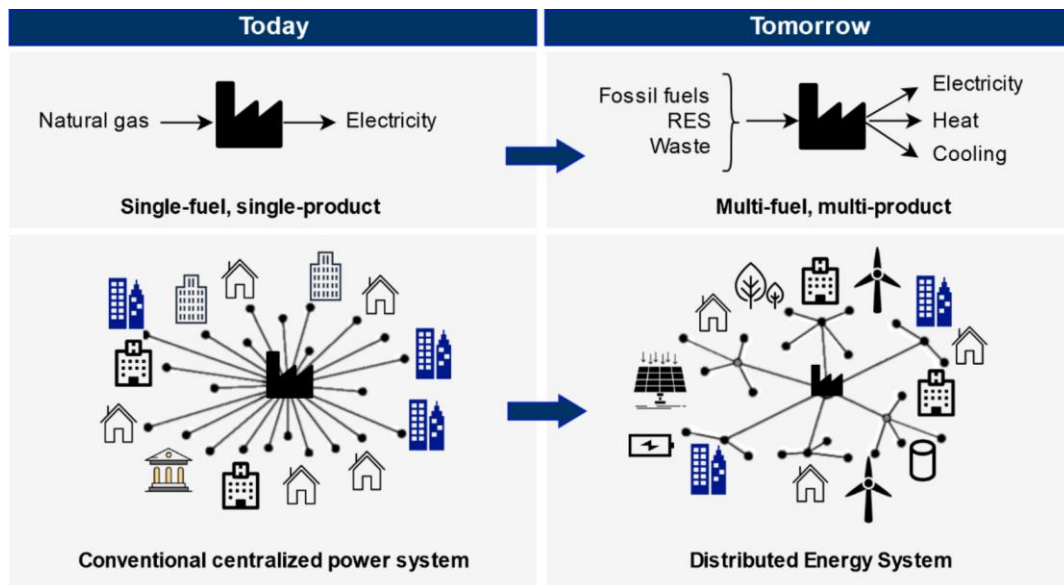


Figure 1.6 – Paradigm shift in the energy landscape (Pina, 2019).

The role of ECs in achieving better economic results as well as reducing environmental emissions has been widely considered and studied by the scientific community, particularly when it comes to the share of heat through a district heating network – DHN (Dorfner and Hamacher, 2014; Sartor, Quoilin and Dewallef, 2014; Vesterlund, Toffolo and Dahl, 2017). For instance, the work developed by Lund et al. (2010), analyzed a set of scenarios in which the Danish energy system is converted to a 100% RE scenario by 2060. In this scenario, DHN technology proved to have the second lowest annual cost (the first was individual electric heating) out of 10 types of heating technology and resulted in the lowest annual fuel consumption option. According to the same authors, the best solution for the energy transition would be to continue the growth of DHNs combined with individual heat pumps for areas not covered by them.

Another important aspect to be considered, when it comes to EC, is the sharing of electricity among the buildings. This is an additional topic that has demonstrated potential for the improvement of ECs. Such approach essentially intends to reduce the amount of electricity purchased from the grid by sharing the self-produced electricity among the EC members. This procedure makes it possible, for example, to share the electricity produced by local photovoltaic plants to power heat pumps and circulation pumps (the main source of operating costs), as in the research carried out by Vivian et al. (2022). In the work developed by Kim et al. (2021), they proposed an “energy prosumer concept” in order to

increase the self-consumption of an EC in terms of thermal and electrical energy. The shared electricity was generated by distributed PV plants and, before the implementation of the mentioned concept, the power sold to the grid was around 60% of the PV power production. After the implementation, such figure dropped to 12.5% of electricity sold to the grid, which shows the increase of self-consumption. Kayo, Hasan and Siren (2014) investigated the electricity sharing approach applied to four types of buildings that could generate and consume electricity and heat from each other. As each building had its own CHP system, one of their main conclusions was that the larger the CHP system, the greater the possibility of sharing electricity with other buildings and the greater the primary energy savings. Another interesting conclusion is that the operating strategy of the CHP system plays a key role when it comes to improvements in energy sharing.

Therefore, the integration of polygeneration systems, characterized by simultaneous generation of electricity, heat, and cooling, offers a versatile and efficient approach towards sustainable energy utilization. The pivotal role of trigeneration systems shows the potential for enhanced thermal and electrical coverage, which can be crucial in a scenario of decentralized generation and storage. The introduction of ECs further extends the discourse, highlighting the combined potential of interconnected consumers and prosumers. The potential of ECs in supporting the transition to a low-carbon future is clear due to key benefits such as (i) highly integrated energy systems, (ii) primary energy savings, and (iii) economic viability. The shared consumption of electricity among buildings within ECs, as demonstrated in the research by Vivian et al. (2022) and Kim et al. (2021), further accentuates the advantages of ECs. Thus, the integration of polygeneration systems and the development of ECs present a coherent strategy for advancing economically viable, resilient, and environmentally friendly urban energy infrastructures.

### *1.1.3.3 On the thermoeconomic analysis of energy supply systems*

In order to design polygeneration systems and to obtain the economic benefits derived from their integration, three main approaches have been applied throughout the literature (Andiappan, 2017): heuristics, thermodynamic-based, and mathematical optimization. The first one cannot provide or ensure an optimal solution since it is based on the knowledge and experience of the designer. Although the thermodynamic-based approach

(such as pinch and exergy analysis) is a proven and effective method for energy systems design, it cannot offer a common framework to evaluate configurations with the aim to find an optimal solution. In alternative, the mathematical optimization approach offers a systematic procedure for searching an optimal solution, which includes the definition of a superstructure consisting of all feasible technologies, the mathematical model of each technology, and a clearly defined objective function.

The design of polygeneration systems must cover two main issues (Chicco and Mancarella, 2009; Lozano, Carvalho and Serra, 2009, 2011; Pina, Lozano and Serra, 2017): (i) the synthesis of the plant configuration (which technology is installed and its capacity), and (ii) the operation of the installed technologies (on/off status, energy flow rates, purchase/selling electricity, etc). When it comes to new plants, both issues must be considered, while only the second issue is considered when dealing with already-in-operation plants (Chun *et al.*, 2021).

After the design of polygeneration systems, a central problem remains: the cost allocation of each energy flow within the optimal configuration and operation of the energy plant (Lozano *et al.*, 1994; Lozano, Valero and Serra, 1996). The complexity of cost allocation increases with the cumulative complexity of energy systems configuration, i.e., when it involves different types of fuels with varying prices, more than one product, several technologies, the integration of thermal energy storage (TES), and complex energy interdependencies where alterations in one flow may influence others (Pina, Lozano and Serra, 2017).

By explaining the optimal operation mode of a polygeneration system through a thermoeconomic analysis, it is possible to obtain a comprehensive understanding of the cost formation process through the marginal costs associated with internal flows and final products (Lozano, Carvalho and Serra, 2009). Furthermore, this analysis makes it possible to assess the economic implications arising from changes in energy demands or changes in the operating conditions of devices. This integrated approach not only unveils the logic behind operational strategies, but also quantifies the economic consequences of dynamic changes in the complex framework of modern energy systems.

The work developed by Lozano, Carvalho and Serra (2009) investigated the operational complexities of a simple trigeneration system integrated with the electric grid for both



purchase electricity and sell self-produced electricity surplus. By using a linear programming model, the study identified the optimal operational mode with the lowest variable cost under diverse energy demand scenarios. A thermoeconomic analysis, based on marginal cost analysis, returned the unit costs for the internal energy flows and final products, offering insights into the optimal operational strategy concerning energy service demands and resource prices. The work systematically described the characteristics of various operation modes and elucidated the logic behind the optimal production mode, interpreting the marginal cost formation process and evaluating economic impacts.

Thermal energy storage (TES) is another key element in the design of polygeneration systems (Buoro *et al.*, 2013; Capuder and Mancarella, 2014; Pina, Lozano and Serra, 2017; Casisi *et al.*, 2019; De Souza *et al.*, 2022). Such technology allows to explore the heat produced within a polygeneration system in a more effective and efficient way, reducing overall energy consumption and carbon emissions (Cabeza *et al.*, 2021). Based on the research of Lozano, Carvalho and Serra (2009), the work developed by Pina, Lozano and Serra (2017) investigated the operational dynamics of a trigeneration system supported by thermal energy storage (TES), aiming to optimize the system's performance and comprehend the role of TES in achieving an optimal solution. The optimal operation of the trigeneration system was also determined through a linear programming model, minimizing the total variable cost, and was supplemented by a thermoeconomic analysis. The marginal cost assessment of internal flows and final products highlighted the system's operational strategy and the complex cost formation process. The incorporation of TES introduced a temporal dimension to the cost allocation problem, revealing how energy storage optimally shifts consumption periods by decoupling the energy production and energy demand periods.

Therefore, the design and optimization of polygeneration systems present a complex challenge, involving the synthesis of plant configurations and the efficient operation of installed technologies. The complex task of cost allocation within the optimal configuration and operation of energy plants, especially those incorporating TES, represents a central problem. The inclusion of TES illustrated how energy storage optimally reshapes consumption periods by decoupling energy production and demand. Such integrated approach elucidated the logic behind optimal operational strategies and quantified the economic consequences of dynamic changes.

## 1.2 Problem Statement

In this section, the foundational elements presented in the preceding sections are consolidated to succinctly articulate the problem statement that sets the stage for the research conducted in this PhD thesis.

### 1.2.1 Foundational elements

The escalating global demand for primary energy reflects the increasing levels of social and economic development worldwide. Over the past 50 years, global energy consumption has surged by over 200%, consequently leading to a substantial rise in greenhouse gas (GHG) emissions and their detrimental environmental impacts, notably contributing to global warming. Recent records, such as the unprecedented November 2023 average global temperature, emphasize the urgency of addressing these challenges. In response, the international community has recognized the imperative for transitioning towards a clean-energy economy, exemplified by the landmark Paris Agreement. Climate anomalies and severe environmental impacts further underscore the urgency of mitigating climate change effects. The scientific community's acknowledgment of the problem has shifted global attention to not only renewable energy sources (IPCC, 2018), but also to more efficient strategies for energy supply systems.

The recent global energy crisis essentially resulted from interconnected issues related to the supply chain and energy prices. Factors such as the economic recovery post-Covid-19 and the Russia/Ukraine war started in February 2022 contributed to a drastic increase in energy prices. The European Union (EU), facing a significant drop in Russian gas supplies, responded by outlining a comprehensive plan in a report (IEA, 2022c), emphasizing energy efficiency improvements in industries and buildings, increased deployment of renewables and electrification of heating to avoid gas shortages in 2023. This initiative aligns with the EU's broader commitment to achieve carbon neutrality by 2050, as outlined in the EU 2030 target plan (EEA, 2023). The "Fit for 55" package, a component of this plan, sets an ambitious target to reduce net GHG emissions by at least 55% by 2030 compared to 1990 levels. It outlines legislative proposals covering various aspects such as energy-efficient transition, energy performance of buildings, and deployment of renewable energy sources. These directives stress the significance of

energy savings and renewable sources in reducing GHG emissions and achieving the EU's climate goals.

It has become clear that the escalation of global energy consumption, while promoting the development of society, imposes environmental threats through increased GHG emissions. In addition, the importance of actions such as improving the efficiency of energy supply systems and the deployment of renewable energy sources also have become clear, as they have the potential to support nations in the transition towards a more self-sufficient scenario in terms of primary energy. Such actions can support coping with unforeseen events, such as an energy crisis, and have progressively gained more attention from the scientific community.

Over the past two decades, numerous works have explored scenarios wherein primary energy supply relies entirely on renewable sources. Despite debates about the feasibility of a 100% renewable energy (RE) scenario, recent studies (Sadiqa, Gulagi and Breyer, 2018; Bogdanov *et al.*, 2019, 2021; Hansen, Breyer and Lund, 2019b; Ram, Aghahosseini and Breyer, 2020; Potrč *et al.*, 2021) have evaluated energy transition pathways, addressing diverse challenges such as the RE intermittency through substantial energy storage capacities. Country-specific studies, exemplified by Bogdanov *et al.* (2021) for Kazakhstan and Borasio and Moret (2022) for Italy, provide models and simulations supporting the plausibility of transitioning to energy systems less dependent on fossil-based fuels. In the context of polygeneration systems, highlighted by Bogdanov *et al.* (2021), these technologies emerge as vital components facilitating the transition by offering flexibility regarding the energy sources. Polygeneration systems, particularly at building scale, as explored by Buoro (2013), Casisi *et al.* (2019), De Souza *et al.* (2022), Pina *et al.* (2020), and Pinto (2021) present efficiency gains through process integration, reducing primary energy needs while meeting energy demands.

When it comes to polygeneration systems (typically categorized into cogeneration and trigeneration systems), energy process integration is fundamental, which involves the optimization of interconnected energy conversion processes to produce electricity, heat, and cooling simultaneously. Such process integration aligns with the paradigm shift towards distributed energy systems (DES) and has the potential to contribute with better performance standards in energy communities (which corroborates with a transition

towards DES). The role of energy communities sharing thermal energy and/or electricity among its members, has been extensively studied (Dorfner and Hamacher, 2014; Kayo, Hasan and Siren, 2014; Sartor, Quoilin and Dewallef, 2014; Vesterlund, Toffolo and Dahl, 2017; Kim *et al.*, 2021; De Souza *et al.*, 2022; Volpato *et al.*, 2022; Terrier *et al.*, 2024) demonstrating their potential to reduce fuel consumption, overall costs, and environmental impacts.

The design of polygeneration systems involves synthesizing plant configurations and managing the operation of installed technologies. After design, a significant challenge is the cost allocation of energy flows within optimal configurations, considering complexities such as different fuels, multiple products, various technologies, and thermal energy storage (TES). A thermoeconomic analysis enables a comprehensive understanding of the cost formation process, assessing economic implications of changing energy demands or device operating conditions. For instance, the work developed by Lozano, Carvalho and Serra (2009), investigated a trigeneration system integrated with the electric grid. Their study identified optimal operational modes using a linear programming model and explained the cost formation process of internal energy flows and final products through marginal cost analysis. Based on the work of Lozano, Carvalho and Serra (2009), the implementation of TES to the trigeneration system was explored by Pina, Lozano and Serra (2017). Their work also used a linear programming model and thermoeconomic analysis to evaluate the trigeneration system's operational strategy by means of the marginal cost analysis. Such study demonstrated how TES introduces a temporal dimension to the cost allocation problem, i.e., how TES can support the optimization of energy consumption by decoupling production and demand periods.

### **1.2.2 Identification of the research problem**

Despite the important developments achieved in the field of polygeneration systems applied to residential/commercial/public buildings, there are crucial aspects that still need to be explored. The complexity of designing polygeneration systems for buildings is intensified when considering energy interconnections between them, not only through a local electricity grid, but also through a district heating and cooling network that facilitates thermal energy sharing. Addressing this challenge requires interdisciplinary approaches to accommodate the multifaceted nature of the problem, such as the

involvement of diverse energy resources, multiple energy products, an array of technology alternatives, and distinct operation periods. Furthermore, in the context of polygeneration systems with a high level of process integration, the issue of cost allocation and marginal cost analysis assumes a higher level of complexity. Thus, in the context of cost allocation, assigning resources to internal flows and final products becomes an especially complex task. When the focus is shifted to studies about energy communities, they generally present the following characteristics: (i) tend to focus on one type of energy sharing: electricity or thermal energy (Buoro, 2013; Barroco Fontes Cunha *et al.*, 2021; Musolino *et al.*, 2023; Trevisan, Ghiani and Pilo, 2023), and (ii) consider a limited number of technologies (Asim *et al.*, 2020; Edtmayer *et al.*, 2021; Calise *et al.*, 2022; Jebamalai, Marlein and Laverge, 2022). In the context of marginal cost analysis, several previously referred works have been developed for simple polygeneration systems. However, to the best of our knowledge, it has not been developed yet to a complex polygeneration system containing central and distributed energy supply systems highly interconnected.

Finally, the role of energy communities, powered by polygeneration systems, in the economic and environmental aspects of a future low-carbon energy system scenario has not been evaluated in the literature, especially for the case of the Italian energy system.

It is important to state that the starting point of the research developed within the present thesis is the optimization model of a distributed generation energy system developed in the PhD thesis of Dario Buoro (Buoro, 2013). He developed a comprehensive work which allowed the design of a polygeneration system to a district heating and cooling network (DHCN), applied to a case study of a small town city center in the northeast of Italy.

Therefore, the aim of this thesis is to address the abovementioned research gaps by (i) updating and expanding the optimization model developed by Buoro (2013) to design and optimize an energy community powered by polygeneration systems and sharing not only heating and cooling among its members, but also purchased electricity (from the electric grid) and self-produced electricity, (ii) developing a thermoeconomic analysis through the marginal costs interpretation of each internal energy flow and final product for the entire energy community, (iii) proposal of a methodology to evaluate and interpret marginal costs when there is thermal energy transfer through heating and/or cooling pipelines

(DHCN) in the optimal solution of the energy supply system, and (iv) evaluate the role of such energy communities in the economic and environmental aspects of a future energy system scenario with a high level of renewable energy deployment. With this, it is expected that the work developed in this thesis can provide a deeper understanding about the integration of polygeneration system in an energy community, new insights to better understand the optimal operation of the whole system, and an idea about potential benefits for the Italian energy system.

## **1.3 Objectives**

In order to provide a better understanding of the main goals of the work, the objectives of this thesis are divided into general and specific.

### **1.3.1 General**

The general objective of this PhD thesis is to advance the understanding and development of a sustainable and efficient integration of polygeneration systems into energy communities through a comprehensive optimization of their energy systems. Such knowledge advancement rests over three main pillars: (i) development of a mathematical model which constitutes an effective tool to optimally design and operate polygeneration systems integrated into energy communities; (ii) adoption of a thermoeconomic analysis, aiming to provide an optimal operational strategy and quantify the consequences of dynamic changes (such as on the energy demand and/or on the technologies' performance) in the complex framework of energy communities powered by polygeneration systems; and (iii) evaluation of the role that such energy communities can play in the economic and environmental aspects of a future Italian energy system scenario with a high level of renewable energy deployment.

### **1.3.2 Specific**

Based on the presented background and context and the discussed problem statement, the following specific objectives are established in order to cover the identified research gaps:

- Update and expand the optimization model developed by Buoro (2013) to design and optimize an energy community dealing, at the same time, with a district heating and cooling network (DHCN) of pipelines connecting the buildings, a

central unit to support the buildings, thermal and cooling storage, management and distribution of self-produced and purchased electricity among the buildings and between the EC and the national electric grid, integration of solar technologies, hourly electricity purchase price, hourly electricity selling price, and hourly CO<sub>2</sub> emissions factors.

- Perform a single-objective optimization detailing the optimal (i) polygeneration system structure of each building, (ii) DHCN pipeline's structure, (iii) central unit structure, and (iv) technologies operation with all energy flows within each building, through pipelines, and within the central unit.
- Develop a multi-objective optimization presenting a range of trade-off solutions through which it is possible to have important pieces of information about installed capacities, structure for the DHCN pipelines, total annual costs and CO<sub>2</sub> emissions, cost of moving from one solution to another, and cost of choosing a more environmentally friendly solution.
- Implement an analysis and interpretation of the hourly marginal costs of the highly integrated polygeneration system, applied to the energy community, and supported by (i) TES, which decouples energy service production from consumption (it becomes relevant knowing not only the amount of energy produced, but also the time at which it took place), (ii) the incorporation of DHCN pipelines, which adds a new difficulty level, i.e., besides the necessity of knowing the amount and time in which the energy production took place, it becomes also necessary to know in which building it took place, and (iii) the management and sharing of purchased and self-produced electricity among members, i.e., the management of the electricity connections among buildings and between the energy community and the main electric grid.
- Delineate different marginal paths (energy production pathways with the lowest marginal cost) through (i) advanced and delayed energy services production, thanks to the implementation of TES, (ii) simultaneous service production, and (iii) remote energy services production, due to the implementation of DHCN pipelines.

- Implement the local optimization of energy systems into the global Italian energy system in order to evaluate the role of such energy communities in the economic and environmental aspects of a future Italian energy system scenario with a high level of renewable energy diffusion.

## 1.4 Thesis structure

Besides the present introductory chapter, the structure of the thesis is divided into five chapters.

Chapter 2 discusses the methodology through the presentation of the research framework. The chapter provides an overview about the optimization process of energy systems by discussing four main steps. The first step discusses the importance of defining the energy supply system's superstructure by taking into account the boundaries of the problem, the type of technology (generation, transformation, and storage), and the interactions among them. The second step regards the critical role owned by the data collection and analysis phase since the quality of data directly affects the integrity and credibility of the results. The third step concerns the translation of all gathered information into a mathematical model which represents the characteristics and performance of all technologies, the desired detail level, and the optimization criteria. Finally, the fourth step regards the calculation of an optimal solution for the energy supply system by solving the mathematical model.

Chapter 3 presents the development of the multi-objective optimization model, based on the MILP method, for an energy community (EC) consisting in a group of nine buildings plus a central unit sharing electricity, heating, and cooling among each other. The EC buildings (from tertiary sector) are located in the city of Pordenone, northeast of Italy, and one of the main objectives of the model is the integration of cogeneration systems and renewable energy technologies in order to reduce overall annual costs and CO<sub>2</sub> emissions. In fact, the objective functions are the total annual cost (related to maintenance, investment, and hourly operation) and total annual CO<sub>2</sub> emissions (related to the hourly operation). As a preliminary step, this chapter presents the superstructure for both the buildings and central unit, the gathering of the input data, the mathematical model, and the reference case scenario. In accordance with the objective function, the results from the model indicate the optimal (i) energy supply system structure within each building,



(ii) hourly operation of each technology, (iii) connections between buildings in terms of DHCN pipelines, (iv) distribution (among the building) of self-produced electricity and electricity purchased from the grid, and (v) energy supply system structure and hourly operation for the central unit.

Chapter 4 develops a thermoeconomic analysis of the energy community through the analysis and interpretation of the hourly marginal costs related to each energy flow and final product. Such analysis and interpretation allow the obtention of insights that the optimization developed in chapter 4 cannot provide. The mentioned insights regard mainly the determination of the optimal operation of the system when the energy demand of a given building is increased. As already discussed in the literature (Pina, Lozano and Serra, 2017), the consideration of TES decouples energy service production from consumption, i.e., it becomes relevant knowing not only the amount of energy produced, but also the time at which it took place. Besides considering TES, the incorporation of DHCN pipelines adds a new complexity layer, i.e., besides the necessity of knowing the amount of energy and time in which the energy production took place, it becomes also necessary to know (i) in which building such energy production took place, (ii) what is the related marginal path, and (iii) the reasons why some paths are more expensive than others. These points constitute the main contributions from this chapter. The results are presented by dividing the marginal cost values by energy service type (electricity, heating, and cooling) and building.

Chapter 5 is developed with the aim of answering a research question by using the thermoeconomic local optimization (LO) methodology. Considering all the research work developed in chapters 3 and 4, the research question is: *what the role of ECs (such as the case study of this thesis) in the economic and environmental aspects of a future Italian energy system scenario with a high level of renewable energy deployment could be?* In order to answer the question, three main elements will be considered: a local subsystem, a global system, and the abovementioned methodology. The local subsystem will be the EC (or a group of ECs) while the global system will be the Italian national energy system (NES). The results demonstrated the potential that a reasonable deployment of ECs has to promote even further the usage of more efficient energy conversion technologies in the Italian NES with a tendency of decreasing the total primary energy supply.

Chapter 6 presents a synthesis with the main results and conclusions obtained from the development of the work, the main contributions provided by the thesis, and suggestions for future work developments.

Chapter 7 lists all the references used throughout the text.

Appendix A provides detailed information about the buildings and adopted technologies.

---

*CHAPTER 2 – Synthesis of  
Optimized Energy Systems: An  
Overview*

---



## **CHAPTER 2 – Optimization and Thermoeconomics of Energy Systems**

### **2.1 Synthesis and Optimization of Energy Systems**

One of the most fundamental problems that energy supply systems aim to solve is the alignment between the different energy demands of a consumer center, the available energy resources (renewable and non-renewable) and the most appropriate energy conversion technologies converting the energy resources into the required energy services. There are indeed several ways to arrive at solutions for such a problem. At the country level, for example, there are different types of energy supply systems (or power plants) with characteristics that will vary depending on the primary energy source, i.e., coal, diesel, natural gas, hydroelectric, solar, wind, etc. However, to derive effective and efficient solutions, each case should be carefully assessed, considering, among others, the intrinsic characteristics of the country (for the sake of this example), accurate energy profiles demand data along the year, the availability of local primary energy resources, or the technical and economic data of the available energy resources and technologies. This simple example illustrates some relevant aspects that should be considered in the development of a mathematical model representing a given problem dealing with the complex problem of addressing the optimal synthesis and operation of energy supply systems.

#### **2.1.1 Research framework**

Optimal synthesis and operation models, aiming to provide feasible and optimal solutions for an energy supply system, can be applied not only at the country level but also at any desired scale, including regions, cities, neighborhoods, buildings, and even individual homes. Polygeneration systems refer to the combined production of electricity, heat, cold and any other useful products such as potable water, dry air, biofuels and/or synthetic fuels, among others, thanks to an efficient energy process integration. Such systems can comprise a variety of technologies, such as combined heat and power (CHP) systems (e.g., internal combustion engines and gas turbines), absorption chillers, solar panels, and

energy storage systems to meet the diverse demands of different consumers. However, it is not always necessary to incorporate all these technologies in every case; rather, their selection should be determined through an optimization process.

The expression “their selection” is actually a strong simplification of the mentioned optimization process. In reality, this process involves the decision of whether a given technology should be installed in the energy supply system, as well as determining the optimal size of such technology, the number of units to be installed, and their operating strategies (Pina, 2019). Therefore, in order to identify the optimal design of energy supply systems, several aspects including different feasible alternatives (feasible combinations of different technologies) need to be considered and compared.

This is when combinatorial optimization comes into place, i.e., it solves the optimization problem through the comparison of different technically feasible alternatives characterized with a certain number of “aspects” (or variables), the so-called discrete variables (Baños *et al.*, 2011). When it comes to the combinatorial optimization of energy supply systems, it is necessary to tackle two essential problems: the synthesis of the system (i.e., defining number and size of each installed technology) and the operational strategy (such as the technology operation status, buying/selling electricity decision, etc.) (Lozano, Carvalho and Serra, 2009). For existing facilities, the focus of these aspects is solely to the operational strategy. However, for new facilities, both issues (synthesis and operation) are interconnected. Moreover, from a design standpoint, if the capacity of the technology is set lower than the required energy demand, the system might struggle to meet peak-hours. Conversely, if the capacity greatly exceeds the optimal level, the economic viability of the system could be compromised due to heavy investment expenses (Liu, Georgiadis and Pistikopoulos, 2013).

In order to solve synthesis and operation problems regarding energy supply systems, the optimization models might deal with a huge number of variables (both continuous and discrete). These can be related to the system itself and its boundaries (Pina, 2019), as well as to the decision variables (Buoro *et al.*, 2011). Variables related to the system itself can include energy demands, available energy resources and their purchase prices, capital costs of technologies and their technical parameters, and local weather data. At the same time, decision variables might include the number of technologies that need to be installed

(as well as their sizing), the hours of operation of these technologies, management of energy flows, and the amount of purchased (or sold) electricity from (to) the electric grid in a specified time period, e.g. each hour.

Mathematical programming emerges as a powerful problem-solving method to deal with such complex optimization models. It uses mathematical techniques to optimize decisions and find the most suitable solution, given certain constraints. Due to its rigorousness, flexibility, and extensive modeling capability (Floudas and Lin, 2005), the mixed integer linear programming (MILP) became one of the most suitable mathematical techniques to deal with optimization models comprising both continuous and discrete variables. MILP models embrace the niceties of the design challenge through the utilization of both binary and continuous variables. The former variables account for various potential alternatives in energy supply systems configuration and operational approaches, whereas the latter can represent, for instance, the energy flows, economic factors, and environmental aspects (Casisi, Pinamonti and Reini, 2007; Buoro *et al.*, 2010).

Grounded in the principles of mathematical programming techniques (such as MILP), the superstructure-based optimization approach plays a crucial role in enabling a comprehensive evaluation of numerous alternative configurations (Umeda, Hirai and Ichikawa, 1972), as it is the case of energy supply systems optimization. The superstructure-based approach involves four main consecutive phases (Pina, 2019; Mencarelli *et al.*, 2020):

- **Definition of a superstructure**, which captures the set of all feasible alternative structures, given the energy resources and energy demands.
- **Data collection and analysis**, which constitutes a crucial part of the whole optimization process, i.e., the inputs.
- **Translation of the superstructure into an algorithm**, which will establish the optimization model.
- **Calculation of an optimal structure** by solving the optimization model.

### 2.1.2 Definition of a superstructure

In the initial synthesis stage, defining the energy system's superstructure is fundamental. This structure comprises possible technologies and their interconnections, personalized to meet the due energy demand. Then, after the optimization process, the superstructure is updated to an optimal form containing the layout of the optimized energy supply system consisting of the pieces of installed equipment (model, size, and number of pieces) as well as their interconnections. A clear superstructure definition provides the optimization model with essential data for identifying optimal technology combinations and interactions (Gong and You, 2015; Mencarelli *et al.*, 2020). On the contrary, an imprecise representation yields suboptimal solutions, which could technical and economically compromise the project. Additionally, the superstructure must address a balance between the number of technologies and optimization complexity since one of the main trade-offs lies between technology variety and computational effort (Klotz and Newman, 2013).

The superstructure complexity can be simplified by defining specific conditions that express the boundaries of the problem. Such conditions comprehend the required energy demands and the accessible energy resources. Energy demands refer to the profile of the consumer energy needs along the time, such as electricity, domestic hot water, space heating, and cooling, whereas energy resources include local renewables, fossil fuels, and grid electricity. Once the energy demands and available resources have been defined, both the amount of each one as well as their distribution along the time, the technologies can be selected considering their characteristics when interacting between them. These characteristics include their types of inputs and products, operation modes, temperature levels, and how they can cooperate to make better use of resources.

Three primary technology categories can be highlighted within the energy system landscape: generation, transformation, and storage technologies (Pina *et al.*, 2020). Generation technologies comprises processes that convert energy resources into intermediate or final products, e.g., internal combustion engines, gas turbines, boilers, photovoltaic panels, or solar thermal collectors. Transformation technologies, in contrast, convert energy resources or intermediate products into final products, e.g., absorption chillers, mechanical chillers, or heat pumps. Lastly, energy storage technologies play a crucial role in preserving energy services produced by generation and transformation



technologies. Examples include hot water storage tanks, chilled water storage tanks, ice storage, electric batteries, and Carnot batteries.

The importance of the interaction between the mentioned technologies, i.e., the synergies among them have been highlighted in several works throughout literature (Ng, Zhang and Sadhukhan, 2013; Comodi *et al.*, 2019; Pina *et al.*, 2020; Pina, Lozano and Serra, 2021; Pinto, Serra and Lázaro, 2022) since they can supply crucial information when selecting technologies for a given energy supply system. For instance, some technologies can supply the very same energy product and, for this reason, compete between each other to attend the same energy demand (e.g., solar thermal panels and boilers). However, at the same time, the redundancy in energy systems supply is extremely important in order to provide a good system reliability level. Energy cascading is another important practice when it comes to the interaction between polygeneration systems (Gao *et al.*, 2008; Wu *et al.*, 2017; Bose *et al.*, 2022), since the product of a given technology can be used as the fuel of another. In addition, the integration of energy storage units (whether it is thermal- and/or electrical-based) adds the benefit of the mismatch between the energy production and the energy consumption, which is vital for the increasing incorporation of renewable energy sources (De Souza *et al.*, 2022; Nadalon *et al.*, 2023). Furthermore, if a given analysis will be performed to evaluate an energy supply system for long periods (months, years, etc.), the operation mode of some technologies should also be taken into account, as it is the case of heat pumps (cooling mode for summer and heating mode for other periods of the year) and solar collectors (during summer, the higher temperatures can drive an absorption chiller, whereas during the other periods of the year they can attend the heating demand).

Figure 2.1 generically illustrates possible ways through which polygeneration technologies can transform energy resources into useful products to meet the due energy demands (without considering the different temperature levels within an energy supply system). As highlighted by Pina (2019), thermal energy flows under different temperature levels should not be overlooked since they are produced/consumed by different technologies, as it is, in fact, evaluated throughout literature for different applications (Kasaeian *et al.*, 2020; Bellos and Tzivanidis, 2021). This imposes additional constraints to the energy system modeling that should be tackled through specific process integration techniques.

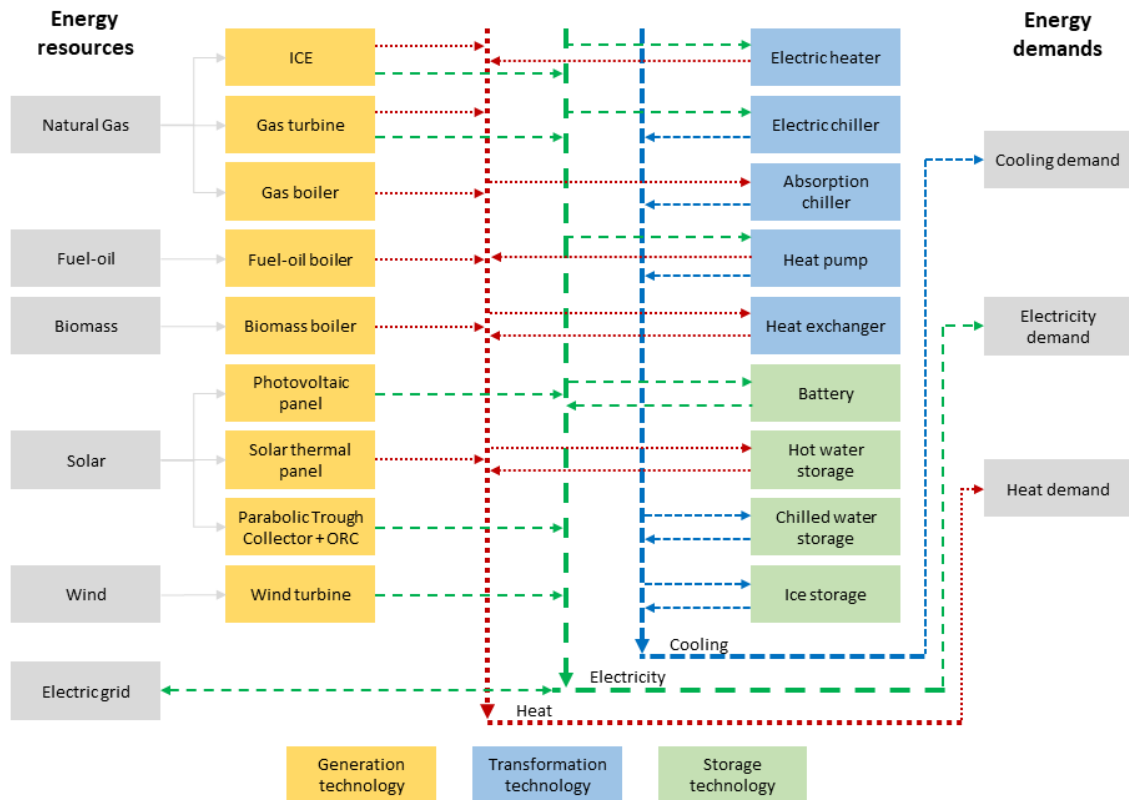


Figure 2.1– Interactions among polygeneration systems including energy resources, technology types, and demanded energy services for a typical building. Source: own elaboration.

Among the generation technologies, the CHP owns a critical role in determining the superstructure. For instance, as revised by De Souza et al. (2021), the different heat products (at different temperature levels, including exhaust gas and jacket water) derived from an internal combustion engine, can be used for different applications including space heating and feeding thermally activated technologies (TATs). Such fact will determine the presence or absence of other technologies in the superstructure. In any case, it is important to pay close attention to the thermal and power load profiles of the consumer (as well as the required temperature levels) and to the energy demand required by both the consumer and other technologies (TATs).

### 2.1.3 Data collection and analysis

This step has a crucial role in the modeling process for the synthesis and optimization of energy supply systems since the quality of the data directly affects the integrity and

credibility of the resulting outcomes. Once the superstructure of the system is defined, the subsequent phase involves searching and collecting specific data according to the superstructure composition and its boundaries. Such collected data will be the input information for the optimization model. This information can be obtained from several sources including literature, utilities supply companies, datasheets from manufacturers, experimental or simulation studies, and official government reports (Pina, 2019).

The gathered set of information must comprise a good representation of both the energy supply system and the consumption unit, encompassing attributes such as:

- the energy demands of the consumption unit,
- the local available renewable and non-renewable energy resources,
- technical specifications of technologies within the superstructure,
- local weather data,
- legislation concerning environmental issues and grid connection, and
- other potential constraints such as specific characteristics of the consumption unit.

Furthermore, the data should be aligned with the analysis criteria, i.e., it should incorporate economic and environmental aspects concerning equipment manufacturing, installation, and system operation, when economic and environmental criteria are considered.

One of the most important and fundamental pieces of data is the demand profile of the consumption unit. With the demand profile, one can guarantee that the designed energy supply system is optimized specifically for its intended use. When it comes to consumption centers in the design phase, obtaining demand profiles is more complicated and may involve the utilization of specific estimation methods or simulation software. Conversely, for already-existent consumption centers, the energy demand profiles can be obtained through data acquisition systems or directly from the consumption unit manager.

### 2.1.3.1 Modeling temporal resolution and technology detail level

When it comes to energy system optimization, and particularly in the synthesis of optimized energy supply systems, defining the temporal resolution of analysis and the level of detail in the optimization model are crucial considerations. These choices significantly impact the accuracy and reliability of the obtained results (Hoevenaars and Crawford, 2012; Shirizadeh and Quirion, 2022).

The temporal resolution determines the granularity of the analysis, such as daily, hourly, or even minute-based intervals. Higher temporal resolution provides more accurate results but demands increased computational effort. For instance, hourly periods are frequently used for optimization studies (Limpens *et al.*, 2019; Bogdanov *et al.*, 2021; Borasio and Moret, 2022), however one should bear in mind that this may lead to computationally heavy models, especially for year-long simulations. For this reason, balancing computational efficiency with model accuracy is a critical challenge. To address this, researchers often employ the concept of representative days (Casisi *et al.*, 2019; Limpens *et al.*, 2019; De Souza *et al.*, 2022). By assuming that days within a certain period share similar characteristics in terms of energy demand, prices, and climatic conditions, computational complexity can be reduced. However, this approach introduces a trade-off between computational efficiency and model fidelity.

Another dimension of model detail concerns the description of technology performance. Many technologies used in polygeneration systems present variances in their performance behavior depending on load and ambient conditions (Urbanucci, Testi and Bruno, 2018; Nadalon *et al.*, 2023). A highly detailed description of those varying performances introduces nonlinear equations to the optimization models that can significantly increase computational effort. Generally, the technology descriptions are simplified in order to optimize efficiently, although this may compromise result accuracy.

### 2.1.3.2 Use of representative days

As stressed in the previous section, handling a high temporal resolution can be computationally intensive when it comes to the synthesis of optimized energy supply systems, especially when binary variables are involved. A commonly employed solution to this challenge is the concept of representative days, which assumes that days within a

specific period share similar characteristics. By doing so, the computational effort is substantially reduced without losing essential information (Borasio and Moret, 2022). Such solution makes the optimization process feasible for large-scale energy supply systems and extensive simulation periods.

The use of representative days for the optimization of energy supply systems enhances efficiency, however it introduces a trade-off with result accuracy. The assumption that all days within a period are equivalent introduce errors that, depending on the assumptions, can set the results away from a more-accurate scenario (Shirizadeh and Quirion, 2022). At the same time, there are some factors such as seasonal energy storage, variable and irregular along the time (stochastic) renewable energy sources (such as wind), and real-time electricity prices that are hard to fit into the solution of representative days. Therefore, reaching the right balance between computational efficiency and result accuracy remains a key consideration.

As already explained, the use of representative days is a valuable tool to reduce the computational effort derived from energy supply systems optimization. However, some challenges must be addressed in order to harness the benefits of such approach. For instance, the intermittent behavior of renewable energy sources and the incorporation of energy storage might be examples of the challenges that must be addressed (Pinto, Serra and Lázaro, 2020). Thus, when the considered representative days are not sequential in time, it is not possible to consider periods of energy storage longer than the extension of the typical day.

It is possible to find several approaches in literature dealing with the problem of defining representative days. For instance, Poncelet et al. (2017) stated the main difficulties when selecting representative days: (i) the computational cost and complexity of analyzing all possible combinations, especially for a high-resolution data; (ii) the lack of a consistent criterion to evaluate the representativeness of the selected days; (iii) the absence of optimization-based approaches in the field of energy systems research. Domínguez-Muñoz et al. (2011) presented a method to reduce a whole-year time series data to a few representative days that preserve important characteristics such as peak demands, duration curves, and temporal relationships between different demand curves (power, heating, and cooling). The main challenges found by them are the requirement of a trade-

off between accuracy and computational effort, the subjectiveness often employed in the definition of representative days, and the variability of the demand data, which depends on factors such as weather, occupancy, and market conditions. In the work conducted by Park and Jun (2009), they proposed an algorithm for K-medoids clustering in order to reduce computational effort. According to them, their novel approach considers both energy and peak demands as well as the temporal connection between the different types of demands, which are some of the difficulties encountered by them when selecting typical days. Pinto, Serra and Lázaro (2020) developed a new method for the selection of representative days by combining the k-Medoids and the method developed by Poncet et al. (2017) OPT methods, taking the advantage of both methods.

### *2.1.3.3 Economic and environmental data*

Every optimization process relies on specific criteria, typically encompassing economic, environmental, and/or energy efficiency considerations. Once these criteria are chosen, defining a quantifiable measure for the objective function of the model becomes imperative. For instance, objective functions aligning with these criteria might include economic considerations (e.g., total annual cost, and profit), environmental concerns (e.g., total annual pollutant emissions or emissions reduction), and energy efficiency aspects (e.g., primary energy consumption or primary energy savings) (Rong and Su, 2017; Pina, 2019). Thus, the character of the analysis depends on these criteria and their corresponding objective functions, necessitating data collection that mirrors these choices. For instance, a total annual cost objective function usually comprises a fixed component encompassing equipment investment and maintenance costs (capital cost), alongside a variable aspect accounting for system operation costs (fuel and electricity purchases, and electricity selling revenues).

When an optimization model incorporates two or more criteria, it's crucial to ensure that all elements receive equivalent attention to detail. In the context of energy design combining economic and environmental considerations, this implies that economic data should align with their environmental counterparts and vice versa. This proves to be a challenging task, as acquiring or identifying such information is not always straightforward. Consider the purchase of electricity from the grid, which is typically subject to time-of-use tariffs wherein prices fluctuate according to the time of day and

month of the year. Consequently, environmental data should also incorporate CO<sub>2</sub> emissions linked to grid electricity on an hourly basis. However, while hourly electricity prices are readily available, associated hourly CO<sub>2</sub> emissions data is often elusive. Some countries such as Spain, for instance, make the hourly CO<sub>2</sub> emissions (from electricity production) available online (REE, <https://www.ree.es/es>). For other countries such as Italy, for example, the hourly CO<sub>2</sub> emissions from electricity production is not available.

#### **2.1.4 Translation of the superstructure into a mathematical model**

After defining the superstructure and collecting the necessary data, the next step is the translation of all this information into an algorithm, or mathematical model. Such model should represent the characteristics and performance patterns of all components of the superstructure, according to the desired detail level and optimization criteria. The later will define the aim of the optimization through an objective function, which is set to be minimized or maximized.

As explained in the section Economic and environmental data, the objective function can be based on different optimization criteria such as economic, environmental, or energy efficiency. Such optimization model is called single-objective optimization (SOO) model, as the optimal solution relies only on one criterion (e.g., the optimization procedure applied by De Souza et al. (2022)). However, there is also another modality of optimization models called multi-objective optimization (MOO) models, which allows the optimal solution to rely on two or more criteria (De Souza *et al.*, 2023).

As introduced in section 2.1.1, in the realm of optimization problems, a first classification can be done by dividing the problems in terms of continuous and discrete variables. According to Biegler and Grossmann (2004), such division can be further subdivided into linear programming (LP) and non-linear programming (NLP) (for continuous variables), and mixed-integer linear programming (MILP) and mixed-integer non-linear programming (MINLP) (for discrete variables), with the general formulation presented from Equations (2.1) to (2.4) (Yokoyama, Hasegawa and Ito, 2002; Biegler and Grossmann, 2004). Figure 2.2 illustrates the classification of the optimization problems according to the type of the involved variables.

$$\min f(x, y) \quad (2.1)$$

$$h(x, y) = 0 \quad (2.2)$$

$$g(x, y) \leq 0 \quad (2.3)$$

$$x \in X, y \in \{0,1\} \quad (2.4)$$

Equation (2.1) represents the objective function, Eq. (2.2) can describe the performance of systems, energy balances, production rates, etc., and Eq. (2.3) presents to the model the boundaries of the optimization, i.e., the constraints to which the model is restricted, such as capacity limits and number of components allowed to be installed. Equation (2.4) indicates that  $x$  represents continuous variables, while  $y$  denotes binary variables.

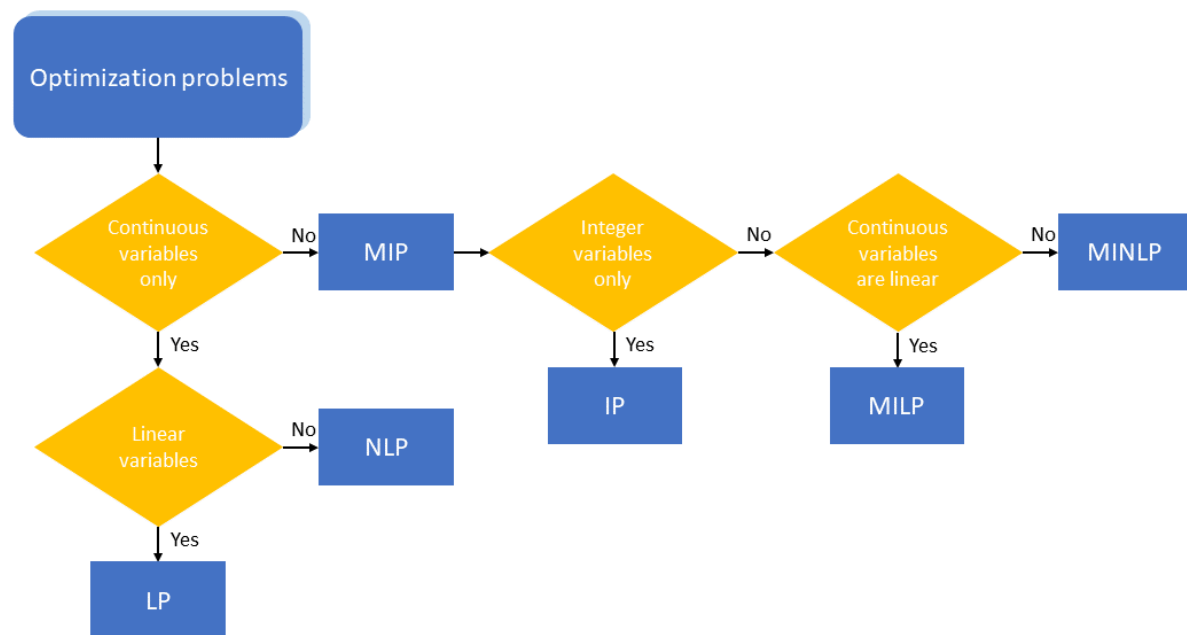


Figure 2.2 – Optimization problems classification. Source: own elaboration.

For the case of synthesis and optimization of supply energy systems, one of the main methodologies that has been used by researchers is the MILP method, which is a special case of the MIP (mixed-integer programming) method (see Figure 2.2) (Biegler and Grossmann, 2004). For instance, in the work developed by Miguel A. Lozano et al. (2009), a MILP model was built to determine the capacity, number, and type of cogeneration units for a project involving tertiary sector buildings. With the minimization of the total annual costs as the objective function, their model has also the feature of



defining (in hourly resolution) the optimal operation mode of the energy supply system throughout a whole year. In literature, it is possible to find many other types of applications for the MILP methodology, such as on the oil & gas sector (Méndez *et al.*, 2006; Zhang and Hua, 2007; Zhang and Rong, 2008) to define, for example, operation and maintenance strategies, on renewable energy supply sector (Pezic and Cedres, 2013; Lamedica *et al.*, 2018; Zare *et al.*, 2018) to optimize, for instance, the triad generation-storage-demand, and on the chemical industry sector to address the water and energy stream distribution on a pulp and paper process (Kermani *et al.*, 2017), to find the optimal layout for process plant storage vessels (de Lira-Flores, Gutiérrez-Antonio and Vázquez-Román, 2018), and to optimize the pipe arrangement in a chemical industry plant (Wu and Wang, 2017). In summary, the MILP methodology has demonstrated its adaptability and effectiveness across various fields.

The MILP method can be defined as an operations research method consisting in maximize or minimize a given objective function subjected to input parameters, continuous, integer and/or binary variables, and several constraints (Haeseldonckx and D'haeseleer, 2011). Such method is frequently used in the field of process integration (Becker and Maréchal, 2012) and to analyze and optimize large and complex systems (Kantor *et al.*, 2020).

According to A Floudas (1995), the general formulation of MILP models is defined through the Equations (2.5) to (2.8).

$$\min \quad cx + dy \tag{2.5}$$

$$\text{Subject to} \quad Ax + By \leq b \tag{2.6}$$

$$x \geq 0, x \in X \subseteq \mathfrak{R}^n \tag{2.7}$$

$$y \in \{0,1\} \tag{2.8}$$

Equation (2.5) represents the linear objective function, which is subjected to a set of constraints represented by Eq. (2.6). Letters  $c$  and  $d$  in Eq. (2.5) represent vectors of parameters that can hold, for instance, input performance data of equipment, while letters  $x$  and  $y$  represent, respectively, a vector of continuous decision variables and a vector of binary decision variables. In Eq. (2.6), letters  $A$  and  $B$  represent matrices which dimension

will depend on the problem under analysis, whereas  $b$  represents a vector of inequalities. Letter  $X$ , in Eq. (2.7), represents a continuous variables subset and  $n$  represents the number of continuous variables.

### 2.1.5 Calculation of an optimal structure

After having defined the superstructure of the energy supply system, the details concerning the data collection phase (temporal resolution, representative days, and optimization criteria) and the mathematical model describing the superstructure, the next step is the calculation of an optimal solution for the energy supply system by solving the MILP-based algorithm.

As introduced in section 2.1.3.3, the search for such optimal solution can be based on a single objective optimization (SOO) model or on a multi objective optimization (MOO) model. However, several works in literature have highlighted the importance of bear in mind crucial differences between both. For instance, Pina (2019) states that the mathematical optimal solution from SOO models deviates from the real-world optimal solutions due to aspects such as the impossibility of identify and introduce all the constraints that will influence the system configuration and the fact that a mathematical model cannot perfectly represent every single aspect of a real-world problem. According to Cohon (1978), the consideration of a MOO model can provide substantial improvements in the problem-solving process, such as: (i) well-defined roles for people working in the decision-making process, i.e., the analyst (or modeler) takes care of defining alternative scenarios for the problem, whereas the decision maker takes advantage of such pieces of information to take informed decisions; (ii) wide range of different scenarios; (iii) closer-to-reality models when more than one objective is considered. Therefore, the consideration of more than one objective can be a solution to overcome the strict optimal solution from SOO models by providing different scenarios based on multiple factors, which can lead to the obtention of meaningful insights rather than numbers representing a very specific condition (Frangopoulos, Von Spakovsky and Sciubba, 2002; Savic, 2002; Voll *et al.*, 2015; Uniyal, Pant and Kumar, 2020).

This was exemplified in studies conducted by Casisi *et al.* (2019) and De Souza *et al.* (2023), where a Multi-Objective Optimization (MOO) approach was employed. The

objective was to minimize both total costs and emissions in a district heating and cooling network situated in a northeast Italian city. Their investigation revealed that, with a relatively marginal rise in total costs, there could be a substantial reduction in the overall CO<sub>2</sub> emissions of the system. Similar findings were reported by Pinto, Serra and Lázaro (2022), who focused on the integration of polygeneration systems in the residential sector of Zaragoza, Spain. Employing a MOO-based approach, they concluded that noteworthy reductions in emissions could be achieved with a relatively modest increase in costs, given the current available technology.

Indeed, real-world problems are rarely based on only one criterion such as the interaction between economic and environmental aspects in designing sustainable energy systems. Instead, such kind of problems involves several conflicting objectives. This requires the application of a MOO approach, which considers multiple objective functions. However, while numerous objective functions can help on evaluating energy systems, increasing the number of objectives complicates the optimization model. Therefore, balancing model accuracy and computational effort is essential. Additionally, the choice of the objective function significantly impacts optimization results, even for the same criterion as economic costs, where different objective functions, such as total annual cost, net present value, or profits, yield distinct outcomes.

As mentioned before, there is no single optimal solution when using a MOO model; instead, it offers a range of trade-off solutions, so that decision-makers are able to determine the best among them, according to their interests. Then, in order to help the decision-taking process, the concept of "dominance" is used to identify suboptimal solutions, which, ultimately, leads to a set of non-dominated solutions (Alarcon-Rodriguez, Ault and Galloway, 2010) (known as Pareto-optimal solutions) where no improvement in one objective comes without losing something in the other one (Figure 2.3).

Analyzing Figure 2.3 (left), it is possible to observe the main details of the MOO approach. The main function under analysis is  $F(x)$ . This could be a function depending on multiple other functions. However, for the sake of the illustration, it depends only on the functions  $g_1(x)$  and  $g_2(x)$ . As indicated in the figure, the optimal  $g_1(x)$  solution is the point where  $g_1(x)$  function reaches its minimum value and  $g_2(x)$  its maximum value (and

vice-versa). The other solutions, along with the Pareto front, represent trade-off solutions, i.e., solutions where it is still possible to benefit from lower  $g_2(x)$  values by giving up an acceptable value for  $g_1(x)$  (and vice-versa). Then, the feasible and infeasible regions represent, respectively, a region of possible (but non-optimal) solutions and a region of non-possible solutions (where the system's boundaries would be exceeded).

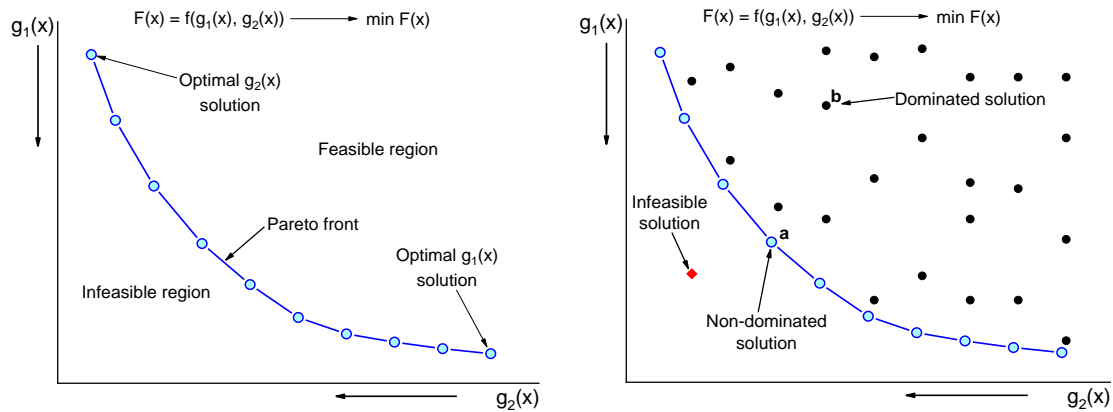


Figure 2.3 – Pareto front diagram indicating feasible and infeasible regions, optimal solutions for  $g_1$  and  $g_2$  functions (left); dominated and non-dominated solutions (right). Source: own elaboration.

Figure 2.3 (right) illustrates the concept of “dominance” to identify the optimal and sub-optimal solutions. As observed, there are two named solutions in the feasible region: a non-dominated (solution **a**) and a dominated one (solution **b**). According to such a concept, solution **a** dominates solution **b** if (i) **a** is no worse than **b** in all objective functions and (ii) **a** is better than **b** in at least one objective function (Pina, 2019). In other words, when dealing with minimizing the objective function in MOO, if solution **a** has the same  $g_1$  value as solution **b** but, on the other hand, solution **a** has a lower  $g_2$  value than solution **b**, then solution **a** dominates solution **b** (dominated or sub-optimal solution). The same is true if solution **a** has the same  $g_2$  value as solution **b** but a lower  $g_1$  value. The non-dominated solutions represent the limit for feasible solutions, i.e., if the  $g_1$  value of solution **a**, for instance, is fixed there is no better solution with a lower  $g_2$  value. This would violate the intrinsic constraints of the system under analysis. The same is true if a similar analysis is performed by fixing the  $g_2$  value of solution **a**. Therefore, the solutions within the Pareto front are a set of non-dominated solutions.

Different methods have been used in the literature in order to solve MOO problems. One of the most common involves transforming MOO problems into a series of SOO problems. The  $\epsilon$ -constraint method, finds application in optimizing energy supply systems, as demonstrated by various authors (Alarcon-Rodriguez, Ault and Galloway, 2010; Carvalho, Lozano and Serra, 2012; Fazlollahi *et al.*, 2012; Buoro *et al.*, 2013; Balaman, 2016; Batista and Batista, 2018; Pina, 2019; De Souza *et al.*, 2023). This method optimizes the single objective function, while upper/lower bounds ( $\epsilon$ -constraints) are established for the remaining functions. The problem is iteratively solved for different  $\epsilon$  values, yielding diverse trade-off solutions comprising the Pareto front.

Efforts to identify as many Pareto-optimal solutions as possible within the Pareto front are critical for a more realistic problem representation. However, due to the impractical size of the entire Pareto front and the time-consuming nature of the  $\epsilon$ -constraint method, full identification becomes practically impossible. Consequently, it is recommended that decision-makers investigate the obtained Pareto-optimal solutions to assess different trade-off solutions and make more informed decisions.

Given the number of optimal obtained solutions, defining metrics to evaluate these solutions becomes crucial. Metrics such as marginal and average costs could be considered in this context. The marginal cost represents the cost of moving from one Pareto-optimal solution to the next one in the Pareto front, while the average cost represents the cost of moving from a specific Pareto-optimal solution to any other Pareto-optimal solution (Pina, 2019). Therefore, the mentioned metrics could serve as criteria for selecting a solution among a diverse spectrum of trade-off solutions.

## **2.2 Thermoconomics**

Thermoconomics combines thermodynamic principles with economic assessments in order to identify energy and cost-saving opportunities within energy conversion systems (Gaggioli, 1983; Lozano and Valero, 1993; Reini, Lazzaretto and Macor, 1995). In this sense, the next two sections will briefly present two of the main thermo-economic methodologies used to analyse and optimize energy conversion systems. Such methodologies are adopted in the analyses presented in chapters 4 and 5.

### 2.2.1 Marginal costs

As stated by Lozano, Carvalho and Serra (2009), the core of thermoconomics is the determination of unit costs for energy system flows and outputs, distinguishing between average and marginal costs. These cost metrics are vital for in-depth economic evaluations of energy supply systems, facilitating optimization and diagnostic endeavours. The distinction between average (unit) costs and marginal costs is fundamental in the economics of energy systems, as highlighted by Pina (2019) and Li et al. (2015). Unit costs, reflecting the average production cost of energy flows, fall short in accurately guiding optimal operations under changing conditions such as fluctuating energy demands. Marginal costs, on the other hand, calculated as the cost to produce an additional unit of energy, offer precise insights for managing and understanding system cost dynamics, facilitating more informed decision-making.

Marginal cost calculation, especially in highly integrated energy systems, presents significant complexities. Computational tools, particularly those incorporating linear programming optimization models such as FICO Xpress, have become indispensable for accurately determining marginal costs and analysing the impact of input data variations. These models yield hourly dual values for constraints, which indicate the marginal effect on the objective function. Specifically, dual values for energy balance constraints represent the marginal cost ( $\lambda$ ) of the corresponding energy demand, offering critical insights into system responses to demand fluctuations, as detailed by Reini, Lazzaretto and Macor (1995) and Lozano, Valero and Serra (1996). This approach provides a nuanced understanding of energy supply system dynamics under varying energy demand scenarios.

### 2.2.2 Local optimization

The aim of an optimization of energy supply systems is to determine the value of the independent design variables associated to the minimum consumption of resources by the entire system, given the same energy demand levels. This type of optimization can be regarded also as “global optimization”, i.e., all the subsystems comprising the energy supply system are optimized together in order to obtain a solution for the independent design variables.

The local optimization (LO) approach has the same goal, i.e., optimize the energy supply system and obtain results associated with the minimum consumption of resources by the entire system, but optimizing separately each subsystem as if they were isolated units (Reini, 1994). Once the internal costs of a given system are known, it is possible to analyze its subsystems separately. Also, the correct use of such costs allows the LO of subsystems, even for complex energy systems, which simplifies the problem since, instead of performing the optimization of an entire system, it is possible to optimize only a target subsystem (Serra, 1994). The procedure to develop a LO is better explained in section 5.1.

## **2.3 Conclusion**

Addressing the optimal synthesis and operation of energy supply systems is a critical task that aligns energy demands with suitable conversion technologies and resources. This process involves assessing detailed energy demand profiles, resource availability, and technological data, besides of being applicable to a wide range of energy supply systems scales. Polygeneration systems, integrating various technologies such as CHP systems and solar panels, are able to provide energy services to a diverse range of energy demands through efficient energy process integration. The core of optimizing these systems lies in a combinatorial process that selects and sizes technologies based on detailed information, such as energy balances, economic viability, and environmental impacts. The mixed integer linear programming (MILP) modelling method, as reviewed in this chapter, is one of the main mathematical tools for handling such complex problems. Moreover, the superstructure-based optimization approach enables the comprehensive evaluation of feasible configurations for the polygeneration system under analysis, ensuring a high efficiency standard with the lower impact in the objective function.

Thermoeconomics is another important methodology considered within this thesis. It is essential for optimizing energy conversion systems, particularly through methods such as marginal cost analysis and local optimization. Marginal costs provide critical insights for efficient system management under varying energy demands, while local optimization offers a simplified approach for subsystem improvements. Together, these methods improve understanding and decision-making in energy system optimization, paving the way for more sustainable and economical energy solutions.





---

*CHAPTER 3 – Multi-Objective  
Optimization of Energy  
Communities*

---



---

## CHAPTER 3 – Multi-Objective Optimization of Energy Communities

Based on the research framework described in chapter 2, a case study analysis is developed in chapter 3. A multi-objective optimization model is developed using the mixed integer linear programming (MILP) method to determine optimal solutions according to economic and environmental criteria. The case study is an energy community (EC) comprising nine tertiary sector buildings (plus a central unit) in the city of Pordenone, northeast of Italy, demanding electricity, heat, and cooling. Moreover, the buildings are set to (i) share heat and cooling through a set of pipelines network (district heating and cooling network – DHCN), (ii) share electricity among them through a local electric grid, which is connected to the main national electric grid, and (iii) consume only natural gas and solar energy as local resources.

The nine EC buildings are: Town hall, Theater, Library, Primary school, Retirement home, Museum, Hospital, Secondary school, and Swimming pool. The EC model was developed to design the structure and operation of the polygeneration system and DHCN pipelines for each building individually, as well as the local electric grid. The design of the structure means the installation (or not) of a given equipment, whether it be a component of a given building or a pipeline (heating and/or cooling) connection between two buildings. The operation design corresponds to the on/off operation status for the set of installed equipment. Both the structure and operation are defined through binary variables, while the other variables such as energy, economic, and environmental flows, are defined through continuous variables.

The model is also based on dynamic operation conditions, i.e., the production of energy services is optimized according to a set of data representing the time variations of such conditions. The mentioned set of data includes the variability of weather conditions, energy demands, energy resources prices, CO<sub>2</sub> emission factors, and performance of the different considered technologies.

To offer the reader a comprehensive overview of the entire optimization process applied to the EC and drawing inspiration from the works of Pina (2019) and Wakui, Kawayoshi and Yokoyama (2016), Figure 3.1 illustrates the key phases of the optimization process

along with some of their key details. The phases encompass superstructure definition, data gathering, development of the optimization model, and support for optimal decision-making.

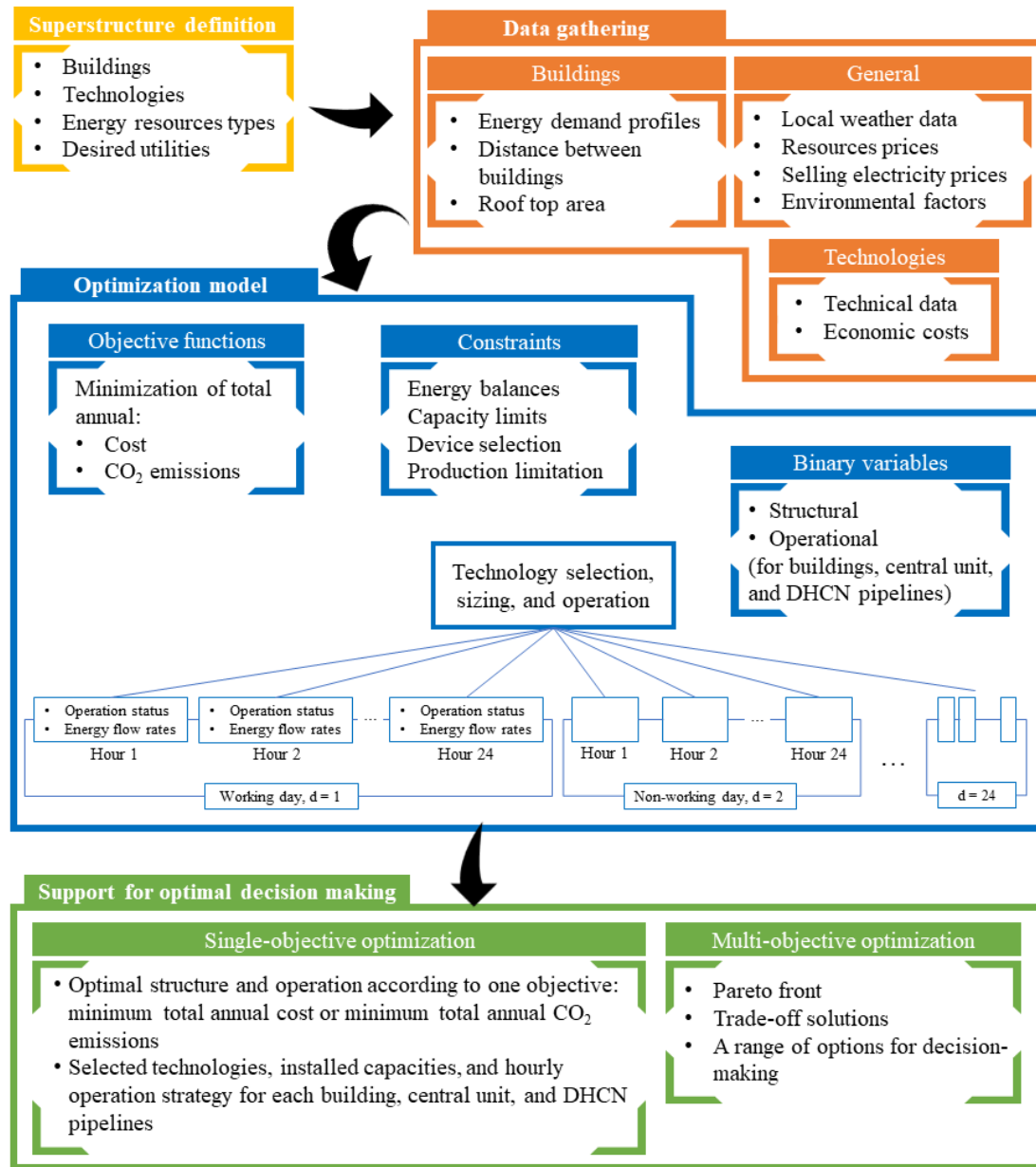


Figure 3.1 – Multi-objective optimization framework applied to the energy community. Source: own elaboration.

Following the same reasoning as Pina (2019), the optimization of the case study under analysis does not provide solutions with final designs. Instead, the provided solutions constitute a foundation for a subsequent and more comprehensive analysis, within the

---

optimization process. Such procedure will determine the actual final design according to the decision-maker interests.

The main contributions and novelties from the study developed in this chapter include:

- Optimization of an EC dealing, at the same time, with a district heating and cooling network (DHCN) of pipelines connecting the buildings, a central unit to support the buildings, thermal and cooling storage, management and distribution of self-produced and purchased electricity among the buildings and between the EC and the national electric grid, integration of solar technologies, hourly electricity purchase price, hourly electricity selling price, and hourly CO<sub>2</sub> emissions factors;
- Single-objective optimization detailing the optimal energy supply system structure of each building, DHCN pipelines, and central unit, plus the optimal technologies operation with all annual energy flows within the building, through pipelines, and within the central unit;
- Multi-objective optimization presenting a range of trade-off solutions through which it is possible to have important pieces of information about installed capacities, structure for the DHCN pipelines, total annual costs and CO<sub>2</sub> emissions, cost of moving from one solution to another, and cost of choosing a more environmentally friendly solution.

The chapter is organized according to the following structure: section 3.1 presents the superstructure for entire EC (all possible building connections to the DHCN and the local electric grid) as well as for each building plus central unit (all possible technologies that can be installed); section 3.2 introduces the input data (energy demand profiles, as well as technical, economic, and environmental data); section 3.3 develops the mathematical model for the EC, detailing the objective functions and constraints based on the MILP method; section 3.4 describes the reference case (or conventional solution) to which the results from the optimized EC will be compared; section 3.5 presents and discuss the results obtained from the single-objective optimization solutions (for total annual costs and environmental viewpoints); and section 3.6 develops the multi-objective optimization

approach applied to the EC and presents a range of possible solutions (Pareto front) that can be used to support the decision-making process.

### 3.1 Superstructure of the Energy Community

According to the superstructure definition provided in section 2.1.2, specific conditions should be defined in order to express the boundaries of the case study. Such conditions comprise not only the energy demand profiles of each building, but also the locally available energy resources. With such pieces of information, the technologies can be selected according to interactions between them. This will determine the proper fulfillment of the energy demands.

In order to better understand the superstructure of the entire EC, it should be divided into two main parts:

- the EC superstructure; and
- the superstructure of a given building.

#### 3.1.1 EC Superstructure

The EC superstructure is depicted in Figure 3.2. As observed, this representation is intended to illustrate all possible connections between the buildings in terms of heating, cooling, and electricity. When it comes to heating and cooling, the buildings can connect to each other through the district heating network (DHN) and the district cooling network (DCN). The central unit is also connected to the EC through a heating pipeline (there is no cooling produced in the central unit). An observation should be made at this point since a given building cannot possibly connect to all the other buildings, due to physical distance constraints. Figure 3.3 provides the actual location of each EC building and the possible DHCN connections.

Regarding the electricity connections, the EC is designed to concentrate the communication with the national electric grid through a distribution substation (DS). It means that the buildings are not directly connected to the national electric grid. Instead, the buildings are connected to the DS which has the role to manage the electricity balance among the buildings and between the EC and the national electric grid.

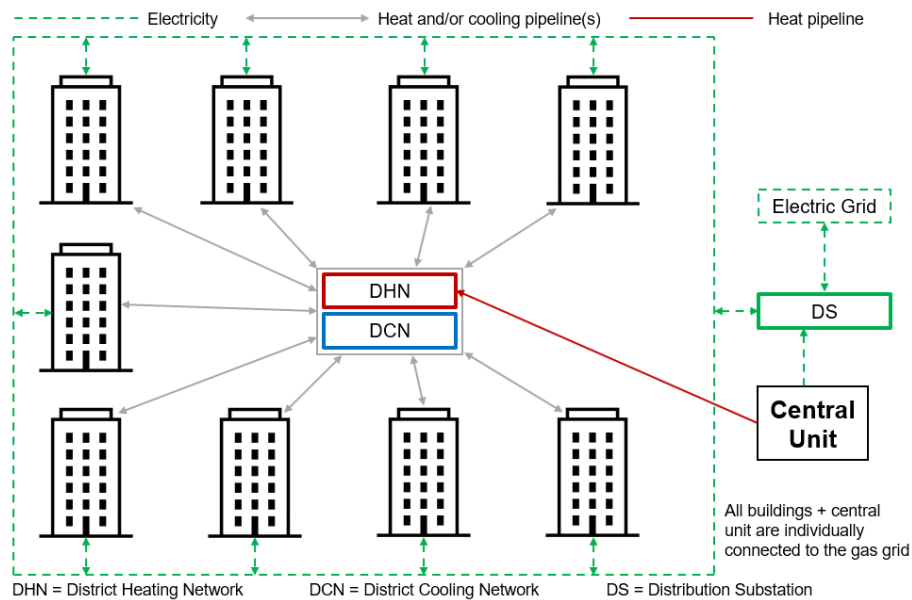


Figure 3.2 – Energy community superstructure. Source: own elaboration.

The DS electricity balance management is one of the main details of the EC superstructure. Figure 3.3 illustrates the main idea behind the DS balance management. As mentioned before, the buildings are not directly connected to the national electric grid. Instead, they are connected to the DS. Such connection is set to function in both directions (not at the same time), i.e., depending on the obtained solution, a given building will be: (i) sending electricity to the DS at some hours of the year (self-production surplus), (ii) receiving electricity from the DS at some other hours of the year (self-production deficit), or (iii) neither receiving nor sending electricity from/to the DS at some other hours of the year (self-production is equal to the electricity demand at these hours). The central unit does not have an electricity demand. For this reason, all produced electricity would be sent to the DS. Then, in agreement with the objective function, the DS will (i) purchase (or not) the necessary amount of electricity from the national electric grid, or (ii) sell (or not) the total surplus of self-produced electricity by the entire EC, after having satisfied the electricity demand of each building. The DS balance management strategy has been published in De Souza et al. (2022).

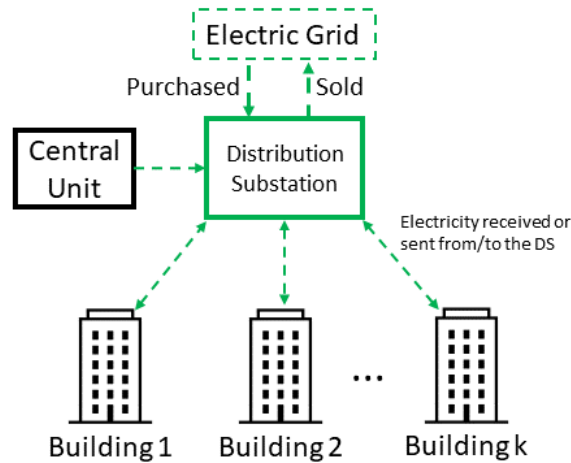


Figure 3.3 – Electricity balance management of the distribution substation. Source: own elaboration.

### 3.1.2 Superstructure: building and central unit

The superstructure of a given building is presented in Figure 3.5. This figure can be thought of as a “zoom-in” in a given building of Figure 3.2. For the better understanding of the reader, the analysis of Figure 3.5 can be focused on the five main details specified in the figure itself: (i) the Building  $k$  Superstructure, i.e., all the pieces of equipment (components) that are possible to be installed in a given building  $k$ ; (ii) the Central Unit Superstructure; (iii) the three possible ways of connecting the buildings in terms of electricity, heating, and cooling, that is, DS, DHN, and DCN; (iv) all the other EC buildings but  $k$ , i.e., the representation of the other EC buildings; and (v) the available energy resources.



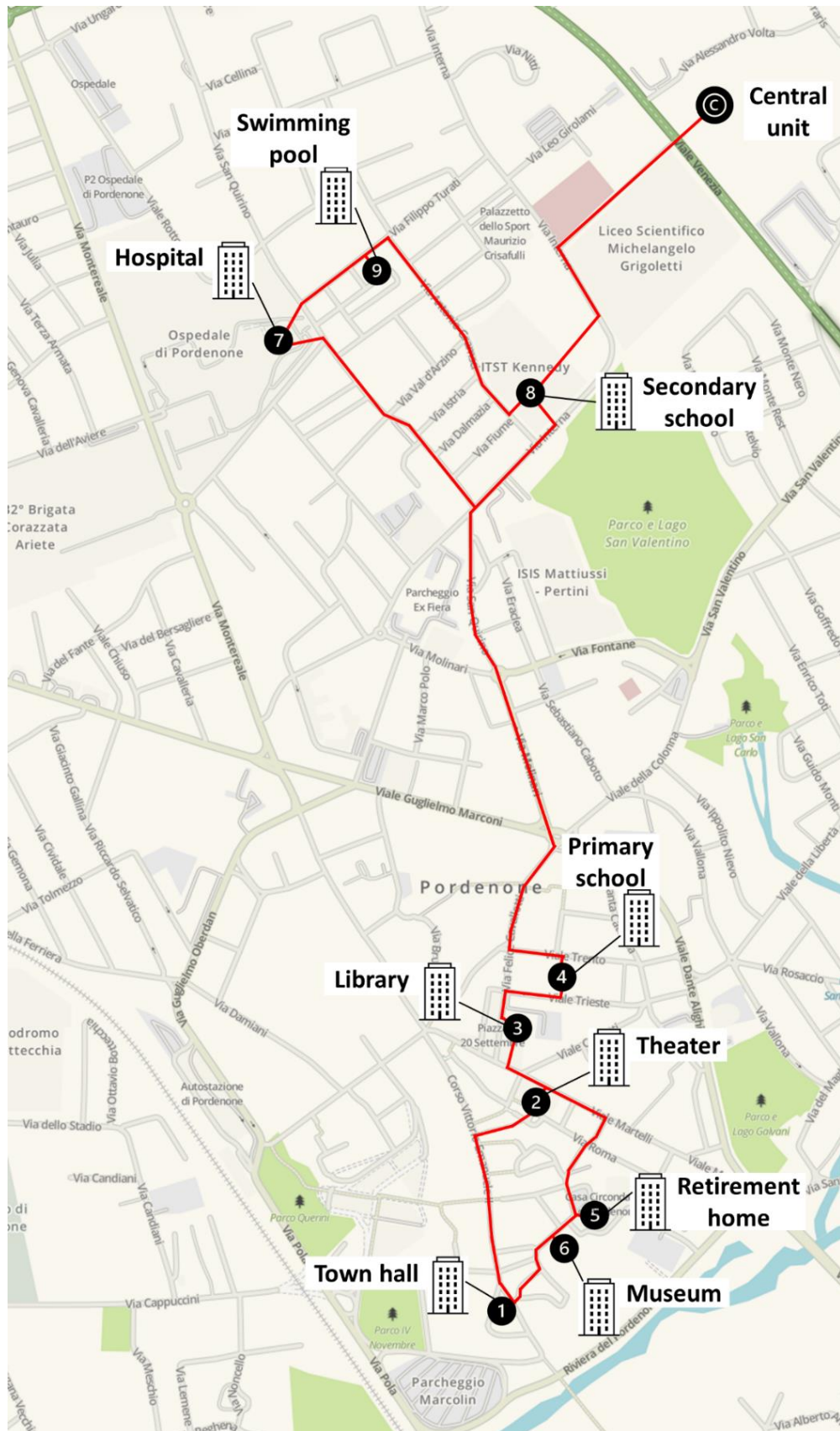


Figure 3.4 – DHCN superstructure for nine buildings plus central unit located in Pordenone, Italy. Source: own elaboration.

#### *Building k Superstructure*

The Building k Superstructure comprises the following technologies.

- Solar technologies: photovoltaic and flat-plate solar thermal panels (PV and ST).
- Natural gas cogeneration units: micro gas turbine (MGT) and internal combustion engine (ICE).
- Natural gas auxiliary boiler (BOI).
- Cooling technologies: single-effect absorption chiller (ABS) and compression chiller (CC).
- Heat pump (HP).
- Thermal energy storages: hot water storage (HST) and chilled water storage (CST).

The MGT, ICE, and BOI are fed with natural gas, while the ST produces heat from the incident solar irradiation and the HP (when working in heat mode) from an electricity input (whether it be from the cogeneration units, PV, or electric grid). Then, after the balance of the produced heat between these five technologies (at a given hour) and the building heat demand (at the same hour), the system will have two options (in the case of a heat surplus): (i) store it in the HST, and/or (ii) send it to another building through the DHN. In the case of a heat deficit, the building will need to receive heat from another building.

Electricity inputs can be derived from the cogeneration units, PV panels, other buildings, and/or electric grid. The PV panels are fed with the incident solar irradiation. At this point it is important to highlight that the EC model separates the building electricity demand from the CC and HP electricity demands. After balancing the electricity, the building can (i) send the surplus to the DS, (ii) require electricity from the DS, in the case of a deficit, or (iii) neither send nor require electricity to/from the DS (self-sufficiency).

The cooling demand can be provided by the ABS, CC, and/or HP (working under cooling mode). The ABS is allowed to be fed only by heat from the cogeneration units and/or ST. Then, in an analogous way as for the heat production, after the balance of the produced cooling between these three technologies (at a given hour) and the building cooling demand (at the same hour), the system will have two options (in the case of a cooling surplus): (i) store it in the CST, and/or (ii) send it to another building through the DCN. In the case of a cooling deficit, the building will need to receive cooling from another building.

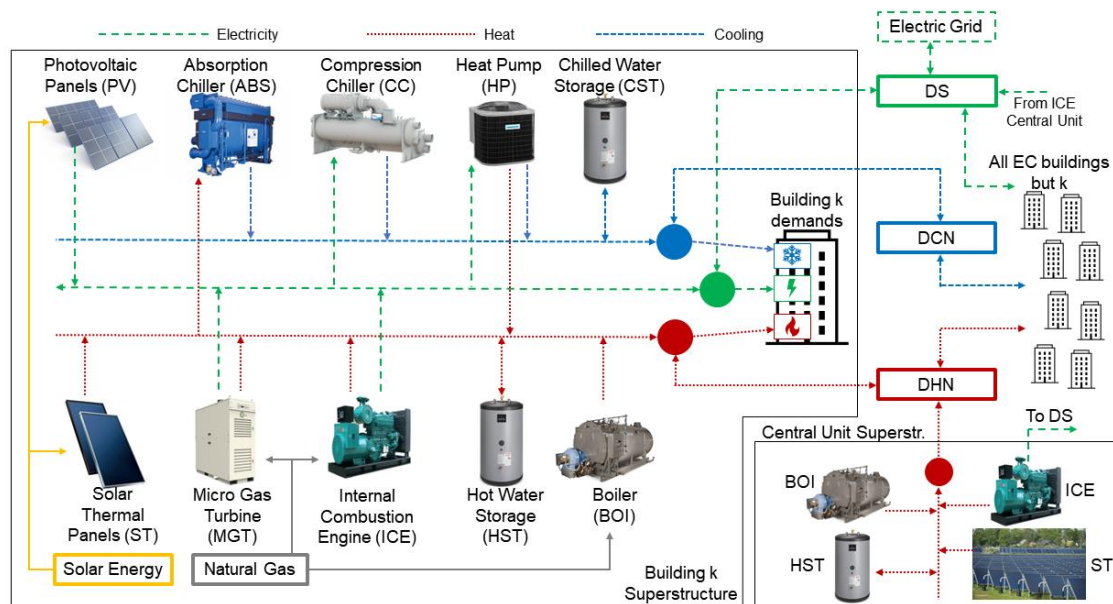


Figure 3.5 – Superstructure of a given building plus the central unit.

### *Central Unit Superstructure*

As observed in Figure 3.5, the available technologies for the Central Unit are:

- Natural gas auxiliary boiler (BOIc).
- Natural gas internal combustion engine (ICEc).
- Seasonal hot water storage (HSTc).
- Flat-plate solar thermal field (STc).

The natural gas ICEc is intended to send electricity to the DS (if needed) and the cogenerated heat can be stored or sent to the DHN. The BOIc can support the EC heat demand in the case of no installed ICEc (or if it is off at the time) or during the night. The HSTc is able to store a great amount of heat and the solar thermal field (STc) allows the EC to increase its percentage of renewable energy sources. The heat produced by the Central unit is then sent to the EC buildings, which have the opportunity to produce less heat from natural gas.

#### *DS, DHN, and DCN*

As already mentioned, the Distribution Substation, District Heating Network, and District Cooling Network provide all EC buildings with the opportunity to share the three demanded utilities, namely electricity, heat, and cooling. In this way, the EC model is allowed to search for favorable solutions by producing the needed utility where its production will be more advantageous for the EC, according to the objective function.

#### *Representation of the other EC buildings*

All the other EC buildings, depicted in Figure 3.5, have the same superstructure of building k, i.e., available energy resource types, technologies, and DS, DHN, and DCN connections.

#### *Available energy resources*

Solar energy, natural gas, and electricity from the national electric grid.

### **3.2 Data gathering**

As showed in Figure 3.1, the data gathering phase is essentially composed by three categories: buildings, technologies, and general related data. The gathering data phase represents an initial step in which all the necessary input data for the development of the optimization model phase is searched, collected, evaluated, and organized. Since the MILP model requires linear equations only, the phase of data gathering should identify non-linear equations and perform the due linearization.

Therefore, this section is intended to describe the gathered input data that is used in the EC model. This section is organized as follows: section 3.2.1 gives a brief description of the buildings, while section 3.2.2 provides the energy demands for each building. The technical data of the technologies considered for the building superstructure is presented in section 3.2.3. Section 3.2.4 presents the economic data for both technologies and energy resources, and, lastly, section 3.2.5 specifies the adopted environmental data.

### **3.2.1 Buildings description**

The EC comprises nine buildings. As observed in Figure 3.4, the buildings can be divided into two groups: (i) the south group, composed of town hall, theater, library, primary school, retirement home, and museum; and (ii) the north group, comprising hospital, secondary school, swimming pool, and central unit. Depending on the found solution, these two groups might be interconnected through the DHCN or not. Differently from residential buildings, the buildings under analysis are characterized by very different energy demand profiles, as shown in the next section.

### **3.2.2 Energy demands**

When it comes to energy supply systems optimization for buildings, the energy demand profile is one of the most important pieces of information regarding the building. This information determines the technology that the model should install, the capacity it should have, and the operational strategy according to the hourly variations in the energy demand profile. For the specific case of the EC and bearing in mind (i) the energy demand profiles of each building, (ii) the DHCN connections between buildings, and (iii) the objective function under analysis, at some hours the optimal solution might find more interesting to produce the demanded energy in a different building. Such dynamics between the hourly energy demand of a given building and the actual place where the energy will be generated is explained in more depth in chapter 5, through marginal cost analysis.

As illustrated in Figure 3.5, the energy demands of the buildings consist of electricity, heating, and cooling.

- The heat demand is intended to comprise sanitary hot water (SHW) and spacing heating (SH). However, due to the lack of more detailed data, the heat demand of

the building is composed by one hourly value corresponding to the composition of SHW plus SH. Moreover, the heat demanded by the ABS is not included in the heat demand of the building; instead, the ABS heat demand depends on the optimal solution of the MILP model.

- The electricity demand of each building is composed of (i) consumption due to electric driven equipment, lighting, etc., which is an input of the model, and (ii) consumption of CC and HP (if installed), which is calculated by the optimal solution of the MILP model.
- For what concerns the cooling demand, there are three main aspects to bear in mind: (i) the majority of the cooling demand of the EC buildings is concentrated from June to August (as it is the case for cooling demand profiles of buildings located in the north hemisphere), (ii) not all the buildings have cooling demand during the mentioned months (e.g., the schools and swimming pool), and (iii) the hospital maintains a cooling demand level even in the cold months due to specific equipment and procedures.

The EC model was developed to cover a period of one year represented by 24 typical days for each building. Such group of typical days is composed by two typical days (with hourly resolution) per month representing one working day (Monday to Friday) and one non-working day (Saturday and Sunday). Since the EC under study is composed by tertiary sector buildings, the following assumptions were adopted regarding their energy demand profiles: (i) working days have the same-order-of-magnitude energy demands, and (ii) same logic for non-working days. Therefore, it was considered two energy demand profiles (per building and per month): one representing all working days and another one representing all non-working days. Then, the model transforms, for each month, the two typical days into four weeks of five working days and two non-working days. Thus, each month comprises 28 days and the whole year is composed of 8064 hours, instead of 8760 hours.

The model is based on 24 typical days for all variables, except for the ones related to the thermal energy storages – TES (heat and cooling). Therefore, these cannot be based on the typical days. This is because every single day of the year needs to be connected to

each other in order to properly represent the energy flows in and out of the TES, i.e., the charging and discharging phases.

The energy demand for the typical days and for each building was defined based on: (i) search on the literature, technical reports, etc., and (ii) direct contact with the building administration. Section A.1 provides a detailed description of the procedure for obtaining the buildings energy demands.

Table 3.1 – Total annual energy services demands and peak demand per building.

Building	Electricity		Heating		Cooling	
	Annual MWh/y	Peak kW <sub>el</sub>	Annual MWh/y	Peak kW <sub>th</sub>	Annual MWh/y	Peak kW <sub>c</sub>
<b>1. Town hall</b>	346.6	189	618.9	397	148.5	150
<b>2. Theater</b>	852.2	270	947.7	1572	457.7	458
<b>3. Library</b>	492.2	110	523.8	287	112.4	115
<b>4. Primary school</b>	73.8	54	926.9	572	0	0
<b>5. Retirement home</b>	489.0	101	637.4	238	173.4	138
<b>6. Museum</b>	82.5	36	387.3	231	78.7	91
<b>7. Hospital</b>	8840.2	1659.4	23,992.2	6902.9	1475.5	2001.5
<b>8. Secondary school</b>	410.3	200	3603.9	2822.6	0	0
<b>9. Swimming pool</b>	126.2	23.7	360.8	241.6	0	0

The total annual electricity, heating, and cooling demands for the entire EC are, respectively, 11,713.2 MWh/y, 31,998.9 MWh/y, and 2446.1 MWh/y. Table 3.1 presents the total annual energy demands for each building individually. The values are the summation of the 8064 hours considered for this study. Sections 3.2.2.1 to 3.2.2.2 describe the energy demand profiles of each energy utility in more detail.

### 3.2.2.1 Electricity demand

Figure 3.6 and Figure 3.7 show the hourly electricity demand for the nine buildings and for each typical day. The horizontal axis represents two 24-hours typical days per month. As observed, electricity is demanded throughout the whole year, for the majority of the buildings. For some buildings such as the library, schools, and swimming pool, the electricity demand follows the occupancy levels, i.e., it is higher during the school year (from September to June). The theater and hospital have an approximately constant electricity demand throughout the year since their occupancy level does not depend on

vacation or non-vacation periods. The town hall, retirement home, and museum are buildings that should operate during the entire year. For this reason, they also have electricity demand throughout the entire year, but with lower levels during the period of daylight-saving time.

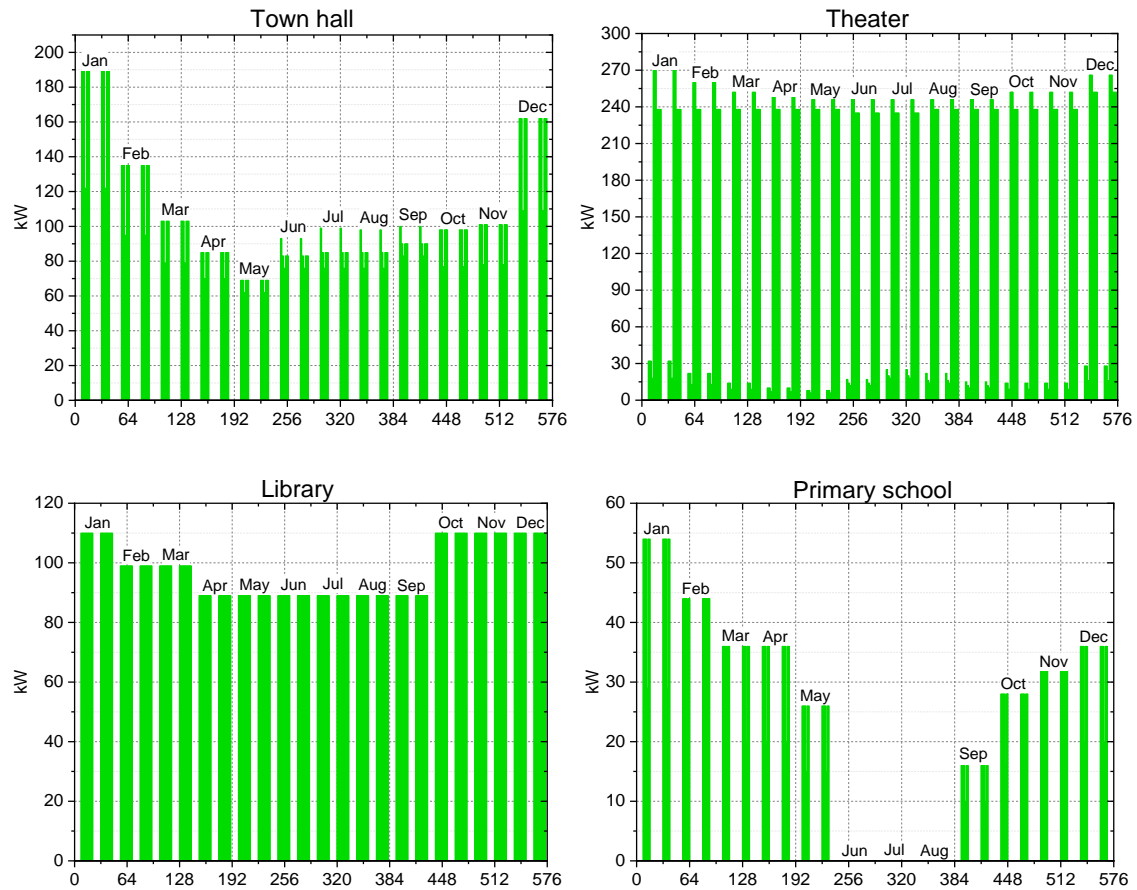


Figure 3.6 – Annual electricity demand profiles (two 24-hours typical days per month) for the buildings: town hall, theater, library, and primary school.

Section A.1 provides the numerical values of electricity demand for each building and for one January and July working days.



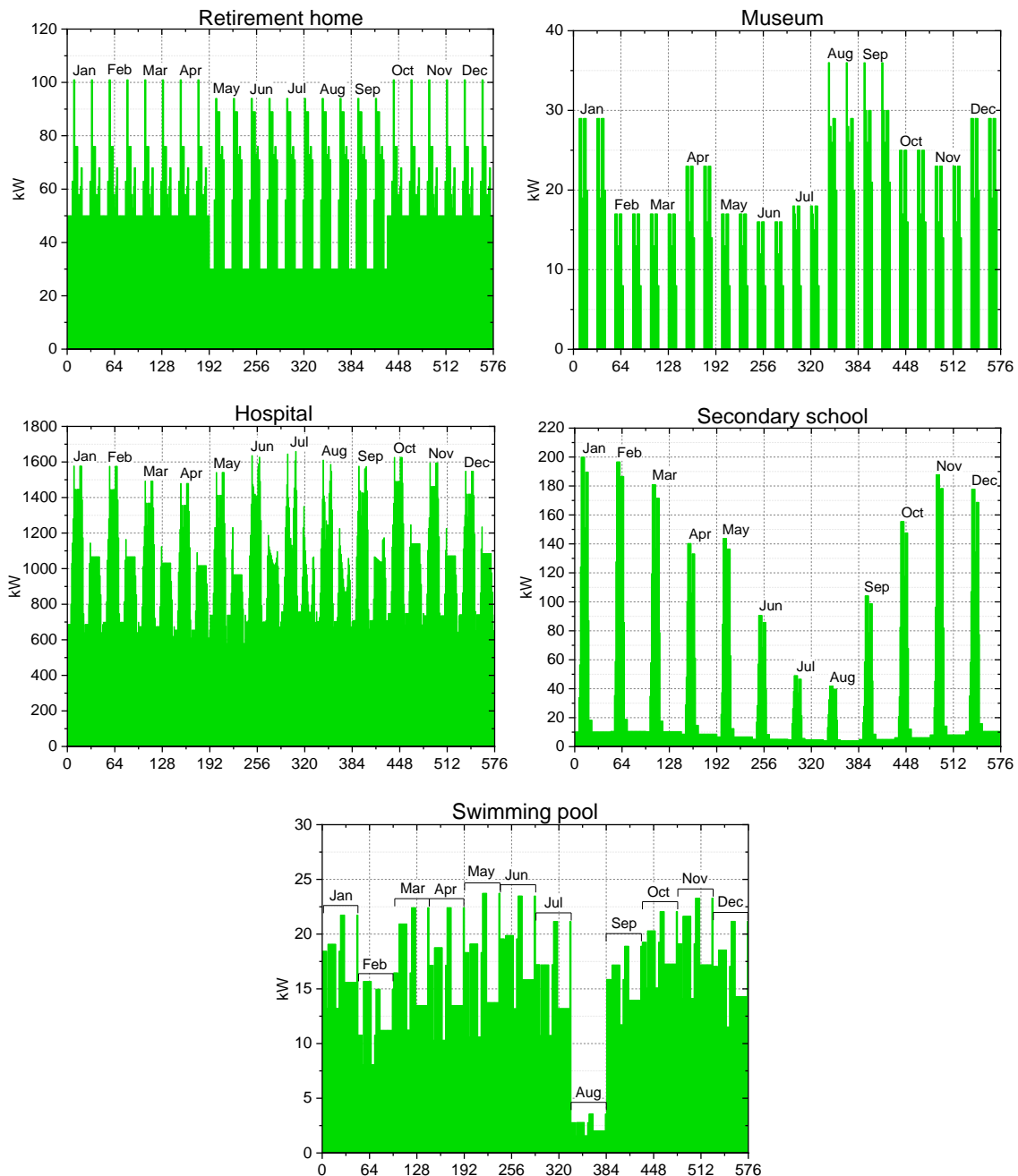


Figure 3.7 – Annual electricity demand profiles (two 24-hours typical days per month) for the buildings: retirement home, museum, hospital, secondary school, and swimming pool.

### 3.2.2.2 Heating demand

Figure 3.8 and Figure 3.9 present the hourly heating demands for the nine buildings and for each typical day. The horizontal axis represents two 24-hours typical days per month. As can be seen, heating is demanded throughout the whole year, for most of the buildings,

and the heating demand level follows the seasons of the year. It is worth remembering that the heating demand during summer represents the sanitary hot water (SHW) demand; also, during the cold months, the heating demand is higher due to the composition of SHW plus spacing heating (SH) demands. As observed in Figure 3.9, the retirement home and hospital are buildings with 24/7 heating demand during the cold months of the year. During the end of spring, summer, and beginning of autumn the heating demand is due only to SHW. The hospital, however, has a 24/7 SHW even during the mentioned period.

Section A.1 provides the numerical values of heat demand for each building and for one January and July working days.

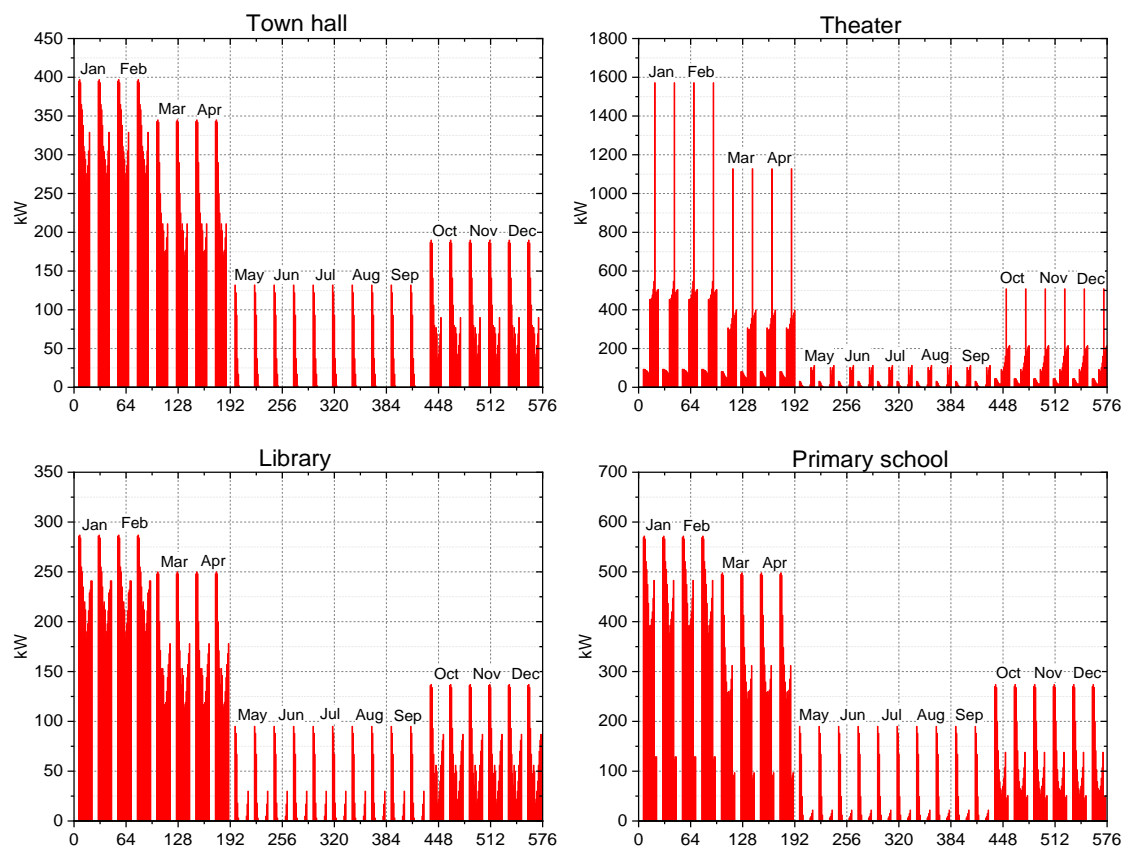


Figure 3.8 – Annual heating demand profiles (two 24-hours typical days per month) for the buildings: town hall, theater, library, and primary school.

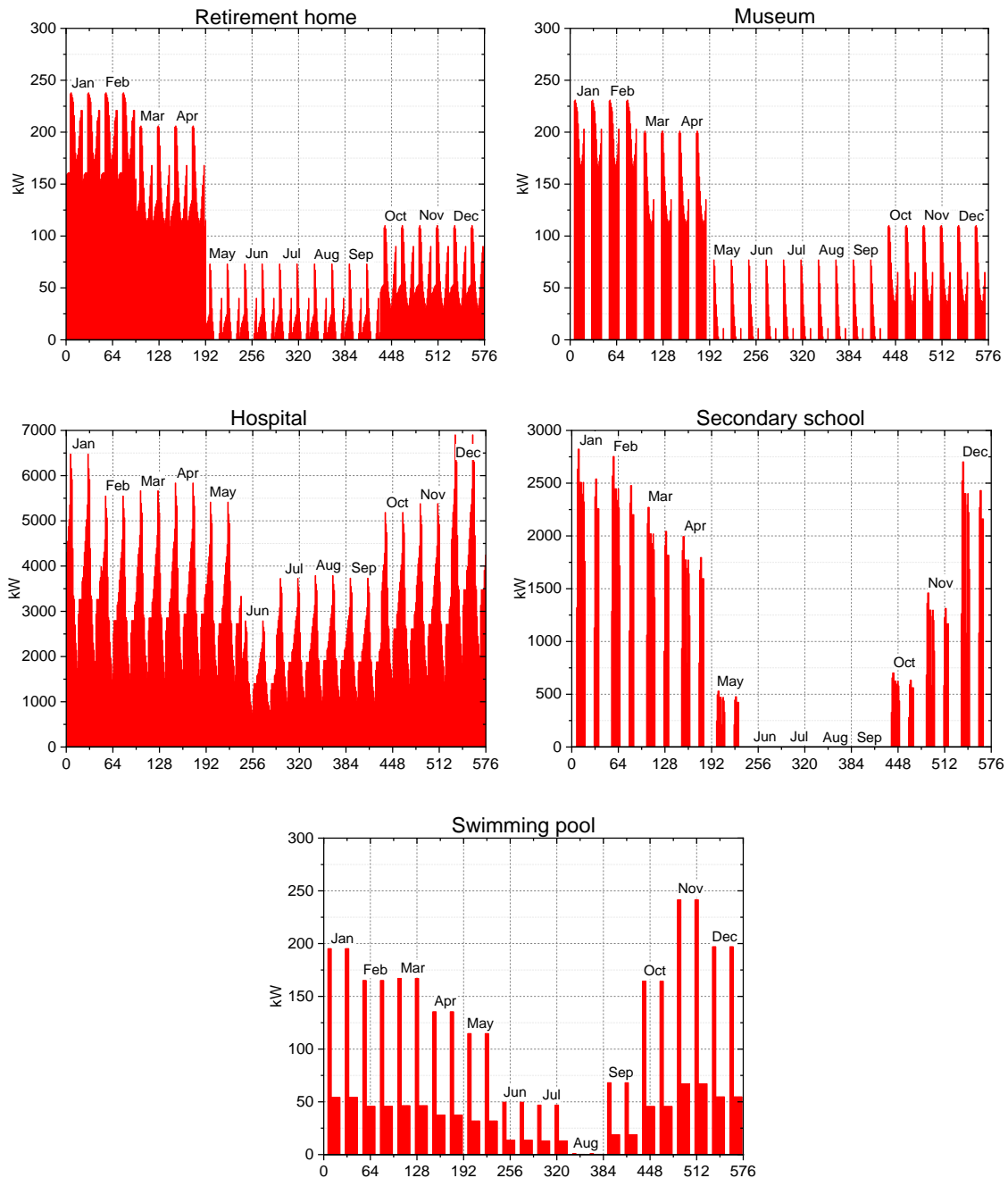


Figure 3.9 – Annual heating demand profiles (two 24-hours typical days per month) for the buildings: retirement home, museum, hospital, secondary school, and swimming pool.

### 3.2.2.3 Cooling demand

Figure 3.10 and Figure 3.11 present the hourly cooling demands for the nine buildings and for each typical day. The horizontal axis represents two 24-hours typical days per month. At a first glance, one can observe two main aspects from those figures: (i) there

are three buildings with no cooling demand, and (ii) one of the buildings has cooling demand even during the cold months.

The buildings with no cooling demand are the schools and the swimming pool. Such buildings do not work during the hot months of the year (vacation period).

Besides during the hot months, the hospital also demands cooling throughout the whole year due to specific procedures that are out of the scope of the present thesis.

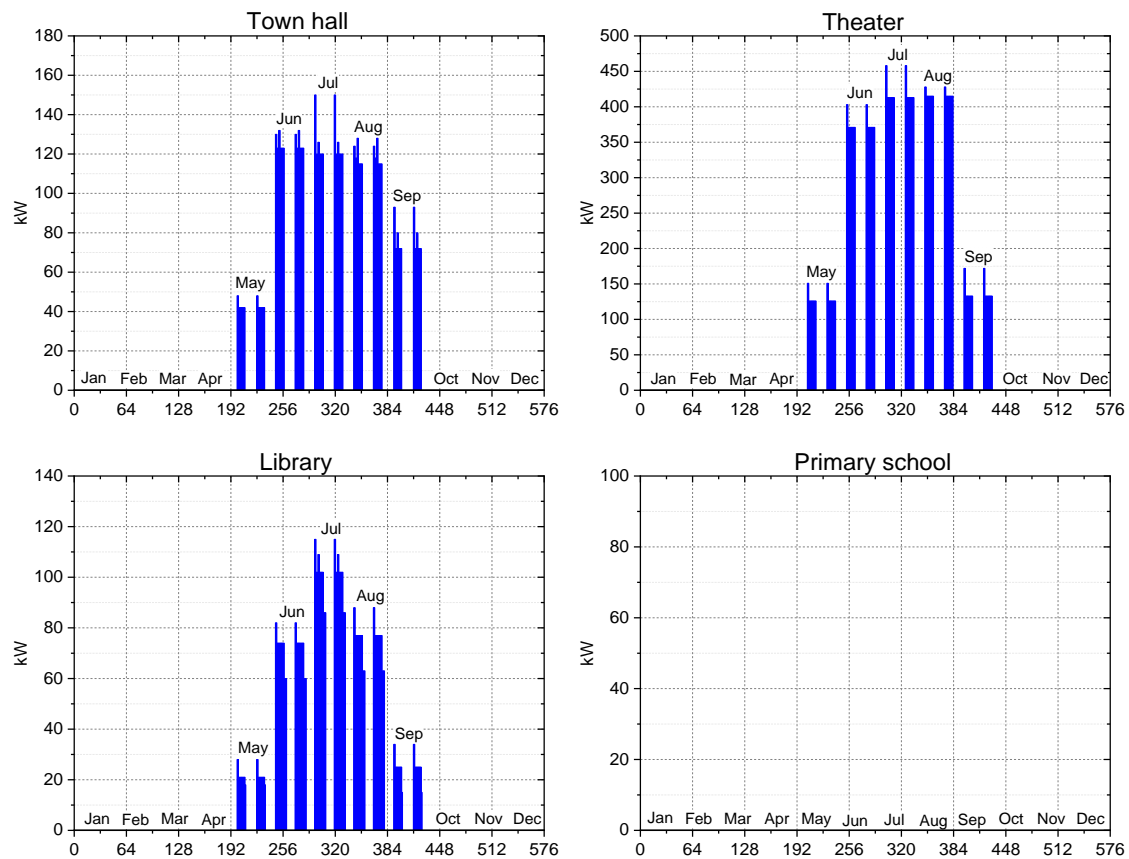


Figure 3.10 – Annual cooling demand profiles (two 24-hours typical days per month) for the buildings: town hall, theater, library, and primary school.

For all the other buildings, the cooling demand is present only from end of spring to the beginning of autumn. As observed in Figure 3.11, the retirement home and hospital are buildings with 24/7 cooling demand during the hot months of the year. Section A.1 provides the numerical values of cooling demand for each building and for one January and July working days.

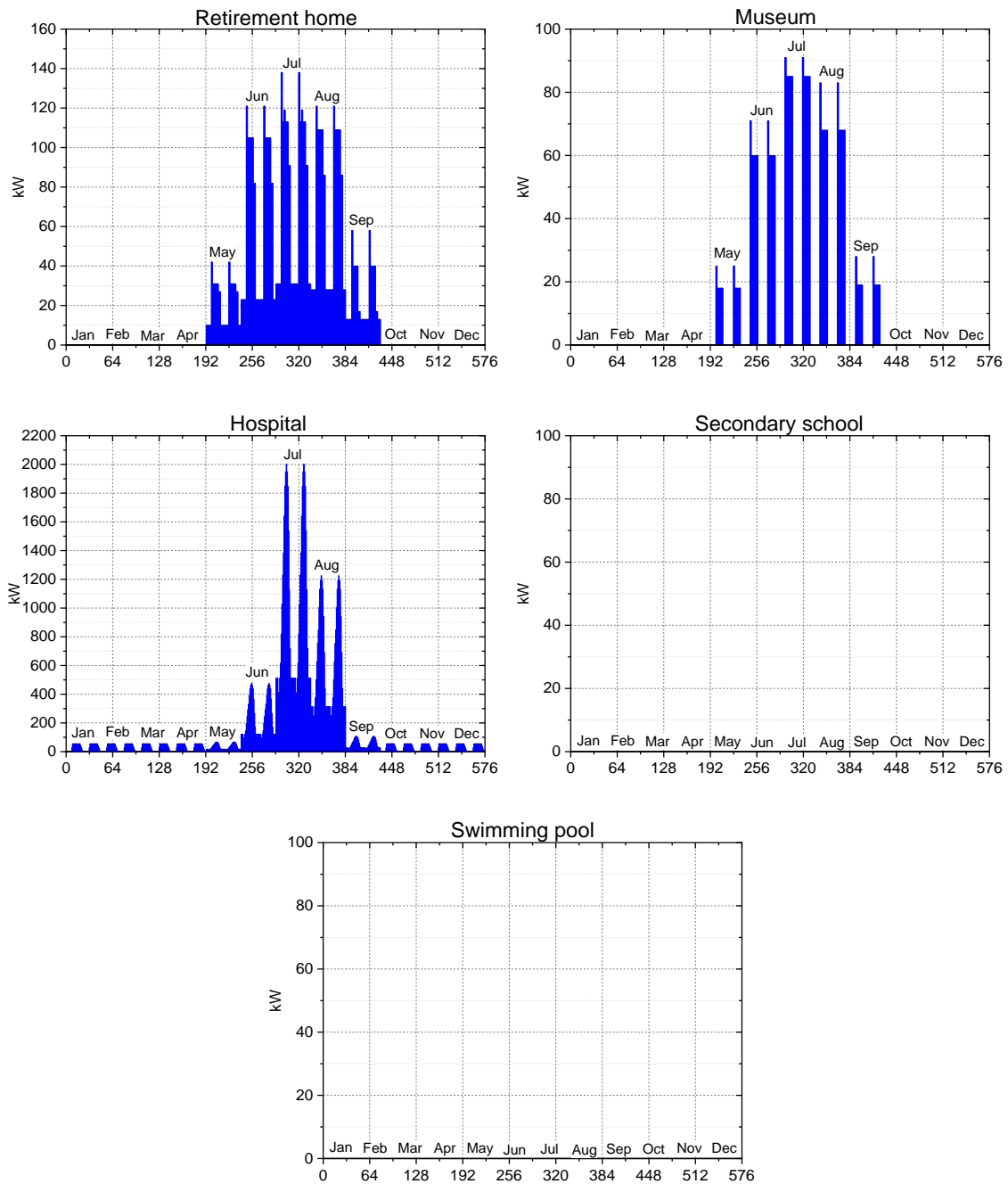


Figure 3.11 – Annual cooling demand profiles (two 24-hours typical days per month) for the buildings: retirement home, museum, hospital, secondary school, and swimming pool.

### 3.2.3 Technical related data

The technical data of the technologies involved in the superstructure of each building plus central unit is another very important set of input data to the EC model. Bearing in mind the fact that the EC model is based on a MILP algorithm and that all equations must be linear, the performance of all technologies must be expressed through linear equations.

However, some technologies hold intrinsically non-linear behavior describing their performances. This is the case of the micro gas turbine (MGT), internal combustion engine (ICE), absorption chiller (ABS), and heat pump (HP). Therefore, the performance curves of these technologies were approximated to a linear behavior through their linearization. This procedure as well as the obtained results are explained in more detail in the section A.3. Besides the data regarding the installed technologies for each building, the data concerning the DHCN pipelines is another crucial element for the model.

For this reason, the next two sections (3.2.3.1 and 3.2.3.2) briefly provide the main technical data related to, respectively, the (i) candidate technologies for building *k* superstructure (see Figure 3.5) plus central unit and (ii) DHCN pipelines.

### 3.2.3.1 Building *k* superstructure technologies

The technical data of the MGT, ICE, ABS, and HP are based on real and commercially available equipment, which are presented in detail in section A.3. For these technologies, different nominal capacities were selected, according to the energy demand magnitude of each building. Table 3.2 shows the nominal installed capacities that are allowed to be installed in each building. Then, the optimization model is allowed to install up to six components in a given building.

Table 3.3 provides the electric and thermal efficiencies for the ICE and MGT, while Table 3.4 presents the COP values for the ABS. Table 3.5 provides the COP values regarding the heating and cooling modes of the HP throughout the year. As observed, the COP values of the HP varies according to the ambient temperature.

Table 3.2 – ICE, MGT, ABS, and HP nominal capacities per building. Values in kW.

Tech.	Buildings								
	1	2	3	4	5	6	7	8	9
ICE	70	140	50	50	50	50	200	70	140
MGT	65	100	30	30	30	30	200	65	100
ABS	70	105	35	35	35	35	105	70	105
HP	80	100	35	35	35	35	100	80	100

Table 3.3 – Electric and thermal efficiencies for ICE and MGT at nominal capacity.

ICE nominal capacity (kW <sub>el</sub> )	Electric efficiency %	Thermal efficiency %	MGT nominal capacity (kW <sub>el</sub> )	Electric efficiency %	Thermal efficiency %
50	34.4	56.8	30	26.2	51.2
70	34.6	56.6	65	29.2	48.8
140	36.3	54.3	100	30.1	45.4
200	37.2	53.9	200	33.4	36.3

Table 3.4 – COP values for ABS at nominal capacity.

ABS nominal capacity (kW <sub>cooling</sub> )	COP
35	0.71
70	0.71
105	0.69

Table 3.5 – Annual COP values for the HP in heating (H) and cooling (C) modes.

Build.	Jan to Feb		Mar		Apr		May		Jun to Jul	
	H	C	H	C	H	C	H	C	H	C
1	2.26	4.63	2.45	4.63	2.72	4.63	2.96	4.09	3.21	3.59
2	2.30	4.51	2.51	4.51	2.77	4.51	2.99	3.95	3.27	3.40
3	2.17	4.90	2.31	4.90	2.61	4.90	2.90	4.40	3.10	4.00
4	2.17	4.90	2.31	4.90	2.61	4.90	2.90	4.40	3.10	4.00
5	2.17	4.90	2.31	4.90	2.61	4.90	2.90	4.40	3.10	4.00
6	2.17	4.90	2.31	4.90	2.61	4.90	2.90	4.40	3.10	4.00
7	2.30	4.51	2.51	4.51	2.77	4.51	2.99	3.95	3.27	3.40
8	2.26	4.63	2.45	4.63	2.72	4.63	2.96	4.09	3.21	3.59
9	2.30	4.51	2.51	4.51	2.77	4.51	2.99	3.95	3.27	3.40
Build.	Aug		Sep		Oct		Nov		Dec	
	H	C	H	C	H	C	H	C	H	C
1	3.21	3.12	3.21	4.09	2.96	4.63	2.45	4.63	2.26	4.63
2	3.27	2.94	3.27	3.95	2.99	4.51	2.51	4.51	2.30	4.51
3	3.10	3.50	3.10	4.40	2.90	4.90	2.31	4.90	2.17	4.90
4	3.10	3.50	3.10	4.40	2.90	4.90	2.31	4.90	2.17	4.90
5	3.10	3.50	3.10	4.40	2.90	4.90	2.31	4.90	2.17	4.90
6	3.10	3.50	3.10	4.40	2.90	4.90	2.31	4.90	2.17	4.90
7	3.27	2.94	3.27	3.95	2.99	4.51	2.51	4.51	2.30	4.51
8	3.21	3.12	3.21	4.09	2.96	4.63	2.45	4.63	2.26	4.63
9	3.27	2.94	3.27	3.95	2.99	4.51	2.51	4.51	2.30	4.51

The solar technologies production was simulated for the city of Pordenone, Italy, through the System Advisor Model (SAM) software, from National Renewable Energy Laboratory (NREL, 2023). The production for both PV and ST were calculated per square meter of the installed technology (detailed information on section A.3.5). The maximum total available rooftop area was set to 200 m<sup>2</sup> per building. Both PV and ST compete between them to occupy such space, however it is the MILP algorithm which will decide the installed percentage of each one or even to not install at all.

For what concerns the boiler (BOI) and compression chiller (CC), they are based, respectively, on a typical efficiency and COP of such technologies. Their optimal installed capacities are essentially based on the fuel cost, technology purchase cost, maintenance cost, and other installed technologies providing the same product. The thermal energy storage technologies (HST and CST) are essentially centered on a dissipation factor and a maximum installed capacity. Table 3.6 presents the main technical data regarding these technologies.

Table 3.6 – Main technical data regarding BOI, CC, HST and CST.

<b>Technologies</b>	<b>Efficiency</b>	<b>COP</b>	<b>Dissipation factor</b>	<b>Maximum capacity</b>
<b>BOI</b>	95%	-	-	Decision variable
<b>CC</b>	-	3	-	Decision variable
<b>HST</b>	-	-	2%	4 MWh
<b>CST</b>	-	-	2%	4 MWh

Regarding the central unit superstructure, it is possible to highlight the following details about the technical data: (i) larger capacity technologies are needed here, since the central unit is intended to support (in terms of electricity and/or heat) the entire or part of the EC, (ii) the ICE is based on a typical electricity and heat efficiencies for larger capacity components, (iii) the BOI, ST, and HST follow the same logic as for the ones considered for the buildings. Table 3.7 provides the technical details regarding the central unit technologies.



Table 3.7 – Main technical data regarding central unit technologies.

Central unit technologies	Parameter	Value	Maximum capacity
ICE	Electric efficiency	0.38	6.5 MW <sub>el</sub>
	Thermal efficiency	0.44	
BOI	Thermal efficiency	0.955	7.5 MW <sub>th</sub>
ST	Efficiency		45000 m <sup>2</sup>
HST	Hourly loss factor	0.005 h <sup>-1</sup>	400 MWh

### 3.2.3.2 DHCN technical data

The technical data regarding the pipelines of the district heating and cooling network is essentially based on: (i) maximum and minimum capacities of each pipeline, i.e., the minimum and maximum amount of heat (or cooling) that a given pipeline is allowed to transport, (ii) the length of the pipeline between two buildings, and (iii) the loss factors regarding heat or cooling dissipation. Table 3.8 presents the minimum and maximum capacities for pipelines between buildings as well as for the pipeline between central unit and buildings.

Table 3.8 – Capacity limits for pipelines connecting buildings and for the central unit pipeline.

	Min. capacity (kW)	Max. capacity (kW)
Pipelines between buildings	40	2100
Pipelines between central unit and buildings	1000	7500

Table 3.9 shows the actual pipeline length between the buildings. Zero-values means that the model is not allowed to connect the buildings with pipelines. As observed, there are two main highlights in this table: (i) one building cannot send thermal energy (heat and/or cooling) to itself, and (ii) one building cannot connect to another one due to very long distances (e.g., buildings 1 and 7) or simply because it can connect to another building through a third building (e.g., buildings 2 and 4 connecting through building 3). For a graphical aid visualization, the reader may refer to Figure 3.4. Table 4.8 and Table 4.9

provide the dissipation factors for heating and cooling pipelines, respectively. These factors represent a percentage loss per unit of length (8% for heating and 5% for cooling pipelines).

Table 3.9 – DHCN pipeline length between buildings allowed to connect. Zero-values means that the model is not allowed to connect the buildings. Values in meters.

Buildings	Buildings								
	1	2	3	4	5	6	7	8	9
1	0	450	0	0	230	200	0	0	0
2	450	0	80	0	250	260	0	0	0
3	0	80	0	200	0	0	0	0	0
4	0	0	200	0	0	0	1400	1400	0
5	230	250	0	0	0	30	0	0	0
6	200	260	0	0	30	0	0	0	0
7	0	0	0	1400	0	0	0	0	250
8	0	0	0	1800	0	0	0	0	400
9	0	0	0	0	0	0	250	400	0

### 3.2.4 Economic data

The economic data relating to the EC comprise a fixed component, concerning the investment costs and maintenance factors of technologies, and a variable component, concerning the hourly operation cost. Moreover, the price of resources is another very important economic input data, which, in this case, is related to natural gas and electricity. The mentioned components are described in sections 3.2.4.1 to 3.2.4.3.

#### 3.2.4.1 Fixed costs plus maintenance factors

The investment costs and maintenance factors of the technologies comprising the building k, central unit, and DHCN pipelines superstructures are based on catalogues of commercially available devices as well as on the scientific literature. Table 3.10 provides the referred figures for each considered device.

As explained in section 3.2.3.1, MGT, ICE, ABS, and HP were selected based on different nominal capacities, according to the energy demand magnitude of each building. As observed in Table 3.10, the cost of the different nominal capacities (for the same

technology) varies accordingly, although the maintenance factor has been considered the same for each nominal capacity. BOI, CC, PV, ST, HST, and CST were not modelled considering fixed investment costs. Instead, their costs are based on the final installed capacity, i.e., these are variable costs, which are detailed on the next section.

Table 3.10 – Investment costs and maintenance factors for the EC selected technologies.

<b>Technologies</b>	<b>Fixed investment cost k€</b>	<b>Maintenance factor €/kWh</b>
<b>Building k superstructure</b>		
<b>ICE 50 kW<sub>el</sub></b>	89	
<b>ICE 70 kW<sub>el</sub></b>	103	
<b>ICE 140 kW<sub>el</sub></b>	185	0.01
<b>ICE 200 kW<sub>el</sub></b>	245	
<b>MGT 30 kW<sub>el</sub></b>	74	
<b>MGT 65 kW<sub>el</sub></b>	148	
<b>MGT 100 kW<sub>el</sub></b>	207	0.002
<b>MGT 200 kW<sub>el</sub></b>	340	
<b>ABS 35 kW<sub>c</sub></b>	31	
<b>ABS 70 kW<sub>c</sub></b>	60	0.001
<b>ABS 105 kW<sub>c</sub></b>	89	
<b>HP 35 kW<sub>el</sub></b>	30	
<b>HP 80 kW<sub>el</sub></b>	53	0.001
<b>HP 100 kW<sub>el</sub></b>	78	
<b>BOI</b>	-	0.001
<b>CC</b>	-	0.002
<b>PV</b>	-	0
<b>ST</b>	-	0
<b>HST</b>	-	0
<b>CST</b>	-	0
<b>Inst. DHCN pipeline</b>	300	0
<b>Central unit superstructure</b>		
<b>ICE</b>	340	0.01

<b>BOI</b>	290	0.001
<b>ST</b>	-	0
<b>HST</b>	-	0
<b>Inst. DHN pipeline</b>	600	0

#### 3.2.4.2 Variable costs

The hourly operation costs of the technologies comprising the building k, central unit, and DHCN pipelines superstructures were also based on catalogues of commercially available devices as well as on the scientific literature. Table 3.11 provides the variable costs for each considered device.

Table 3.11 – Variable costs for the EC selected technologies.

<b>Technologies</b>	<b>Variable investment cost</b>
<b>Building k superstructure</b>	
<b>BOI</b>	80 €/kW <sub>th</sub>
<b>CC</b>	150 €/kW <sub>c</sub>
<b>PV</b>	250 €/m <sup>2</sup>
<b>ST</b>	600 €/m <sup>2</sup>
<b>HST</b>	20 €/kWh
<b>CST</b>	20 €/kWh
<b>Installed DHCN pipeline</b>	300 €/m 0.25 €/kW.m
<b>Central unit superstructure</b>	
<b>ICE</b>	990 €/kW <sub>el</sub>
<b>BOI</b>	45 €/kW <sub>th</sub>
<b>ST</b>	300 €/m <sup>2</sup>
<b>HST</b>	5 €/kWh
<b>Installed DHN pipeline</b>	600 €/m 0.04 €/kW.m

### 3.2.4.3 Electricity and gas economic data

As illustrated in Figure 3.5, the available resources for the EC are solar energy, natural gas, and electricity from the national grid. The EC purchases natural gas, from the main gas grid, and is allowed to purchase and sell electricity from/to the main electric grid. This section aims to provide the data related to the input natural gas price, as well as the electricity price for both purchasing and selling.

Table 3.12 provides the natural gas purchase price. In Italy, the natural gas price is composed of (i) natural gas expenses, i.e., the cost of various activities carried out by the seller before supplying natural gas to the end customer, (ii) transportation and metering management expenses, (iii) system charges expenses, which is an amount used by the state to support expenditures and works in the public interest, such as the incentive for renewable sources or economic support for disadvantaged households, and (iv) tax expenditures (ARERA, 2023).

Another important detail regarding natural gas price in Italy, is an incentive to self-producers who adopt cogeneration devices into their own energy systems (Casisi *et al.*, 2008). Such incentive allows a gas price reduction of 25% (Table 3.12) for the amount of gas used in the mentioned devices.

Table 3.12 – Natural gas price.

	<b>Price</b>
<b>NG for cogeneration</b>	0.064 €/kWh
<b>NG for boilers</b>	0.085 €/kWh

Regarding electricity prices, the data were taken from the Italian energy markets manager (GME, 2019). In this case, the prices are based on the PUN (acronym for *Prezzo Unico Nazionale* or National Unique Price), which is the wholesale reference price of electricity that is purchased on the Italian Power Exchange (IPEX) market. The PUN prices data can be obtained as a monthly average value divided into three hour bands (Table 3.13). The data was taken from a pre-pandemic period, in this case for 2019. Then, these bands are used to specify the hourly electricity price for each day, according to Table 3.14. Such

specification is regulated by ARERA (2006) and have different electricity prices: F1 (On-peak); F2 (Mid-level); and F3 (Off-peak).

Table 3.13 – Monthly average PUN divided into three hour bands (GME, 2019).

€/MWh	Jan	Feb	Mar	Apr	May	Jun	Jul	Aug	Sep	Oct	Nov	Dec
<b>F1</b>	76.64	61.79	55.61	59.2	53.6	54.02	57.64	51.54	57.4	60.17	57.73	53.03
<b>F2</b>	72.48	63.65	57.81	59.14	56.09	52.49	56.51	54.78	56.35	58.39	52.43	47.91
<b>F3</b>	58.46	51.11	48.15	46.7	45.64	42.65	45.59	45.18	43.96	43.7	39.17	35.33

Table 3.14 – Hourly distribution of the time bands (F1, F2, and F3) for purchasing electricity, according to ARERA (2006).

Hour	1	2	3	4	5	6	7	8	9	10	11	12	13	14	15	16	17	18	19	20	21	22	23	24
<b>Mon</b>	3	3	3	3	3	3	3	2	1	1	1	1	1	1	1	1	1	1	1	2	2	2	2	3
<b>Tue</b>	3	3	3	3	3	3	3	2	1	1	1	1	1	1	1	1	1	1	1	2	2	2	2	3
<b>Wed</b>	3	3	3	3	3	3	3	2	1	1	1	1	1	1	1	1	1	1	1	2	2	2	2	3
<b>Thu</b>	3	3	3	3	3	3	3	2	1	1	1	1	1	1	1	1	1	1	1	2	2	2	2	3
<b>Fri</b>	3	3	3	3	3	3	3	2	1	1	1	1	1	1	1	1	1	1	1	2	2	2	2	3
<b>Sat</b>	3	3	3	3	3	3	3	2	2	2	2	2	2	2	2	2	2	2	2	2	2	2	2	3
<b>Sun</b>	3	3	3	3	3	3	3	3	3	3	3	3	3	3	3	3	3	3	3	3	3	3	3	3

Bearing in mind that the PUN value corresponds only to the electricity production cost, some calculations should be made in order to estimate what would be the electricity bill value, which is the actual electricity price input to the EC model. The calculation was procedure as follows: (i) according to ARERA (2023), the percentages provided in Table 3.15 represent the portion of the final electricity bill value regarding the electricity production cost, (ii) as the PUN corresponds to the electricity production cost, it was divided by the percentages in Table 3.15 in order to obtain the estimated prices shown in Table 3.16.

Table 3.15 – Portion of the final electricity price regarding electricity production cost (per trimester).

2019	Electricity price % regarding electricity production cost
Trimester I	49.8
Trimester II	42.3
Trimester III	43.9
Trimester IV	45.6

Table 3.16 – Monthly average electricity price divided into three time bands. Values in €/MWh.

	Jan	Feb	Mar	Apr	May	Jun	Jul	Aug	Sep	Oct	Nov	Dec
<b>F1</b>	153.28	123.58	111.22	140.95	127.62	128.62	131.00	117.14	130.45	130.80	125.50	115.28
<b>F2</b>	144.96	127.30	115.62	140.81	133.55	124.98	128.43	124.50	128.07	126.93	113.98	104.15
<b>F3</b>	116.92	102.22	96.30	111.19	108.67	101.55	103.61	102.68	99.91	95.00	85.15	76.80

For the price of the electricity sold to the grid, it was considered the data regarding the “Dedicated collection” or *Ritiro Dedicato* managed by GSE (2008). This is an Italian simplified available procedure to producers for selling self-produced electricity to the grid. According to the *Deliberazione AEEG 280/07*, the considered time bands for the hourly selling electricity price is established as shown in Table 3.17, which is slightly different from Table 3.14. Then, the data regarding the selling electricity price was retrieved from GSE (2023) for the north zone, as presented in Table 3.18.

Table 3.17 – Hourly distribution of the time bands (F1, F2, and F3) for selling electricity, according to GSE (2008).

Hour	1	2	3	4	5	6	7	8	9	10	11	12	13	14	15	16	17	18	19	20	21	22	23	24
<b>Mon</b>	3	3	3	3	3	3	2	1	1	1	1	1	1	1	1	1	1	1	2	2	2	2	3	3
<b>Tue</b>	3	3	3	3	3	3	2	1	1	1	1	1	1	1	1	1	1	1	2	2	2	2	3	3
<b>Wed</b>	3	3	3	3	3	3	2	1	1	1	1	1	1	1	1	1	1	1	2	2	2	2	3	3
<b>Thu</b>	3	3	3	3	3	3	2	1	1	1	1	1	1	1	1	1	1	1	2	2	2	2	3	3
<b>Fri</b>	3	3	3	3	3	3	2	1	1	1	1	1	1	1	1	1	1	1	2	2	2	2	3	3
<b>Sat</b>	3	3	3	3	3	3	2	2	2	2	2	2	2	2	2	2	2	2	2	2	2	2	3	3
<b>Sun</b>	3	3	3	3	3	3	3	3	3	3	3	3	3	3	3	3	3	3	3	3	3	3	3	3

Table 3.18 – Monthly average electricity selling price divided into three time bands. Values in €/MWh.

	Jan	Feb	Mar	Apr	May	Jun	Jul	Aug	Sep	Oct	Nov	Dec
<b>F1</b>	75.96	59.19	55.28	56.66	52.36	52.93	56.63	47.87	55.1	59.4	57.08	50.43
<b>F2</b>	69.17	56.61	47.38	49.4	51.34	42.12	49.28	43.07	46.9	49.16	49.79	44.96
<b>F3</b>	58.51	48.26	47.95	43.61	43.82	35.28	40.92	38.12	42.67	40.43	39.3	33.98

### 3.2.5 Environmental data

Another important aspect when it comes to the set of input data to the EC model is the environmental impact considered for the system. For this study, the considered environmental impacts concern only the operation phase, i.e., the consumption of natural gas and electricity from the main grid, which are expressed by the total annual CO<sub>2</sub> emissions. Therefore, it is necessary to determine the CO<sub>2</sub> emissions associated with such consumption.

The CO<sub>2</sub> emission factor associated with the local consumption of natural gas was assumed to be constant throughout the entire year and equal to 0.202 kg CO<sub>2</sub>/kWh (ISPRA, 2021).

The hourly CO<sub>2</sub> emissions from the generated electricity in Italy is not available, as it is for other European countries such as Spain. The truth is that, for most European countries, current official reports provide only annual estimates for their national CO<sub>2</sub> emissions (Ke *et al.*, 2023). Therefore, in order to provide the model with hourly CO<sub>2</sub> emissions data for the Italian generated electricity, two main pieces of information were needed: (i) the hourly generated electricity in Italy (from the entire electricity mix), and (ii) the hourly CO<sub>2</sub> emissions from the Italian power sector. The first one was obtained from the European Network of Transmission System Operators for Electricity (ENTSO-E, 2023), which is an association for the cooperation among the European transmission system operators (TSOs). On their webpage, it is possible to obtain the hourly electricity generation from all primary energy sources divided by country. The Italian related data was selected. The second piece of information was obtained from the online application



“Figshare” or “Carbon Monitor Europe” (Ke *et al.*, 2022), which provides the daily average CO<sub>2</sub> emissions divided by sector and for all European countries. Thus, the data regarding the Italian power sector was selected. As noted, there is a divergence between both pieces of data, i.e., *hourly* generated electricity and *daily* CO<sub>2</sub> emissions. Bearing in mind that the EC model was developed considering two typical days per month, the procedure to converge both pieces of data was (i) calculate the average daily CO<sub>2</sub> emissions corresponding to the working days of each month, (ii) perform the same procedure for non-working days, (iii) assume that CO<sub>2</sub> emissions are constant for the 24 hours of a given working day and equal to the value obtained in step (i), and (iv) assume that CO<sub>2</sub> emissions are constant for the 24 hours of a given non-working day and equal to the value obtained in step (ii).

Figure 3.12 shows the daily CO<sub>2</sub> emissions obtained from Carbon Monitor Europe (Ke *et al.*, 2022) and the hourly CO<sub>2</sub> emissions calculated for this work, which is the data representing the environmental impacts associated to the electricity available in the Italian electric grid for each hour of each typical day. The data was obtained from the year 2019 in order to be coherent with the electricity price data. Table 3.19 provides the exact CO<sub>2</sub> emission values for each typical day (working and non-working day) of each month.

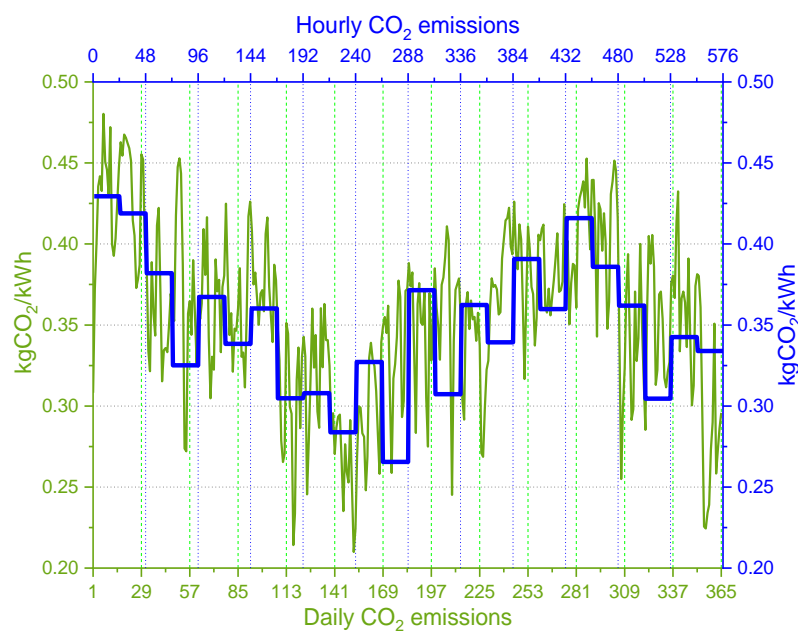


Figure 3.12 – Hourly CO<sub>2</sub> emissions for two typical days per month (input data to the EC model) and daily CO<sub>2</sub> emissions (reference data).

Table 3.19 – CO<sub>2</sub> emission factors for each typical day and for each month. Values in gCO<sub>2</sub>/kWh.

	Jan	Feb	Mar	Apr	May	Jun	Jul	Aug	Sep	Oct	Nov	Dec
<b>WD</b>	429.4	382.0	367.3	360.2	307.9	327.2	371.5	362.4	390.7	416.0	361.9	342.5
<b>NWD</b>	418.9	325.1	338.4	304.8	283.8	265.5	307.3	339.3	359.8	385.9	304.6	334.0

### 3.3 Mathematical model

Sections 3.1 and 3.2 provided, respectively, the superstructure of the entire EC and the necessary input data for the EC model. The next step is the development of the mathematical model representing (i) the essential aspects regarding behavior and performances of technologies, (ii) the boundaries of the system, and (iii) the targeted objective functions.

For this work, a MILP model was developed to identify the optimal system configuration, including installed technologies and their capacities, along with the optimal hourly operation strategy throughout the year from economic and environmental perspectives. The MILP model incorporates binary variables to enforce specific conditions on the system's structure (e.g., permission to install technologies in the superstructure) and operation (e.g., operation modes of the reversible heat pump and flat-plate solar thermal collectors). Additionally, continuous variables are employed to represent energy, economic, and environmental flows. The MILP model was implemented and solved using FICO XPress software (FICO, 2023).

Before dive into the mathematical expressions of the model, it is important to bear in mind the assumptions that have been made in order to keep an acceptable balance between the accuracy of the model and computational effort:

- hourly energy demands, solar radiation, energy prices, and CO<sub>2</sub> emission factors are known before-hand and are considered constant in each time interval;
- TES units (heating and cooling) work as a buffer in which thermal energy is stored (with losses) and consumed later at the same temperature level;

- the typical days have been defined considering the energy demand profiles of each building, i.e., working days and non-working days.

This section is subdivided as follows: section 3.3.1 presents and describes the considered objective functions, i.e., the minimum total annual cost and minimum total CO<sub>2</sub> emissions regarding the entire EC; sections 3.3.2 to 3.3.4 provides the equations representing the boundaries of the model, i.e., constraints, energy balances, and structural and operational restrictions.

### 3.3.1 Objective functions

Equation (3.1) expresses the economic objective function which minimizes the total annual cost  $TAC$  (in €/y) for the entire EC and is composed by the total annual operation cost ( $AOC_{tot}$ ), total annual maintenance cost ( $AMC_{tot}$ ), total annual investment cost ( $AIC_{tot}$ ), total annual purchased electricity cost via distribution substation ( $E_P$ ), and total annual sold electricity revenue via distribution substation ( $E_S$ ) (for the better understanding of the last two terms, in the context of this work, the reader may refer to Figure 3.3). The reader may refer to section A.2 for further details about the equations (3.2) to (3.4).

$$TAC = AOC_{tot} + AMC_{tot} + AIC_{tot} + E_P - E_S \quad (3.1)$$

The total annual operation cost is expressed by Eq. (3.2), which calculates the total costs with purchased gas for boilers and/or cogeneration technologies.

$$AOC_{tot} = OC_{central} + \sum_{B=1}^{Building} OC_{building}(B) \quad (3.2)$$

where  $OC_{central}$  is the operation cost regarding the central unit and  $OC_{building}(B)$  is the operation cost of each building  $B$ . Equation (3.3) represents the total annual maintenance cost.

$$AMC_{tot} = mC_{central} + \sum_{B=1}^{Building} mC_{building}(B) \quad (3.3)$$

where  $mC_{central}$  is the maintenance cost regarding the central unit and  $mC_{building}(B)$  is the maintenance cost of each building  $B$ .

Equation (3.4) expresses the total annual investment cost of the EC.

$$AIC_{tot} = IC_{central} + IC_{pipes} + \sum_{B=1}^{Building} IC_{building}(B) \quad (3.4)$$

where  $IC_{central}$  is the investment cost regarding the central unit,  $IC_{pipes}$  is the investment cost of the DHCN pipelines, and  $IC_{building}(B)$  is the investment cost of each building  $B$ .

As explained in section 3.1.1, only the distribution substation (DS) is allowed to communicate with the national electric grid and, for this reason, all purchased and/or sold electricity is concentrated in the DS. Therefore, all electricity purchase expenses should be accounted by the variable  $E_p$  (Eq. (3.5)) while all electricity selling revenues is computed by the variable  $E_s$  (Eq. (3.8)).

$$E_p = \sum_{m=1}^{12} \sum_{d=1}^2 \sum_{h=1}^{24} Elec_{cost}(m, d, h) \cdot \tau(d) \quad (3.5)$$

where  $Elec_{cost}(m, d, h)$  is the hourly electricity cost (in €, Eq. (3.7)) for all 24 hours  $h$  of each one of the 2 typical days  $d$  and for each one of the 12 months  $m$  of the year. The  $\tau(d)$  term (non-dimensional), represented by Eq. (3.6), expresses the transformation of a given variable (calculated for the typical days) into a specific number of days representing the whole year. In another words, the term  $\tau(d)$  plays a crucial role in transforming a given variable (excluding the ones representing the TES charging and discharging), calculated for two specific days in a month (specifically, one working day and a non-working day), into a value representing a standardized month of 28 days. The operational mechanism of term  $\tau(d)$  involves a two-step process. Firstly, for a working day, term  $\tau(d)$  multiplies the value of a given variable by 5, producing the variable's value associated with one week from Monday to Friday. Secondly, for a non-working day, term  $\tau(d)$  multiplies the value of the same given variable by 2, resulting in the variable's value associated with one weekend. This process effectively computes the given variable for a whole 7-days week. Subsequently, the computed weekly value is multiplied by 4 to derive

the same given variable for a month encompassing 28 days. This entire procedure is iteratively applied for each month throughout the year, resulting in an annual representation of the given variable based on a standardized month. This methodology ensures a comprehensive evaluation over the span of a year, amounting to 336 days or 8064 hours, as explained in section 3.2.2.

$$\tau(d) = 4 \cdot rep(d) \quad (3.6)$$

where  $rep$  corresponds to the matrix [5,2]. It means that, since  $d$  varies from 1 to 2, when  $d = 1$   $\tau(d) = 4 \cdot 5$  which represents 20 weekdays; when  $d = 2$   $\tau(d) = 4 \cdot 2$  which represents 8 weekend days.

The hourly electricity price is given by Eq. (3.7), where  $Elec_{price}(m, d, h)$ , in €/kWh, is the hourly electricity price provided in Table 3.16 while  $E_{bgt}(m, d, h)$  is the hourly amount of purchased electricity, in kWh.

$$Elec_{cost}(m, d, h) = Elec_{price}(m, d, h) \cdot E_{bgt}(m, d, h) \quad (3.7)$$

The electricity selling revenues, in €, are calculated by Eq. (3.8).

$$E_S = \sum_{m=1}^{12} \sum_{d=1}^2 \sum_{h=1}^{24} Elec_{sold}(m, d, h) \cdot \tau(d) \quad (3.8)$$

where  $Elec_{sold}(m, d, h)$  is the hourly electricity revenue (in €, Eq. (3.9)) for all 24 hours  $h$  of each one of the 2 typical days  $d$  and for each one of the 12 months  $m$  of the year. The  $\tau(d)$  term is equal to the one of Eq. (3.5).

$$Elec_{sold}(m, d, h) = Elec_{sold\_price}(m, d, h) \cdot E_{sold}(m, d, h) \quad (3.9)$$

where  $Elec_{sold\_price}(m, d, h)$ , in €/kWh, is the hourly electricity selling price provided in Table 3.18 while  $E_{sold}(m, d, h)$  is the hourly amount of sold electricity, in kWh.

The second objective function is the total annual environmental emissions ( $TAE$ ), expressed by Eq. (3.10), in kg CO<sub>2</sub>/y. As explained before, the emissions considered in this work are due only to the operation of the system. Therefore,  $TAE$  is equal to the total annual operation emissions  $OE_{tot}$ , in in kg CO<sub>2</sub>/y, which is composed of total annual

emissions due to natural gas consumption ( $gas_{em}$ ), total annual emissions due to electricity purchased from the grid ( $E_{P_{em}}$ ), and total annual emissions compensation due to electricity sold to the grid ( $E_{S_{em}}$ ).

$$TAE = OE_{tot} = gas_{em} + E_{P_{em}} - E_{S_{em}} \quad (3.10)$$

The  $gas_{em}$  term is composed of the CO<sub>2</sub> emissions generated from the gas consumption in the central unit and buildings, represented by Eq. (3.11).

$$gas_{em} = gas_{em\_centralunit} + \sum_{B=1}^{Building} gas_{em\_building}(B) \quad (3.11)$$

The terms  $E_{P_{em}}$  (Eq. (3.12)) and  $E_{S_{em}}$  (Eq. (3.14)) are both dependent on the hourly CO<sub>2</sub> emissions  $Elec_{emissions}(m, d, h)$ , provided by Figure 3.12, and on the purchased  $E_{bgt}(m, d, h)$  and sold electricity  $E_{sold}(m, d, h)$ , respectively.

$$E_{P_{em}} = \sum_{m=1}^{12} \sum_{d=1}^2 \sum_{h=1}^{24} Elec\_purch_{CO_2}(m, d, h) \cdot \tau(d) \quad (3.12)$$

$$Elec\_purch_{CO_2}(m, d, h) = Elec_{emissions}(m, d, h) \cdot E_{bgt}(m, d, h) \quad (3.13)$$

$$E_{S_{em}} = \sum_{m=1}^{12} \sum_{d=1}^2 \sum_{h=1}^{24} Elec\_sold_{CO_2}(m, d, h) \cdot \tau(d) \quad (3.14)$$

$$Elec\_sold_{CO_2}(m, d, h) = Elec_{emissions}(m, d, h) \cdot E_{sold}(m, d, h) \quad (3.15)$$

### 3.3.2 Models of the adopted technologies

The energy production as well as the boundary of the system are two of the main details described in the models of each technology. The following two subsections describe the models of each technology considered in the superstructure of the EC (see Figure 3.5), for both the buildings and central unit.

### 3.3.2.1 Buildings

As explained in section 3.1.2, the superstructure of each building comprises: micro gas turbine (MGT), internal combustion engine (ICE), boiler (BOI), absorption chiller (ABS), compression chiller (CC), heat pump, (HP), photovoltaic panels (PV), solar thermal panels (ST), hot water storage (HST), and chilled water storage (CST). In this section, the model of each one of these technologies is presented. The reader should bear in mind that, from Eq. (3.16) to Eq. (3.52), the hourly dependency of the variables, represented by  $m$  (month),  $d$  (day), and  $h$  (hour), is replaced by  $t$  for simplicity.

#### Micro gas turbine (MGT)

As shown in Table 3.2, there are four nominal MGT sizes that can be installed, depending on the building: 30, 65, 100, and 200 kW. The performance data for each nominal size was obtained from manufacture's catalogues and are detailed in section A.3. The linearized equations derived from the performance curves of the MGTs are shown in Eq. (3.16) and Eq. (3.17). They represent, respectively, the heat production ( $Heat_{MGT}$ ) and the fuel consumption ( $Fuel_{MGT}$ ) as function of the produced electricity ( $E_{MGT}$ ). In this way, the model is able to calculate the exact value of the device's efficiencies (electric or thermal ones) for any partial load level, between the minimum ( $MGT_{min}$ ) and maximum ( $MGT_{max}$ ) capacities.

$$Heat_{MGT}(t, c, B) = kh_{MGT}(t, B, 1) \cdot E_{MGT}(t, c, B) + kh_{MGT}(t, B, 2) \cdot O_{MGT}(t, c, B) \quad (3.16)$$

$$Fuel_{MGT}(t, c, B) = kf_{MGT}(t, B, 1) \cdot E_{MGT}(t, c, B) + kf_{MGT}(t, B, 2) \cdot O_{MGT}(t, c, B) \quad (3.17)$$

$$MGT_{min}(t, B) \cdot O_{MGT}(t, c, B) \leq E_{MGT}(t, c, B) \leq MGT_{max}(t, B) \cdot O_{MGT}(t, c, B) \quad (3.18)$$

$$O_{MGT}(t, c, B) \leq X_{MGT}(c, B) \quad (3.19)$$

$$X_{MGT}(c, B) \leq X_{MGT}(c - 1, B) \quad (3.20)$$

The obtainment of the linear coefficients in Eq. (3.16) and (3.17) ( $kh_{MGT}$  and  $kf_{MGT}$ ) are explained in the section A.3. Equation (3.18) represents the limits of electricity production and defines whether the electricity production is zero or not, through the operation binary

variable  $O_{MGT}$ . Equation (3.19) tells the model that the technology is able to operate only if it was installed. The installation decision is made through the binary variable  $X_{MGT}$ . As mentioned in section 3.2.3.1, the model is able to install up to six components of the same technology. Bearing in mind that the model considers lower investment values for installing components starting from the second one on, Eq. (3.20) guarantees that the installation of the second component is allowed only if the first one is already installed.

#### *Internal combustion engine (ICE)*

Table 3.2 also presents the nominal ICE sizes according to the building: 50, 70, 140, and 200 kW. The reasoning about Eq. (3.21) to Eq. (3.25) is analogous to the one of MGT (Eq. (3.16) to Eq. (3.20)).

$$Heat_{ICE}(t, c, B) = kh_{ICE}(t, B, 1) \cdot E_{ICE}(t, c, B) + kh_{ICE}(t, B, 2) \cdot O_{ICE}(t, c, B) \quad (3.21)$$

$$Fuel_{ICE}(t, c, B) = kf_{ICE}(t, B, 1) \cdot E_{ICE}(t, c, B) + kf_{ICE}(t, B, 2) \cdot O_{ICE}(t, c, B) \quad (3.22)$$

$$ICE_{\min}(t, B) \cdot O_{ICE}(t, c, B) \leq E_{ICE}(t, c, B) \leq ICE_{\max}(t, B) \cdot O_{ICE}(t, c, B) \quad (3.23)$$

$$O_{ICE}(t, c, B) \leq X_{ICE}(c, B) \quad (3.24)$$

$$X_{ICE}(c, B) \leq X_{ICE}(c - 1, B) \quad (3.25)$$

#### *Boiler (BOI)*

The auxiliary boiler produces the required amount of heat ( $Heat_{BOI}$ ) limited to the installed capacity  $Cap_{BOI}$ . In this case, there is no variation in the index  $c$  since only one boiler is allowed to be installed. What varies is the size of the equipment. Both  $Heat_{BOI}$  and  $Cap_{BOI}$  are decision variables, which means that the algorithm is free to install (or not) an optimal capacity, according to the objective function under scrutiny.

$$Fuel_{BOI}(t, B) = Heat_{BOI}(t, B) / \eta_{BOI} \quad (3.26)$$

$$Heat_{BOI}(t, B) \leq Cap_{BOI}(B) \quad (3.27)$$

#### *Absorption chiller (ABS)*



As shown in Table 3.2, the ABS nominal sizes, according to each building, are: 35, 70, 105 kW. The hourly cooling production  $Cool_{ABS}$  is expressed by Eq. (3.28) and is related to the heat consumption  $Heat_{ABS}$  through the  $COP_{ABS}$ . The cooling production is limited to a minimum and maximum values, as observed on Eq. (3.29). The binary variables  $O_{ABS}$  and  $X_{ABS}$  define the operation and existence (or installation) of an ABS unit, respectively.

Equation (3.30) tells the model that the technology is able to operate only if it was installed. In a similar way as for MGT and ICE, Eq. (3.31) guarantees that the installation of the second ABS unit is allowed only if the first one is already installed. Another important restriction of the model is to make sure that the ABS can be fed only by heat from solar thermal (ST), MGT, and/or ICE, which is the purpose of Eq. (3.32).

$$Heat_{ABS}(t, c, B) \cdot COP_{ABS}(t, B) - Cool_{ABS}(t, c, B) = 0 \quad (3.28)$$

$$ABS_{min}(t, B) \cdot O_{ABS}(t, c, B) \leq Cool_{ABS}(t, c, B) \leq ABS_{max}(t, B) \cdot O_{ABS}(t, c, B) \quad (3.29)$$

$$O_{ABS}(t, c, B) \leq X_{ABS}(c, B) \quad (3.30)$$

$$X_{ABS}(c, B) \leq X_{ABS}(c - 1, B) \quad (3.31)$$

$$Heat_{ST}(t, B) - Heat_{HST}(t, B) + \sum_{c=1}^6 (Heat_{MGT}(t, c, B) + Heat_{ICE}(t, c, B)) - \sum_{c=1}^6 Heat_{ABS}(t, c, B) \geq 0 \quad (3.32)$$

#### Compression chiller (CC)

The hourly cooling produced by the CC ( $Cool_{CC}$ ) is associated to the hourly consumed electricity  $Elec_{CC}$  through  $COP_{CC}$  (Eq. (3.33)) and is limited to the installed capacity  $Cap_{CC}$  (Eq. (3.34)). Analogously to the BOI case, CC has no variation in the index  $c$  since only one CC is allowed to be installed. What varies is the size of the equipment. Both  $Cool_{CC}$  and  $Cap_{CC}$  are decision variables, which means that the algorithm is free to install (or not) an optimal capacity, according to the objective function under analysis.

$$Elec_{CC}(t, B) = Cool_{CC}(t, B) / COP_{CC} \quad (3.33)$$

$$Cool_{CC}(t, B) \leq Cap_{CC}(B) \quad (3.34)$$

### Heat pump (HP)

As observed in Table 3.2, the HP nominal sizes, according to each building, are: 35, 80, 100 kW. The HP can deliver heat or cooling as products by consuming electricity. The heat  $Heat_{HP}$  and cooling  $Cool_{HP}$  hourly productions are obtained through Eq. (3.35) and Eq. (3.36), and are related to the electricity consumption via the COP of each operation mode. Equation (3.37) expresses the fact that the total electricity consumed by the HP is the summation of the electricity consumed in both operation modes.

The operation in cooling or heat mode is specified through the binary variables  $O_{HP_c}$  and  $O_{HP_h}$ , while  $X_{HP}$  expresses the installation (or not) of the device. Then, for both operation modes, the following equations represent: (i) the electricity consumption limits (Eq. (3.38) and Eq. (3.39)), (ii) the fact that a technology can operate only if it is installed (Eq. (3.40) and Eq. (3.41)), (iii) the constraint to tell the model that cooling and heat mode cannot operate at the same time (Eq. (3.42)), and (iv) the allowance to install a second HP only if the first one have already been installed (Eq. (3.43)).

$$Heat_{HP}(t, c, B) = COP_{HP\_heat}(t, B) \cdot Elec_{HP_h}(t, c, B) \quad (3.35)$$

$$Cool_{HP}(t, c, B) = COP_{HP\_cooling}(t, B) \cdot Elec_{HP_c}(t, c, B) \quad (3.36)$$

$$Elec_{HP}(t, c, B) = Elec_{HP_h}(t, c, B) + Elec_{HP_c}(t, c, B) \quad (3.37)$$

$$HP_{min\_h}(t, B) \cdot O_{HP_h}(t, c, B) \leq Elec_{HP_h}(t, c, B) \leq HP_{max\_h}(t, B) \cdot O_{HP_h}(t, c, B) \quad (3.38)$$

$$HP_{min\_c}(t, B) \cdot O_{HP_c}(t, c, B) \leq Elec_{HP_c}(t, c, B) \leq HP_{max\_c}(t, B) \cdot O_{HP_c}(t, c, B) \quad (3.39)$$

$$O_{HP_h}(t, c, B) \leq X_{HP}(c, B) \quad (3.40)$$

$$O_{HP_c}(t, c, B) \leq X_{HP}(c, B) \quad (3.41)$$

$$O_{HP\_h}(t, c, B) + O_{HP\_c}(t, c, B) \leq 1 \quad (3.42)$$

$$X_{HP}(c, B) \leq X_{HP}(c - 1, B) \quad (3.43)$$

#### *Solar technologies (PV and ST)*

The solar technologies comprise photovoltaic panels (PV) and flat-plate solar thermal panels (ST). The hourly PV electricity production  $Elec_{PV}(t, B)$  is expressed by Eq. (3.44) and depends on two terms: (i)  $k_{PV}(t)$  which is the hourly PV electricity production per  $m^2$  ( $kW/m^2$ ) obtained from local solar irradiation data, and (ii)  $Cap_{PV}(B)$  which is the installed PV capacity (in  $m^2$ ) of a given building and a decision variable. Then, the hourly ST heat production  $Heat_{ST}(t, B)$  is calculated through Eq. (3.45) and also depends on two terms: (i)  $k_{ST}(t)$  which is the hourly ST heat production per  $m^2$  ( $kW/m^2$ ) obtained from local solar irradiation data, and (ii)  $Cap_{ST}(B)$  which is the installed ST capacity (in  $m^2$ ) of a given building and also a decision variable.

$$Elec_{PV}(t, B) = k_{PV}(t) \cdot Cap_{PV}(B) \quad (3.44)$$

$$Heat_{ST}(t, B) = k_{ST}(t) \cdot Cap_{ST}(B) \quad (3.45)$$

$$Cap_{PV}(B) + Cap_{ST}(B) \leq Avail\_area_{rooftop}(B) \quad (3.46)$$

Equation (3.46) restricts the installation of the solar technologies to a maximum available rooftop area. Besides, this equation gives the model the task to decide which solar technology is more advantageous to install, according to the objective function under analysis.

#### *Hot water storage (HST)*

The hourly heat flow in or out of the HST ( $Heat_{HST\_in\_out}$ ) is given by Eq. (3.47). When the heat stored at a given hour  $h$  ( $HST_{stored}(t, B)$ ) is greater than the heat stored at the previous hour (minus heat losses) ( $heat_{loss\_HST} \cdot HST_{stored}(t - 1, B)$ ), it means that the hourly heat flow variable is positive and the HST is being charged. Conversely, if  $heat_{loss\_HST} \cdot HST_{stored}(t - 1, B) > HST_{stored}(t, B)$ , it means that the hourly heat flow variable is negative and the HST is being discharged. The HST model is not based on typical days. It is modelled for the whole year. For that reason, the HST model demanded

more detailed equations to express not only transitions between hours, but also the transitions between days, weeks, and months.

Equation (3.48) limits the allowed hourly amount of heat that can be stored in the HST. The variable  $Size_{HST}(B)$ , in kWh, is the size limit and, at the same time, is a decision variable constrained to a maximum allowed HST capacity for each building (Eq. (3.49)).

$$Heat_{HST\_in\_out}(t, B) = HST_{stored}(t, B) - heat_{loss\_HST} \cdot HST_{stored}(t - 1, B) \quad (3.47)$$

$$HST_{stored}(t, B) \leq Size_{HST}(B) \quad (3.48)$$

$$Size_{HST}(B) \leq Cap_{HST_{max}} \quad (3.49)$$

#### *Chilled water storage (CST)*

The logic of the CST model follows a similar procedure as of HST model.

$$Cool_{CST\_in\_out}(t, B) = CST_{stored}(t, B) - cool_{loss\_CST} \cdot CST_{stored}(t - 1, B) \quad (3.50)$$

$$CST_{stored}(t, B) \leq Size_{CST}(B) \quad (3.51)$$

$$Size_{CST}(B) \leq Cap_{CST_{max}} \quad (3.52)$$

#### *3.3.2.2 Central unit*

As explained in section 3.1.2, the superstructure of the central unit comprises internal combustion engine (ICEc), boiler (BOIc), solar thermal panels (STc), and hot water storage (HSTc). In this section, the model of each one of these technologies is presented. From Eq. (3.53) to Eq. (3.64), the hourly dependency of the variables, represented by  $m$  (month),  $d$  (day), and  $h$  (hour), is replaced by  $t$  for simplicity.

#### *Internal combustion engine (ICEc)*

The ICEc electricity ( $Elec_{ICEc}$ ) and heat ( $Heat_{ICEc}$ ) products are expressed through Eq. (3.53) and Eq. (3.54). Both heat and fuel are written as functions of the produced electricity since the latter is the decision variable. The linear coefficients are  $kh_{ICEc} = 1.175$  and  $kf_{ICEc} = 2.646$ , which means efficiencies of 44.4% and 37.8% for heat and electricity products, respectively. Then, Eq. (3.55) sets the minimum and maximum limits

for  $Elec_{ICEc}$ , where  $Elec_{ICEc\_min} = 0.2$ , and Eq. (3.56) establishes the boundaries for the ICEc size. The  $Size_{ICEc}$  is also a decision variable.

$$Heat_{ICEc}(t) = kh_{ICEc} \cdot Elec_{ICEc}(t) \quad (3.53)$$

$$Fuel_{ICEc}(t) = kf_{ICEc} \cdot Elec_{ICEc}(t) \quad (3.54)$$

$$Elec_{ICEc\_min} \cdot Size_{ICEc} \leq Elec_{ICEc}(t) \leq Size_{ICEc} \quad (3.55)$$

$$Size_{ICEc\_min} \cdot X_{ICEc} \leq Size_{ICEc} \leq Size_{ICEc\_max} \cdot X_{ICEc} \quad (3.56)$$

#### Boiler (BOIc)

The hourly heat ( $Heat_{BOIc}$ ) produced by the central unit boiler is calculated through Eq. (3.57), where  $\eta_{BOIc}$  is the boiler efficiency and  $Fuel_{BOIc}$  is the hourly amount of consumed fuel. In a different way as for the boiler of the buildings' superstructure, a minimum amount of produced heat should be set for the BOIc. Moreover, in order to introduce a linear relation between two decision variables ( $Heat_{BOIc}(t)$  and  $Size_{BOIc}$ ), an auxiliary variable  $\varphi_{BOIc}(t)$  should be introduced. Therefore, Eq. (3.58) to Eq. (3.60) present a set of additional constraints in order to (i) allow the specification of a minimum value for  $Heat_{BOIc}(t)$ , and (ii) provide a linear relation between the hourly produced heat and the boiler size.  $Fuel_{BOIc\_min}$  is set to 10%, while  $O_{BOIc}(t)$  and  $X_{BOIc}$  are binary variables to specify operation and existence status, respectively.

$$Fuel_{BOIc}(t) = Heat_{BOIc}(t)/\eta_{BOIc} \quad (3.57)$$

$$Fuel_{BOIc\_min} \cdot \varphi_{BOIc}(t) \leq Heat_{BOIc}(t) \leq \varphi_{BOIc}(t) \quad (3.58)$$

$$Size_{BOIc} + Size_{BOIc\_max} \cdot (O_{BOIc}(t) - 1) \leq \varphi_{BOIc}(t) \leq Size_{BOIc} \quad (3.59)$$

$$Size_{BOIc\_min} + X_{BOIc} \leq Size_{BOIc} \leq Size_{BOIc\_max} + X_{BOIc} \quad (3.60)$$

#### Solar thermal panels (STc)

The hourly heat produced  $Heat_{STc}$  by the STc installed in the central unit (Eq. (3.61)) is calculated in a similar way as the one for ST on buildings, where  $k_{ST}(t)$  is the hourly STc

heat production per  $m^2$  ( $kW/m^2$ ), obtained from local solar irradiation data, and  $Cap_{STc}$  is the installed capacity in  $m^2$ .

$$Heat_{STc}(t) = k_{ST}(t) \cdot Cap_{STc} \quad (3.61)$$

#### *Hot water storage (HSTc)*

The central unit HSTc is modelled (Eq. (3.62) to Eq. (3.64)) in a similar way as for the buildings HST. Time dependency is the same. The only difference is that HSTc is not building dependent.

$$Heat_{HSTc\_in\_out}(t) = HSTc_{stored}(t) - heat_{loss\_HSTc} \cdot HSTc_{stored}(t - 1) \quad (3.62)$$

$$HSTc_{stored}(t) \leq Size_{HSTc} \quad (3.63)$$

$$Size_{HSTc} \leq Cap\_HSTc_{max} \quad (3.64)$$

### 3.3.3 Energy balances

The energy balance equations are given from Eq. (3.65) to Eq. (3.71). Following the same pattern of the previous sections, the reader should bear in mind that, from Eq. (3.65) to Eq. (3.73), the hourly dependency of the variables, represented by  $m$  (month),  $d$  (day), and  $h$  (hour), is replaced by  $t$  for simplicity.

The hourly heat balance for a given building is calculated through Eq. (3.65),

$$\begin{aligned}
& \left[ \sum_{c=1}^6 (Heat_{MGT}(t, c, B) + Heat_{ICE}(t, c, B) + Heat_{HP}(t, c, B) \right. \\
& \quad \left. - Heat_{ABS}(t, c, B)) \right] \\
& + \left[ \sum_{k=1}^9 (Q_h(t, k, B) \cdot (1 - p_h(B, k)) - Q_h(t, B, k)) \right] \\
& + Heat_{BOI}(t, B) + Heat_{ST}(t, B) - Heat_{HST}(t, B) \\
& - Heat_{Dem}(t, B) + Heat_{cen.unit}(t) - Heat_{waste}(t, B) \geq 0
\end{aligned} \tag{3.65}$$

where  $Heat_{Dem}$  is the hourly heat demand of a given building,  $Q_h(t, k, B)$  and  $Q_h(t, B, k)$  are the variables to express the amount of transported heat through the DHN pipelines and represent, respectively, the hourly heat received by a building  $B$  (from a building  $k$ ) and the hourly heat sent to a building  $k$  (by the building  $B$ ).  $p_h(B, k)$  is the term to express the pipeline heat losses, which was set to impose a 5% heat loss for each kilometer of pipeline length. The hourly central unit heat supply is represented by  $Heat_{cen.unit}(t)$ , while the variable  $Heat_{waste}(t, B)$  represents the hourly wasted heat in each building. The variables carrying the subscripts MGT, ICE, HP, BOI, and ST represent the hourly heat provided by such technologies, whereas the variable with the subscript ABS represents the heat received by the absorption chiller. The variable with HST as subscript represents the in/out heat flow of the hot water storage; for charging mode the variable is positive and for discharging mode it is negative.

The hourly heat balance of the central unit is expressed by Eq. (3.66).

$$\begin{aligned}
& Heat_{ICEc}(t) + Heat_{BOIc}(t) + Heat_{STc}(t) - Heat_{HSTc\_in\_out}(t) \\
& - Heat_{cen.unit}(t) \geq 0
\end{aligned} \tag{3.66}$$

The hourly cooling balance for a given building is determined through Eq. (3.67),

$$\begin{aligned}
& \left[ \sum_{c=1}^6 (Cool_{ABS}(t, c, B) + Cool_{HP}(t, c, B)) \right] \\
& + \left[ \sum_{k=1}^9 (Q_c(t, k, B) \cdot (1 - p_c(B, k)) - Q_c(t, B, k)) \right] \quad (3.67) \\
& + Cool_{CC}(t, B) - Cool_{CST\_in\_out}(t, B) - Cool_{Dem}(t, B) \\
& - Cool_{waste}(t, B) \geq 0
\end{aligned}$$

where  $Cool_{Dem}$  is the hourly cooling demand of a given building,  $Q_c(t, k, B)$  and  $Q_c(t, B, k)$  are the variables to express the amount of transported cooling through the DCN pipelines and represent, respectively, the hourly cooling received by a building  $B$  (from a building  $k$ ) and the hourly cooling sent to a building  $k$  (by the building  $B$ ).  $p_c(B, k)$  is the term to express the pipeline cooling losses, which was set to impose an 8% cooling loss for each kilometer of pipeline length. Variables carrying the subscripts ABS, HP, and CC represent the hourly cooling provided by such technologies, whereas the variable with the subscript *waste* represents the cooling waste from each building. The variable with CST as subscript represents the in/out cooling flow of the chilled water storage; for charging mode the variable is positive and for discharging mode it is negative.

The electricity balance is made up of two parts: (i) balance within each building (Eq. (3.68)), and (ii) balance regarding the distribution substation plus central unit (Eq. (3.69)) (see Figure 3.3). The first part assures that the electricity demand of each building is fulfilled, while the second part guarantees that the electricity demand of the entire EC is fulfilled and that the electricity management between EC and electric grid is performed in an optimal way.

$$\begin{aligned}
& \left[ \sum_{c=1}^6 (Elec_{MGT}(t, c, B) + Elec_{ICE}(t, c, B) - Elec_{HP}(t, c, B)) \right] + Elec_{PV}(t, B) \\
& - Elec_{CC}(t, B) - Elec_{Dem}(t, B) = Elec_{DS}(t, B) \quad (3.68)
\end{aligned}$$

where  $Elec_{Dem}(t, B)$  is the hourly electricity demand of a given building and  $Elec_{DS}(t, B)$  is the hourly amount of electricity that building  $B$  is receiving from the DS (if negative) or sending to the DS (if positive). It will depend on the optimal solution. Variables with the subscripts MGT, ICE, and PV represent the hourly electricity produced



by such technologies, whereas the variables with the subscripts HP and CC represents the electricity consumed by these technologies.

$$\left[ \sum_{B=1}^9 Elec_{DS}(t, B) \right] + Elec_{ICEc}(t) - E_{bgt}(t) - E_{sola}(t) = 0 \quad (3.69)$$

$$E_{bgt}(t) \geq 0 \quad (3.70)$$

$$E_{sola}(t) \geq 0 \quad (3.71)$$

### 3.3.4 DHCN pipelines model

As introduced in the previous section,  $Q_h(t, k, B)$  is the hourly amount of heat transported through the DHN pipelines. Nevertheless, it should be highlighted that this variable is restricted to a certain limit. The same goes for  $Q_c(t, k, B)$ . Therefore, Eq. (3.72) and Eq. (3.73) provide the boundary for those two variables.

$$Q_h(t, k, B) \leq S_h(k, B) \quad (3.72)$$

$$Q_c(t, k, B) \leq S_c(k, B) \quad (3.73)$$

where  $S_h(k, B)$  and  $S_c(k, B)$  are, respectively, the maximum amount of heat and cooling (both in kW) that a pipeline connection between building  $k$  and  $B$  can transport. These variables are also decision variables, i.e., it is up to the optimization engine to decide the optimal size of the pipeline. For this reason, the limits for these sizes should be also introduced (Eq. (3.74) and Eq. (3.75)).

$$S_{min} \cdot X_{pipe\_h}(k, B) \leq S_h(k, B) \leq S_{max} \cdot X_{pipe\_h}(k, B) \quad (3.74)$$

$$S_{min} \cdot X_{pipe\_c}(k, B) \leq S_c(k, B) \leq S_{max} \cdot X_{pipe\_c}(k, B) \quad (3.75)$$

where,  $S_{min} = 40 \text{ kW}$ ,  $S_{max} = 2100 \text{ kW}$ , and  $X_{pipe\_h}(k, B)$  and  $X_{pipe\_c}(k, B)$  are the binary variables expressing the existence (or not) of pipeline connection between two buildings.

It is also important to specify the model that a pipeline connection between two buildings (whether it is part of the DHN or DCN) is allowed to exist only in one direction. This is the purpose of Eq. (3.76) and Eq. (3.77).

$$X_{pipe\_h}(k, B) + X_{pipe\_h}(B, k) \leq 1 \quad (3.76)$$

$$X_{pipe\_c}(k, B) + X_{pipe\_c}(B, k) \leq 1 \quad (3.77)$$

In order to assure that the model will not install pipelines between two buildings that cannot physically connect, Eq. (3.78) and Eq. (3.79) are set up for every zero-value in Table 3.9.

$$X_{pipe\_h}(k, B) = 0 \quad (3.78)$$

$$X_{pipe\_c}(k, B) = 0 \quad (3.79)$$

### 3.4 Conventional solution (reference case)

A primary step before even starting the single- or multi-objective optimizations is the definition of a reference case with the aim to evaluate the enhancement provided by the optimization process. Therefore, this section is intended to describe the considered reference case and provide the obtained results from such a scenario.

The reference case scenario (or conventional solution, as often called in literature) is characterized by the buildings (the same ones composing the EC) individually fulfilling their energy demands. Neither DHCN pipelines nor central unit are considered in this scenario. In other words, the reference case represents how the energy demands are fulfilled in most of the cases, i.e., total electricity demand purchased from the national electric grid, heat demand covered by a gas boiler, and cooling demand fulfilled by electric chiller. Figure 3.13 illustrates the individual electricity connections, where the buildings are allowed to only purchase electricity, and the technologies structure to cover energy demands. The reader may compare this figure with Figure 3.2 and Figure 3.5 for a better understanding.

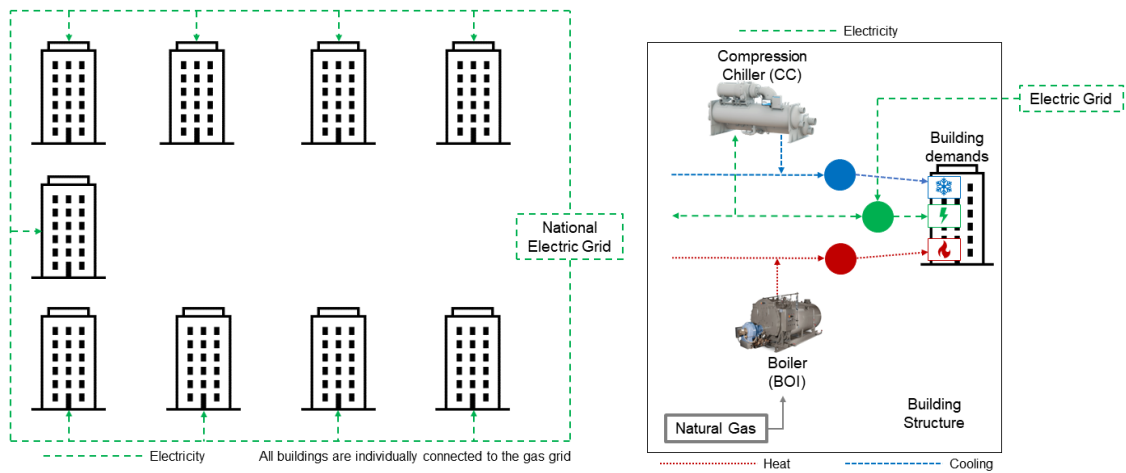


Figure 3.13 – Electricity connections for each building in the reference case (left). Structure of each building (right). Source: own elaboration.

Table 3.20 provides the main results obtained from the reference case scenario, i.e., the annual expenses due to operational, maintenance, and amortization costs as well as the total expenses regarding the total amount of electricity purchased from the grid and the total revenue from the electricity sold to the grid. These are the parameters used to calculate the total annual cost (4.6 M€/y). The total annual emissions are composed of emissions due gas and electricity consumption, and was equal to 7.1 kt CO<sub>2</sub>/y.

Table 3.20 – Main results from the reference case.

Building	Reference case						
	<sup>a</sup> Oper. cost (€/y)	<sup>b</sup> Maint. cost (€/y)	<sup>c</sup> Amort. cost (€/y)	<sup>d</sup> Total E <sub>P</sub> cost (€/y)	<sup>e</sup> Total E <sub>S</sub> revenue (€/y)	<sup>f</sup> Oper. CO <sub>2</sub> emissions (kg CO <sub>2</sub> /y)	<sup>g</sup> E <sub>P</sub> CO <sub>2</sub> emissions (kg CO <sub>2</sub> /y)
1. Town Hall	55,371	916	7027			131,588	
2. Theater	84,798	1863	25,183			201,520	
3. Library	46,863	748	5207			111,370	
4. Primary School	82,934	927	5926			197,091	
5. Retirement home	57,027	984	5147	1,515,710	0	135,524	301,520
6. Museum	34,653	545	4161			82,351	
7. Hospital	2,146,675	26,943	110,397			5,101,509	
8. Secondary School	322,458	3604	29,243			766,313	
9. Swimming Pool	32,283	361	2503			76,720	
<b>Total</b>	2,863,062	36,891	194,794	1,515,710	0	6,803,986	301,520
	(A)	(B)	(C)	(D)	(E)	(F)	(G)
<b>TOTAL</b>	4,610,457 €/y (A+B+C+D-E)					7,105,506 kg CO <sub>2</sub> /y (F+G)	

<sup>a</sup> Total annual operation cost

<sup>b</sup> Total annual maintenance cost

<sup>c</sup> Total amortization cost

<sup>d</sup> Total annual electricity purchase expenses (for all buildings)

<sup>e</sup> Total annual electricity selling revenue (for all buildings)

<sup>f</sup> Total annual operation CO<sub>2</sub> emissions

<sup>g</sup> Total annual CO<sub>2</sub> emissions due to electricity purchased

### 3.5 Single-Objective optimization

Before diving into the multi-objective optimization analysis, this section provides the results of the objective functions analyzed separately. Such results offer essential insights when (i) compared to the results of the reference case, and (ii) compared between themselves (which is a preliminary step towards the multi-objective optimization).

Table 3.21 and Table 3.22 provide the main results obtained by separately evaluating the objective functions, i.e., total annual cost and total annual CO<sub>2</sub> emissions. Then, sections 3.5.1 and 3.5.2 present both analysis in a more detailed way.

Table 3.21 – Main results from the optimal economic solution.

Building	Optimal economic solution							
	<sup>a</sup> Oper. cost (€/y)	<sup>b</sup> Maint. cost (€/y)	<sup>c</sup> Amort. cost (€/y)	<sup>d</sup> Total EP cost (€/y)	<sup>e</sup> Total ES revenue (€/y)	<sup>f</sup> Oper. CO <sub>2</sub> emissions (kg CO <sub>2</sub> /y)	<sup>g</sup> EP CO <sub>2</sub> emissions (kg CO <sub>2</sub> /y)	<sup>h</sup> ES CO <sub>2</sub> emissions (kg CO <sub>2</sub> /y)
<b>1. Town Hall</b>	4586	413	17,740			10,898		
<b>2. Theater</b>	121,985	7814	65,829			384,258		
<b>3. Library</b>	0	104	7180			0		
<b>4. Primary School</b>	171	2	4043			405		
<b>5. Retirement home</b>	902	251	8670	1,495,991	0	2143	4,659,527	0
<b>6. Museum</b>	817	19	4357			1942		
<b>7. Hospital</b>	701,512	43,006	147,153			2,203,912		
<b>8. Secondary School</b>	421	1038	27,918			1001		
<b>9. Swimming Pool</b>	0	1039	28,435			0		
<b>Buildings pipelines</b>	0	0	79,021	-	-	-	-	-
<b>Central unit</b>	0	0	355,797	0	0	0	0	0
<b>Cent. unit pipelines</b>	0	0	15,056	-	-	-	-	-
<b>Total</b>	830,394	53,686	761,199	1,495,991	0	2,604,559	4,659,527	0
	(A)	(B)	(C)	(D)	(E)	(F)	(G)	(H)
<b>Obj. functions</b>	<b>3,141,270 €/y (A+B+C+D-E)</b>					<b>7,264,086 kg CO<sub>2</sub>/y (F+G-H)</b>		

<sup>h</sup> Total annual CO<sub>2</sub> emissions due to electricity sold

The other letters have the same meanings as described on Table 3.20

Table 3.22 – Main results from the optimal environmental solution.

Optimal environmental solution								
Building	<sup>a</sup> Oper. cost (€/y)	<sup>b</sup> Maint. cost (€/y)	<sup>c</sup> Amort. cost (€/y)	<sup>d</sup> Total E <sub>P</sub> cost (€/y)	<sup>e</sup> Total E <sub>S</sub> revenue (€/y)	<sup>f</sup> Oper. CO <sub>2</sub> emissions (kg CO <sub>2</sub> /y)	<sup>g</sup> E <sub>P</sub> CO <sub>2</sub> emissions (kg CO <sub>2</sub> /y)	<sup>h</sup> E <sub>S</sub> CO <sub>2</sub> emissions (kg CO <sub>2</sub> /y)
<b>1. Town Hall</b>	0	85	94,522			0		
<b>2. Theater</b>	90,779	5074	172,151			286,522		
<b>3. Library</b>	6708	506	82,200			19,485		
<b>4. Primary School</b>	18,729	1306	78,371			58,911		
<b>5. Retirement home</b>	77	112	54,794	1,280,394	87,595	183	3,737,743	740,102
<b>6. Museum</b>	0	89	60,385			0		
<b>7. Hospital</b>	530,277	30,668	222,308			1,658,485		
<b>8. Secondary School</b>	0	118	60,752			0		
<b>9. Swimming Pool</b>	114,378	6679	204,462			361,004		
<b>Buildings pipelines</b>	0	0	524,758	-	-	-	-	-
<b>Central unit</b>	0	0	1,129,348	0	0	0	0	0
<b>Cent. unit pipelines</b>	0	0	17,564	-	-	-	-	-
<b>Total</b>	760,948	44,637	2,701,615	1,280,394	87,595	2,384,590	3,737,743	740,102
	(A)	(B)	(C)	(D)	(E)	(F)	(G)	(H)
<b>Obj. functions</b>	<b>4,699,999 €/y (A+B+C+D-E)</b>					<b>5,382,231 kg CO<sub>2</sub>/y (F+G-H)</b>		

<sup>a</sup> Meaning of the letters: see Table 3.20 and Table 3.21

### 3.5.1 Optimal economic solution

The annual economic and environmental costs for the optimal economic solution are presented in Table 3.21. The present section has the aim to dig deeper into the results by detailing, for each building, the following aspects: (i) which technologies were in fact installed, (ii) the installed capacity of each technology, (iii) the energy flows regarding primary energy sources, electricity, heating, and cooling, (iv) the distribution of electricity among the EC buildings, and (v) which buildings are interconnected through the DHCN pipelines. Figure 3.14 to Figure 3.22 provide visual aid, to analyze such aspects, by illustrating the optimal structure for each building.

#### 3.5.1.1 Optimal structure for each building

##### *Building 1 – Town hall*

Figure 3.14 depicts the optimal energy supply system structure for the Town hall. The reader should bear in mind that all energy flows are annual values. As observed, only the ABS, MGT, and ICE were not installed. It means that, in terms of electricity, the whole demand (building demand + HP + CC) is covered by PV (only 4%) and electricity coming from the distribution substation (DS). Most of the heat demand is produced by the HP due to three main reasons: (i) electricity is cheaper than natural gas, (ii) HP is more efficient than BOI, and (iii) there is a space limitation for installing more ST panels. When it comes to cooling, the entire demand is covered by CC (38%) and HP (62%).

In this solution, the Town hall was the only building that does not have any heating or cooling pipeline connection with other building(s). According to the results data and observing the buildings' location in Figure 3.4, the solution went in the direction of concentrating a substantial amount of heat production in building 2 (Theater) and distributing that heat to buildings 3, 4, 5, and 6 through the DHN pipelines. Building 1 (Town hall) was probably left behind due to the distance between it and building 2, i.e., installing the pipelines between them and accounting for the heat losses would be more costly than the self-production scenario for building 1.

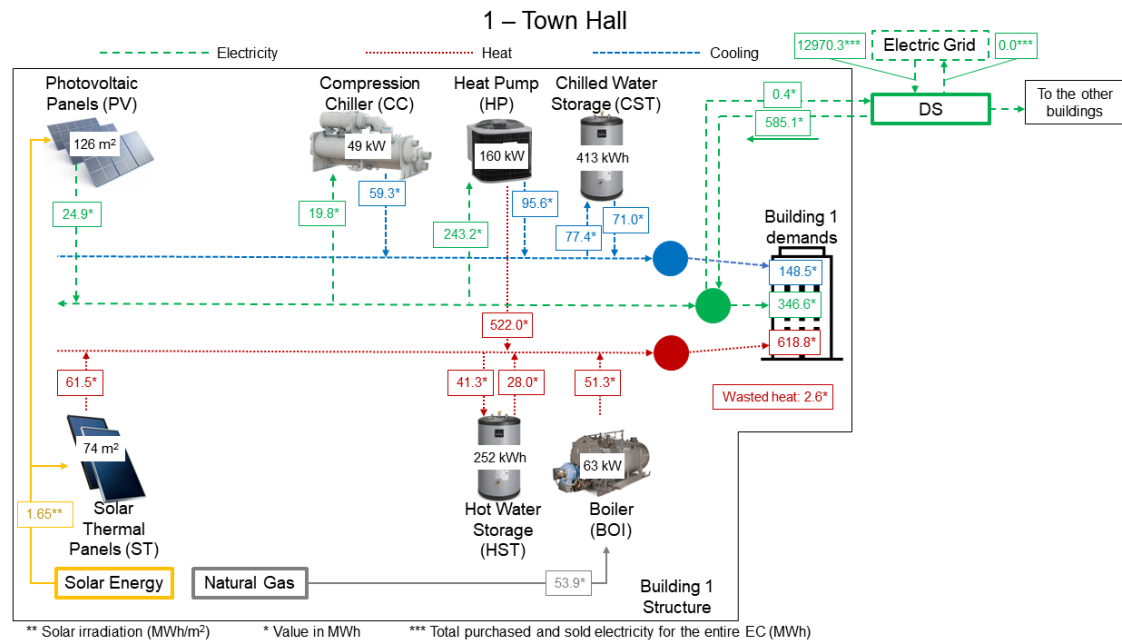


Figure 3.14 – Installed capacities and annual energy flows for building 1 (Town Hall).

### *Building 2 – Theater*

Observing Figure 3.4, it is possible to note that building 2 is located between two couple of buildings: 3 and 4 to the north and 5 and 6 to the south. Moreover, the distances between building 2 and the mentioned buildings are less than 300 meters. Therefore, this group of buildings has the opportunity to cover their energy needs by sharing thermal energy (heating and cooling) through the DHCN pipelines since there will be not so long installed pipelines length (as between buildings 1 and 2) and, consequently, heat losses will be lower.

As observed in Figure 3.15, building 2 does not have ABS, CC, or MGT, but it was granted the installation of two 140 kW ICEs. In this way, the group of buildings are benefited not only by the self-generated electricity, but also by the substantial amount of cogenerated heat. Besides, focusing in the heat balance (same figure), it is possible to note three main aspects: (i) when it comes to the solar technologies, the optimal solution prioritized ST over PV (indicating that, in this case, building 2 need to produce large amounts of heat), (ii) the HP is responsible for 65% of the total heat produced (indicating the search for more efficient ways to produce the heat), and (iii) 71% of the total produced heat is sent to the buildings 3 and 6.



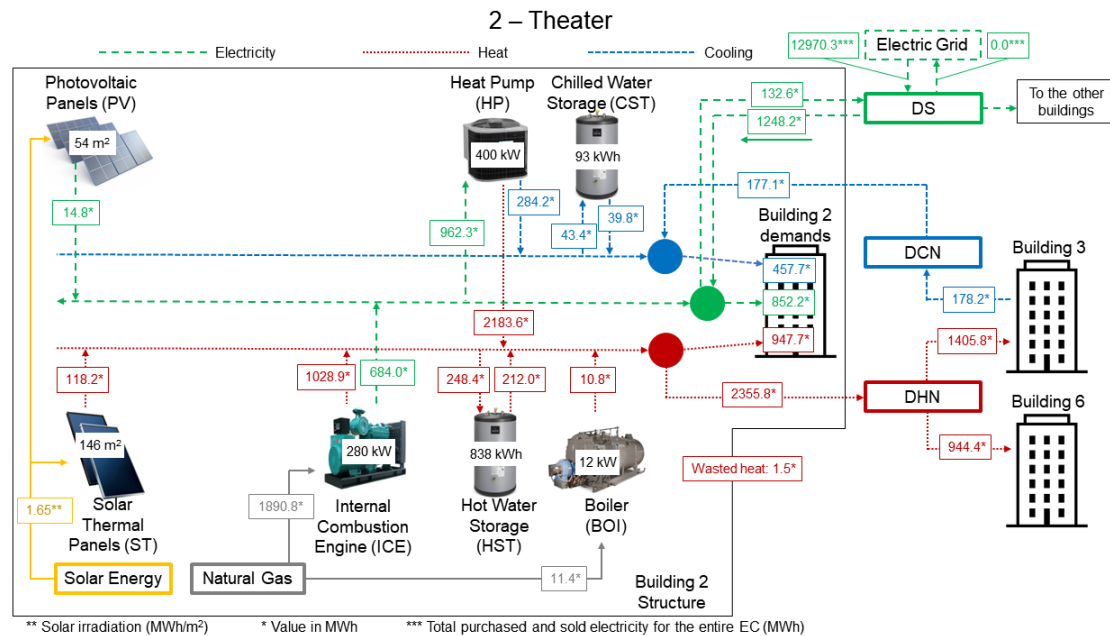


Figure 3.15 – Installed capacities, annual energy flows, and DHCN connections for building 2 (Theater).

Another interesting detail regards the cooling balance. The only technology responsible for producing the building 2 demanded cooling is the HP. Since building 2 is allowed to install up to four 100 kW HPs, the other options would be either installing a CC and /or an ABS. Installing a CC would imply less electricity sent to the DS, which would have to be produced in another building or purchased from the grid. Installing an ABS would imply an additional heat demand or less heat being sent to buildings 3 and 6. Therefore, the optimal solution took advantage of installing a HP in building 3 (which has a lower cooling demand) by connecting both buildings (2 and 3) through a DCN pipeline. Since these buildings are only 80 meters away from each other, the cost of installing the pipes and the low heat losses would be more attractive from the economic viewpoint.

### *Building 3 – Library*

Figure 3.16 illustrates the optimal structure of building 3, which includes only PV panels, CC, HP, and CST. Also, there are heating and cooling pipelines with buildings 2 and 4. As seen, the installed HP supplies only 10% of the total Library heat demand, while providing more than double the demanded cooling. This is because part of the produced cooling is sent to building 2. Moreover, taking into account the heat provided by the HP,

only 34% of the heat received from building 2 is consumed by building 3; the remaining goes to building 4. The available area for installing solar technologies is fully occupied by PV panels. However, they provide only 6% of the total demanded electricity.

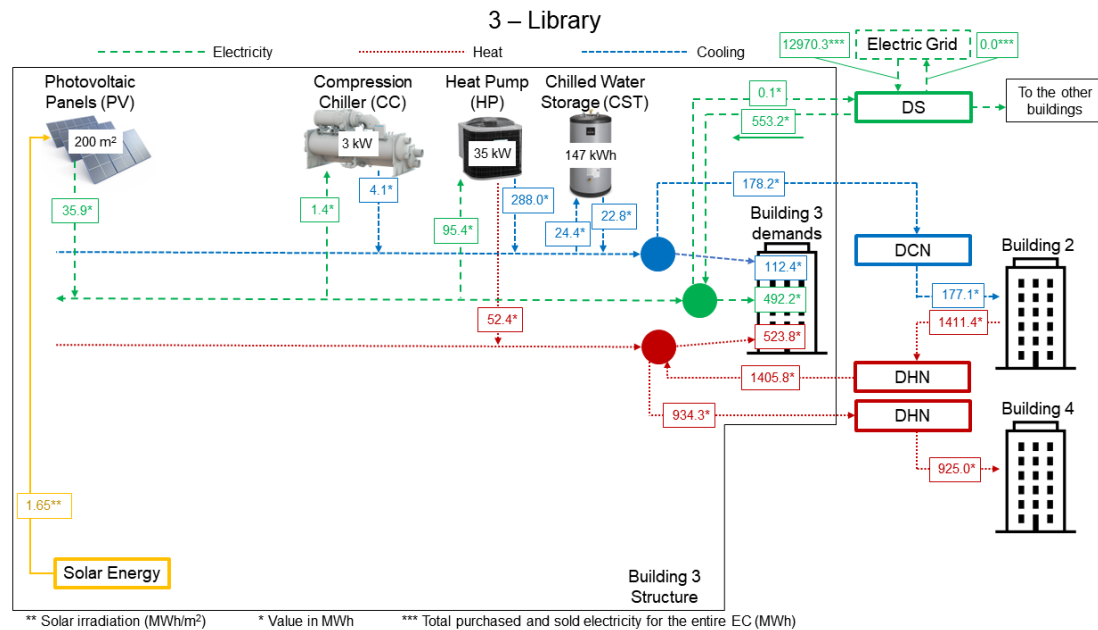


Figure 3.16 – Installed capacities, annual energy flows, and DHCN connections for building 3 (Library).

#### *Building 4 – Primary school*

First, this building has no cooling demand (Figure 3.17) since the school is closed during summer vacations. Moreover, this school has one of the lowest electricity demands among the EC buildings and, for that reason, the electricity supply is focused on (i) self-production through PV panels (49% of the total demand), and (ii) electricity imported from DS. Also, during some periods of the year, especially in summer, the building is able to send part of the self-produced electricity (or even the full amount in June, July, and August) to the DS. For what concerns heat demand, the heat received from building 3 covers almost all the heat needs, with only a tiny amount left for the BOI.

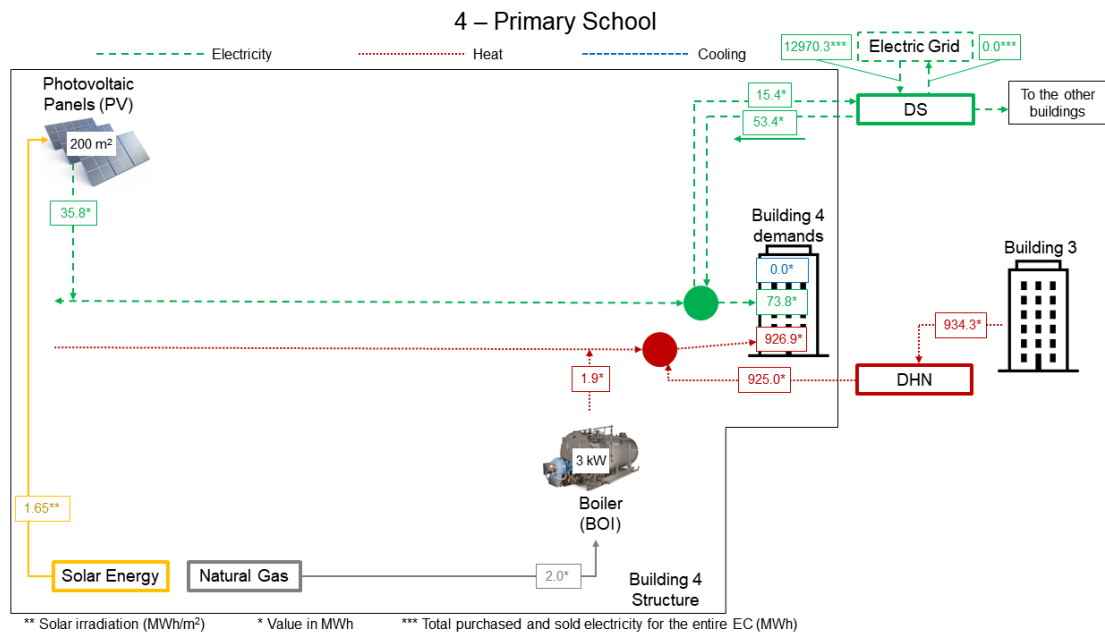


Figure 3.17 – Installed capacities, annual energy flows, and DHN connection for building 4 (Primary school).

*Building 5 – Retirement home*

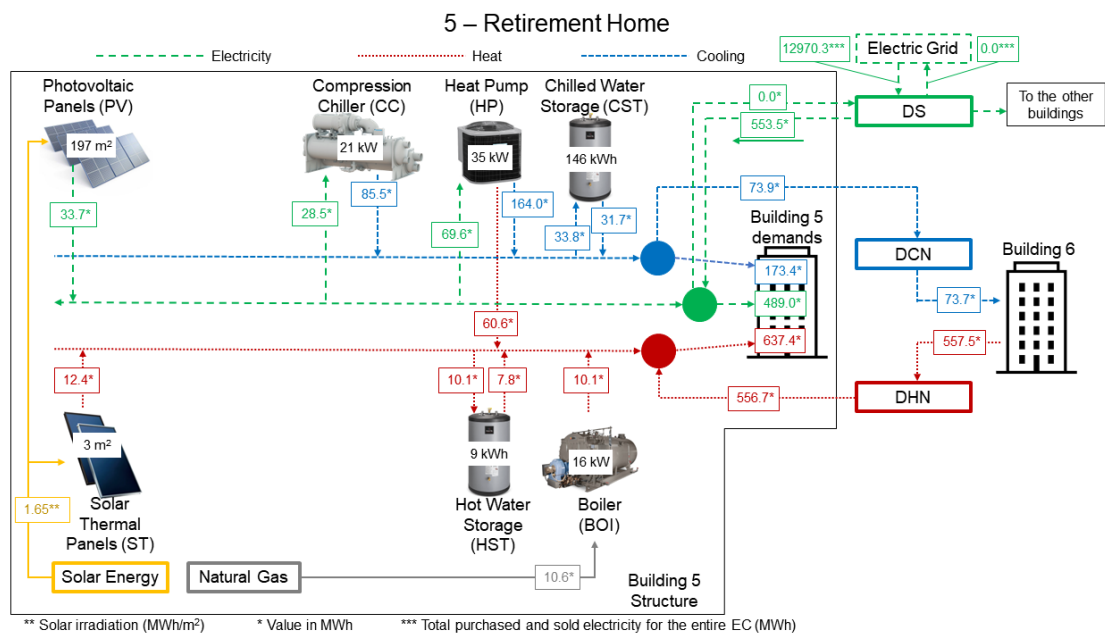


Figure 3.18 – Installed capacities, annual energy flows, and DHCN connection for building 5 (Retirement home).

The optimal structure of building 5 is illustrated through Figure 3.18. As observed, 87% of its heat demand is received from building 6. This explains the fact that no MGT or ICE was installed and, hence, no ABS. The installed CC and HP capacities produce 44% more cooling than the internal demand, which surplus is sent to building 6 (which is only 30 meters away). For what concerns the electricity balance, 6% is covered by PV panels while the major part is imported from the DS.

### Building 6 – Museum

The museum optimal structure is pictured through Figure 3.19. As noted, the only installed technology for cooling production is the CC, which contributes with only 7% of the cooling demand. The remaining amount comes from building 5 as previously explained. For what concerns solar technologies, the solution prioritized the installation of PV panels, which contribute with 43% of the museum electricity demand. The self-produced heat (ST and BOI) constitutes only 3% of the total heat demand of building 6. The remaining portion is received from building 2. However, only 40% of that heat remains at the museum. The other part is sent to building 5.

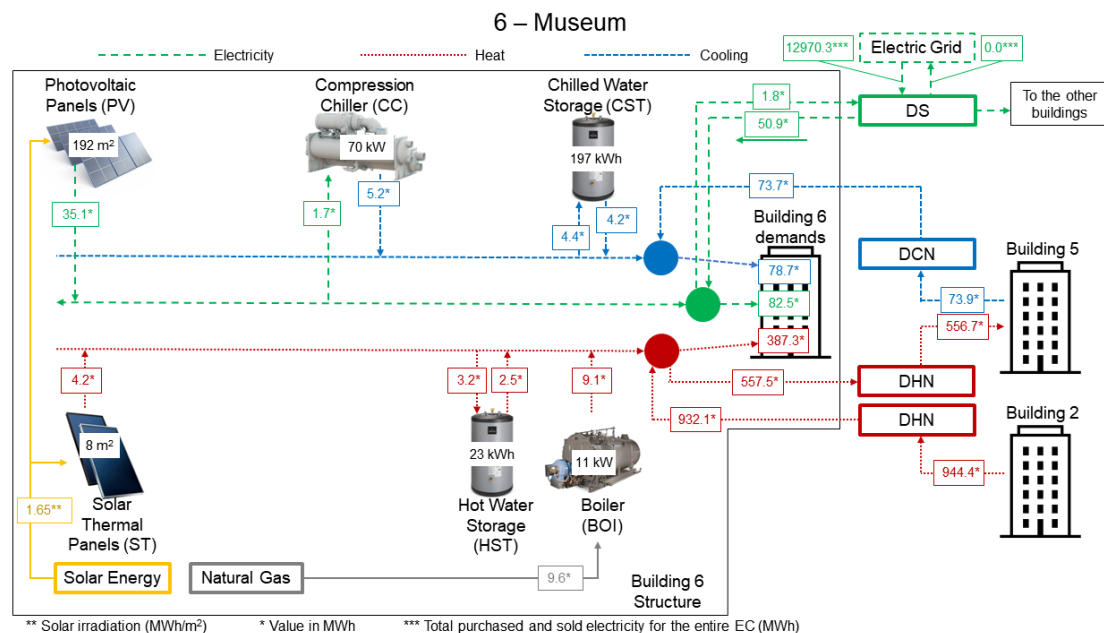


Figure 3.19 – Installed capacities, annual energy flows, and DHCN connection for building 6 (Museum).

### Building 7 – Hospital

Building 7 is the greatest energy consumer in the EC. It is responsible for 75.4%, 74.9%, and 60.3% of the total electricity, heating, and cooling demands of the EC, respectively. As observed in Figure 3.20, the only technologies not installed were MGT and ABS. The following installed technologies have reached their full allowed capacity (or have come very close): (i) solar technologies, where ST panels were prioritized by covering 70% of the available area, (ii) ICE, with four 200 kW installed units (max. six), (iii) HP, with six 100 kW installed units, and (iv) HST, with 4000 kWh.

Focusing on the cooling balance, the total cooling demand is covered by the CC and HP, with the latter contributing with 93% of the demand. The most likely reasons for a full HP installed capacity are (i) the hospital has an extremely high heat demand and therefore it needs all self-produced heat available, and (ii) installing an ABS would require an additional amount of heat, and the cooling produced would not be obtained as efficiently as that obtained by means of the HP.

When it comes to the electricity balance, it is worth noting that (i) self-produced electricity covers 35% of the total electricity demand (the remaining part comes from the DS), (ii) the solution could have installed two additional 200 kW ICE units to obtain not only more electricity, but also more heat.

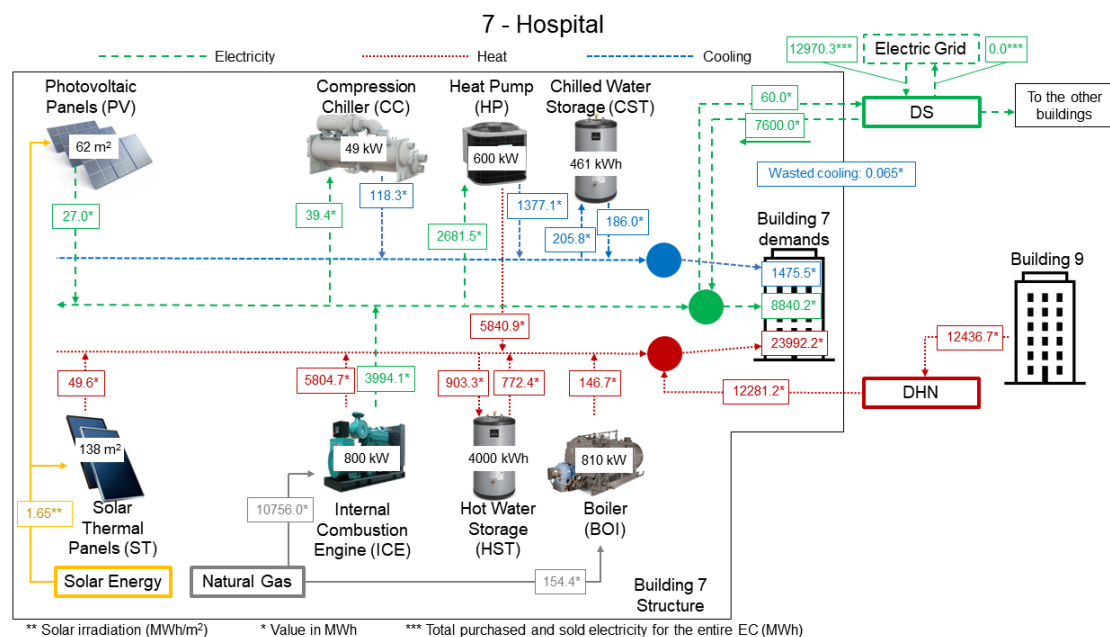


Figure 3.20 – Installed capacities, annual energy flows, and DHN connection for building 7 (Hospital).

The heat balance shows that self-produced heat covers about half (49%) of the total heat demand. In the case of one additional ICE installed unit, such percentage would be higher. However, the cost of purchasing, maintaining, and operating this additional unit would be higher than importing heat from another building. Moreover, most part of the heat received through the DHN pipeline comes from the central unit, where it is produced by means of ST panels.

### *Building 8 – Secondary school*

The secondary school (Figure 3.21) has no cooling demand. With regard to electricity balance, only 2.5% of the total electricity demand is covered by PV panels, while the remaining part is imported from the DS. Six HP units of 80 kW each are installed to cover 69% of the total heat demand of building 8 while the remaining part by the heat coming from the central unit. The central unit supplies a considerable amount of heat, derived from solar thermal panels, which is internally used by building 8 (22%) and the remaining heat is sent to building 9.

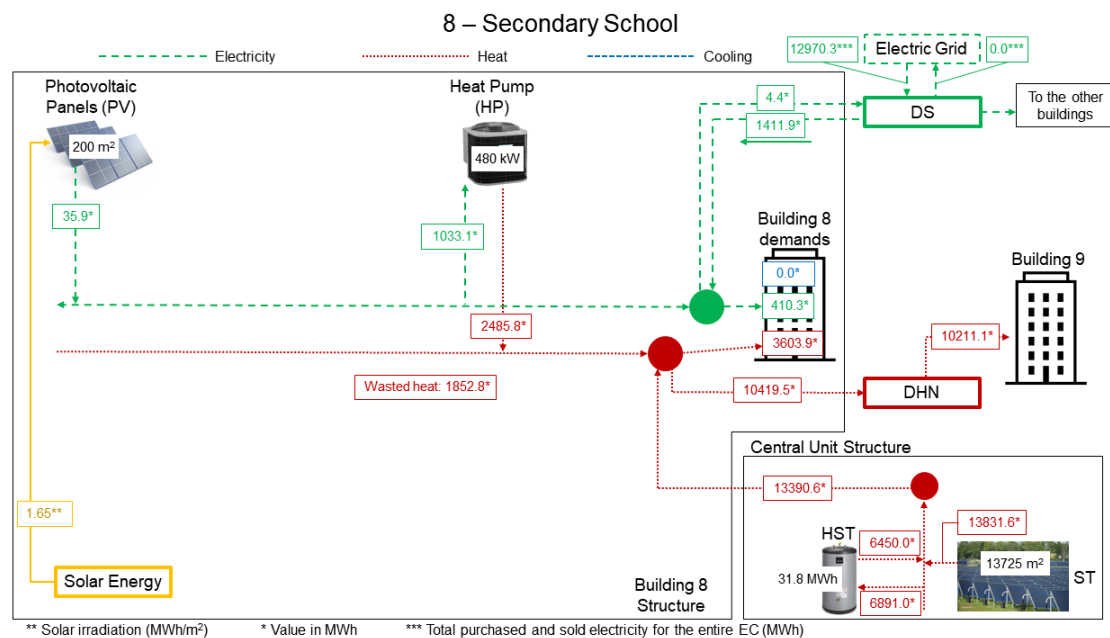


Figure 3.21 – Installed capacities, annual energy flows, and DHN connection for building 8 (Secondary school).

*Building 9 – Swimming pool*

The swimming pool has no cooling demand (Figure 3.22) either since it is closed during the summer vacation period. The main highlight for this building is the installation of five 100 kW HP units, with an annual heat production of 2609.1 MWh which is seven times higher than the heat demand of building 9. Such additional amount of heat covers the internal heat demand and complements the heat coming from building 8 in order to be sent to building 7. The main reasons for such an additional amount of heat production are:

- As observed in Table 3.9, the only possible DHCN pipeline connections for building 7 (hospital) are with buildings 4 and 9. Building 4 is 1400 meters away from building 7, a fact that does not make it economically attractive. Therefore, the only remaining option for building 7 is building 9 (250 meters away).
- Since the optimal solution installed all permitted HP capacity (six 100 kW units) for building 7 (hospital), the only left options to produce more heat (within building 7) would be higher BOI capacity, one additional ICE unit, and/or MGT. However, these options are way more expensive, than HP, in terms of investment and operation costs. Therefore, installing these technologies in building 7 would be more expensive than installing additional HP capacity in building 9 and sending the heat to building 7.

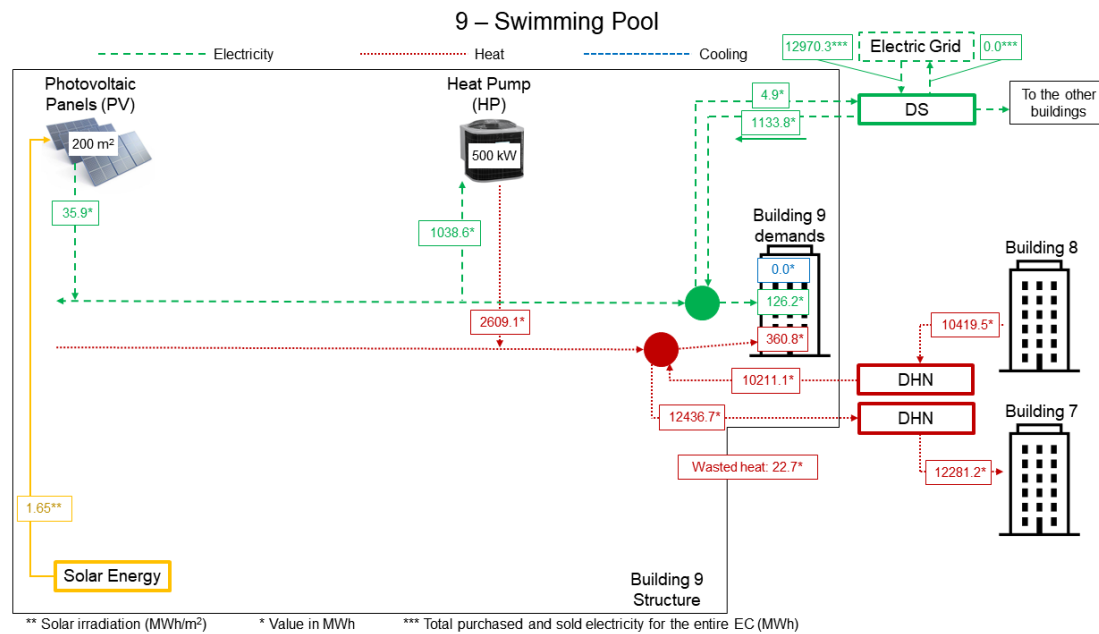


Figure 3.22 – Installed capacities, annual energy flows, and DHN connection for building 9 (Swimming pool).

### 3.5.1.2 Energy balances for the entire EC

This section aims to provide the reader with a graphic visualization of the electricity, heat, and cooling balances for the entire EC and for one typical day in January and July. It should be noted that the following balances are the results of the energy balances of all buildings together. Obviously, in this way there is no possibility to evaluate the energy magnitudes within each building, but it is possible to have an idea about (i) which technologies play the most important roles in the EC, (ii) knowing in what extent renewable energy source (solar) is supporting the energy demands fulfilment, and (iii) the differences between the energy demand profiles in January (winter) and July (summer). The graphics with the energy demand profiles for each building are provided in chapter 5 since they are one of the key elements for the marginal cost analysis and interpretation.

Figure 3.23 provides the electricity balances derived from two working days: one in January and the other one in July. It is possible to note that ICE and HP play an essential role especially during the winter. Since there is a large heat demand during this period, using a cogeneration system becomes economically attractive due to the fact that, providing the two products (electricity and heat), the efficiency increases to around 90%.



The HP electricity demand also constitutes an important portion of the total electricity demand due to the fact that its heat production is economically attractive. During summer (July – working day), the electricity production from ICE becomes less attractive since there is no heat demand to be covered. Instead, HP electricity demand continues making up an important part of the total electricity demand, since during this period it will have to cover most of the cooling demand. In the economic optimal solution, the EC does not sell electricity at any moment during the entire year. However, it purchases from the grid 72% of the total electricity demand (including CC + HP demands).

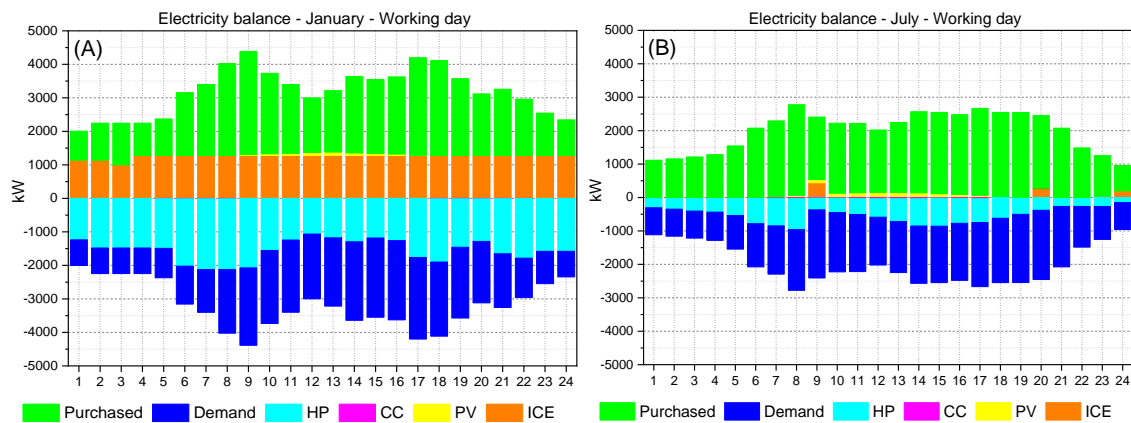


Figure 3.23 – EC electricity balance for a working day in January (A) and a working day in July (B).

The total EC heat balance is shown in Figure 3.24. As seen, winter period is characterized by a substantial contribution of ICE and HP (Figure 3.24 A). Also, the heat received from central unit – which is exclusively produced by solar thermal panels (STc) and supported by hot water storage (HSTc) (Figure 3.24 B) – plays an important role to cover the total EC heat demand. The boiler only comes to place when the mentioned technologies are at full load and there is still a missing portion of the heat demand to be covered, as observed in hours 7 and 8 of Figure 3.24 (A).

In summer period, as explained in section 3.2.2.2, the EC buildings (especially the hospital) still demand a certain heat demand level due to sanitary hot water needs (Figure 3.24 C). During the same period, the central unit heat production is naturally higher than in cold months (Figure 3.24 D) and, for that reason, is covers most of the EC total heat

demand. At hours 9, 20, and 24 (Figure 3.24 C), the heat is partially covered by ICE since its electricity production is required at the same times (Figure 3.24 B).

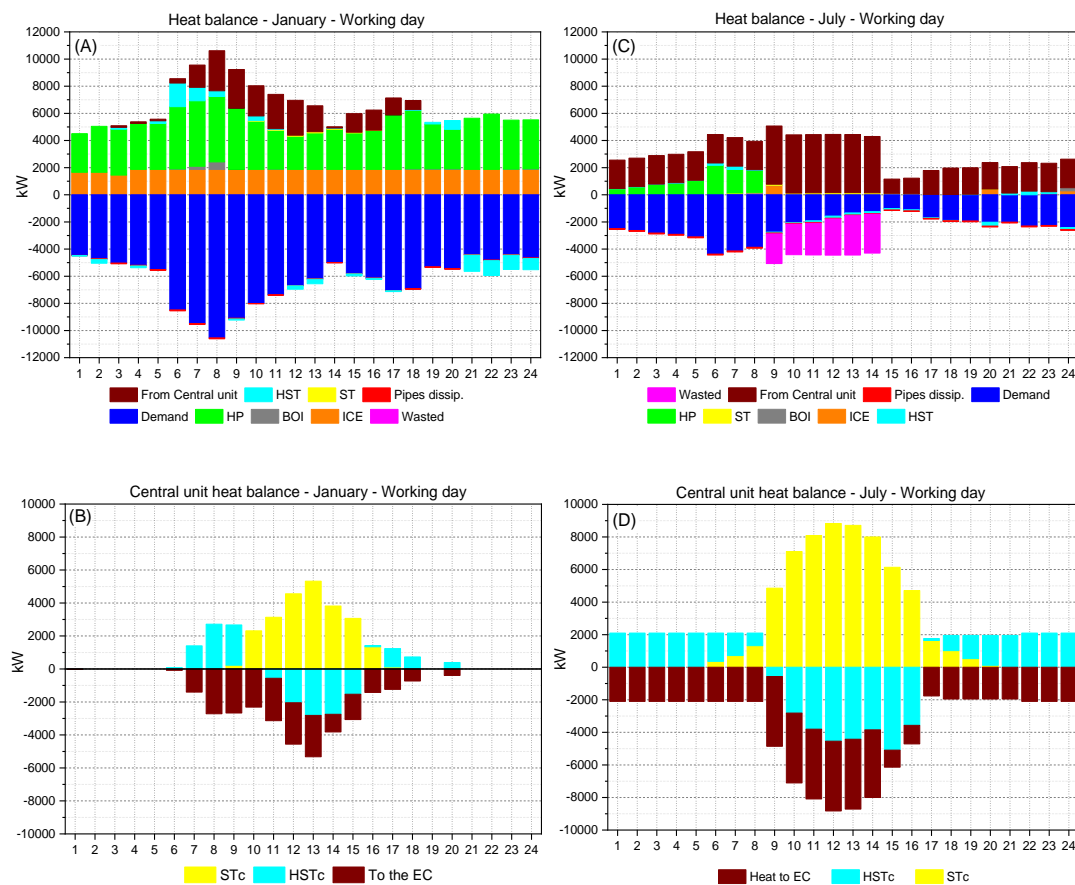


Figure 3.24 – EC and central unit heat balance for a working day in January (A) and (B) and a working day in July (C) and (D).

The cooling balance charts are presented in Figure 3.25. First, as explained on section 3.2.2.3, the hospital has a cooling demand even during the winter. A tiny portion of this demand is covered by CC while the major part is fulfilled by running the HP at hour 9, storing cooling in the CST, and using it throughout the day (Figure 3.25 A).

Figure 3.25 B demonstrates the higher cooling demand during summer and how the installed HP capacity plays a crucial role in covering it. Indeed, since there are no installed ABS, the only two ways to produce the needed cooling is either by CC and/or HP. However, bearing in mind that the HP capacity can be used also during the winter, the

only sense in installing CC is for covering summer cooling peak demands when the HP is at full load.

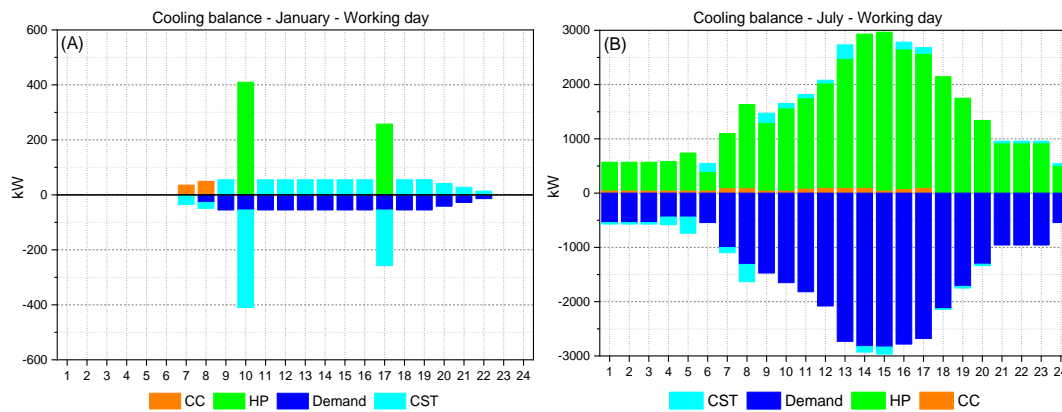


Figure 3.25 – EC cooling balance for a working day in January (A) and a working day in July (B).

### 3.5.2 Optimal environmental solution

The annual economic and environmental costs for the optimal environmental solution are presented in Table 3.22. This section has the purpose to provide some of the results regarding buildings' energy supply system structure and EC energy balances. For the sake of brevity, this section will present the optimal structure of only two buildings. The buildings chosen were the theater (building 2) and the hospital (building 7), as they received the largest energy supply system structures in the optimal economic solution. It is worth noting that, differently from the optimal economic solution, the present solution resulted in a total annual amount of electricity sold to the grid in the order of 2 GWh, which corresponded to a revenue of 87.6 k€.

#### 3.5.2.1 Optimal structure of selected buildings

##### *Building 2 – Theater*

Figure 3.26 presents the optimal energy supply system structure for building 2 when the EC is optimized with the objective to minimize CO<sub>2</sub> emissions only. At a first glance and comparing with Figure 3.15, it is possible to observe that the optimal environmental solution resulted in more installed technologies, higher installed capacity levels, DHCN

connections with two times more buildings, four times more DCN pipelines, and two times more DHN pipelines.

Focusing on the electricity balance, 71% of the self-produced electricity is sent to the DS, which demonstrates that during some periods of the year, the optimization model finds it more attractive to send that self-produced electricity to the DS. It happens mainly during the winter months when the heat demand is higher. Moreover, 84% of the total electricity demanded by building 2 is imported from the DS.

The internal cooling production is made by the ABS and CC, with support of the CST. However, 88% of the cooling demand (including the portion sent to building 1) is covered by the cooling imported from buildings 3, 5, and 6.

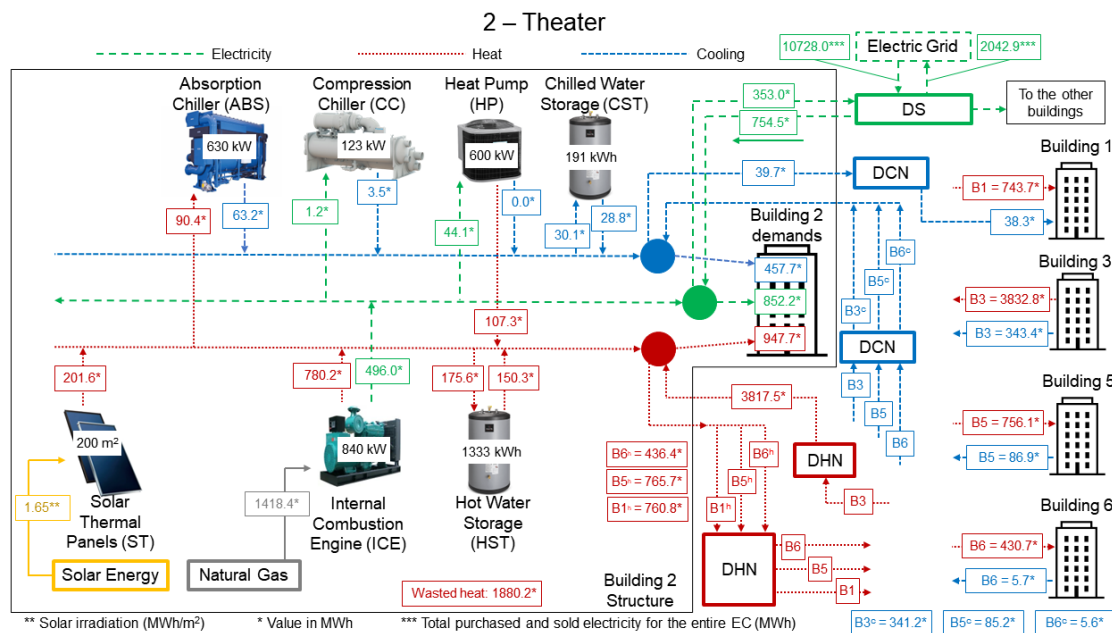


Figure 3.26 – Installed capacities, annual energy flows, and DHCN connections for building 2 (Theater). Optimal environmental solution.

In the case of the heat balance, 78% of the total annual heat demand (including the part sent to buildings 1, 5, and 6) is covered by heat coming from building 3. If such heat is traced back to the place where it was produced, it is possible to arrive at the central unit. The heat produced by solar thermal panels in the central unit is sent to building 8 which covers its own heat demand and sends the remaining heat to buildings 4 and 8. A major

part of the heat supplied to building 4 is sent to buildings 3 and 7. Building 3, in its turn, sends 85% of the received heat to building 2.

### Building 7 – Hospital

As mentioned in section 3.5.1.1, the hospital is responsible for most of the EC energy consumption. With almost 24 GWh of heat demand, the optimization model focused on the installation of almost all heat-producer technologies and with high installed capacities (Figure 3.27).

For what concerns the electricity balance, 72% of the total electricity demand is imported from the DS, while 11% of the self-produced electricity is sent to the DS.

Although the building has ABS, CC, and HP to generate cooling, 89% of the cooling is received through the DCN pipelines from buildings 4 and 9. A similar situation happens for the heat balance since 77% of building 7 heat demand is covered by the heat imported from buildings 4 and 9. In both cases, the origin of the heat is the solar thermal panels production in central unit.

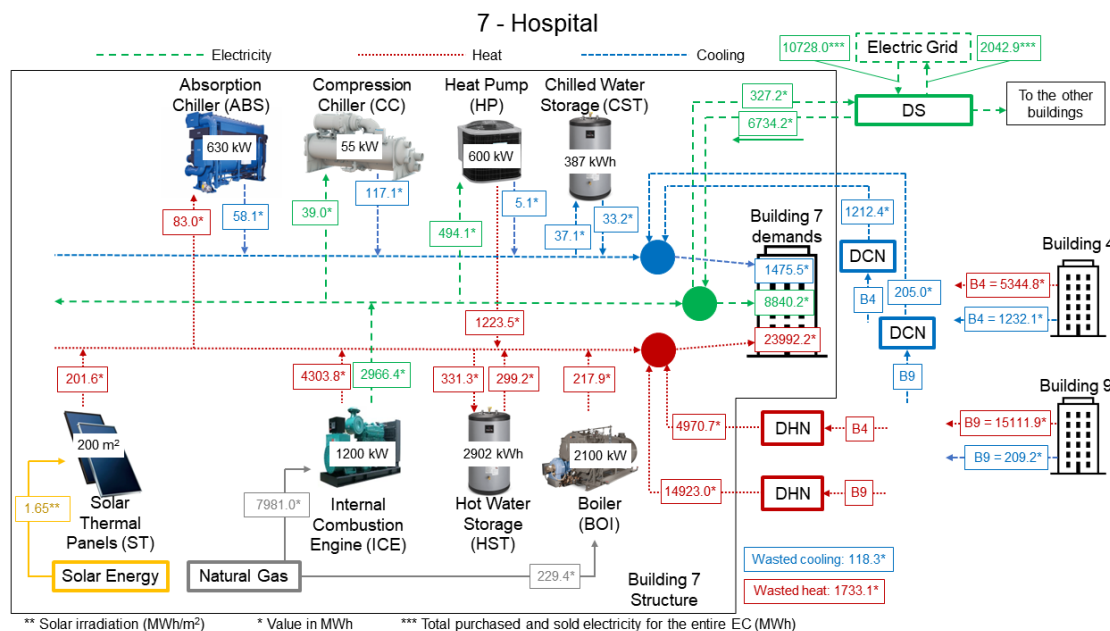


Figure 3.27 – Installed capacities, annual energy flows, and DHCN connections for building 7 (Hospital). Optimal environmental solution.

### 3.5.2.2 Energy balances for the entire EC

This section is analogous to section 3.5.1.2 and has the goal to offer the reader with a graphic picture of the electricity, heat, and cooling balances for the entire EC (one typical day in January and July), based on the optimal environmental solution. The following balances are also the results of the energy balances of all buildings together. In this way, it is possible to have an idea about (i) which technologies play the most important roles in the EC, (ii) knowing in what extent renewable energy source (solar) is supporting the energy demands fulfilment, and (iii) the differences between the energy demand profiles in January (winter) and July (summer).

Figure 3.28 provides the electricity balance for a typical winter and summer day. From Figure 3.28 (A) it is possible to note that (i) most of the electricity is covered by ICEs, (ii) most of the electricity is sold at non-working hours, and (iii) a small amount of electricity is purchased from hour 10 to hour 19. In fact, this solution installed ICE in the buildings 2, 3, 4, 7, and 9, and they run mainly during the cold months. HP is the other main way to produce heat in the EC, however the solution prioritized the cooling production during hot months. Moreover, there is a huge amount of ICE heat production in January which, together with the heat from central unit, covers the majority of the January heat demand. That is why electricity demand from HP does not appear in Figure 3.28 (A). Instead, Figure 3.28 (B) provides the electricity balance for a summer day, and it is possible to see a HP demand.

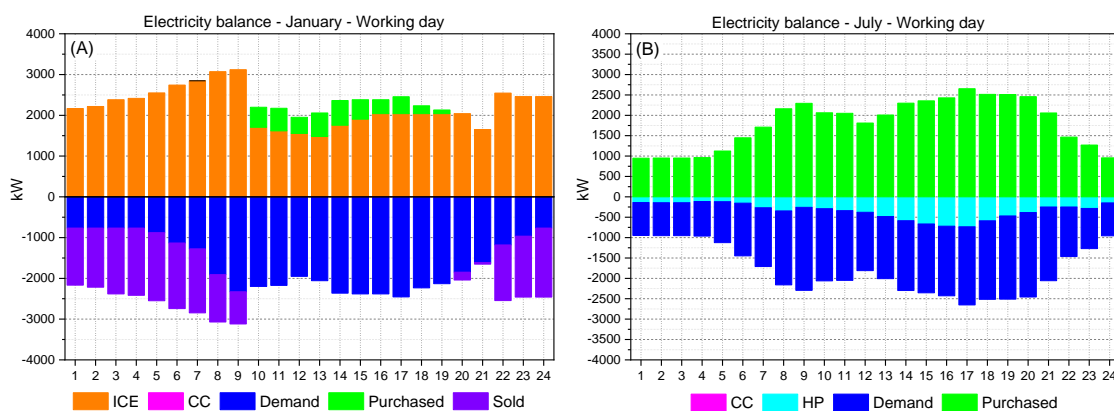


Figure 3.28 – Optimal environmental solution: EC electricity balance for a working day in January (A) and a working day in July (B).

Figure 3.29 shows the graphics of heat balances for EC and central unit. As observed, a major part of the demand is covered by ICE and heat from the central unit. In this solution the central unit is able to provide a higher amount of heat since there is more STc and HSTc installed capacity. As explained before, the HP does not produce heat during the period illustrated by Figure 3.29 (A) because there is already a large amount of heat being cogenerated by ICE and produced by solar thermal panels in the central unit. Therefore, from an environmental viewpoint, it would not be so attractive producing heat from HP in that period.

During the summer, a huge amount of heat is produced in the central unit which, with the support of a hot water storage (HSTc) sends such heat to the EC (Figure 3.29 C). That heat covers almost the entire heat demand of the EC together with the solar thermal panels installed in the buildings (Figure 3.29 D). The total heat demand, in the same period, comprises also a small portion dedicated to the ABS, which covers a small percentage of the summer cooling demand (Figure 3.30 B).

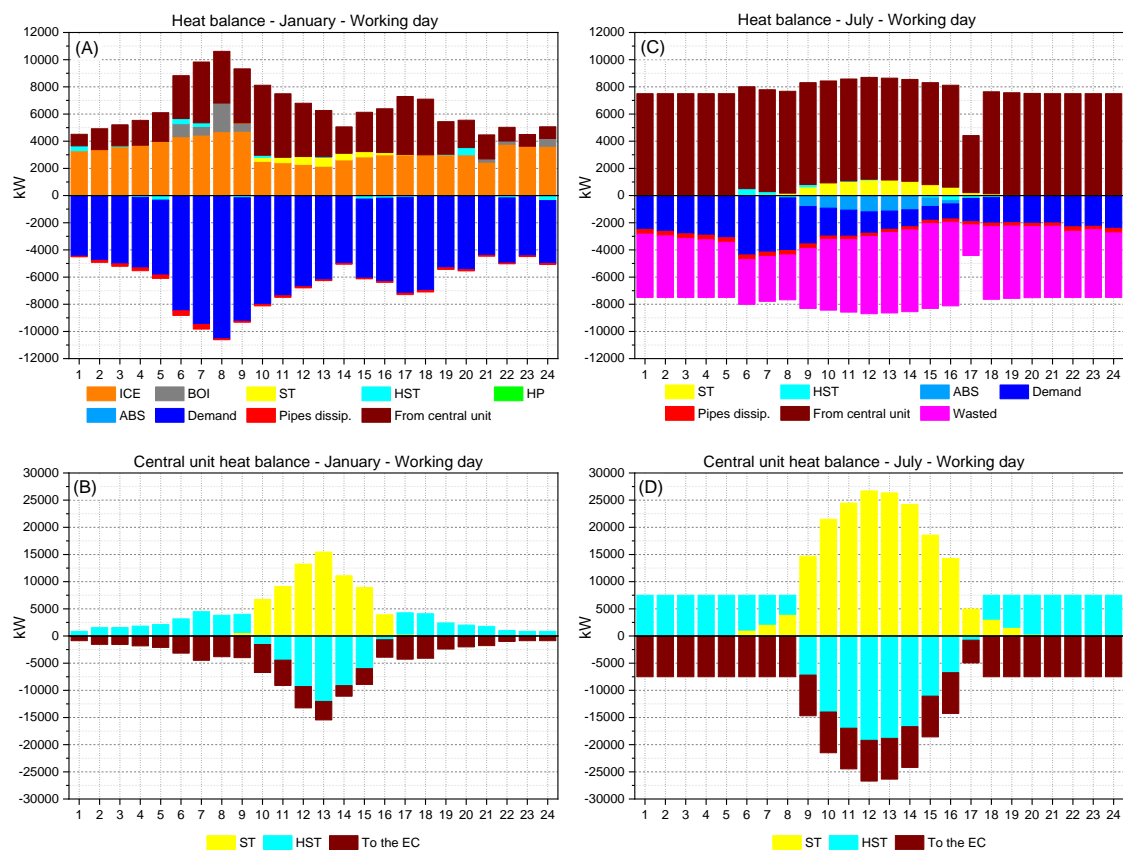


Figure 3.29 – Optimal environmental solution: EC and central unit heat balances for a working day in January (A) plus (B) and a working day in July (C) plus (D).

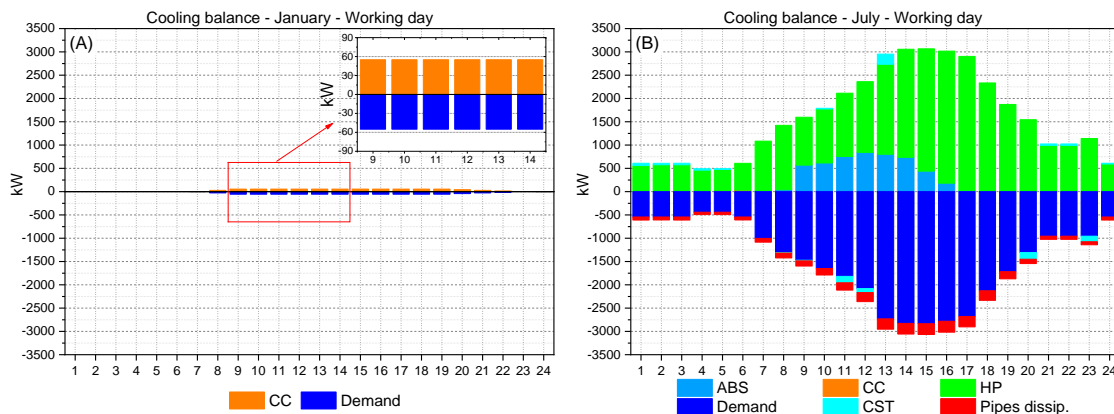


Figure 3.30 – Optimal environmental solution: EC cooling balances for a working day in January (A) and a working day in July (B).

Figure 3.30 provides the EC cooling balance for a typical day in winter and summer derived from the optimal environmental solution. Coherently with the electricity balance, in this solution there is no cooling produced by HP in January (Figure 3.30 A), as in the optimal economic solution. For this reason, the small cooling demand (from the hospital) is fully covered by CC. For a typical summer day (Figure 3.30 B), it is worth noting the differences between it and Figure 3.25 (B). At a first glance, the two main differences are the contribution of the ABS cooling and the pipelines heat dissipation. While the optimal economic solution did not install any ABS unit, the optimal environmental solution installed it in all buildings. Moreover, the optimal environmental solution way more DCN pipeline connections which increased considerably the heat losses into the cooling pipes.

### 3.6 Multi-Objective optimization

Real-world problems are rarely dependent on one objective only. Instead, they generally depend on two or more conflicting objectives. The resolution of such conflicting objectives, exemplified by the simultaneous minimization of total annual cost and total annual CO<sub>2</sub> emissions, is addressed through a multi-objective optimization approach. In this type of optimization, a singular optimal solution, satisfying both objectives, is not possible. Instead, a group of trade-off solutions forms the Pareto front, in which enhancing one objective requires compromising the other.



In this study, the  $\varepsilon$ -constraint method is employed to determine the solutions in the Pareto front. As explained in section 2.1.5, this method optimizes the single objective function, while upper (in the case of minimization) bounds ( $\varepsilon$ -constraints) are established for the remaining function. Then, the problem is iteratively solved for different  $\varepsilon$  values, yielding the trade-off solutions comprising the Pareto front.

By designating the total annual cost as the primary objective function, the secondary objective function is transformed into an inequality constraint, establishing an upper limit on the total annual CO<sub>2</sub> emissions. The single-objective optimization solutions detailed in section 3.5 delineate the boundaries of the Pareto front. As illustrated in Figure 3.31, the Pareto front is confined within an upper limit of 7.26 kt CO<sub>2</sub>/y (regarding the optimal economic solution) and a lower limit of 5.38 kt CO<sub>2</sub>/y (regarding the optimal environmental solution).

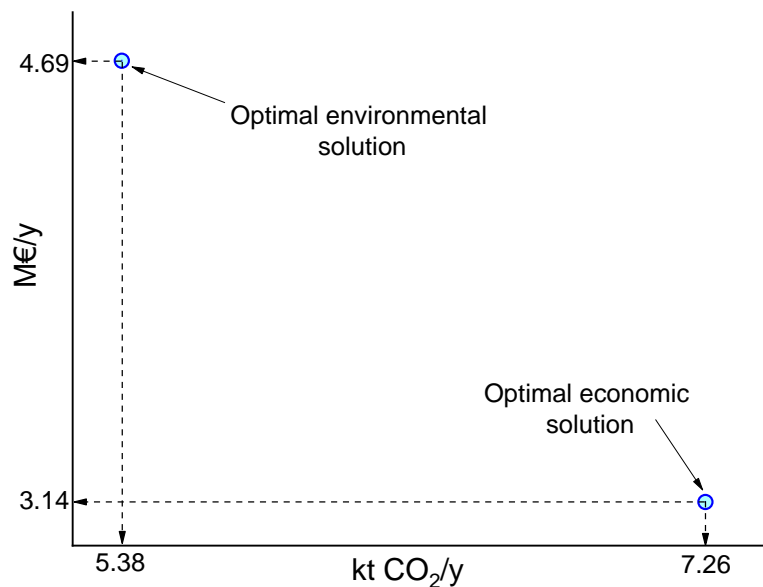


Figure 3.31 – Single-objective optimization solutions: boundaries of the Pareto front. Total annual costs in the vertical axis and total annual CO<sub>2</sub> emissions in the horizontal axis.

Table 3.23 presents the results derived from successively solving the EC model for different  $\varepsilon$  values. The process started with the optimal economic solution and went all the way to the other end of the Pareto front, i.e., the optimal environmental solution. In this case, the  $\varepsilon$  values were consecutively lower total annual CO<sub>2</sub> emissions and the

consequence was the Pareto front depicted in Figure 3.32 with 29 solutions and different energy supply system structures as well as installed capacities. As indicated in the same figure, there are four sets of solutions (*a*, *b*, *c*, and *d*) which will be explained in the following paragraph.

It is interesting noting that the EC buildings can be divided into two groups of buildings: Group I in the south and Group II in the north (Figure 3.33). The distances between buildings within each group are never more than 450 meters. However, the distance between these two groups of buildings can reach up to 1800 meters. It means more investment costs with pipelines and more heat losses, which consequently increases the overall operation cost. For that reason, the optimal economic solution (Figure 3.32) and the following ten solutions (solutions *a*) do not install any DHCN pipeline connection between the two groups of buildings. On the other hand, starting from solutions *b*, the optimization installs pipelines between the two groups of buildings. In both points, within solutions set *b*, a heat pipeline connection between buildings 8 and 4 is installed, which means that the heat produced by the solar thermal panels, in the central unit, starts to benefit not only buildings in Group II, but also the buildings in Group I.

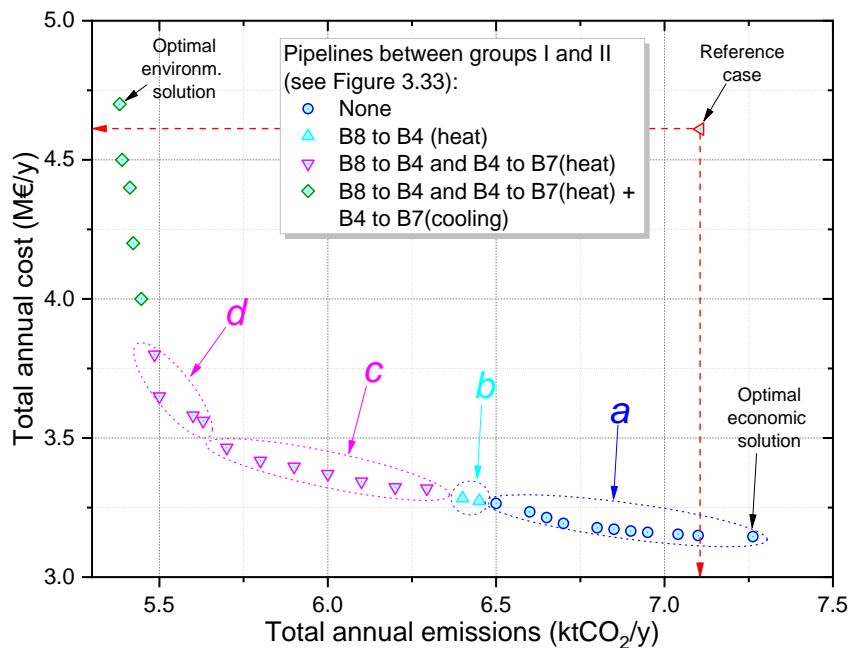


Figure 3.32 – Pareto front for the multi-objective optimization of the EC.

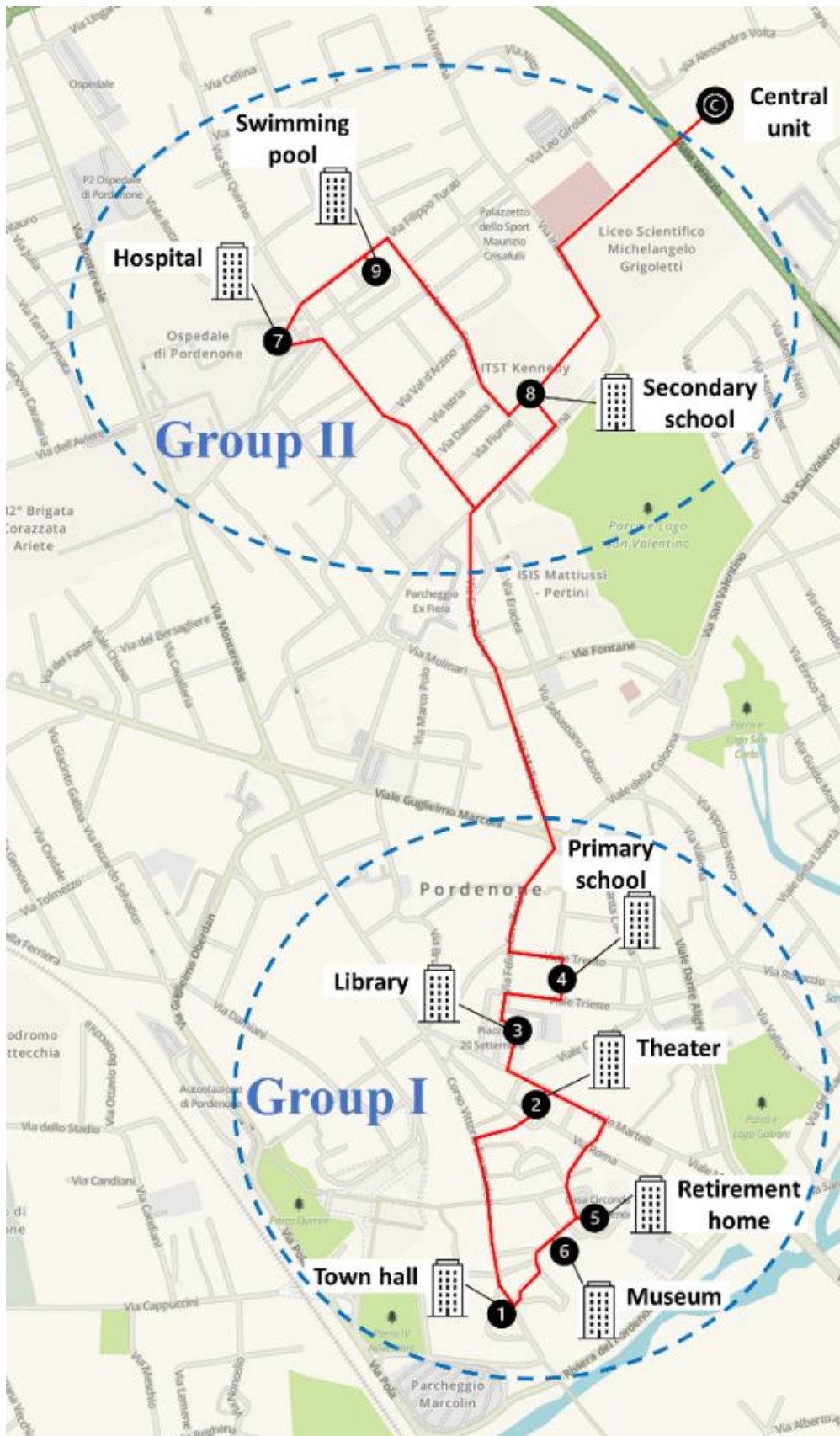


Figure 3.33 – Groups of buildings: Group I (south) and Group II (north).

The set of solutions  $c$  installs not only the heat pipeline connection between buildings 8 and 4, but also between buildings 4 and 7. It is worth noting that building 8 is already connected to building 7 through building 9. However, in the solutions  $c$ , the pipelines between buildings 8–9–7 are at full load. For that reason, if building 7 needs an additional amount of heat, it should come from building 4 (if it is more interesting than installing additional capacity for self-produce heat). Solutions  $d$  have the same characteristics as solutions  $c$  in terms of pipeline connections between the two groups of buildings. Nevertheless, they differ in two main aspects: (i) the installed capacities of STc and HSTc start to substantially increase in the central unit, and (ii) the installed capacities of two very-expensive technologies start to increase in the buildings – ICE and ABS. The remaining set of solutions, in the Pareto front (including the optimal environmental solution), has a considerably high marginal cost when compared with the preceding solutions.

Table 3.23 – Data regarding installed capacities, costs, and CO2 emissions from the Pareto front solutions.

*	Sol. #	Total cost (k€/y)	Total emissions (t CO <sub>2</sub> /y)	Installed capacities												Marg. cost (€/tCO <sub>2</sub> )	Average cost (€/tCO <sub>2</sub> )
				For the nine buildings together									Central unit				
				ICE (kW)	MGT (kW)	BOI (kW)	ABS (kW)	HP (kW)	CC (kW)	PV (m <sup>2</sup> )	ST (m <sup>2</sup> )	HST (kWh)	CST (kWh)	STc (m <sup>2</sup> )	HSTc (kWh)		
	1	3145.7	7262.6	1330	0	852	0	2100	237	1577	223	5542	1236	13,786	31,793	-	-
	2	3149.6	7100	1480	0	402	0	2030	258	1429	371	5322	699	15,384	31,516	24	24
	3	3153.8	7040.3	1480	0	495	0	1960	205	1439	361	5392	1791	16,328	31,352	69.8	36.3
	4	3160.8	6950	1480	0	446	0	1925	232	1344	456	5286	992	17,595	35,428	78.1	48.4
	5	3165.4	6900	1480	0	403	0	1890	378	1337	463	5517	737	18,376	36,659	91.2	54.3
⊙	6	3171.9	6850	1390	0	503	0	1820	362	1388	412	5836	650	19,502	38,532	131.1	63.6
	7	3177.1	6800	1480	0	468	0	1890	312	1322	478	5396	909	19,926	39,947	103.7	67.9
	8	3192.9	6700	1480	0	434	0	1890	252	1180	620	5617	805	21,422	43,280	157.4	83.8
	9	3214	6650	1480	0	400	0	1925	416	1180	620	5656	1103	22,740	49,568	422.4	111.5
	10	3234.6	6600	1760	0	384	0	1645	134	1258	542	5858	1249	22,711	49,431	411.5	134.1
	11	3264.7	6500	1900	0	265	0	1890	87	906	894	8506	904	24,323	57,126	301.7	156.1
△	12	3274.1	6450	1550	0	230	0	1715	60	1399	401	5284	826	24,501	57,973	186.5	157.9
	13	3283	6400	1530	0	365	0	1610	52	1600	200	4899	1449	25,304	61,806	178.7	159.2
	14	3318.3	6294.3	1410	0	280	0	1435	270	1688	112	4010	775	26,527	67,641	334.4	178.3
▽	15	3322.8	6200	1410	0	140	0	1435	193	1640	160	3046	674	27,773	73,590	47.6	166.7
	16	3343.5	6100	1340	0	109	0	1470	135	1722	78	2269	522	29,403	81,371	206.8	170.1
	17	3370.5	6000	1620	0	47	0	1365	58	1735	65	1751	822	30,347	85,874	270.3	178.1

\* Refer to Figure 3.32

Cont. Table 3.22 – Data regarding installed capacities, costs, and CO<sub>2</sub> emissions from the Pareto front solutions.

*	Sol. #	Total cost (k€/y)	Total emissions (t CO <sub>2</sub> /y)	Installed capacities												Marg. cost (€/tCO <sub>2</sub> )	Average cost (€/tCO <sub>2</sub> )
				For the nine buildings together										Central unit			
				ICE (kW)	MGT (kW)	BOI (kW)	ABS (kW)	HP (kW)	CC (kW)	PV (m <sup>2</sup> )	ST (m <sup>2</sup> )	HST (kWh)	CST (kWh)	STc (m <sup>2</sup> )	HSTc (kWh)		
	18	3397	5900	1340	0	90	0	1645	164	1731	69	1336	1577	33,056	98,804	264.5	184.4
	19	3418.2	5800	1340	0	88	0	1470	149	1670	130	1476	1124	34,931	107,752	212.1	186.3
	20	3464.8	5700	1620	0	0	0	1295	0	1795	5	857	616	35,651	139,737	466.6	204.2
	21	3561.7	5630	2040	0	0	0	1400	0	1645	155	2027	550	37,200	208,540	1383.2	254.8
▽	22	3580.7	5600	2040	0	0	0	1785	0	1614	186	1898	564	37,689	230,298	633.8	261.6
	23	3649.4	5500	2090	0	20	70	1295	0	1271	529	2340	426	39,662	317,947	687.3	285.8
	24	3800	5485.7	2270	0	772	315	1295	569	762	1038	3947	1046	40,368	349,299	10,515.90	368.2
	25	4000	5446	2980	0	1213	420	1645	848	984	816	4318	871	41,509	400,000	5046.3	470.3
	26	4200	5422.3	3480	0	645	875	2660	454	466	1334	6393	3281	41,509	400,000	8439.5	572.9
◇	27	4400	5412.5	3480	0	2507	1155	2870	733	389	1411	8132	5634	41,509	400,000	20,251.10	678
	28	4500	5389.3	3280	0	2379	3535	3430	125	0	1800	21219	13051	41,509	400,000	4322.3	723
	29	4700	5382.2	4010	200	2435	3570	3570	380	0	1800	7983	1343	41,509	400,000	28,149.20	826.6

\* Refer to Figure 3.32

Another interesting analysis from Figure 3.32 is the comparison between the reference case solution and the optimal economic and environmental solutions. As observed in the figure, from the reference case viewpoint, both optimal economic and environmental solutions are not advantageous. Although the optimal economic solution (Sol. #1 – Table 3.23) is way cheaper (comparing to the reference case), it emits 2.2% (or 157 t CO<sub>2</sub>/y) more CO<sub>2</sub>. On the other side, the optimal environmental solution (Sol. #29 – Table 3.23) emits way less CO<sub>2</sub> than the reference case but is 1.9% (or 89 k€/y) more expensive. Therefore, the analysis of the solutions can be concentrated in the remaining points (Sol. #2 to #28 – Table 3.23).

Solution #2 (Table 3.23) presents approximately the same CO<sub>2</sub> emissions level as for the reference case but generates a total annual cost 32% lower (or 1,460,856 €/y less) than the one from the reference case. Focusing on the points from the same set of solutions *a* (Sol. #2 to #11), solution #11 requires an increase, in the total annual cost, of 3.6% (or 115.1 k€/y) while providing a reduction of 8.4% (or 600 t CO<sub>2</sub>/y) in the total annual CO<sub>2</sub> emissions, when compared to Sol. #2. Solutions *b* (Sol. #12 and #13) do not provide a substantial enhancement in terms of total annual costs and CO<sub>2</sub> emissions when compared to Sol. #11. Moreover, solutions *b* would require the installation of almost 2 km of DHN pipeline between buildings 8 and 4.

The set of solutions *c* (Sol. #14 to #20) comprises the results in which the total annual cost remained under 3.5 M€/y (Figure 3.32). Comparing Sol. #20 with Sol. #14, the increase in the total annual cost was 4.4% (or 146.5 k€/y) while the total annual CO<sub>2</sub> emissions decreased by 9.4% (or 594.3 t CO<sub>2</sub>/y). By analyzing Table 3.23, it is possible to note that the main reason for this was the gradual decrease (up to zero) in the BOI installed capacity and the gradual increase of the STc and HSTc installed capacities in central unit. Since, for these solutions, the buildings are better interconnected through DHN pipelines, the central unit is able to distribute its heat to the whole EC.

By analyzing the set of solutions *d* (Figure 3.32), Sol. #21 to #24, it is possible to note that the CO<sub>2</sub> emissions reduction starts to become very expensive due to the fact that the installed capacities of ICE, BOI, ABS, and HSTc started to sharply increase. Thus, from those solutions on, the trade-off between costs and CO<sub>2</sub> emissions starts to become imbalanced.

Still analyzing Table 3.23, some other key aspects are worth commenting on, although a more in-depth discussion is compromised by the fact that this table presents the installed capacities of all the buildings together. The comments are separated into bullet points as follows:

- MGT and ABS are not installed for the majority of the solutions; they are installed only when the optimization model is not too “worried” about total costs. The MGT is an alternative cogeneration component to the ICE. However, MGT are more expensive and less efficient comparing to ICE. A similar reasoning goes to ABS. As an alternative technology for cooling production, it is more expensive and less efficient than HP and CC. Moreover, heat from MGT, ICE, and/or ST should be available to feed ABS. Therefore, since there is plenty of heat coming from central unit, the self-produced heat within the buildings can be used to drive ABS. MGT remains a not interesting choice up to the last solution.
- Solar technologies are implemented in every solution, whether it be in the buildings (PV + ST) or in the central unit. In the buildings, PV and ST share the available rooftop area in nearly every single solution. However, as observed in Table 3.23, the solutions near the optimal economic one prioritize PV over ST, while the solutions near the optimal environmental one prioritize ST over PV. In the first case, MGT is not installed and ICE owns a relatively low installed capacity. For that reason, there are only two left options to cover electricity demand: purchase from the grid and PV. In the second case, the ICE installed capacities are around the double compared to the first case. For that reason, there is no need for additional electricity production from PV.

### **3.7 Conclusions**

This chapter presented the development of a multi-objective optimization model, based on the MILP method, for an energy community (EC) consisting in a group of nine buildings plus a central unit sharing electricity, heating, and cooling among each other. The EC buildings (from tertiary sector) are located in the city of Pordenone, northeast of Italy. One of the main objectives of the model was the integration of cogeneration systems and renewable energy technologies in order to reduce overall annual costs and CO<sub>2</sub>



emissions. In fact, the objective functions were the total annual cost (related to maintenance, investment, and hourly operation) and total annual CO<sub>2</sub> emissions (related to the hourly operation). As a preliminary step, this chapter presented the superstructure for both the buildings and central unit, the gathering of the input data, the mathematical model, and the reference case scenario.

In accordance with the objective function, the results from the model indicated the optimal (i) energy supply system structure within each building, (ii) hourly operation of each technology, (iii) connections between buildings in terms of DHCN pipelines, (iv) distribution (among the building) of self-produced electricity and electricity purchased from the grid, and (v) energy supply system structure and hourly operation for the central unit.

The results were presented by dividing them into two main categories: single-objective optimization (SOO) and multi-objective optimization (MOO). The SOO section described and illustrated in detail the optimal configuration of each building for both the optimal economic and environmental solutions. The MOO section demonstrated the importance of this kind of approach by presenting a range of trade-off solutions through the Pareto front. Such trade-off solutions constitute a set of valuable pieces of information that can support decision-makers to take informed choices based on their interests.



---

*CHAPTER 4 – Thermoeconomic  
Analysis of Energy Communities*

---



---

## CHAPTER 4 – Thermo-economic Analysis of Energy Communities

Thermoeconomics, as outlined by Gaggioli (1983) and further developed by Lozano and Valero (1993), represents a merge between thermodynamic principles and economic analysis. Its primary objective is to demonstrate opportunities for energy and cost savings in the assessment, diagnosis, and optimization of energy conversion systems. The foundation of several thermoeconomic methodologies, as stressed by Lozano, Carvalho and Serra (2009), revolves around obtaining unit costs of internal flows and final products of energy supply systems. Such unit costs can be of two different types, average costs and marginal costs. They play a crucial role in various analyses, allowing for a comprehensive understanding of the energy system economics (Reini and Lozano, 1994b, 1994a; M.A. Lozano *et al.*, 2009). For the sake of clarity, in this Ph. D. Thesis when dealing with unit costs of internal and final products, the unit average costs will be called only unit costs, and unit marginal costs will be denoted only as marginal costs.

It is crucial in energy system economics the distinction between unit (or average) costs and marginal costs (Pina, 2019). When changing external conditions (such as variations in energy demand), unit costs are not able to properly explain the optimal plant operation and system behavior, since they are only indicative of the average production cost of a given flow (how much it costed, i.e. how many resources have been consumed for its production, divided by how much was produced). In contrast, a marginal cost is a derivative regarding the cost of producing one additional unit of a given energy flow. As emphasized by Li *et al.* (2015), marginal costs provide a clear path to understanding and managing cost behavior throughout the system.

For instance, the study developed by Lozano, Carvalho and Serra (2009) analyzed a grid-connected trigeneration system under various operational scenarios. Employing a linear programming model, it identified the most cost-efficient operational mode based on a marginal cost analysis. Based on this study, the paper published by Pina, Lozano and Serra (2017) also analyzed the optimization of trigeneration systems, emphasizing the role of thermal energy storage (TES) in improving efficiency by separating production and consumption phases. Through a thermoeconomic approach, the paper assessed the

---

marginal costs of internal flows and final products, elucidating the system's optimal operation and the pivotal contribution of TES. The analysis delineated the formation of marginal costs, tracing a clear path from final products back to resource consumption.

While marginal costs offer valuable insights, their calculation poses challenges, particularly in systems characterized by high levels of energy integration. In this sense, computational tools have emerged as essential aids in overcoming these challenges, facilitating the calculation of marginal costs and the analysis of the influences of changes in input data. In combination with the optimal system operation, a linear programming optimization model, such as those built in FICO Xpress software, provides the hourly dual values for each constraint. Such dual values indicate the amount by which the objective function will vary when the constant term of a constraint is increased by one unit (Lozano, Valero and Serra, 1996). For instance, for an energy balance constraint, the dual values serve as the marginal cost ( $\lambda$ ) of the related energy demand, providing a pathway which offers detailed information about how the energy supply system would react in the case of energy demand increase.

The results obtained from chapter 3 provide valuable and detailed insights about the optimal energy supply system installed in each building (plus central unit), the optimal set of installed DHCN pipelines, the costs and environmental impacts related to the entire system, and the trade-off solutions between total annual costs and CO<sub>2</sub> emissions. However, the mentioned insights do not provide information to determine the optimal operation of the system when the electricity, heat, or cooling demand of a given building is increased.

Therefore, the aim of this chapter is to analyze and interpret the hourly marginal costs related to the energy supply system of the energy community (EC) studied in chapter 3. Such system consists of a complex polygeneration structure comprising different electricity-, heat-, and cooling-producing technologies installed in nine different buildings of the EC plus central unit. Such polygeneration structure is also supported by thermal energy storages (heat and cooling), district heating and cooling network (DHCN) pipelines, and the sharing of electricity among the buildings. The mentioned analysis and interpretation are developed for a typical winter day (January working day) and based on the optimal economic solution presented on section 3.5.1.

The main contributions and novelties from this chapter include:

- The analysis and interpretation of the hourly marginal costs of a complex and highly integrated polygeneration system supported by (i) thermal energy storages, (ii) DHCN pipelines, and (iii) the sharing of purchased and self-produced electricity among the nine buildings.
- The outline of different optimal marginal paths through advanced, delayed, simultaneous, and remote energy services production types.

The structure of the chapter is organized as follows: section 4.1 provides visual aids to better understand the optimal operation of each building by means of the their individual energy balances; section 4.2 offers preliminary and essential pieces of information for the analysis and interpretation of the marginal costs, such as balance equations, dual values, and the mathematical expressions related to thermal losses in both thermal storage devices and DHCN pipelines; section 4.3 develops the analysis and interpretation of the hourly marginal costs for each energy service and for each building; and, finally, section 4.4 provides the main conclusions about the present chapter.

### **4.1 Optimal operation of each building**

In order to develop the analysis and interpretation of the hourly marginal costs associated with the entire EC, two pieces of information are essential: the hourly energy balances of the entire energy supply system and the hourly dual values for the constraints that will be evaluated. Section 3.5.1.2 provided the hourly energy balances for electricity, heating, and cooling for all buildings together, which is useful to have a big picture about the whole EC. However, the marginal cost analysis requires a more detailed energy balance information which, in this case, is achievable by the hourly energy balances of each building individually. For what concerns the hourly dual values, they can be obtained from the software through which the optimization is performed (FICO Xpress, in this case) by writing the appropriate code lines.

The marginal cost analysis will be focused on the optimal operation of the entire EC system for one January working day. The analyzed optimal solution is the same as the one discussed on section 3.5.1, i.e., the optimal economic solution. However, it is worth

knowing that the same marginal cost study can be performed for any other solution, including the ones depicted in the Pareto front (Figure 3.32).

Figure 4.1 to Figure 4.10 present the hourly energy balances, from one working day in January, of electricity, heating, and cooling for each building plus central unit individually. It is important to note that the negative part of the graphics showed in those figures can represent different parameters.

For the electricity balances, the negative part can represent:

- the electricity demand of the building (the portion not related to HP or CC),
- the electricity demanded by HP and/or CC, and/or
- part of the self-generated electricity that is being sent to the distribution substation (DS) to be sold to the grid or sent to other building(s).

For the heat balances, the parameters represented by the negative part can be:

- the heat demand of the building,
- the charging process of the hot water storage (HST or HSTc),
- the amount of heat sent to another building(s), and/or
- the heat dissipated through DHCN pipelines.

As explained in section 3.2.2.3, there is a cooling demand in January due to specific needs of the hospital only. For the cooling balance of that building, the negative part can represent:

- the cooling demand of the building, and
- the charging process of the chilled water storage (CST).

All possible mentioned meanings are duly indicated in each graphic.

It is also important to bear in mind that, as will be observed in the electricity balance graphs, there is not a term called “electricity purchased” or any other related term. Instead,



there is the term “DS connection”. As explained on section 3.1.1, the buildings are not directly connected to the national electric grid; they are connected to the distribution substation (DS), which manages the communication with the electric grid. Such connection (building  $\leftrightarrow$  DS) is set to function in both directions (not at the same time). For the optimal economic solution, analyzed herein through a January working day, a given building (in a given hour) will be: (i) sending electricity to the DS (self-production surplus), which will be graphically represented in the negative region, or (ii) receiving electricity from the DS (self-production deficit), which will be graphically represented in the positive region.

#### **4.1.1 Energy balance per building**

As mentioned before, the analyzed optimal solution is the same as the one discussed on section 3.5.1 and, for that reason, the reader may refer to Figure 3.14 to Figure 3.22 for a visual aid, i.e., for the illustration of the optimal energy supply system structure of each building.

The hourly electricity and heat balances of the Town hall (building 1) are presented through Figure 4.1. As observed, both electricity and heat are required only during the working hours, with a peak in the morning and a peak in the afternoon. The hourly electricity demand (Figure 4.1 A) is composed by 53% for HP and 47% for the electricity demand of the building. Such demand is mostly covered by electricity received from the DS and a tiny percentage by PV panels. Regarding the hourly heat demand (Figure 4.1 B), it is covered by BOI, HP, and ST. From hour 6 to 9 the HP is at full load (361.6 kW), and, for this reason, the BOI operation was needed from hours 6 to 8. From hours 9 to 17 the energy supply system of building 1 receives a small help from solar thermal energy produced by 61 m<sup>2</sup> of ST panels. At this day, the hot water storage (HST) of the Town hall is neither charging nor discharging. As noted, there is no heat dissipation due to heat transportation through DHN pipelines since, for the analyzed solution, building 1 is not connected to any other building by means of pipelines.

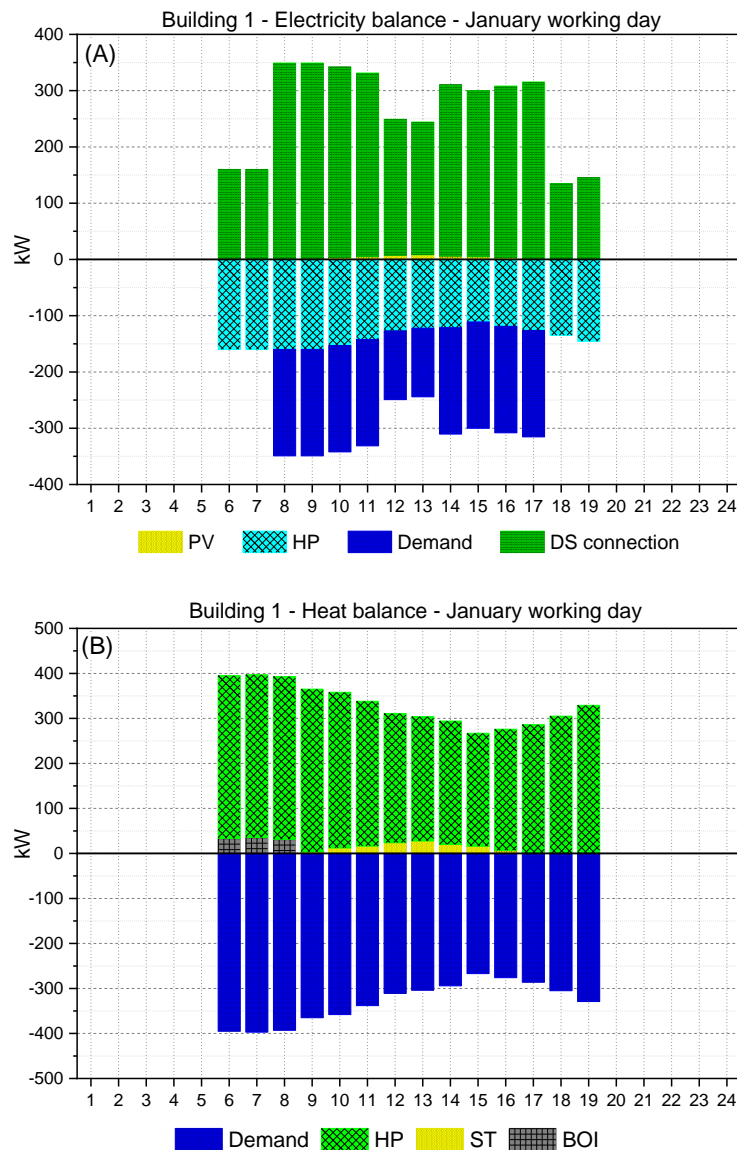


Figure 4.1 – Electricity and heat balances for building 1 (Town hall). The reader may refer to section 4.1 for a better understanding of “DS connection”.

The theater (building 2) is located in a strategic position as shown in Figure 3.4. As explained in section 3.5.1.1, building 2 is situated between buildings 3 and 4 to the north and buildings 5 and 6 to the south within distances not over 300 meters. This is one of the main reasons why building 2 receives the installation of four HP units of  $100 \text{ kW}_{el}$  each,  $117 \text{ m}^2$  of ST, and two ICE units of  $140 \text{ kW}_{el}$  each, i.e., with such energy supply system, building 2 is able to cover its heating demand and send the surplus to the other buildings.

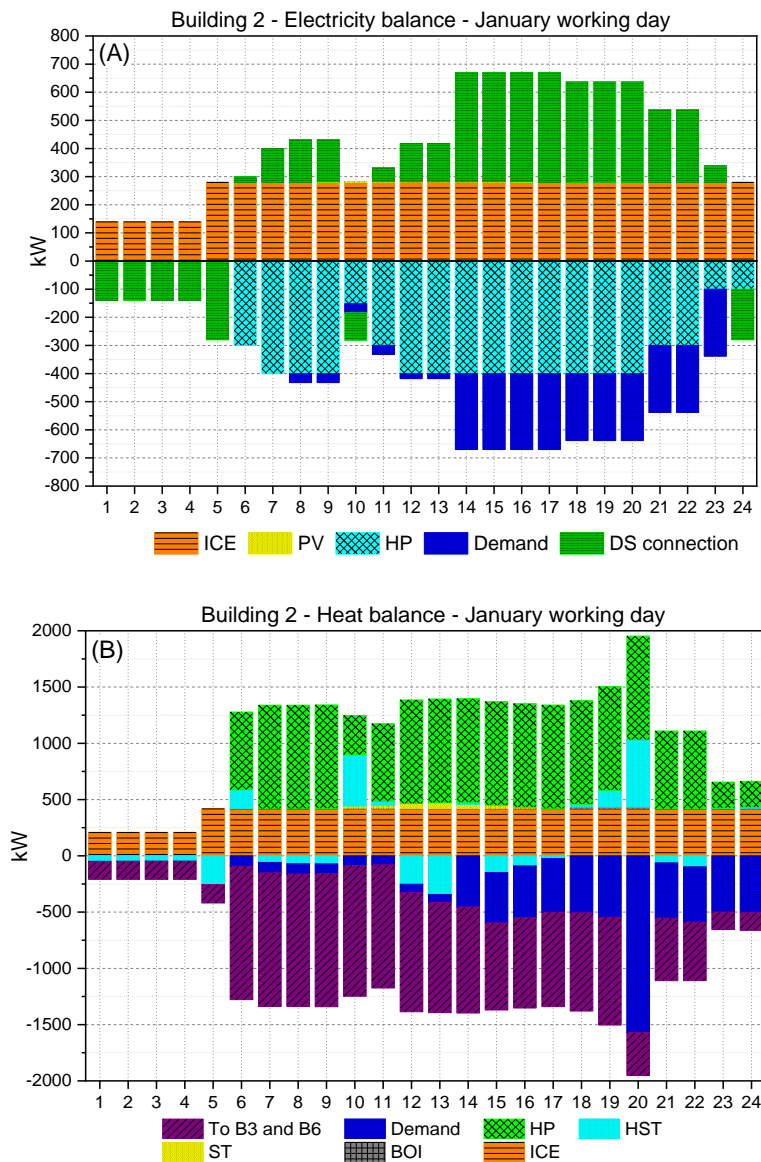


Figure 4.2 – Electricity and heat balances for building 2 (Theater). The reader may refer to section 4.1 for a better understanding of “DS connection”.

Figure 4.2 (A) presents the electricity balance of building 2. As seen, the HP electricity demand constitutes a great part of the total electricity demand of the building and takes place from hour 6 to 24. The installed ICE capacity allows self-generated electricity for all 24 hours; in the first four hours only one ICE is at full load operation while from hour 5 to 24 both ICE units are operating at full load. It allows the building to (i) send 100% of the self-produced electricity to the DS from hour 1 to 5 (at this period there is no electricity demand), and (ii) send a percentage of the self-produced electricity to the DS

at hours 10 and 24 since the production is higher than the demand at these times. At all the other hours, building 2 needs to receive electricity from the DS.

Regarding the heat balance of building 2, Figure 4.2 (B) demonstrates that (i) the ICE heat supply profile is coherent with the ICE electricity supply profile, (ii) there is a substantial amount of heat being sent to buildings 3 and 6, (iii) 61% of the heat is supplied by HP, and (iv) HST is charged at the hours 1 to 5, 7 to 9, 12 to 13, 15 to 17, and 21 to 22. The heat balance of building 2 does not have any heat dissipation through pipelines because it does not receive heat from other building; instead, it sends heat to other two buildings and, therefore, the heat dissipation is charged to the receiving buildings.

The only technologies, installed in building 3 (the reader may refer to Figure 3.16), for self-producing electricity are the 200 m<sup>2</sup> of PV panels, although they can supply only a small amount of the total electricity demand, as observed in Figure 4.3 (A). Most of the electricity demand is supplied by electricity coming from the DS. At hours 6 to 8, 11, and 15 to 20 the 35 kW<sub>el</sub> HP is operating at full capacity, as shown in Figure 4.3 (A) and (B). Figure 4.3 (B) shows that the majority of the Library heat demand is covered by heat provided by building 2 (Theater) and that 64% of the heat supplied to building 3 (Library) is sent to building 4 (Primary school). It is also possible to observe the small hourly portion regarding the heat pipeline dissipation, which in this case is due to the heat received from building 2.

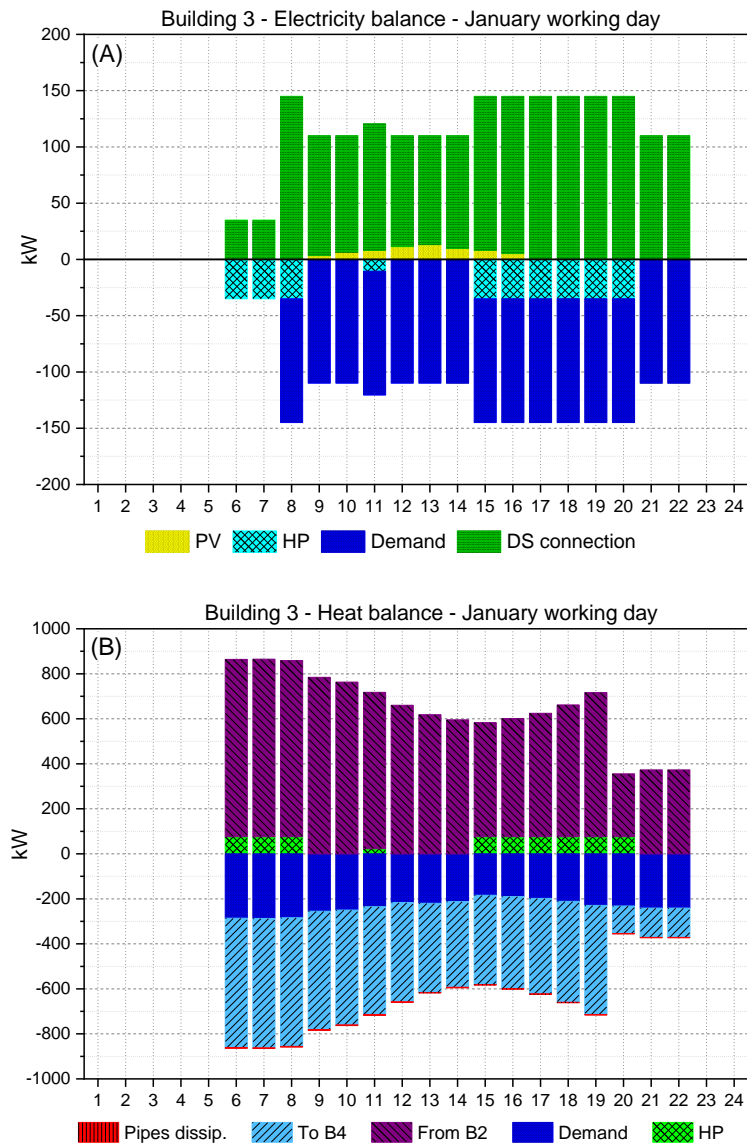


Figure 4.3 – Electricity and heat balances for building 3 (Library). The reader may refer to section 4.1 for a better understanding of “DS connection”.

Building 4 (Primary school) has the simplest energy supply system structure (the reader may refer to Figure 3.17) among all nine buildings of the EC. The structure is composed by a 200 m<sup>2</sup> PV plant and a 3 kW BOI. From Figure 4.4 (A) it is shown that the PV electricity covers only 14% of the total electricity demand of the typical day under analysis, while the remaining part is received from the DS. The BOI contributes with a tiny amount of heat at hours 7 and 18 to 20, whereas the heat coming from building 3 comprises 99.8% of the heat supplied to building 4 (Figure 4.4 B). For that reason, the

option of not installing the BOI at building 4 could be evaluated considering the annual and peak values. It is also possible to perceive the hourly heat dissipation through pipelines due the heat received from building 3.

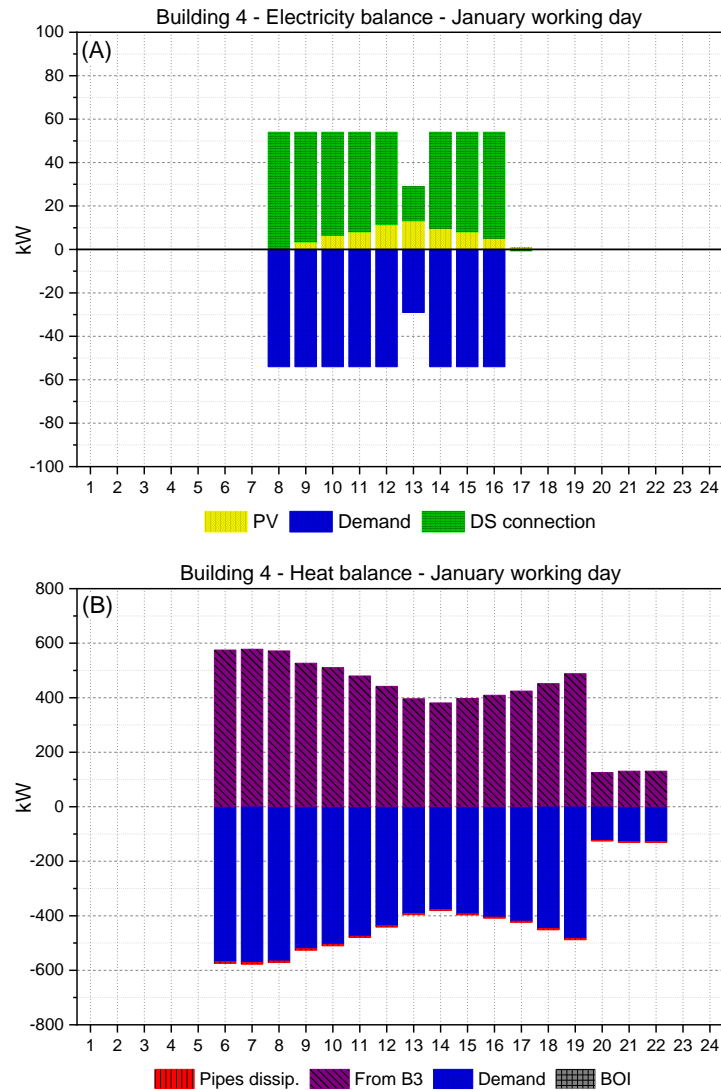


Figure 4.4 – Electricity and heat balances for building 4 (Primary school). The reader may refer to section 4.1 for a better understanding of “DS connection”.

Figure 4.5 provides the electricity and heat balances for building 5 (retirement home) in a January working day. Differently from the previous buildings, this building demands electricity 24/7 all year long, whereas the heat demand behaves the same way only during the cold months. Figure 4.5 (A) reveals that 22% of the total electricity demand from a January working day is due the HP operation at the hours 6 to 10 and 15 to 22 (at the

hours 9, 10, and 21 the HP is at part load operation), while most electricity supply comes from the DS. Figure 4.5 (B) exposes five main aspects regarding the heat balance of the retirement home: (i) 79% of the buildings' heat demand is covered by the heat received from building 6, (ii) the HP operates at the peak hours, (iii) at hour 11 the BOI should operate because the HP is off and the heat from building 6 (at the same hour) is not enough to cover the heat demand, (iv) at hours 18 to 20 the BOI should operate because the HP is at full load and the heat from building 6 (at the same hours) is not enough to cover the heat demand, and (v) the hourly pipeline heat dissipation due to the heat coming from building 6.

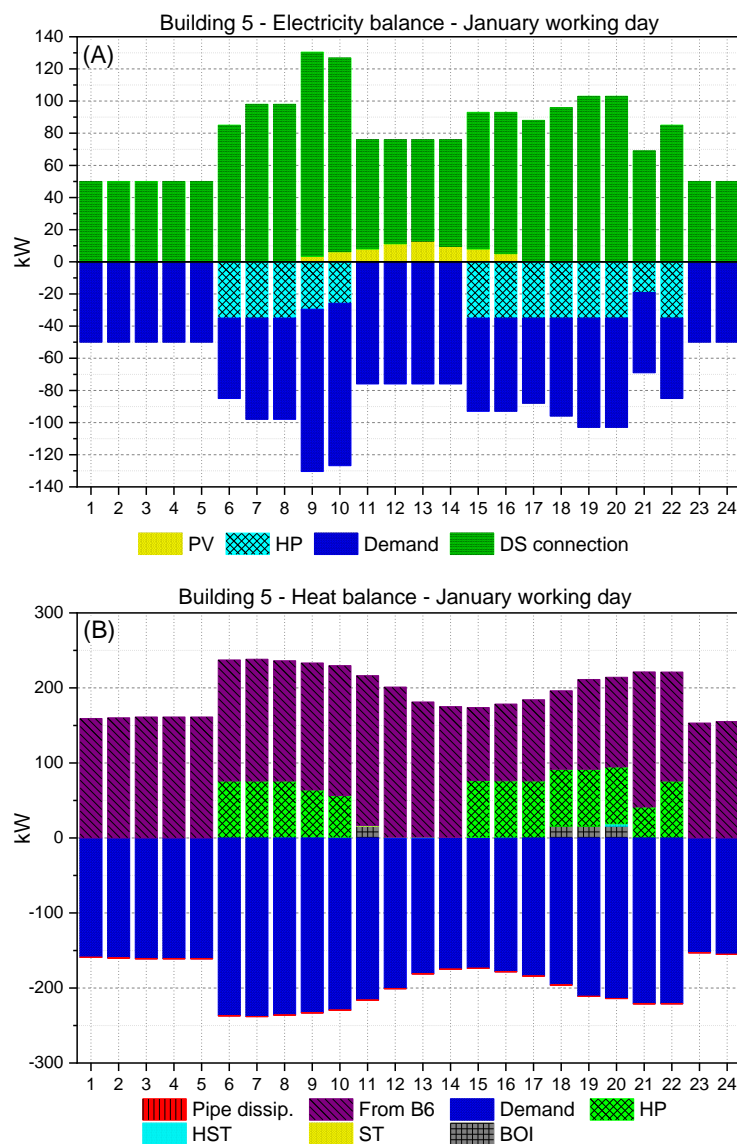


Figure 4.5 – Electricity and heat balances for building 5 (Retirement home). The reader may refer to section 4.1 for a better understanding of “DS connection”.

The graphs corresponding to the museum (building 6) energy balances are shown in Figure 4.6. Figure 4.6 (A) reveals that the electricity demand takes place only from hour 8 to hour 19, with peak hours from 8 to 11 and 14 to 17. As observed, 20% of the hourly electricity demand is covered by its 196 m<sup>2</sup> PV plant and the remaining part is supplied by the DS. Regarding the heat balance, the major heat supply comes from building 2 (Theater), as seen in Figure 4.6 (B). The BOI only comes to play (at full load – 11 kW) at hours 11 and 18 to 20. From hour 1 to 5 and from hour 20 to 24, all the heat received from building 2 is sent to building 5, whereas from hour 6 to 19 part of the heat received from building 2 covers building 6 heat demand and the remaining part is sent to building 5. Lastly, there is the hourly heat dissipation part due to the heat received from building 2.



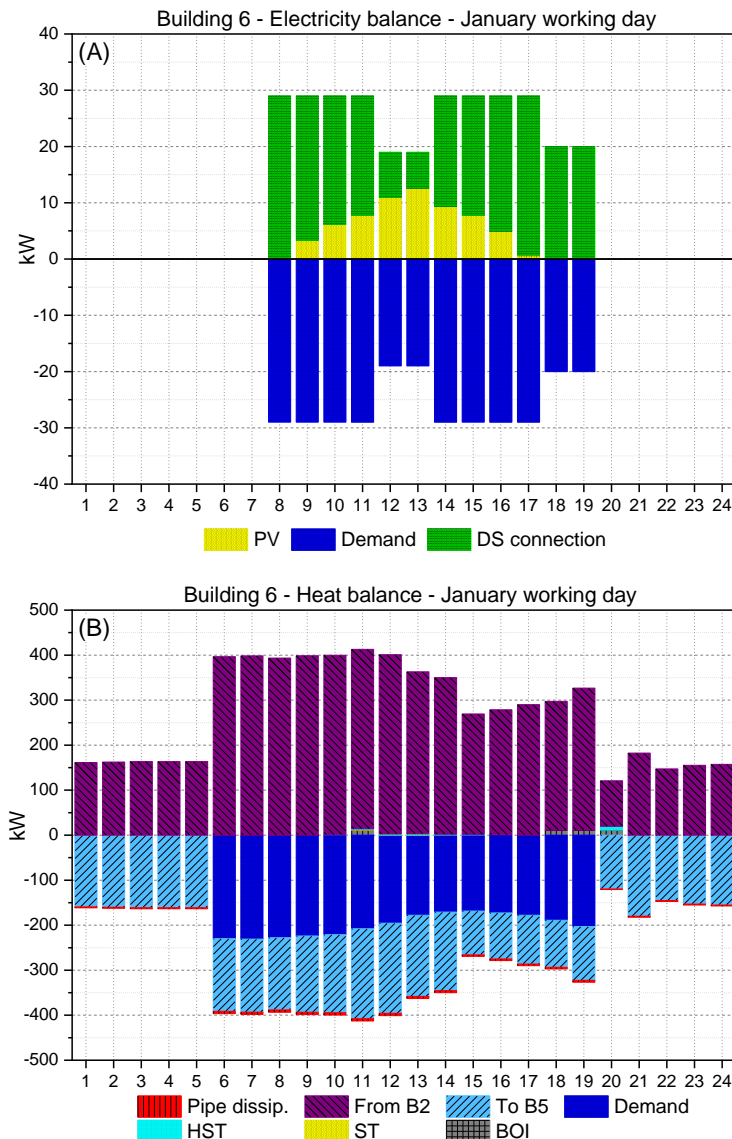


Figure 4.6 – Electricity and heat balances for building 6 (Museum). The reader may refer to section 4.1 for a better understanding of “DS connection”.

Building 7 (hospital) received the largest energy supply system in terms of number of installed technologies, installed capacity, and magnitude of the energy flows (Figure 3.20). The solution under scrutiny installed five ICE units of  $200 \text{ kW}_{\text{el}}$  each, six HP units of  $100 \text{ kW}_{\text{el}}$  each, an  $810 \text{ kW}_{\text{th}}$  BOI, a  $41 \text{ kW}_{\text{el}}$  CC, a  $4000 \text{ kWh}$  HST, a  $609 \text{ kWh}$  CST,  $151 \text{ m}^2$  of PV panels, and  $49 \text{ m}^2$  of ST panels. Figure 4.7 (A) shows that 47% of the total supplied electricity is provided by four ICE units operating at full load for all 24 hours, while the remaining amount of electricity comes from the DS. The total building electricity demand is composed by 32% regarding HP, a tiny little amount concerning CC, and the remaining part corresponding to non-HP and non-CC electricity demand. The CC

electricity demand takes place only at hours 7 and 8 to cover a specific cooling demand of the hospital, whereas the electricity generated by the PV plant comprises an insignificant amount when compared to the hourly electricity demanded by the hospital.

Figure 4.7 (B) presents the heat balance of the hospital. As seen, the supplied heat comes from ICE, HP, BOI, HST, ST, and building 9. The four ICE units are at full load for all 24 hours. The BOI enters into operation from hour 5 to 8 because (i) ICE and HP are at full load, (ii) at these hours there is not enough heat to be supplied from the HST, and (iii) the amount of heat coming from building 9 cannot increase. Moreover, the HST is charged at the hours 1, 2, 15, 16, and 19 to 24, and is discharged at the hours 3 to 8 and 17 to 18. From hour 9 to 14 the HST is neither charged nor discharged.

It is interesting to note that the operation of the HP units is configured according to the hourly heat demand level and the hourly amount of heat coming from building 9. From hour 1 to 12, the six HP units are operating at full capacity. At hour 13 the HP operation reduces to four units at full capacity and gradually reduces to two units at full load. Then, at hour 17, the HP operation increases to five units at full load and, from hour 18 to 24, all six HP units are operating again at full capacity. Finally, there is the hourly pipeline heat losses due to the heat coming from building 9.

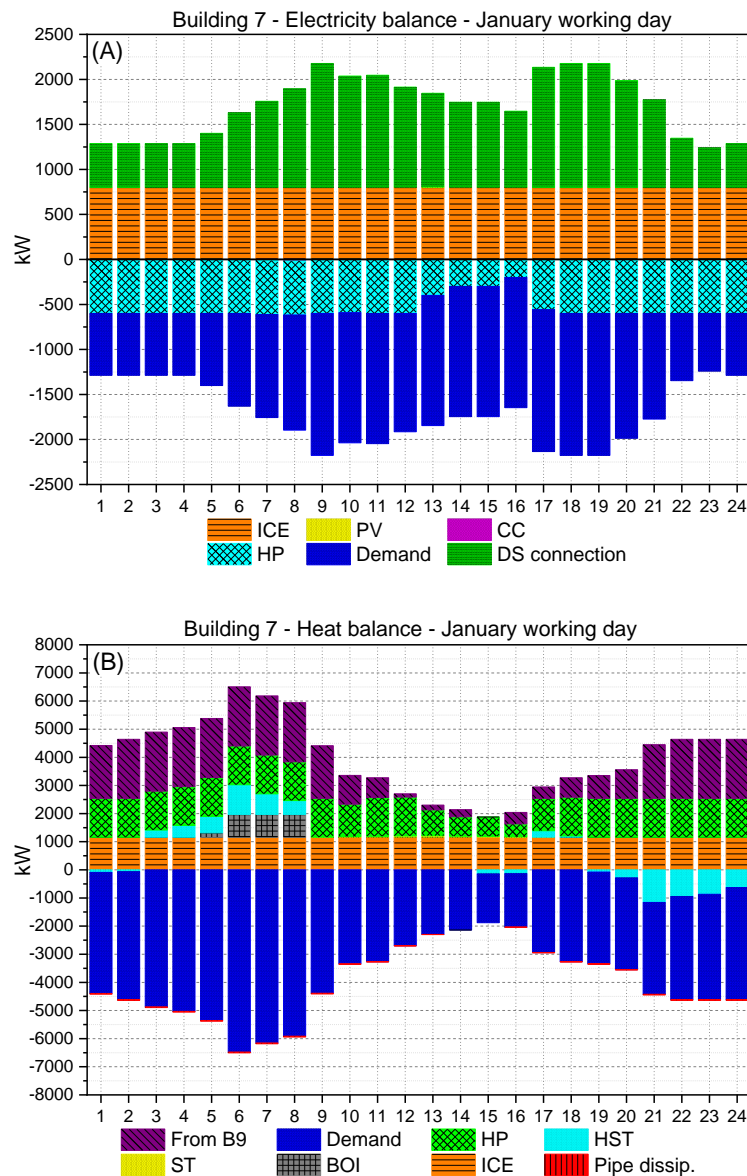


Figure 4.7 – Electricity and heat balances for building 7 (Hospital). The reader may refer to section 4.1 for a better understanding of “DS connection”.

Figure 4.8 provides the hourly electricity and heat demands for the secondary school (building 8). As deduced from Figure 4.8 (A), 77% of the building’s electricity demand is dedicated to feed the six HP units of  $80 \text{ kW}_{el}$  each. The HP operation profile is very diversified throughout the 24 hours of the analyzed day. At hour 1 there are four HP units working at full load, whereas from hour 2 to 5 there are five HP units operating at full load and one HP unit at partial load. From hour 6 to 9 all six HP units are operating at full load since the heat demand starts to increase around these hours (Figure 4.8 B). Then, at

hour 10, the HP operation falls to three units at full load plus another one at partial load. This is because the heat that should be sent to building 9 substantially decreases at hour 10 and there is a considerable amount of heat coming from the central unit at this same hour (Figure 4.8 B). Next, from hour 11 to 13, all HP units are shut down since, at these hours, the heat coming from central unit is enough to cover the heat demand. From hour 14, the HP units start to get back into operation up to hour 16 when all six HP units are working again at full load, a behavior that is maintained until hour 18, as there is not enough heat coming from the central unit at these times. From hour 19 on, building 8 does not have heat demand; instead, the only heat demand at such hours is the heat that should be sent to building 9. Thus, at hour 19 only one HP unit is at operation (full load) and, at hour 20, this HP goes off since there is enough heat coming from central unit. From hour 21 on, there is no heat coming from central unit and, for that reason, four HP units at full load plus one at partial load go back into operation at hour 21. From hour 22 to 24, the fifth HP unit reaches full load and the sixth starts to operate at partial load.

Figure 4.8 (B) also shows the hourly amount of heat received from the central unit (from hour 6 to 20), which is in accordance with Figure 4.10 (A), and the hourly amount of heat sent to building 9. It is interesting noting that, for the typical day under analysis, most of the heat received from central unit covers the hourly heat demand of building 8, whereas the majority of the heat sent to building 9 is produced by the HP units.

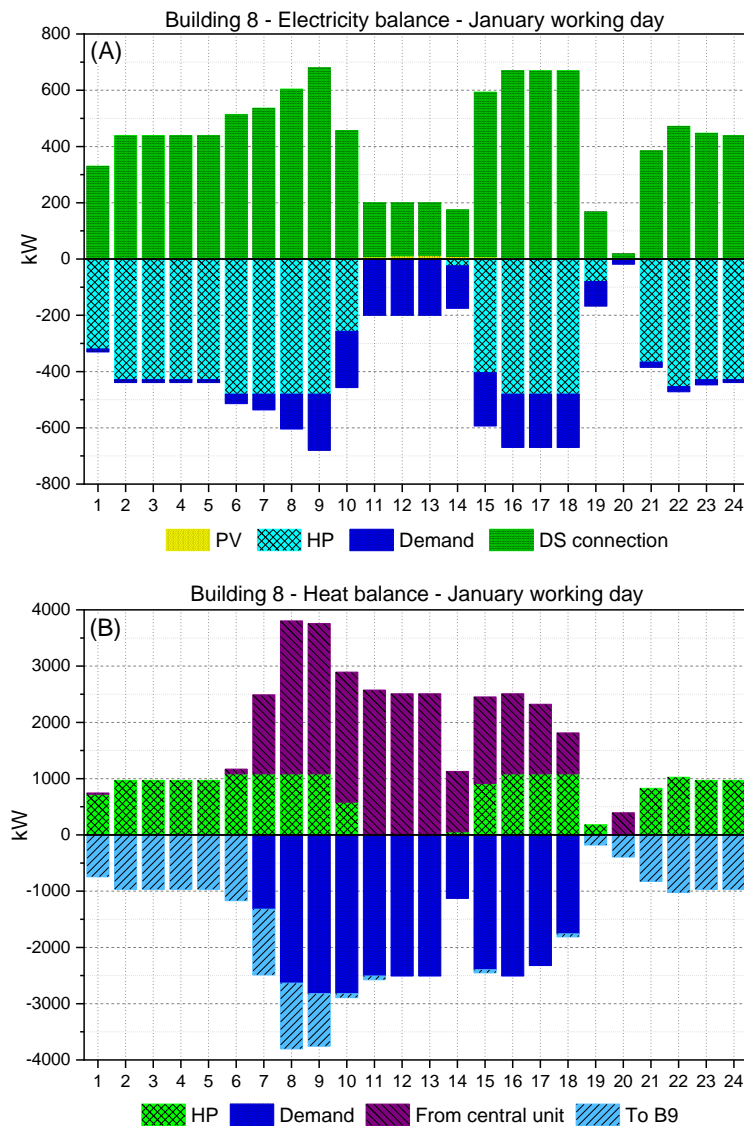


Figure 4.8 – Electricity and heat balances for building 8 (Secondary school). The reader may refer to section 4.1 for a better understanding of “DS connection”.

The swimming pool (building 9) is one of the buildings with the simplest energy supply system structure. It is composed of a 200 m<sup>2</sup> PV plant and five HP units of 100 kW<sub>el</sub> each. As observed in Figure 4.9, building 9 has a very low electricity and heat demand. However, it has a considerably high hourly electricity demand regarding the HP units (Figure 4.9 A), which should complement the heat received from building 8 and send it to building 7. From hour 1 to 10 and 21 to 24, the five HP units are operating at full capacity, which are the periods of peak heat demand in the hospital. From hour 11 to 20,

the heat demand levels of the hospital are lower, which is coherent with the HP units operation profile within the same period.

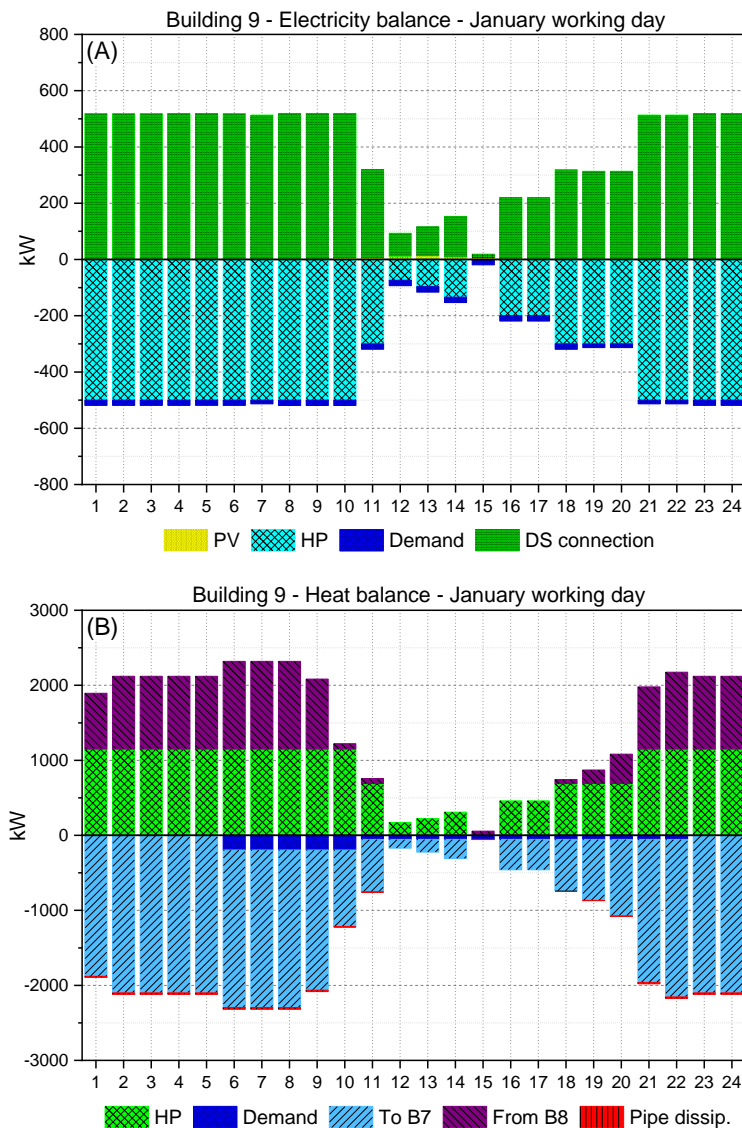


Figure 4.9 – Electricity and heat balances for building 9 (Swimming pool). The reader may refer to section 4.1 for a better understanding of “DS connection”.

Figure 4.10 shows the hourly heat balance of the central unit and the hourly cooling balance of the building 7 (hospital). As explained before, only this building has a cooling demand in January. Figure 4.10 (A) shows that all heat production comes from solar energy, by means of flat-plate collectors (STc), and is supported by hot water storage (HSTc). Figure 4.10 (B) reveals that the low hourly cooling demand of building 7 is covered by CC and HP, and is supported by the CST.

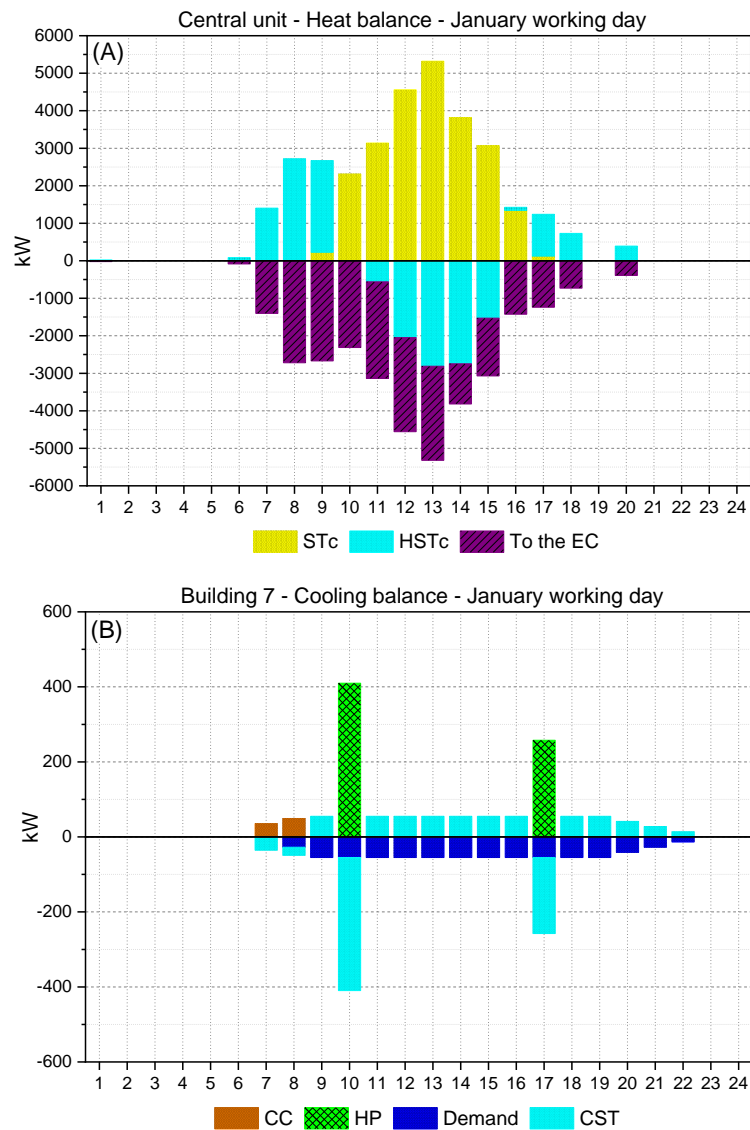


Figure 4.10 – Central unit heat balance (A) and building 7 (Hospital) cooling balance (B).

## 4.2 Marginal cost analysis: preliminary information

As explained in the introduction section of this chapter, the reader should bear in mind that the mathematical model used to obtain the marginal costs associated with the optimal operation of the entire EC is the same as the one described in chapter 3, section 3.3. In fact, a complete and exact operational strategy is an essential source of data to perform the analysis and interpretation of the marginal costs.

### 4.2.1 Energy balances: hourly dual values obtention

The mentioned EC model determines the hourly optimal operational strategy (of the energy supply system for the whole EC and for all typical days) that minimizes the total

annual costs  $TAC$  (in €/y), which has been already presented and explained in section 3.3.1. For convenience, the  $TAC$  equation is repeated through Eq. (4.1),

$$TAC = AOC_{tot} + AMC_{tot} + AIC_{tot} + E_P - E_S \quad (4.1)$$

where  $AOC_{tot}$  is the total annual operation cost,  $AMC_{tot}$  is the total annual maintenance cost,  $AIC_{tot}$  is the total annual investment cost,  $E_P$  is the total annual purchased electricity cost via distribution substation (DS), and  $E_S$  is the total annual sold electricity revenue via DS.

The equations connecting energy supply resources with the energy demands of each building are the energy balances (section 3.3.3). For that reason, the marginal cost analysis will be concentrated in such constraints through the obtention of the dual values associated to them. It has the aim to evaluate the effect in the objective function when the hourly demand of any energy product (heat, cooling, and electricity) increases or decreases without changing the operation mode of the whole system. For convenience, the equations are repeated in this section from Eq. (4.2) to Eq. (4.5). The hourly dependency of the variables, represented by  $m$  (month),  $d$  (day), and  $h$  (hour), is replaced by  $t$  for simplicity.

Equation (4.2) provides the heat balance for building 8. For buildings 1 to 7 and 9, the heat balance is the same equation without the term  $Heat_{cen.unit}(t)$ . As observed, the equation comprises the variables regarding (i) heat producing technologies plus heat storage (within the building superstructure), (ii) heat coming from central unit, (iii) net amount of heat received through DHN pipelines, (iv) wasted heat, and (v) heat demand of a given building.



$$\begin{aligned}
& \left[ \sum_{c=1}^6 (Heat_{MGT}(t, c, B) + Heat_{ICE}(t, c, B) + Heat_{HP}(t, c, B) \right. \\
& \quad \left. - Heat_{ABS}(t, c, B)) \right] \\
& + \left[ \sum_{k=1}^9 (Q_h(t, k, B) \cdot (1 - p_h(B, k)) - Q_h(t, B, k)) \right] \\
& + Heat_{BOI}(t, B) + Heat_{ST}(t, B) - Heat_{HST}(t, B) \\
& - Heat_{Dem}(t, B) + Heat_{cen.unit}(t) - Heat_{waste}(t, B) \geq 0
\end{aligned} \tag{4.2}$$

The term regarding the heat received from the central unit (Eq. (4.2)) is obtained from another heat balance applied to the technologies comprising the central unit (Eq. (4.3)).

$$\begin{aligned}
& Heat_{ICEc}(t) + Heat_{BOIc}(t) + Heat_{STc}(t) - Heat_{HSTc.in.out}(t) \\
& - Heat_{cen.unit}(t) \geq 0
\end{aligned} \tag{4.3}$$

In a similar way as Eq. (4.2), Eq. (4.4) provides the cooling balance for a given building of the EC. As seen, the equation comprises the variables regarding (i) cooling producing technologies plus cooling storage (within the building superstructure), (ii) net amount of cooling received through DCN pipelines, (iii) wasted cooling, and (iv) cooling demand of a given building.

$$\begin{aligned}
& \left[ \sum_{c=1}^6 (Cool_{ABS}(t, c, B) + Cool_{HP}(t, c, B)) \right] \\
& + \left[ \sum_{k=1}^9 (Q_c(t, k, B) \cdot (1 - p_c(B, k)) - Q_c(t, B, k)) \right] \\
& + Cool_{CC}(t, B) - Cool_{CST.in.out}(t, B) - Cool_{Dem}(t, B) \\
& - Cool_{waste}(t, B) \geq 0
\end{aligned} \tag{4.4}$$

Equation (4.5) provides the electricity balance of the distribution substation (DS). The first term regards the summation of the electricity sent or received to/from the buildings, whereas the second term refers to the electricity received from the engine installed in the central unit. The last two terms refer to the purchased (or bought) and sold electricity,

respectively. Equations (4.6) and (4.7) guarantee that the purchased or sold electricity cannot be a negative number.

$$\left[ \sum_{B=1}^9 Elec_{DS}(t, B) \right] + Elec_{ICEc}(t) + E_{bgt}(t) - E_{sold}(t) = 0 \quad (4.5)$$

$$E_{bgt}(t) \geq 0 \quad (4.6)$$

$$E_{sold}(t) \geq 0 \quad (4.7)$$

## 4.2.2 Dual values

Following the same reasoning of Pina (2019), the hourly dual values associated to the constraints presented through Eq. (4.2) to Eq. (4.5) are presented in Table 4.1. Such dual values can be interpreted as the Lagrange multipliers or the marginal costs  $\lambda$  associated with variations in the demand of products (Lozano *et al.*, 1994; Lozano, Valero and Serra, 1996).

For the present analysis, such demand variation can happen on the (i) hourly heat demand of each building ( $\lambda \cdot Heat_{Dem}(t, B)$ ), (ii) hourly cooling demand of each building ( $\lambda \cdot Cool_{Dem}(t, B)$ ), (iii) hourly heat demanded from central unit ( $\lambda \cdot Heat_{cen.unit}(t)$ ), and (iv) hourly electricity demand resulted from the summation  $\lambda \cdot \sum_{B=1}^9 Elec_{DS}(t, B)$ .

### 4.2.2.1 Marginal cost values

Table 4.1 presents the marginal costs associated with the variation of the above-mentioned energy demands. The reader should bear in mind three aspects regarding this table: (i) the presented hourly marginal costs correspond to one typical day (working day) of January for the entire EC, (ii) the marginal costs regarding the heat and cooling demands refer to all nine buildings together, and (iii) the hourly marginal costs regarding the electricity demand are not divided by building since the only communication with the external electric grid is done through the DS, i.e., the DS determines the necessity or not of buying electricity from the grid based on the summation  $\sum_{B=1}^9 Elec_{DS}(t, B)$  (Eq. (4.5)).

Table 4.1 – Hourly marginal costs (in €/kWh) associated with electricity, heat, and cooling demand variations for all buildings plus central unit. Values for a January working day.

Hour	Buildings			Central unit
	$\lambda \cdot \sum_{B=1}^9 Elec_{DS}(t, B)$	$\lambda \cdot Heat_{Dem}(t)$	$\lambda \cdot Cool_{Dem}(t)$	$\lambda \cdot Heat_{cen.unit}(t)$
1	0.1169	0.4055	0.0363	0.0759
2	0.1169	0.3634	0.0370	0.0763
3	0.1169	0.3686	0.0378	0.0766
4	0.1169	0.3740	0.0386	0.0770
5	0.1169	0.3795	0.0394	0.0774
6	0.1169	0.6830	0.0402	0.0778
7	0.1169	0.7382	0.0410	0.0782
8	0.1169	0.6735	0.0418	0.0786
9	0.1450	0.6692	0.0427	0.0790
10	0.1533	0.6213	0.0342	0.0683
11	0.1533	0.8099	0.0349	0.0669
12	0.1533	0.6370	0.0356	0.0672
13	0.1533	0.6305	0.0363	0.0676
14	0.1533	0.6382	0.0371	0.0679
15	0.1533	0.6480	0.0378	0.0683
16	0.1533	0.6557	0.0386	0.0686
17	0.1533	0.6666	0.0342	0.0690
18	0.1533	0.7473	0.0349	0.0693
19	0.1533	0.7547	0.0356	0.0696
20	0.1533	0.7004	0.0363	0.0700
21	0.1450	0.5317	0.0371	0.0704
22	0.1450	0.5471	0.0378	0.0707
23	0.1450	0.4163	0.0317	0.0711
24	0.1450	0.4222	0.0324	0.0714

The next two pages present the tables with the hourly marginal costs, for heating and cooling demands, separated by buildings and for the mentioned January typical day.

Table 4.2 – Hourly marginal costs (in €/kWh) associated with the hourly heat demand variations ( $\lambda \cdot \mathbf{Heat}_{Dem}(t, \mathbf{B})$ ) for the nine buildings. Values for a January working day.

Hour	1	2	3	4	5	6	7	8	9
1	0	0.0559	0	0	0.0567	0.0567	0.0799	0.0774	0.0789
2	0	0.0571	0	0	0.0579	0.0578	0.0852	0.0522	0.0532
3	0	0.0582	0	0	0.0591	0.0590	0.0869	0.0522	0.0532
4	0	0.0594	0	0	0.0603	0.0602	0.0887	0.0522	0.0532
5	0	0.0606	0	0	0.0615	0.0614	0.0905	0.0522	0.0532
6	0.0905	0.0619	0.0621	0.0627	0.0628	0.0627	0.0923	0.0793	0.0809
7	0.0905	0.0631	0.0634	0.0640	0.0787	0.0785	0.0942	0.0797	0.0813
8	0.0905	0.0644	0.0647	0.0653	0.0654	0.0653	0.0961	0.0801	0.0817
9	0.0905	0.0657	0.0660	0.0667	0.0673	0.0672	0.0832	0.0805	0.0822
10	0.0683	0.0671	0.0673	0.0680	0.0711	0.0710	0.0705	0.0683	0.0697
11	0.0683	0.0684	0.0687	0.0694	0.1655	0.1652	0.0691	0.0669	0.0683
12	0.0683	0.0698	0.0701	0.0708	0.0833	0.0724	0.0679	0.0672	0.0671
13	0.0683	0.0713	0.0716	0.0723	0.0723	0.0722	0.0679	0.0676	0.0671
14	0.0683	0.0727	0.0730	0.0738	0.0738	0.0737	0.0679	0.0679	0.0671
15	0.0683	0.0742	0.0745	0.0753	0.0753	0.0752	0.0674	0.0683	0.0697
16	0.0683	0.0757	0.0760	0.0768	0.0768	0.0767	0.0688	0.0686	0.0679
17	0.0683	0.0773	0.0776	0.0784	0.0784	0.0783	0.0702	0.0690	0.0693
18	0.0683	0.0926	0.0930	0.0939	0.0940	0.0938	0.0716	0.0693	0.0707
19	0.0683	0.0945	0.0949	0.0959	0.0959	0.0958	0.0709	0.0686	0.0700
20	0	0.0964	0.0968	0.0978	0.0979	0.0977	0.0723	0.0700	0.0714
21	0	0.0663	0.0666	0.0672	0.0673	0.0672	0.0667	0.0646	0.0659
22	0	0.0676	0.0679	0.0686	0.0686	0.0685	0.0753	0.0646	0.0659
23	0	0.0690	0	0	0.0700	0.0699	0.0769	0.0646	0.0659
24	0	0.0704	0	0	0.0715	0.0714	0.0784	0.0646	0.0659

Table 4.3 – Hourly marginal costs (in €/kWh) associated with the hourly cooling demand variations ( $\lambda \cdot Cool_{Dem}(t, \mathbf{B})$ ) for the nine buildings. Values for a January working day.

Hour	1	2	3	4	5	6	7	8	9
1	0	0	0	0	0	0	0.0363	0	0
2	0	0	0	0	0	0	0.0370	0	0
3	0	0	0	0	0	0	0.0378	0	0
4	0	0	0	0	0	0	0.0386	0	0
5	0	0	0	0	0	0	0.0394	0	0
6	0	0	0	0	0	0	0.0402	0	0
7	0	0	0	0	0	0	0.0410	0	0
8	0	0	0	0	0	0	0.0418	0	0
9	0	0	0	0	0	0	0.0427	0	0
10	0	0	0	0	0	0	0.0342	0	0
11	0	0	0	0	0	0	0.0349	0	0
12	0	0	0	0	0	0	0.0356	0	0
13	0	0	0	0	0	0	0.0363	0	0
14	0	0	0	0	0	0	0.0371	0	0
15	0	0	0	0	0	0	0.0378	0	0
16	0	0	0	0	0	0	0.0386	0	0
17	0	0	0	0	0	0	0.0342	0	0
18	0	0	0	0	0	0	0.0349	0	0
19	0	0	0	0	0	0	0.0356	0	0
20	0	0	0	0	0	0	0.0363	0	0
21	0	0	0	0	0	0	0.0371	0	0
22	0	0	0	0	0	0	0.0378	0	0
23	0	0	0	0	0	0	0.0317	0	0
24	0	0	0	0	0	0	0.0324	0	0

As explained before, with the exception of the electricity demand and the heat from central unit, the marginal costs related to heat and cooling demands should be divided by building, otherwise it would not be possible to individually analyze the hourly values. For that reason, Table 4.2 and Table 4.3 provide the hourly marginal costs, separated by building, associated with the hourly heat and cooling demands, respectively. The mentioned tables can be thought of as a zoom-in in the correspondent values provided in Table 4.1. As expected, most of the values in Table 4.2 are non-zero since the analysis is performed in a winter day and, for that reason, all buildings have heating demands. Conversely, most of the values in Table 4.3 are zero since most buildings do not have cooling demand during the winter. Only building 7 (hospital) has a small cooling demand and, for this reason, its dual values are not zero.

### *4.2.2.2 Marginal cost values associated with technologies*

With the aim to support the marginal cost analysis, this section is intended to calculate and present the marginal cost values associated with heat and cooling production from key technologies within the optimal economic solution. The goal is to know how much it would cost to produce one extra kWh of (i) heat by using BOI or HP, and (ii) cooling by using CC or HP. The calculations and marginal cost values for ICE will not be included since they were not necessary for the marginal cost analysis of the EC optimization solution evaluated in this chapter (the optimal economic one).

#### *Heat production*

Table 4.4 presents the equations and input data necessary to calculate the marginal cost value associated with the production of 1 kWh of heat by using the BOI. The result from such calculation can be used for a BOI installed in any building since the efficiency and associated costs are the same. The input data can also be found on Table 3.6, Table 3.10, and Table 3.12.

Table 4.4 – Marginal cost value associated with 1 kWh of heat production from the BOI.

[A] Marginal amount of heat to be produced	$Heat_{BOI} = 1 \text{ kWh}_h$
[B] Efficiency equation	$Fuel_{BOI} = \frac{Heat_{BOI}}{\eta_{BOI}}$
BOI efficiency ( $\eta_{BOI}$ )	95%
[C] Natural gas price (€/kWh <sub>NG</sub> )	0.085
[D] Maintenance cost (€/kWh <sub>h</sub> )	0.001
<b>[C · B] + [D · A] Marginal cost of heat from BOI (€/kWh<sub>h</sub>)</b>	<b>0.0905</b>

Table 4.5 shows the equations and the necessary input data to calculate the marginal cost value associated with the production of 1 kWh of heat by using HP. In this case, there is not only one result; instead, the associated marginal cost will depend on the three different HP nominal capacities. Only one type of such HP technologies is allowed to be installed in a given building. Table 3.2 and Table 3.4 can support the reader to understand which HP nominal capacity is installed in which building. Input data related to maintenance cost and electricity price were taken from Table 3.10 and Table 3.16.

Table 4.5 – Marginal cost values associated with 1 kWh of heat production from HP.

Marginal amount of heat to be produced		$Heat_{HP} = 1 kWh_h$	
[A] Efficiency equation		$EleC_{HP} = \frac{Heat_{HP}}{COP}$	
[B] Maintenance cost (€/kWh <sub>el</sub> )		0.001	
COP	[C] Elect. price (€/kWh)	[A · B] + [A · C] Marginal cost from HP (€/kWh <sub>h</sub> )	
		0.1169	0.0522
2.26		0.1450	0.0646
		0.1533	0.0683
		0.1169	0.0513
2.3		0.1450	0.0635
		0.1533	0.0671
		0.1169	0.0543
2.17		0.1450	0.0673
		0.1533	0.0711
		0.1169	

*Cooling production*

Table 4.6 shows the equations and input data needed to calculate the marginal cost value associated with the production of 1 kWh of cooling by using the CC. The result from such calculation can be used for a CC installed in any building since the efficiency and associated costs are the same. The input data can also be found on Table 3.6, Table 3.10, and Table 3.16.



Table 4.6 – Marginal cost value associated with 1 kWh of cooling production from the CC.

[A] Marginal amount of cooling to be produced	$Cool_{BOI} = 1 kWh_c$
[B] Efficiency equation	$Elec_{CC} = \frac{Cool_{CC}}{COP_{CC}}$
CC COP	3
[C] Electricity price (€/kWh)	0.1169 0.1450 0.1533
[D] Maintenance cost (€/kWh <sub>c</sub> )	0.002
[C · B] + [D · A] Marginal cost (€/kWh <sub>c</sub> ) of cooling from CC, according to electricity price	<b>0.0410</b> <b>0.0503</b> <b>0.0531</b>

Table 4.7 – Marginal cost values associated with 1 kWh of cooling production from HP.

Marginal amount of cooling to be produced	$Cool_{HP} = 1 kWh_c$	
[A] Efficiency equation	$Elec_{HP} = \frac{Cool_{HP}}{COP}$	
[B] Maintenance cost (€/kWh <sub>el</sub> )	0.001	
COP	[C] Elect. price (€/kWh)	[A · B] + [A · C] Marginal cost from HP (€/kWh <sub>c</sub> )
	0.1169	0.0261
4.51	0.1450	0.0324
	0.1533	0.0342
4.63	0.1169	0.0255
	0.1450	0.0315
	0.1533	0.0333
4.9	0.1169	0.0241
	0.1450	0.0298
	0.1533	0.0315

Table 4.7 presents the equations and the essential input data to calculate the marginal cost value associated with the production of 1 kWh of cooling by using HP. In this case, the associated marginal cost also depends on the three different HP nominal capacities. As stated before, only one type of such HP technologies is allowed to be installed in a given

building. Input data related to maintenance cost and electricity price were taken from Table 3.10 and Table 3.16.

### 4.2.3 TES and DHCN pipelines thermal losses

Thermal energy storage (TES) devices, both for heat and cooling, as well as the district heating and cooling network (DHCN) pipelines own the benefit of supporting the energy supply system of the EC. However, they bring their intrinsic characteristic: heat losses. As reported in Table 3.6 and Table 3.9, the heat loss factor regarding TES is 2% (for both HST and CST), whereas the loss factors for pipelines are calculated per unit of pipeline length (5% for heating and 8% for cooling pipelines). Therefore, the aim of this section is to provide the equations related to the heat losses in TES and DHCN pipelines. Such equations will be crucial to the analysis and interpretation of the marginal cost values associated with the optimal operation of the EC.

#### 4.2.3.1 TES: simultaneous, advanced, and delayed production of energy services

These three types of energy service (heat or cooling) productions are essential to understand the contribution of the TES to the marginal cost associated with the energy supply system at a given hour  $h$ . In accordance with Pina (2019), the three mentioned energy service production types will be detailed below.

Simultaneous production means that the energy service can be produced at the same hour  $h$  it is demanded, i.e., if a marginal energy service unit is demanded at hour  $h$ , the energy service can be produced at that very same hour since (i) there is available capacity to do so, and (ii) using the support of the TES would be more costly.

Advanced production means that the energy service cannot be produced at the same hour  $h$  it is demanded and must be shifted to a previous hour  $k$ . The reason for this depends on the optimal structure and operation of the energy supply system. For instance, one reason could be that all heat-producing technologies are at full capacity at the same analyzed hour  $h$ . If an additional unit of heat is demanded at that hour, the only left option would be the TES. Assuming that this additional heat taken from the TES (at hour  $h$ ) will be needed in the following hours, it means that this additional heat must be compensated for in an earlier hour  $h - k$ . Considering the required heat discharge at hour  $h$ ,  $Heat_{out}(h)$ ,

the amount of heat that must be produced and stored at hour  $k$ ,  $Heat_{prod_{in}}(k)$ , can be obtained through Eq. (4.8). The same logic applies to the cooling storage.

$$Heat_{out}(h) = Heat_{prod_{in}}(k) \cdot (1 - heat_{loss_{HST}})^{(h-k)} \quad (4.8)$$

It means that, when it comes to advanced production, more energy should be produced to compensate for the heat losses inherent to the TES device.

Delayed production means that the energy service cannot be produced at the same hour  $h$  it is demanded and must be shifted to a later hour  $k$ . The reason for this can also vary according to the energy supply system structure and its optimal operation. Equation (4.8) can also be used to calculate how much energy should be produced at hour  $k$  in order to compensate for the heat withdraw at hour  $h$ , bearing in mind that the exponent  $(h - k)$  can be negative. It means that, when it comes to delayed production, less energy should be produced at hour  $k$  since the marginal unit of energy demanded at hour  $h$  will not lose heat in the TES device from hour  $h$  to  $k$ .

#### 4.2.3.2 DHCN: remote production of energy services

The production of an energy service (heat or cooling) in a different building will be referred herein as remote production, which must take into account the pipeline heat losses that will occur when transferring the energy from one building to another. Equation (4.9) provides the heat loss equation for DHCN pipelines. If buildings X and Y are connected through a DHN pipeline and building X is sending heat to building Y, it means that, if building Y needs an additional unit of heat ( $Heat_{building_Y}$ ) from building X, the latter should send the amount of heat ( $Heat_{building_X}$ ) expressed in Eq. (4.9). The same logic applies to cooling pipelines.

$$Heat_{building_X} = \frac{Heat_{building_Y}}{(1 - loss_{pipe})} \quad (4.9)$$

Table 4.8 and Table 4.9 present the loss factors for heat and cooling pipelines, respectively. All non-zero values represent possible connections between the buildings.

Table 4.8 – Loss factors ( $loss_{pipe}$ ) regarding heat pipelines.

		Buildings								
From \ To	1	2	3	4	5	6	7	8	9	
1	-	0.0225	0	0	0.0115	0.01	0	0	0	
2	0.0225	-	0.004	0	0.0125	0.013	0	0	0	
3	0	0.004	-	0.01	0	0	0	0	0	
4	0	0	0.01	-	0	0	0.07	0.07	0	
5	0.0115	0.0125	0	0	-	0.0015	0	0	0	
6	0.01	0.013	0	0	0.0015	-	0	0	0	
7	0	0	0	0.07	0	0	-	0	0.0125	
8	0	0	0	0.09	0	0	0	-	0.02	
9	0	0	0	0	0	0	0.0125	0.02	-	

Table 4.9 – Loss factors ( $loss_{pipe}$ ) regarding cooling pipelines.

		Buildings								
From \ To	1	2	3	4	5	6	7	8	9	
1	0	0.036	0	0	0.0184	0.016	0	0	0	
2	0.036	0	0.0064	0	0.02	0.0208	0	0	0	
3	0	0.0064	0	0.016	0	0	0	0	0	
4	0	0	0.016	0	0	0	0.112	0.112	0	
5	0.0184	0.02	0	0	0	0.0024	0	0	0	
6	0.016	0.0208	0	0	0.0024	0	0	0	0	
7	0	0	0	0.112	0	0	0	0	0.02	
8	0	0	0	0.144	0	0	0	0	0.032	
9	0	0	0	0	0	0	0.02	0.032	0	

### 4.3 Marginal cost analysis and interpretation

Chapter 4 presented the superstructure of each building, central unit, and DHCN pipelines for the EC. It means that, from the point of energy supply resource (solar energy and natural gas, in this case) to the point of energy demand fulfillment of each building, there are several alternative production routes (or operational strategies) that can take place. For instance, the heat demand of a given building can be covered by HP, consuming electricity, BOI, consuming natural gas, and/or even heat produced in another building.

For this reason, this section aims to analyze in detail and interpret the hourly marginal costs, for a January working day, related to electricity, heat, and cooling demands for the nine EC buildings plus central unit, provided in Table 4.1, Table 4.2, and Table 4.3. Such

analysis and interpretation will provide a deeper understanding about the optimal operation of the system and a better insight about operational strategies regarding EC comprising TES (heat and cooling), DHCN pipelines, and sharing electricity (both self-produced and purchased from the grid) among its buildings.

According to Pina (2019), marginal costs should be evaluated individually for each final product. For this reason, sections 4.3.1, 4.3.2, and 4.3.3 will individually evaluate the marginal costs related to electricity, heat, and cooling, respectively.

#### **4.3.1 Electricity marginal costs**

The hourly marginal costs associated with the electricity demand (Table 4.1), are equal to the electricity purchase price for each time band (Table 3.16), and hourly distributed according to Table 3.17 for any working day. As the marginal cost analysis of this chapter is dealing with the optimal economic solution, it is important for the reader to bear in mind that, for this solution, the EC does not sell electricity at any time throughout the year. Instead, it buys electricity most of the time. In fact, for the January working day, DS is buying electricity from the grid for all 24 hours (Figure 3.23 A). It means that, if any building of the EC would need an additional kWh unit of electricity, the DS would have to buy it from the electric grid at the price of the corresponding hour. For example, if a given building needs an additional kWh unit of electricity at hour 10, the DS would have to require it from the grid at the cost of 0.1533 €/kWh.

At this point, a plausible question would be: wouldn't it be possible (and cheaper) for any EC building to self-produce this additional amount of demanded electricity instead of buying it from the grid? To obtain the answer, the reader may refer to two group of figures: (i) Figure 3.14 to Figure 3.22 to see that, based on the optimal energy supply system structure of each building, the only two ways of self-producing electricity are PV plants or ICE, and (ii) Figure 4.1 to Figure 4.9 to see that both types of technologies are at full capacity. Therefore, the only left way to obtain one additional unit of electricity is by purchasing it from the grid.

### 4.3.2 Heat marginal costs

The hourly marginal costs, associated with the buildings heat demand (for the nine buildings together) and the heat demanded from central unit are provided through Table 4.1. Table 4.2, can be thought of as a zoom-in in the third column of Table 4.1, i.e., Table 4.2 presents the hourly marginal costs associated with the buildings heat demand, separated by building. Therefore, differently from the electricity case, the marginal cost analysis associated with the heat demand is performed for each building individually.

This section presents the analysis and interpretation of several relevant marginal cost cases for each building, in order to show the applicability and useful insights that can be obtained with this type of analysis.

#### 4.3.2.1 Building 1 (Town hall)

From hour 1 to 5 and 20 to 24 this building has no heat demand and, therefore, the associated marginal costs are equal to zero.

According to the optimal economic solution, there are three ways to produce heat in building 1 (Figure 3.14): HP, BOI, and ST. From hour 6 to 9 the two HP units are at full load (Figure 4.1) and the ST is not able to produce more heat with the same solar irradiance. Therefore, within the mentioned hours, the only way to produce a marginal amount of heat is by turning the BOI on at a marginal cost of 0.0905 €/kWh (see Table 4.4), which is a case of simultaneous energy service production.

In the following hours (from 10 to 19) the HP units are not at full load anymore. For that reason, it would be cheaper to produce a marginal amount of heat by using the HP units, which are at partial load. Thus, the marginal cost for each hour within this period is 0.0683 €/kWh<sub>h</sub> since the COP<sub>h</sub> of the HP is 2.26 and the hourly electricity price within the same period is 0.1533 €/kWh (see Table 4.5). This is also a case of simultaneous energy service production.

#### 4.3.2.2 Building 2 (Theater)

Comparing to buildings 3, 4, 5, and 6, this building has a more robust energy supply system (section 3.5.1.1). In fact, building 2 performs the four types of energy service

production: simultaneous, advanced, delayed, and remote. Although the heat demand of the theater is only from hour 6 to 24, it has marginal cost values for all 24 hours under analysis. This is because it should send heat to buildings 3 and 6, through the DHN pipelines, and thus, produce heat during all 24 hours. Then, buildings 3 and 6 can send heat to buildings 4 and 5, respectively (Figure 4.11).

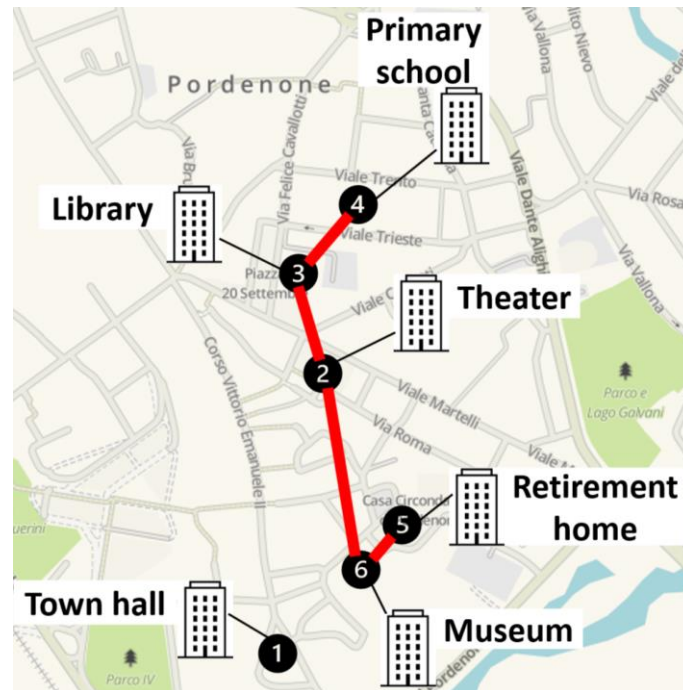


Figure 4.11 – Optimal economic solution: DHN pipeline connections between buildings 2, 3, and 4 (to the north) and 2, 6, and 5 (to the south).

According to the optimal economic solution, there are four ways to produce heat in building 2 (Figure 3.15): HP, BOI, ICE, and ST. From hour 1 to 4, one of the ICE units is at full load. Then, from hour 5 to 24, both ICE units installed in the theater are at full capacity (Figure 4.2). The ST plant cannot deliver more heat due to limitations in its size and solar irradiance. Thus, the only two left options are the HP and BOI.

According to Table 4.4 and Table 4.5, the lower marginal cost value would be derived from HP. In fact, looking at Table 4.2, it is possible to identify that, at hour 10, the marginal cost (0.0671 €/kWh<sub>h</sub>) is equal to the one regarding the HP (Table 4.5) with COP<sub>h</sub> = 2.3 and electricity price = 0.1533 €/kWh (the reader may refer to Table 3.2 and Table 3.5 to see the reason for this COP). Therefore, hour 10 is a case of simultaneous energy

service production, i.e., if building 2 needs a marginal amount of heat at that time, it can be obtained from the HP since, from the two HP units in operation at that time, one is at full load and the other one is at partial load. Another important aspect from hour 10 is that building 2 is sending an electricity surplus to the DS, which means that, if the heat demand increases at that time, the theater would send less electricity to the DS in order to power the HP. Such lack of electricity would obligate the DS to purchase more electricity from the grid at the price in force at hour 10 (0.1533 €/kWh).

From hour 1 to 9 and 11 to 17, the energy service production types are delayed and advanced, respectively, as observed on Table 4.10. At these hours, both ICE and HP units are at full load. Instead of turning the BOI on (which would be more costly), the energy supply system can rely on the hot water storage (HST) to link each one of the mentioned hours to hour 10. The difference is that, for a marginal increase in the heat demand at hours 1 to 9, the HP will have to produce less heat at hour 10 since the heat will not be in the storage from any of these hours up to hour 10 (heat losses will not take place). On the contrary, for a marginal increase in the heat demand at hours 11 to 17, the HP will have to produce more heat at hour 10 in order to compensate for HST heat losses.



Table 4.10 – Marginal costs calculation for building 2, regarding hours 1 to 9 and 11 to 17.

Advanced and delayed cases.

Hour	Marginal costs building 2 (Table 4.2)	$Heat_{out}(h)$ Eq. (4.8) for $k = 10$	Prod. type	$[A \cdot B] + [A \cdot C]$ Calculated marginal cost at hour $k$ (€/kWh <sub>h</sub> )
Marginal amount of heat to be produced at hour 10 $Heat_{HP} = Heat_{out}(h)$				
[A] Efficiency equation	$Elec_{HP} = \frac{Heat_{HP}}{COP}$			
[B] Maintenance cost (€/kWh <sub>el</sub> )	0.001			
[C] Electricity price at hour 10	0.1533			
1	0.0559	0.8337	Delayed	0.0559
2	0.0571	0.8508		0.0571
3	0.0582	0.8681		0.0582
4	0.0594	0.8858		0.0594
5	0.0606	0.9039		0.0606
6	0.0619	0.9224		0.0619
7	0.0631	0.9412		0.0631
8	0.0644	0.9604		0.0644
9	0.0657	0.9800		0.0657
10	<b>0.0671</b>	<b>1.0000</b>		<b>0.0671</b>
11	0.0684	1.0204	Advanced	0.0684
12	0.0698	1.0412		0.0698
13	0.0713	1.0625		0.0713
14	0.0727	1.0842		0.0727
15	0.0742	1.1063		0.0742
16	0.0757	1.1289		0.0757
17	0.0773	1.1519		0.0773

Hours 18 to 20 are supported by the BOI installed in building 2 for two main reasons: (i) both HP and ICE units installed in that building are at full load at these hours, and (ii) at these hours, all heat-producing technologies installed in buildings 3, 4, 5, and 6 (buildings with which building 2 is connected through heat pipelines) are also at full load. It is interesting to note that, for these reasons, buildings 3, 4, 5, and 6 also need support to cover their possible marginal increase in heat demand from hour 18 to 20. The only way to receive such support is through the DHN pipelines. Therefore, for the solution under analysis, the BOI installed in building 2 covers the possible marginal increase in heat

demand of the building and support the possible marginal increase in heat demand of buildings 3, 4, 5, and 6 by means of the DHN pipelines.

Table 4.11 presents the marginal costs related to the hours 18 to 20 for the buildings 2, 3, 4, 5, and 6. It should be noted that the order of the buildings in the table was altered for convenience (according to Figure 4.11); this is how the buildings are connected. To the north, building 2 is connected to building 3, which is connected to building 4. To the south, building 2 is connected to building 6, which is connected to building 5. Therefore, besides the delayed production type, this group of buildings (within the hours 18 to 20) also presents the remote production type (section 4.2.3.2). The following three examples will better explain the relationship between the marginal costs presented in Table 4.11.

Focusing on building 2, if a marginal amount of heat is demanded at hour 18, it will be provided by the BOI installed in the same building at the cost of 0.0926 €/kWh<sub>h</sub>, which is a case of simultaneous production.

Still on building 2, if a marginal amount of heat is demanded at hour 20, the heat production is advanced to hour 18. The amount of heat that must be produced is obtained through Eq. (4.8) considering the loss factor related to the HST and by making  $h = 20$  and  $k = 18$ . If the marginal demanded heat is  $Heat_{out}(20) = 1 kWh_h$ , then the heat that must be produced by the BOI at hour 18 is  $Heat_{prod_{in}}(18) = 1.0412 kWh_h$ .

If building 4 needs an additional amount of heat at hour 19, it must require more heat from building 3 (remote production) since the BOI installed in building 4 is at full load. Knowing that the heat loss in the pipeline between these two buildings is 0.01 (Table 4.8), the marginal amount of heat that building 3 must send to building 4 is  $Heat_{building_3} = 1.0101 kWh_h$ . At that hour, the HP of building 3 is also at full load. Then, the only left option to building 3 is to ask 1.0101 kWh<sub>h</sub> more from building 2. Then, at hour 19, the amount of heat that building 2 must send to building 3 is  $Heat_{building_2} = 1.0142 kWh_h$  (Eq. (4.9)) since the heat loss in the pipeline between these two buildings is 0.004. Following the same logic of the example explained in the previous paragraph, the marginal demanded heat at the hour 19 of building 2 is  $Heat_{building_2} = Heat_{out}(19) = 1.0142 kWh_h$ . Then, the heat that must be produced by the BOI at hour 18 (building 2) is  $Heat_{prod_{in}}(18) = 1.0349 kWh_h$  (Eq. (4.8)). Such marginal path (from hour 19 of

building 4 to hour 18 of building 2) is the reason why the marginal cost at the hour 19 of building 4 is 0.0959 €/kWh<sub>h</sub>.

Table 4.11 – Marginal costs for building 2, regarding hours 18 to 20. Cases of delayed and remote production.

Hour	Buildings				
	4	3	2	6	5
18	0.0939	0.0930	0.0926	0.0938	0.0940
19	0.0959	0.0949	0.0945	0.0958	0.0959
20	0.0978	0.0968	0.0964	0.0977	0.0979

If building 2 needs a marginal amount of heat at hour 21 it will obtain support from the HP installed in building 5 through the remote production mode. At that hour, HP and ICE of building 2 are at full load, and the BOI is off. Then, a cheaper option to compensate for an increase of one unit of heat demand at hour 21 of building 2 is to send one unit less of heat to buildings 6. However, at hour 21, the only heat source for building 6 is the heat from building 2. For this reason, building 6 should send one unit less of heat to building 5. Since, at this time, building 5 has one HP at partial load, the lack of one unit of heat from building 6 will be compensated with one unit more of heat generated by the HP of building 5 (COP = 2.17 and electricity price = 0.1450 €/kWh) at the marginal cost of 0.0673 €/kWh<sub>h</sub> (see Table 4.2 and Table 4.5) (the reader may refer to Table 3.2 and Table 3.5 to see the reason for this COP). It is interesting noting that, in this case, there is no transferred heat from building 5 to building 2. Instead, as mentioned before, the marginal amount of demanded heat in building 2 is covered by sending less heat to building 6 (which will send less heat to building 5). For this reason, there will be no pipelines heat losses and the HP in building 5 will need to produce less heat to compensate for the lack of heat from buildings 2 and 6. Therefore, based on Eq. (4.9), if building 2 needs  $Heat_{building_2} = 1 kWh_h$ , the amount of heat that building 6 will have to produce is  $Heat_{building_6} = 1 kWh_h \cdot (1 - 0.013) = 0.987 kWh_h$ . Then, the amount of heat that building 5 will have to produce is  $Heat_{building_5} = 0.987 kWh_h \cdot (1 - 0.0015) = 0.9855 kWh_h$ . This is the reason why the marginal cost at hour 21 of building 2 is cheaper (0.0663 €/kWh<sub>h</sub>).

If building 2 needs a marginal unit of heat at hour 22, it delays the production to hour 21. Then, the marginal path is the same for hour 21 (building 2) up to building 5. The difference is that the marginal cost of hour 22 (building 2) takes into account the heat loss of the HST from hour 21 to hour 22. Hours 23 and 24 follow the same logic of hour 22.

#### 4.3.2.3 Building 3 (Library)

From hour 1 to 5 and 23 to 24 this building has no heat demand and, therefore, the associated marginal costs are equal to zero.

According to the optimal economic solution, there is only one way to self-produce heat in building 3 (Figure 3.16): through the 35 kW<sub>el</sub> HP. From hour 6 to 8 and 15 to 20 the HP unit is at full load (Figure 4.3). During the rest of the hours the HP is off, with exception of hour 11 when it is at partial load. However, the marginal cost related to its HP functioning at hour 11 (COP<sub>h</sub> = 2.17, electricity price = 0.1533 €/kWh – Table 4.5) would cost 0.0711 €/kWh<sub>h</sub>, which is more costly than the current marginal cost value (0.0687 €/kWh<sub>h</sub>). For these reasons, from hour 6 to 17, building 3 obtains support from the remote production in building 2, which performs an advanced, simultaneous, or delayed production, depending on the hour (Table 4.12). The following two examples will illustrate the three types of production, in this case, and the relationship between the hourly marginal cost values. The reader should bear in mind that, on Table 4.12, blue arrow means remote production, whereas red arrow means advanced or delayed production.

If building 3 needs a marginal amount of heat at hour 6, it will require building 2 to remotely produce and send it. The problem is that, as explained in the building 2 section, the HP and ICE are at full load at hour 6, and running the BOI would be more costly. For this reason, building 2 does the same as explained through Table 4.10, i.e., it delays the heat production to its HP at hour 10. The amount of heat that should be produced by the HP at that hour can be obtained through Eq. (4.8) and Eq. (4.9). Building 3 requires  $Heat_{building_3} = 1 kWh_h$  to building 2, which must send  $Heat_{building_2} = 1 kWh_h / (1 - 0.004) = 1.0040 kWh_h$  to building 3. Then, the amount of heat that the HP in building 2 will have to produce at hour 10 is  $Heat_{prod_{in}} = 0.9261 kWh_h$ . This is the marginal amount of heat that derives the marginal cost in hour 6 of building 3. For the

hours 11 to 17 the logic would be the same, but instead of delayed, the energy production would be advanced within building 2.

Table 4.12 – Marginal costs for building 3, regarding hours 6 to 17. Cases of advanced, delayed, and remote production.

Hour	Buildings	
	2	3
6	0.0619	0.0621
7	0.0631	0.0634
8	0.0644	0.0647
9	0.0657	0.0660
10	0.0671	0.0673
11	0.0684	0.0687
12	0.0698	0.0701
13	0.0713	0.0716
14	0.0727	0.0730
15	0.0742	0.0745
16	0.0757	0.0760
17	0.0773	0.0776

If building 3 demands a marginal amount of heat at hour 10, it will require building 2 to remotely produce and send it. Since building 2 has a HP at partial load at that time, it will perform a simultaneous and remote production and send the heat to building 3.

Hours 18 to 20 of building 3 were explained in the section dedicated to building 2 since they are intrinsically related to hours 18 to 20 of building 2.

The marginal path for hour 21 of building 3 goes through building 2, then building 6, and finally building 5, as explained next. If building 3 needs an additional unit of heat, it will require to building 2 (if building 3 operates its HP, the heat produced would be more costly). Taking into account the pipeline heat loss, building 2 would have to provide building 3 with  $Heat_{building\_2} = 1.0040 \text{ kWh}_h$  (Eq. (4.9)). At hour 21, all the heat-producing technologies of building 2 are at full capacity. Therefore, the only left option for building 2 is to send  $1.0040 \text{ kWh}_h$  less to building 6. Building 6, at its turn, would have to self-produce  $Heat_{building\_6} = 1.0040 \text{ kWh}_h \cdot (1 - 0.013) = 0.9910 \text{ kWh}_h$  of heat. At the same hour, building 6 has no other option but sending  $0.9910 \text{ kWh}_h$  less heat to building 5. Finally, the HP of building 5 will have to produce the marginal heat amount

of  $Heat_{building_5} = 0.9910 kWh_h \cdot (1 - 0.0015) = 0.9895 kWh_h$  at hour 21. For this reason, the marginal cost of building 3 at hour 21 is 0.0666 kWh<sub>h</sub>. In order to check the numbers, the reader may go to Table 4.5, make  $Heat_{HP} = 0.9895 kWh_h$ , and select the  $COP_h = 2.17$  and electricity price = 0.1450 €/kWh.

The marginal cost regarding hour 22 of building 3 follows the same logic of hour 21. Nevertheless, the production is delayed to hour 21 and, for this reason, the heat loss regarding the HST must be taken into account.

#### 4.3.2.4 Building 4 (Primary school)

Similarly to building 3, building 4 has no heat demand from hour 1 to 5 and 23 to 24. Therefore, the associated marginal costs are equal to zero.



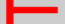
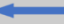



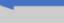



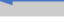












The marginal costs of building 4, related to hours 6 to 17, are presented on Table 4.13. As observed, they are all related to the respective marginal costs of building 2, in a similar way as building 3. The only difference is that the pipeline heat loss between building 4 and 3 should also be taken into account. In order to better understand the relationship between these marginal cost values, the reader may refer to the paragraphs 2, 3, and 4 of the section dedicated to building 3.

Hours 18 to 20 of building 4 were explained in the section dedicated to building 2 since they are intrinsically related to hours 18 to 20 of building 2.

The marginal path for hour 21 of building 4 is similar to the marginal path regarding the same hour for building 3. It goes through buildings 3, 2, 6, and finally building 5 (in that order) as shown in Table 4.14. If building 4 needs a marginal amount of heat at hour 21, it must require to building 3 (if building 4 operates its BOI it would be more costly). Building 3 would have to provide building 4 with  $Heat_{building_3} = 1.0101 kWh_h$  (Eq. (4.9)). At that time, the HP of building 3 is off. Then, the only left option for building 3 is to request 1.0101 kWh<sub>h</sub> to building 2. Building 2, in its turn, would have to provide building 3 with 1.0142 kWh<sub>h</sub>. Since all the heat-producing technologies are at full capacity, the only option for building 2 is to send 1.0142 kWh<sub>h</sub> less heat to building 6. Then, building 6 would have to self-produce  $Heat_{building_6} = 1.0142 kWh_h \cdot (1 - 0.013) = 1.0010 kWh_h$ . At hour 21, building 6 has no other option but sending




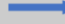
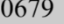

1.0010  $kWh_h$  less heat to building 5. Finally, the HP of building 5 will have to produce  $Heat_{building_5} = 1.0010 kWh_h \cdot (1 - 0.0015) = 0.9995 kWh_h$  more heat at hour 21. This is the reason why the marginal cost at hour 21 of building 4 is very close to the one of building 5.

Table 4.13 – Marginal costs for building 4, regarding hours 6 to 17. Cases of advanced, delayed, and remote production.

		Buildings		
Hour		2	3	4
6		0.0619		0.0621
7		0.0631		0.0634
8		0.0644		0.0647
9		0.0657		0.0660
10		0.0671		0.0673
11		0.0684		0.0687
12		0.0698		0.0701
13		0.0713		0.0716
14		0.0727		0.0730
15		0.0742		0.0745
16		0.0757		0.0760
17		0.0773		0.0776

The marginal cost regarding hour 22 of building 4 follows the same logic of hour 21. However, the production is advanced to hour 21 (Table 4.14) and, for this reason, the heat loss regarding the HST must be taken into account.

Table 4.14 – Marginal costs for building 4, regarding hours 21 and 22. Cases of delayed and remote production.

		Buildings				
Hour		4	3	2	6	5
21		0.0672		0.0666		0.0663
22		0.0686		0.0679		0.0676
						0.0672
						0.0685
						0.0673
						0.0686

#### 4.3.2.5 Building 5 (Retirement home)

Although building 5 receives heat from building 6 during all 24 hours, the former is more independent in terms of covering its hourly marginal increase of heat demand, i.e., for the

solution under analysis, it does not make use of the remote production type at any moment of the typical day under study. The heat-producing technologies installed in building 5 are one 35 kW<sub>el</sub> HP unit ( $COP_h = 2.17$ ), one 10 kW BOI, and 12 m<sup>2</sup> ST plant. At the hours 9, 10, and 21, the HP is at partial load. For this reason, if building 5 needs a marginal amount of heat at these hours, the marginal cost (as indicated on Table 4.15) will be related to operating the installed HP with the correspondent electricity price for each hour. The three mentioned hours are cases of simultaneous production type.

Then, if building 5 needs a marginal amount of heat at the hours 1 to 6 and 8, it will delay the production to hour 10 by using the HST. The exact amount of heat ( $Heat_{out}(h)$ ) can be obtained through Eq. (4.8) and the marginal costs can be calculated by using Table 4.10 with  $k = 10$ ,  $COP_h = 2.17$ , and making  $Heat_{HP} = Heat_{out}(h)$ . In a similar way, if building 5 needs a marginal amount of heat at the hours 13 to 17, it will advance the production to hour 10 by using the HST.

Hours 18 to 20 of building 5 were explained in the section dedicated to building 2 since they are intrinsically related to hours 18 to 20 of building 2.

Finally, if building 5 demands a marginal amount of heat at hours 22 to 24, the heat production is advanced to hour 21 when the HP is at partial load. The exact amount of heat for each hour can be obtained through Eq. (4.8) with  $k = 21$  and the marginal costs can be calculated by using Table 4.10, selecting  $COP_h = 2.17$ , and electricity price = 0.1450 €/kWh for hours 22 to 24.



Table 4.15 – Marginal costs for building 5, regarding hours 1 to 24. Cases of advanced, delayed, and simultaneous production.

Hour	Building 5
1	0.0567
2	0.0579
3	0.0591
4	0.0603
5	0.0615
6	0.0628
7	0.0787
8	0.0654
9	0.0673
10	0.0711
11	0.1655
12	0.0833
13	0.0723
14	0.0738
15	0.0753
16	0.0768
17	0.0784
18	0.0940
19	0.0959
20	0.0979
21	0.0673
22	0.0686
23	0.0700
24	0.0715

B  
2

#### 4.3.2.6 Building 6 (Museum)

As observed in Figure 4.6, the museum heat demand takes place only from hour 6 to 19. However, it actually demands heat during all 24 hours of the day under analysis since it must send heat to building 5 every single hour. Almost the entire hourly heat demand of building 6 is covered by the hourly amount of heat received from building 2 (Figure 4.6 B). In fact, the BOI and ST plant (the only heat-producing technologies in building 6) have small installed capacities compared to the heat demand and cover only 3% of the total annual heat demand of the building.

As illustrated on Table 4.16, if building 6 needs a marginal amount of heat at the day under analysis, four types of scenarios will take place: (i) from hour 1 to 6 plus hour 8, building 6 will take the marginal amount of heat from building 2 which will advance the heat production to hour 10 (running the BOI of building 6 would be more costly), (ii) as the HP in building 5 is at partial load at hours 9 and 10, building 6 will send less heat to

building 5 at these hours, so that its HP can simultaneously produce the required amount of heat at the respective hour, (iii) from hour 13 to 17, building 6 will require the marginal amount of heat to building 2 which will advance the heat production to hour 10 (at these hours, the HP in building 5 is either off or at full capacity, and running the BOI of building 5 or 6 would be more costly), and (iv) as the HP in building 5 is at partial load at hour 21, building 6 will send less heat to building 5 at this hour, so that its HP can simultaneously produce the required amount of heat; then, from hour 22 to 24, building 6 will also send less heat to building 5, however, the production will be advanced to hour 21. The following three examples will help to better understand the mentioned scenarios.

If building 6 needs a marginal amount of heat at hour 1, it will take the heat from building 2. According to Eq. (4.9), the amount of heat that building 2 must send at that hour is  $Heat_{building\_2} = 1 kWh_h / (1 - 0.013) = 1.0132 kWh_h$ . As the production is delayed to hour 10 (building 2) and according to Eq. (4.8), the amount of heat that must be produced is  $Heat_{prod\_in}(k = 10) = 0.8447 kWh_h$ . Since building 2 has a 2.3 COP<sub>h</sub> HP, the electricity price at hour 10 is 0.1533 €/kWh, and making  $Heat_{HP} = Heat_{prod\_in}(k = 10)$  on Table 4.10, the marginal cost value will be 0.0567 €/kWh<sub>h</sub>, which is the marginal cost related to hour 1 of building 6 (Table 4.16). The reader may verify that, as building 5 has a 2.17 COP<sub>h</sub> HP, taking the marginal path through building 5 up to hour 10 would result in a higher marginal cost value (0.0592 €/kWh<sub>h</sub>).

If building 6 requests a marginal amount of heat at hour 9, it will send a marginal amount less of heat to building 5. According to Eq. (4.9), the amount of heat that building 5 must produce to compensate for the lack of heat at that hour is  $Heat_{building\_5} = 1 kWh_h \cdot (1 - 0.0015) = 0.9985 kWh_h$ , i.e., less heat should be produced since it will not be sent through the pipeline and, for this reason, the heat loss will not take place. As it is a simultaneous production type, Eq. (4.8) will not be necessary. Since building 5 has a 2.17 COP<sub>h</sub> HP, the electricity price at hour 9 is 0.1450 €/kWh, and making  $Heat_{HP} = Heat_{building\_5}$  on Table 4.10, the marginal cost value will be 0.0672 €/kWh<sub>h</sub>, which is the marginal cost related to hour 9 of building 6 (Table 4.16).

Table 4.16 – Marginal costs for building 6, regarding hours 1 to 24. Cases of advanced, delayed, and remote production.

Hour	Building					
	5	6	2			
1	0.0567	0.0567	0.0559			
2	0.0579	0.0578	0.0571			
3	0.0591	0.0590	0.0582			
4	0.0603	0.0602	0.0594			
5	0.0615	0.0614	0.0606			
6	0.0628	0.0627	0.0619			
7	0.0787	0.0785	0.0631			
8	0.0654	0.0653	0.0644			
9	0.0673	0.0672	0.0657			
10	0.0711	0.0710	0.0671			
11	0.1655	0.1652	0.0684			
12	0.0833	0.0724	0.0698			
13	0.0723	0.0722	0.0713			
14	0.0738	0.0737	0.0727			
15	0.0753	0.0752	0.0742			
16	0.0768	0.0767	0.0757			
17	0.0784	0.0783	0.0773			
18	0.0940	0.0938	0.0926			
19	0.0959	B2	0.0958	B2	0.0945	B2
20	0.0979		0.0977		0.0964	
21	0.0673	0.0672	0.0663			
22	0.0686	0.0685	0.0676			
23	0.0700	0.0699	0.0690			
24	0.0715	0.0714	0.0704			

Finally, if building 6 needs a marginal amount of heat at hour 24, it will send a marginal amount less of heat to building 5 at the same hour. According to Eq. (4.9), the amount of heat that building 5 must produce to compensate for the lack of heat at that hour is  $Heat_{building\_5} = 1 kWh_h \cdot (1 - 0.0015) = 0.9985 kWh_h$ . As the production is advanced to hour 21 (building 5) and according to Eq. (4.8), the amount of heat that must be produced is  $Heat_{prod\_in}(k = 21) = 1.0609 kWh_h$ , i.e., the heat loss from hour 21 to 24 (regarding the HST) should be taken into account. Since building 5 has a  $2.17 COP_h$  HP, the electricity price at hour 21 is  $0.1450 \text{ €/kWh}$ , and making  $Heat_{HP} = Heat_{prod\_in}(k = 21)$  on Table 4.10, the marginal cost value will be  $0.0714 \text{ €/kWh}_h$ , which is the marginal cost related to hour 24 of building 6 (Table 4.16).

## 4.3.2.7 Building 7 (Hospital)

As already mentioned in section 4.1.1, the hospital has the largest energy supply system in terms of number of installed technologies, installed capacity, and magnitude of the energy flows (Figure 3.20). When it comes to heat-producing technologies, the solution under study installed five  $200 \text{ kW}_{el}$  ICE units, six  $100 \text{ kW}_{el}$  HP units, one  $810 \text{ kW}_{th}$  BOI, and  $49 \text{ m}^2$  of ST panels. Figure 4.12 was added in order to provide the reader with a visual aid regarding the location and connections between buildings 7, 9, 8, and central unit (in that order). This might be a good support when reading the analysis and interpretation of the marginal costs (Table 4.17) corresponding to these mentioned buildings.

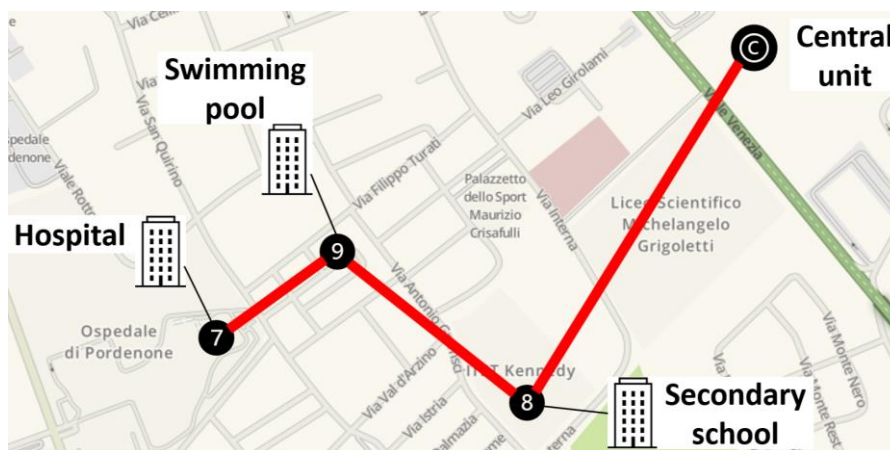


Figure 4.12 – Optimal economic solution: DHN pipeline connections between buildings 7, 9, 8, and central unit.

Next are explained some representative cases of advanced, delayed, simultaneous, and remote production shown in Table 4.17.

When building 7 needs a marginal amount of heat from hour 2 to 8, it would have to generate more heat from the BOI at hour 5, which is at partial load (at the marginal cost of  $0.0905 \text{ €/kWh}_h$ ). The reasons for this are: (i) the ICE and HP of building 7 are at full load, (ii) the HP units, in building 9, are at full load, and (iii) the HP units at building 8 are not at full load (at these hours), however the DHN pipelines between buildings 8, 9, and 7 are at full capacity of heat transport ( $2100 \text{ kWh}_h$ ) and, for this reason, they are not able to send more heat to building 7 at such hours. Therefore, as illustrated in Table 4.17, the BOI at hour 5 would be responsible for generating the marginal demanded heat,

whereas hours 2 to 4 would delay the heat production to hour 5 and hours 6 to 8 would advance the production to hour 5.

At hour 10, the ICE and HP of building 7 are also at full load, while the BOI is off. Although the DHN pipeline with building 9 is not at full load (at this hour), the HP of building 9 is at maximum capacity. However, the DHN pipeline between buildings 9 and 8 and the HP in building 8 are not at full load. For this reason, if building 7 requires a marginal amount of heat at hour 10, it would require such amount of heat to building 9. On its turn, building 9 would have to provide building 7 with  $Heat_{building_9} = 1 kWh_h / (1 - 0.0125) = 1.0127 kWh_h$ . As building 9 cannot generate any amount of heat at hour 10, it would request the heat to building 8. Then, building 8 would have to provide building 9 with  $Heat_{building_8} = 1.0127 kWh_h / (1 - 0.02) = 1.0333 kWh_h$ , which would be generated through the HP. As the HP units installed in building 8 have a  $COP_h = 2.26$  and the electricity price at hour 10 is 0.1533 €/kWh, the marginal cost for building 7 at hour 10 would be 0.0705 €/kWh<sub>h</sub> (Table 4.17). In order to check the numbers, the reader may use Table 4.5 making  $Heat_{HP} = 1.0333 kWh_h$ .

An interesting marginal path is the one related to hour 11 of building 7. As indicated in Table 4.17 (dashed red arrow), the mentioned marginal path passes through buildings 9, 8, and central unit (at the same hour 11), goes from hour 11 to 15 through the heat storage of the central unit (HSTc), and returns to building 8 at hour 15 (where it has a HP at partial load). Therefore, the marginal path (hour 11, building 7) starts by taking the same path as the one regarding hour 10 (up to building 8). The difference is that building 8 is not able to self-generate the extra amount of heat at hour 11. Then, building 8 asks 1.0333 kWh<sub>h</sub> (same amount calculated in the previous paragraph) to the central unit, at hour 11, which is charging its heat storage – HSTc (Figure 4.10) at this time. Thus, the central unit can charge 1.0333 kWh<sub>h</sub> less heat to its storage device and send it to building 7 (through buildings 8 and 9, in this order). However, such missing amount of heat in the HSTc must be offset. The optimal marginal path found is by sending less heat to building 8 at hour 15 since its HP is at partial load (delayed production). Using Eq. (4.8) and knowing that HSTc heat loss is 0.005, it is possible to calculate the exact amount of heat that the central unit will not send to building 8:  $Heat_{prod_{in}}(15) = (1.0333 kWh_h / (1 - 0.005))^{(11-15)} = 1.0128 kWh_h$ . Therefore, taking into account that it was not considered

any heat losses between central unit and building 8, the later must produced  $1.0128 \text{ kWh}_h$  at hour 15, by using a  $2.26 \text{ COP}_h$  HP, and electricity price of  $0.1533 \text{ €/kWh}$  (Table 4.5). The marginal cost value (hour 11, building 7) must be equal to  $0.0691 \text{ €/kWh}_h$ .

Table 4.17 – Marginal costs for buildings 7, 9, 8, and central unit (in this order – see Figure 4.12). Cases of advanced, delayed, simultaneous, and remote production. Blue arrows: marginal path passing through DHN pipeline; red arrows: marginal path passing through the HST of a given building; green arrows: marginal path passing through the HSTc of the central unit; red boxes: cases of simultaneous heat production; red dashed and dotted lines represent specific cases of marginal paths explained throughout the text.

Hour	Building			Central unit
	7	9	8	
1	0.0799	0.0789	0.0774	0.0759
2	0.0852	0.0532	0.0522	0.0763
3	0.0869	0.0532	0.0522	0.0766
4	0.0887	0.0532	0.0522	0.0770
5	0.0905	0.0532	0.0522	0.0774
6	0.0923	0.0809	0.0793	0.0778
7	0.0942	0.0813	0.0797	0.0782
8	0.0961	0.0817	0.0801	0.0786
9	0.0832	0.0822	0.0805	0.0790
10	0.0705	0.0697	0.0683	0.0683
11	0.0691	0.0683	0.0669	0.0669
12	0.0679	0.0671	0.0672	0.0672
13	0.0679	0.0671	0.0676	0.0676
14	0.0679	0.0671	0.0679	0.0679
15	0.0674	0.0697	0.0683	0.0683
16	0.0688	0.0679	0.0686	0.0686
17	0.0702	0.0693	0.0690	0.0690
18	0.0716	0.0707	0.0693	0.0693
19	0.0709	0.0700	0.0686	0.0696
20	0.0723	0.0714	0.0700	0.0700
21	0.0667	0.0659	0.0646	0.0704
22	0.0753	0.0659	0.0646	0.0707
23	0.0769	0.0659	0.0646	0.0711
24	0.0784	0.0659	0.0646	0.0714

In a similar way as for hour 10, if building 7 needs a marginal amount of heat from hour 12 to 14, it cannot obtain such amount of heat from its own energy supply system since it is at full load in the mentioned hours. As there is a HP unit at partial load (at the same hours) in building 9, building 7 can obtain support from it by requesting a marginal amount of heat. Thus, building 9 must provide  $Heat_{building\_9} = 1 kWh_h / (1 - 0.0125) = 1.0127 kWh_h$  to building 7 from hour 12 to 14. As the HP installed in building 9 has a  $COP_h = 2.3$  and the electricity price at hour 12 to 14 is 0.1533 €/kWh, the marginal cost for building 7 at such hours is 0.0679 €/kWh<sub>h</sub> (Table 4.17).

The marginal path for hour 20 follows a similar route as the one for hour 11 (the difference is that, in the central unit, the production is advanced to hour 15), whereas hour 19 is related to hour 20 through the HST of building 7.

Finally, if building 7 demands a marginal amount of heat at hour 21, the logic would be the same as for hour 10, i.e., as the heat-producing technologies are at full load or switched off, building 7 would demand more heat from building 8 since the HP in building 9 is at full load. In order to check the numbers, the reader may perform the same calculations as for hour 10, but with electricity price = 0.1450 €/kWh. The result must be 0.0667 €/kWh<sub>h</sub> (Table 4.17).

#### 4.3.2.8 Building 8 (Secondary school)

As illustrated in Figure 3.21 and Figure 4.8, the secondary school has one of the simplest energy supply systems among the EC buildings and is responsible for receiving the heat from the central unit and distributing it to the other buildings. The installed BOI does not operate during the typical day under analysis since the heat provided by the HP units ( $COP_h = 2.26$ ) plus the heat received from the central unit are enough to cover the internal demand and to send the surplus to building 9.

As indicated in Table 4.17, building 8 has several hours in which the marginal cost values are equal to the one regarding the installed HP units and at the electricity price of the corresponding hour. The following marginal cost values can be directly checked by using Table 4.5.

If building 8 needs a marginal amount of heat at the hours 2 to 5, 10, 15, and 21 to 24, it can obtain the extra amount of heat from its own HP since it is at partial load at these hours. The difference is that, from hour 2 to 5, the electricity price is 0.1169 €/kWh, for hours 10 and 15 the electricity price is 0.1533 €/kWh, and from hour 21 to 24 the electricity price is 0.1450 €/kWh. For that reason, the marginal cost values at these hours are, respectively, 0.0522 €/kWh<sub>h</sub>, 0.0683 €/kWh<sub>h</sub>, and 0.0646 €/kWh<sub>h</sub>.

Bearing in mind that the optimal solution under study did not install any thermal storage in building 8, it is interesting to note how building 8 can make use of the heat storage in central unit to advance or delay the heat production (Table 4.17 – green arrows). If building 8 needs a marginal amount of heat at any hour from 11 to 14, it receives the extra heat from the central unit which charges less its HSTc in the same amount. Then, the central unit offset the lack of heat by delaying the production to hour 15 and sending  $Heat_{prod_{in}}(15) = 1 kWh_h / (1 - 0.005)^{(11-15)} = 0.9802 kWh_h$  (Eq. (4.8) – for  $h = 11$ ) less to building 8, which can produce it by using its HP at partial load.

The same logic goes for hours 16 to 18. The difference is that the production would be advanced to hour 15, at the central unit. The numbers can be checked by using Table 4.5.

Another interesting marginal path for building 8 is the one related to hour 19 (Table 4.17 – dotted red arrows). Since central unit does not send any amount of heat at this hour (Figure 4.10), building 8 cannot obtain support from it. As neither building 8 nor building 9 have heat storages, they can only count on the DHN pipelines. If building 8 needs an marginal unit of heat at hour 19, it will have to send a marginal unit less of heat to building 9, which will need  $1 kWh_h \cdot (1 - 0.02) = 0.98 kWh_h$  (Eq. (4.9)). As building 9 cannot generate more heat at that hour, it will send 0.98 kWh<sub>h</sub> less to building 7. Since building 7 is not able to produce more heat at that hour, it will discharge  $0.98 kWh_h \cdot (1 - 0.0125) = 0.9678 kWh_h$  from its HST (at hour 19 yet). As such amount of heat will not pass through thermal losses in the HST, at hour 20 building 7 will need  $Heat_{prod_{in}}(20) = 0.9678 kWh_h / (1 - 0.02)^{(19-20)} = 0.9484 kWh_h$  to compensate for the lack of heat. The only option is to require such amount of heat to building 9, which will have to send  $0.9484 kWh_h / (1 - 0.0125) = 0.9604 kWh_h$ . As building 9 cannot generate it, the only left way is to request the amount of heat to building 8, which should send  $0.9604 kWh_h / (1 - 0.02) = 0.98 kWh_h$ . Building 8, at its turn, asks the central



unit to send  $0.98 \text{ kWh}_h$  more (no pipeline heat loss was considered here). Then, central unit advances the heat production to hour 15 since it is able to send  $Heat_{prod_{in}}(15) = 0.98 \text{ kWh}_h / (1 - 0.005)^{(20-15)} = 1.0049 \text{ kWh}_h$  less to building 8. Finally, building 8 will have to produce  $1.0049 \text{ kWh}_h$  by using its 2.26  $COP_h$  HP and electricity price of 0.1533 €/kWh. By using the procedure of Table 4.5, the result should be exactly 0.0686 €/kWh<sub>h</sub>.

#### 4.3.2.9 Building 9 (Swimming pool)

The swimming pool energy supply system is even simpler. It only has five HP units of 100 kW<sub>el</sub> each, although it receives a large amount of heat from building 8. As indicated in Table 4.17, from hour 12 to 14 the building can obtain a marginal amount of heat from its own HP units as they are at partial load.

At the hours 2 to 5, 10, 15, and 21 to 24, building 9 can obtain support from the HP units in building 8, which are at partial load. Hour 11 follows the same marginal path as the one for hour 11 of building 7 (Table 4.17 – dashed red arrows), whereas hours 16 to 20 follow a similar marginal path as the one for hour 19 of building 8.

### 4.3.3 Cooling marginal costs

#### 4.3.3.1 Building 7 (Hospital)

As already mentioned, the hospital is the only building which has a small cooling demand even during the winter. According to the optimal economic solution, the only cooling-producing technologies installed in the hospital are six 100 kW<sub>el</sub> HP units and a 41 kW<sub>el</sub> CC, plus the CST to support the cooling production/supply process.

As observed on Table 4.18, the simultaneous cooling production type is in force at hours 7, 10, and 17 (the reader may also refer to Figure 4.10 B). The marginal cost value at hour 7 is the marginal cost derived from the CC, with electricity price = 0.1169 €/kWh (Table 4.6). The marginal cost value at hour 10 and 17 is equal to the marginal cost resulting from operating the HP ( $COP_c = 4.51$ ) under the electricity price of 0.1533 €/kWh.

The marginal path regarding hours 8 and 9 advances the cooling production to the CC at hour 7. Although the CC is in operation at hour 8, it could not generate any additional

amount of cooling since it is at full load (the reader may note that if CC was not at full load, the marginal cost at hour 8 would be lower). The marginal amount of cooling to be advanced can also be calculated using Eq. (4.8). It is interesting to note that the marginal cost of hour 9 would be lower if the cooling production would be delayed to the HP at hour 10. However, as the CST is completely discharged at hour 9, it could not provide any additional amount of cooling (to be offset at hour 10). Therefore, if a marginal amount of cooling is needed at hour 9, the CC at hour 7 would have to compensate for the lack of cooling.

The cooling demand at the hours 11 to 16 and 18 to 22 is completely covered by the CST device, which is charged at hours 10 and 17 by means of the HP. If a marginal amount of cooling is required at the hours 11 to 16 and 18 to 22, the cooling production is advanced to the hours 10 and 17, respectively.

Table 4.18 – Cooling marginal costs regarding building 7. Cases of advanced, delayed, and simultaneous production.

Hour	Building 7
1	0.0363
2	0.0370
3	0.0378
4	0.0386
5	0.0394
6	0.0402
7	0.0410
8	0.0418
9	0.0427
10	0.0342
11	0.0349
12	0.0356
13	0.0363
14	0.0371
15	0.0378
16	0.0386
17	0.0342
18	0.0349
19	0.0356
20	0.0363
21	0.0371
22	0.0378
23	0.0317
24	0.0324

## 4.4 Conclusions

The analysis and interpretation of relevant hourly marginal costs related to the entire energy supply system of the energy community (EC) was presented in this chapter. Such analysis and interpretation of the marginal cost values provided insights that the optimization developed in chapter 3 could not provide. The mentioned insights regard mainly the determination of the optimal operation of the system when the energy demand of a given building is modified without changing the operation mode or configuration of the analyzed system.

The energy supply system of the EC comprises a highly complex polygeneration structure to supply electricity, heat, and cooling to nine buildings. The structure is supported by heat and cooling storages, DHCN pipelines, and the sharing of electricity (both purchased and self-produced) among the buildings. The mentioned analysis and interpretation were developed for a typical winter day (January working day) and based on the optimal economic solution presented in section 3.5.1.

The results were presented by dividing the marginal cost values by energy service type and building. The chapter contributed with valuable insights about several possible marginal paths and the reasons why some paths are more expensive than others. More specifically, the chapter contributed with the analysis and interpretation of the hourly marginal costs of a complex and highly integrated polygeneration system and the outline of different marginal paths through advanced, delayed, simultaneous, and remote energy services production types.



---

*CHAPTER 5 – On the Role of  
Energy Communities in the Italian  
National Energy System: A Local  
Optimization Approach*

---



---

## **CHAPTER 5 – On the Role of Energy Communities in the Italian National Energy System: A Local Optimization Approach**

In a similar way as for chapters 3 and 4, the main focus of the present chapter is the energy community (EC), which has been described in section 3.1. Chapter 3 focused on the optimization of the EC whereas chapter 4 on the analysis and interpretation of the hourly marginal costs related to the energy demands of each EC building. The present chapter proposes an evaluation of the role of such ECs in the economic and environmental aspects of a future Italian energy system scenario with a high level of renewable energy deployment.

In order to do so, three main elements are needed: (i) the EC model, (ii) a model representing the Italian national energy system (NES), and (iii) a methodology that, based on the EC and Italian NES models, systematically answers the abovementioned research question. The EC model is the same as the one presented in chapter 3 (with few modifications to the input data, which will be explained later). The Italian NES was selected from the literature and is duly presented and explained on section 5.3. Finally, the applied methodology is inspired on the thermoeconomic local optimization (LO) method, which states that, when the thermoeconomic isolation is fulfilled, the optimal configuration of a local subsystem is coherent with the optimal configuration of the global system, provided that specific conditions are met (Reini, 1994; Serra, 1994; Lozano, Valero and Serra, 1996).

The motivation to perform such procedure is linked to what has been discussed in the introduction of this thesis, i.e., the global increasing demand for primary energy resources, the consequent increase in greenhouse gas (GHG) emissions, the climate anomalies and environmental impacts that have worsened in recent years, and the need for the scientific community to seek not only renewable energy sources integration, but also more efficient strategies for energy supply systems.

Furthermore, the recent global energy crisis has underlined even further the critical need for a comprehensive response. Events such as a pandemic and geopolitical tensions have

demonstrated the fundamental role of a possible "energy independence" between countries, or at least reducing energy dependence. The European Union (EU), recently facing challenges in gas supplies, has responded with a strategic plan emphasizing, for instance, energy supply systems efficiency improvement and increasing in the deployment of renewables. It makes part of the EU's broader commitment to achieve carbon neutrality by 2050, exemplified by the "Fit for 55" package (European Council, 2023). Therefore, it becomes clear the significance of not only the continuation of deploying renewable sources, but also the enhancement of energy supply systems.

Having said that, it is pertinent going back to the research question of the beginning of this chapter: *what the role of ECs (such as the case study of this thesis) in the economic and environmental aspects of a future Italian energy system scenario with a high level of renewable energy deployment could be?* Answering this question is the main objective of the present chapter.

## **5.1 The local optimization approach**

The optimization performed in chapter 3 can be regarded as a global optimization (GO) of an energy supply system, which objective is identifying optimal values for independent design variables that minimize the overall resource consumption of the system, maintaining constant the energy demand. Similarly, local optimization (LO) aims the minimization of resources consumption within the entire system but optimizing each subsystem independently, as if they were isolated units (Reini, 1994). The knowledge of the internal costs within a given system allows the separate analysis of its subsystems and facilitates the proper application of a LO procedure for complex energy systems since it simplifies the approach by focusing on individual subsystems instead of the entire system (Serra, 1994).

Reini (1994) obtained thermoeconomic isolation conditions (previously proposed also by Evans (1980)) starting from the "cost impact" relation. It allowed the correspondence (or a reasonable approximation) between the optimal solution of the LO problem and the optimal solution of the GO problem. The mentioned thermoeconomic isolation conditions, which are also highlighted by Serra (1994), are:



- A given independent design variable ( $x$ ) must be, in fact, a local variable of the subsystem and must appear only in the equations related to consumptions and to operation-maintenance-investment coefficients,
- The product of the subsystem should be constant, and
- The cost of the flows in the frontier between the global and local system should also be constant.

However, still according to Reini (1994), none of the three conditions are strictly verified in real energy conversion systems since, in general, it is hard to find design variables affecting only one subsystem. Therefore, the concept of a thermoeconomically isolated subsystem is always an approximation and, for that reason, the algorithm presented in Eq. (5.1) can be used in order to develop the LO approach, obtaining an enhancement of the objective function (Reini, 1994; Reini, Lazzaretto and Macor, 1995).

$$\begin{aligned}
 \min: \Phi_L &= \sum_{j:E_j \in E_h} \lambda_j^o k_{hj} + \frac{Z_h}{P_h^o} \\
 k_{hj} &= k_{hj}(x) \\
 Z_h &= z_h(x)
 \end{aligned} \tag{5.1}$$

In Eq. (5.1),  $\Phi_L$  comes from the deduction of the cost impact relation (Reini, 1994; Reini, Lazzaretto and Macor, 1995),  $j$  is a given energy flow,  $h$  is a given subsystem,  $\lambda_j^o$  is the initial marginal cost of an energy flow at the border between the global and local system,  $k_{hj}$  is related to fuel consumption,  $Z_h$  is related to capital costs,  $P_h^o$  is the initial product of the given subsystem, and  $x$  is the independent design variable.

Once the independent design variables have been identified, the LO problem can be solved using Eq. (5.1) by performing an iterative procedure (Lozano, Valero and Serra, 1996; Buoro and Reini, 2010). However, the reader should bear in mind that the LO approach always involves the utilization of a model representing the global system. Therefore, besides a local model as the one presented in Eq. (5.1), a global model is also necessary and such approach can be regarded as local-global optimization (LGO), which is a nomenclature also used by Muñoz and Von Spakovsky (2000). The LGO allows to tackle the problem through two different approaches, as explained in Table 5.1.

Table 5.1 – Detailed description of two approaches to tackle the problem of the local-global optimization.

<p><b>Approach 1</b> (only the local subsystem model is optimized)</p>	<ul style="list-style-type: none"> <li>• Only the LO is performed by using the marginal costs of flows at the frontier between the local subsystem and global system.</li> <li>• The optimal local solution found regards the independent design variables of the local subsystem.</li> <li>• Such optimal local solution is expected to be close to an optimal global solution that could be obtained by optimizing the same local independent design variables through an algorithm comprising both systems (global system and local subsystem).</li> <li>• It is hard to know how much the optimal local solution could improve the optimal global solution, however it is possible to verify by simulation (not optimization) of the global system if the local optimum is consistent with a global optimum of the whole system.</li> </ul>
<p><b>Approach 2</b> (both local subsystem and global system models are optimized)</p>	<ul style="list-style-type: none"> <li>• This approach foresees (i) the availability of a global system model divided into local subsystems, and (ii) interactions between the results obtained from the global system model and the local subsystem model.</li> <li>• For each local subsystem, a LO is performed in the same way as described in the Approach 1.</li> <li>• With this, the locally optimized independent design variables are obtained.</li> <li>• Then, a global optimization is performed, i.e., the costs of the internal flows of the global system are recalculated using the locally optimized independent design variables.</li> <li>• The results of the internal flow costs are used as input to perform a LO for the second time to obtain new locally optimized independent design variables.</li> <li>• In the case of a convergence of the independent design variables, it can be demonstrated that the optimal global solution has been reached. The only possible error would be due to truncation.</li> </ul>

Therefore, the LO problem, related to the research question proposed in the introductory section of this chapter, will be tackled by using the Approach 2 since both models are available (local and global). The next subsection presents the other two important elements to perform the proposed LO.

## 5.2 The proposed local optimization

Besides an appropriated methodology, the other two elements needed to answer the research question, proposed in the beginning of this chapter, are the Italian national energy system (NES) model, representing the global system, and the EC model representing the local system (or subsystem). The next two subsections are dedicated to explaining the global system and the local subsystem. Then, sections 5.3 and 5.4 are dedicated to present and discuss the Italian NES model and the EC model, respectively.

### 5.2.1 The global system

The Italian NES was thought as the global system due to three main reasons: (i) the difficulty of finding a model or even detailed enough data regarding only the Italian region of interest (Friuli Venezia Giulia), (ii) writing a regional model from scratch would probably imply a certain number of assumptions (since it is not the central scope of the thesis) that could increase even further the uncertainties related to the proposed LO procedure, and (iii) the Italian NES model found in the literature is reasonably detailed to properly represent the global system for the analysis developed within this chapter.

Figure 5.1 (A) presents a schematic diagram representing the starting point regarding the global system (Italian NES). As observed and leaving aside for a moment the fact about the difference in size proportions, the starting point represents a scenario where the buildings (the same ones considered for the analysis of the EC case study) are not interconnected to establish an EC yet. Instead, the buildings are directly connected to the electric grid and cover their own energy demands in the conventional way (as explained in section 3.4).

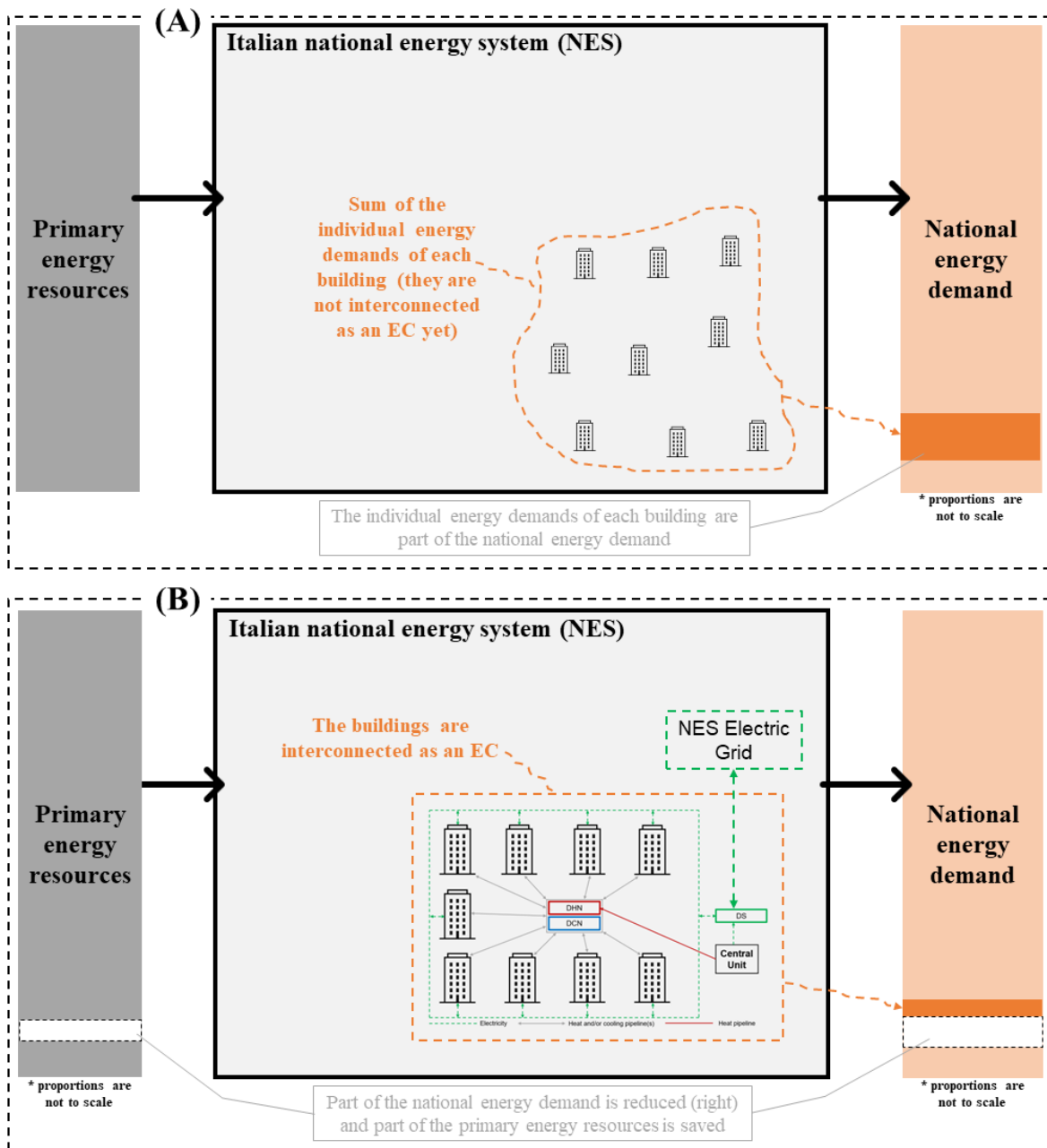


Figure 5.1 – Global system schematic diagram. Part (A) illustrates the starting point for the Italian NES, i.e., buildings of future ECs are connected to the NES in the conventional way (see section 3.4). Part (B) illustrates a future scenario where there is a deployment of ECs throughout the Italian territory.

In the scenario depicted in Figure 5.1 (B), the buildings are interconnected establishing ECs, i.e., in such illustrated future scenario there is a deployment of ECs throughout the Italian territory. Bearing in mind the optimization of these ECs, the consequence is a

reduction in the national energy demand and hence a decrease in the primary energy resource consumption (depending on the boundary conditions for the EC). Thus, as it is easy to infer, such scenario would have the potential to provide economic and environmental benefits to the NES.

### 5.2.2 The local system

As mentioned before, the local system (or subsystem) is the same EC analyzed in chapters 3 and 4. Of course, as the reader may notice, there is an imbalance in terms of size proportions between the global and the local system, i.e., the Italian NES is much larger when compared to the EC. Just to have an idea, the total electricity demand for the entire EC is in the order of 12 GWh/y whereas for the Italian NES it is in the order of 200,000 GWh/y (Borasio and Moret, 2022). In order to come up with a rational compensation to substantially reduce such difference in size proportions, assumptions have been made imagining a scenario in which there is an important deployment of ECs (similar to the one studied in this thesis) throughout the majority of the Italian territory.

The first assumption is based on two main aspects: (i) the EC, as described in chapter 3, comprises nine tertiary sector buildings, in the city of Pordenone (about 50 k inhabitants), northeast of Italy, characterized by building types present in all cities of similar size (town hall, theater, schools, hospital, etc.), and (ii) the energy demands of the buildings do not change significantly if the EC is implemented in a city within a certain range of number of inhabitants.

According to data published by the Italian Department of Internal and Territorial Affairs (*Dipartimento per gli Affari Interni e Territoriali*) (DAIT, 2021), there are 7899 municipalities in Italy. However, to have an idea, only 15% (or 1192 municipalities) have 10 k inhabitants or more. Therefore, in order to restrict the number of cities that could potentially implement an EC, similar to the one studied in this thesis, a further assumption should be made. This is the second assumption, which is based on (i) the candidate cities should not be neither too large nor too small compared to the size of Pordenone (in terms of number of inhabitants), (ii) the chosen range of city sizes is  $30\text{ k} \leq \textit{inhabitants} \leq 70\text{ k}$ , which results in approximately 200 municipalities (DAIT, 2021), and (iii) it is considered the implementation of only one EC per municipality.

Finally, the third assumption has to do with the location of the considered municipalities. Since the Italian NES model, used for the analysis developed in this chapter, is divided according to the Italian major regions (north, center, and south) the 200 municipalities are assumed to be located only in the north and center regions. This is because the heat demand profiles, of buildings located in the south of Italy, tend to be much lower when compared to buildings in the north of Italy (both in terms of magnitude and duration).

Having said that, one may infer that the local system is the group of 200 ECs spread over 200 municipalities located in the north and central Italian regions, as depicted in Figure 5.2 (A). The reader should bear in mind that the locations illustrated in Figure 5.2 (A) do not necessarily coincide with the actual locations of the abovementioned municipalities. Moreover, the definitions of the north and central regions, followed the same as Borasio and Moret (2022). Figure 5.2 (B) illustrates the connections between ECs and NES. As observed, such ECs would cover the energy demands of the buildings and require a lower amount of energy from the NES.

In order to ensure the understanding of the reader, the last bullet point should be explained a bit further. The difference between two crucial definitions should be clear: (i) the total energy demand of the buildings (within an EC), and (ii) the total energy required (by the EC) from the NES in order to cover the total energy demand of the buildings. The first one does not change. Observing Figure 5.1 (A), the total energy demand of the buildings (still in the conventional scenario) is equal to the total energy required (by the buildings) from the NES (highlighted with a dark orange rectangle on the right of Figure 5.1 (A)). After setting the buildings as an EC and implementing and developing the optimization of the polygeneration systems installed in the buildings, the total energy demand of the buildings remains the same. However, due to the high efficiency levels provided by a high integration of processes and deployment of solar energy, the total energy required (by the EC) from the NES reduces, as observed in Figure 5.1 (B) and Figure 5.2 (B). The dark orange rectangle (in both figures) is now smaller than the one in Figure 5.1 (A) and the new white rectangle represents a reduction in the national energy demand. Consequently, it results in savings on the primary energy resources (depending on the boundary conditions for the EC), represented by a white rectangle on the left of Figure 5.1 (B) and Figure 5.2 (B).

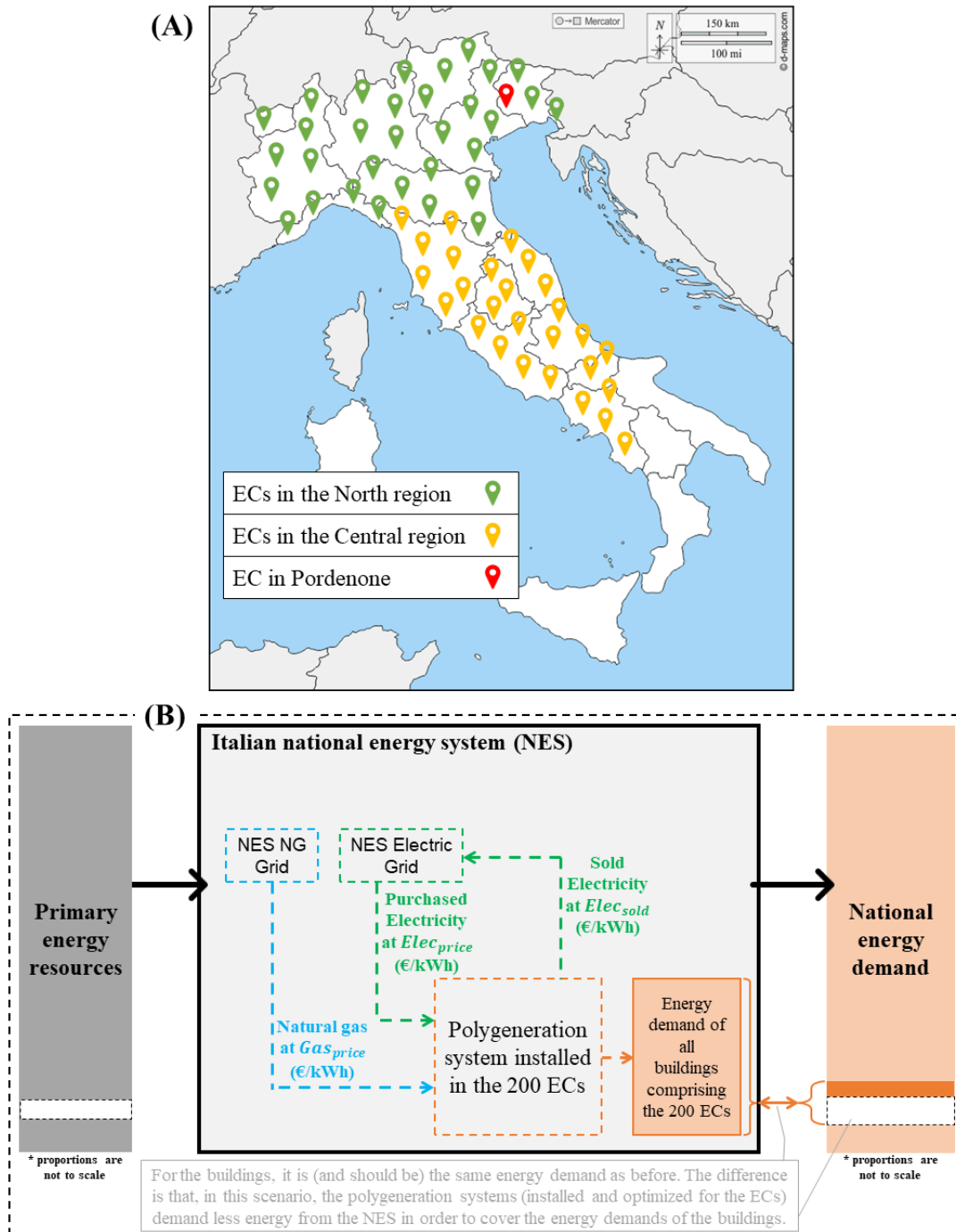


Figure 5.2 – (A) Illustration representing the group of 200 ECs implemented over 200 municipalities located in the north and central Italian regions (the indicated locations do not necessarily coincide with the actual locations of the municipalities). (B) Schematic diagram representing the connections between the group of ECs and the NES.

## **5.3 Global energy system: an Italian national energy system (NES) model**

### **5.3.1 Models applied to the Italian NES**

As mentioned before, the development of a mathematical model representing the Italian NES has not been the scope of the present thesis. Yet, such a model has been needed to develop the local optimization (LO) approach proposed in this chapter. Therefore, a plausible solution was to look at what other researchers have developed in this direction. Thus, in order to go from the starting point (no model whatsoever) to the target point (where there is a selected model, ready to be implemented in the LO approach), the following procedure was applied:

1. searching for appropriate keywords in relevant databases such as Google Scholar and ScienceDirect,
2. selection of the most recent published studies; the selected time range was from 2020 onwards,
3. selection of studies not only specifically developed for the Italian NES, but also with a well described methodology and applied for different economic sectors (or at least for the power sector),
4. the model developed within the selected studies should be open source, i.e., both the model algorithm and the input data must be available online; also, the model must be able to run by using a free software,
5. understanding of the main aspects about the selected study/model and perform several test simulations,
6. configuration of the selected model to be implemented in the LO approach.

After searching for recently published studies in the mentioned databases, five works specifically developed for the Italian NES, have been elected (Table 5.2). As observed in the table, in terms of sectors coverage, all five studies could be good candidates, especially those covering the three types of sectors. However, from the open-source criterion viewpoint, the works of Teske, Morris and Nagrath (2020), Lanati and Gaeta (2020), and Bompard et al. (2020) are not eligible due to (i) lack of open source code and input data availability, and/or (ii) impossibility of running the model in a free software.



Moreover, from the studies developed by Borasio and Moret (2022) and Lombardi et al. (2020), only the former completely covers the open source and sectors criteria.

Table 5.2 – Review of national energy system models applied to Italy. Selected time range: 2020 onwards.

Ref.	Applied model	Open source			Sectors		
		Code	Input data	Software	Power	Heat	Mobility
Teske, Morris and Nagrath (2020)	[R]E 24/7	✗	✗	✗	✓	✓	✓
Lombardi et al. (2020)	Calliope	✓	✓	✓	✓	✗	✗
Lanati and Gaeta (2020)	TIMES & sMTSIM	✗	✗	✓	✓	✓	✓
Bompard et al. (2020)	GenX	✗	✗	✗	✓	✓	✓
Borasio and Moret (2022)	EnergyScope	✓	✓	✓	✓	✓	✓

### 5.3.2 The selected Italian NES model

As explained in the previous subsection, the selected Italian NES model was the EnergyScopeIT, developed by Borasio and Moret (2022). The main objectives of their work were twofold: firstly, to extend and regionalize the EnergyScope model Limpens et al. (2019), thereby enhancing its applicability to more complex energy systems; secondly, to utilize this advanced model to explore and formulate deep decarbonization scenarios for the Italian energy system, specifically targeting the year 2050, while evaluating uncertainties.

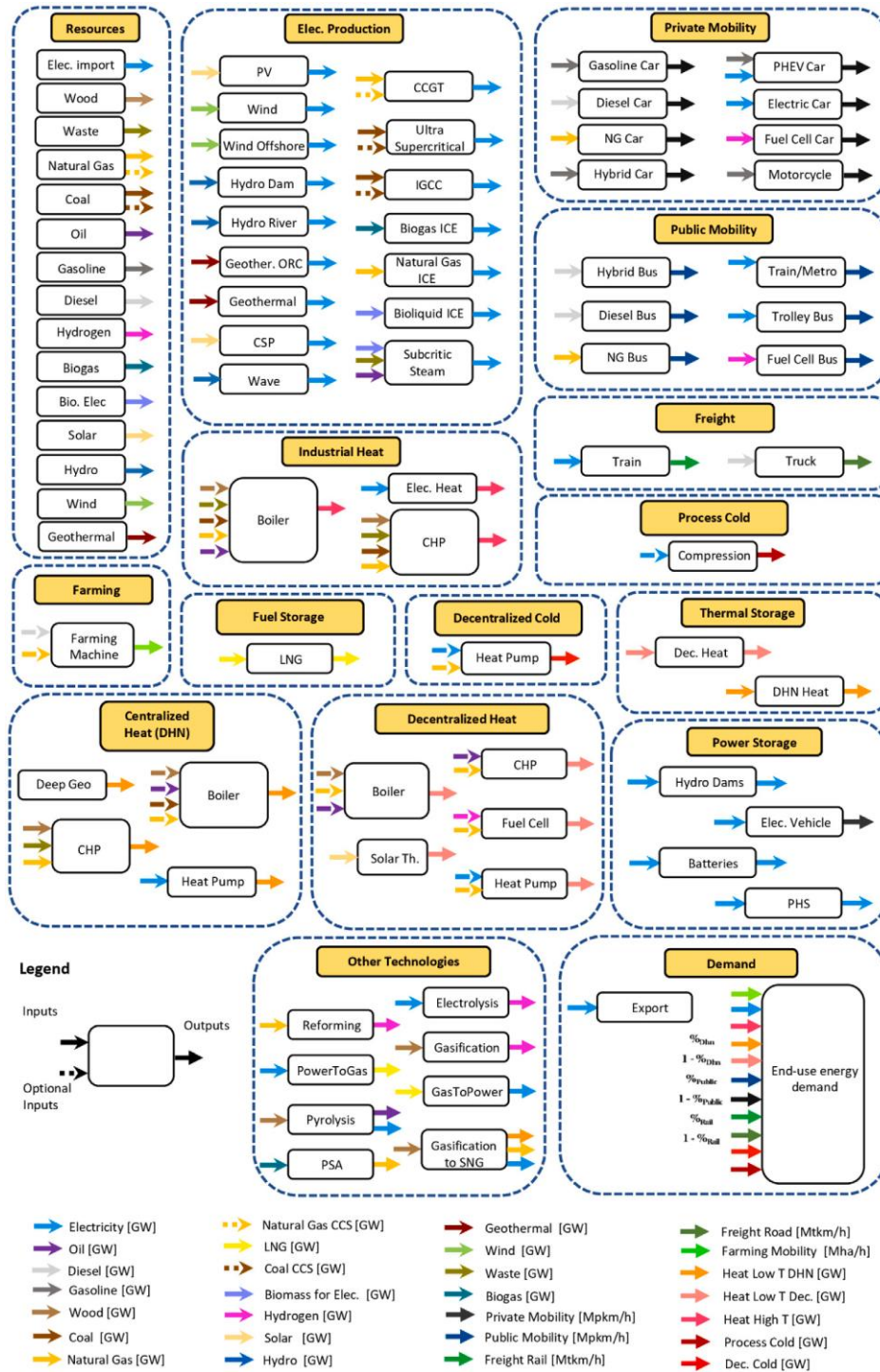


Figure 5.3 – Schematic diagram of the energy flows within the EnergyScopeIT model (Borasio and Moret, 2022). Abbreviations: natural gas (NG), carbon capture and storage (CCS), synthetic natural gas (SNG), geothermal (geoth.) combined cycle gas turbine (CCGT), integrated gasification combined cycle (IGCC), photovoltaic (PV), temperature (T), plug-in hybrid electric vehicle (PHEV), cogeneration of heat and power (CHP), biomass for electricity generation (Bio. Elec), pressure swing adsorption (PSA).

The authors developed a regionalized version of EnergyScope, an open-source linear programming model that, according to the authors, is capable to perform optimizations with high temporal and spatial resolution and for the whole-energy system design and operation. The Italian energy system was divided into 20 distinct regions, incorporating 10 end-use demand types, 17 energy resources, and 67 energy conversion technologies. The authors then defined a reference scenario alongside three decarbonization scenarios, each with varying emission reduction targets (50%, 80%, and 100% compared to 1990 levels) and different assumptions regarding the availability of carbon capture and storage (CCS) and renewable technologies. A sensitivity analysis was also performed to evaluate the impact of uncertainties in cost, demand, and weather parameters on the energy system's optimal configuration and performance.

The study found that the deep decarbonization of the Italian energy system is not only feasible but also cost-effective, primarily driven by a substantial shift towards electrification, augmented by a widespread deployment of renewable and efficient energy conversion technologies. The availability of CCS and renewable technologies emerged as critical factors influencing the optimal energy mix, the extent of inter-regional exchanges, and overall system costs and emissions.

For these reasons, the EnergyScopeIT model was considered detailed and robust enough to translate the reduction in the national energy demand into changes to the Italian national energy system. Figure 5.3 presents a diagram of the energy flows within the EnergyScopeIT model.

#### *5.3.2.1 Procedure to modify energy demand input data*

Because the Italian territory is divided into three main regions (north, center and south), it was possible to modify the energy demand input data for a specific region separately. Table 5.3 provides the input data of the EnergyScopeIT regarding the energy demand for the north and central regions divided by economic sector and energy demand type.

Table 5.3 – EnergyScopeIT: energy demand input divided by type, economic sector, and region (Borasio and Moret, 2022). Values in GWh. Abbreviations: (HT) high temperature, (LTSH) low temperature spacing heat, (LTHW) low temperature hot water, (PRO) process, (SC) spacing cooling, (P) passenger, (FR) freight, (FA) farming.

	Region	Households	Services	Industry	Agriculture	Transport
<b>Electricity</b>	NO	<b>9065.9</b>	17,416.5	48,859.6	2330.2	0
	CN	<b>6388.3</b>	12,272.5	25,500.9	1006.8	0
<b>Lighting</b>	NO	<b>6635.6</b>	13,271.2	6614.2	258.9	0
	CN	<b>4675.8</b>	9351.5	3452.1	111.9	0
<b>Heat HT</b>	NO	0	2549.3	75,635.1	0	0
	CN	0	1796.4	39,475.7	0	0
<b>Heat LTSH</b>	NO	<b>89,342.2</b>	26,799.2	12,904.0	0	0
	CN	<b>62,954.8</b>	18,884.0	6734.9	0	0
<b>Heat LTHW</b>	NO	<b>19,306.1</b>	5399.2	0	0	0
	CN	<b>13,604.0</b>	3804.5	0	0	0
<b>Cold PRO</b>	NO	0	12,279.7	15,042.9	0	0
	CN	0	8652.8	7851.2	0	0
<b>Cold SC</b>	NO	20,269.3	34,514.8	13,717.1	0	0
	CN	14,282.7	24,320.8	7159.3	0	0
<b>Mobility P</b>	NO	0	0	0	0	485,118.7
	CN	0	0	0	0	341,837.7
<b>Mobility FR</b>	NO	0	0	0	0	93,460.8
	CN	0	0	0	0	65,856.9
<b>Mobility FA</b>	NO	0	0	0	3.5	0
	CN	0	0	0	1.5	0

After applying the assumptions described in the section 5.2.2, the bold numbers in Table 5.3 were modified by following the procedure below.

1. Calculation of the total electricity saved by the EC by comparing the total amount of purchased electricity in the conventional solution and in the optimal economic solution of one EC.
2. Estimation of the total electricity saved by 200 ECs.
3. Proportional division of such value into (i) “Electricity” and “Lighting” demand types, and (ii) north and central regions.
4. Similar procedure is made for each iteration of the LO approach, but always comparing the total amount of purchased electricity with the value of the previous iteration.

5. The entire heat demand of all buildings together was removed from Heat LTSH and Heat LTHW, assuming that such demand is now self-covered by the EC. The proportion division was applied into (i) “Heat LTSH” and “Heat LTHW” demand types, and (ii) north and central regions.

According to the authors, such annual values are optimally allocated into typical days to form a 365-day sequence, which allows the integration of daily and seasonal storage.

#### 5.3.2.2 LCOE and electricity price calculation procedure

The levelized cost of electricity (LCOE), which essentially represents a specific average cost of producing the electricity, is relatively simple to calculate. For the EnergyScopeIT model, the authors Borasio and Moret (2022) calculated the LCOE through Eq. (5.2).

$$LCOE = \frac{PS_{investment} + PS_{resources} + PS_{grid}}{Total\ electricity\ production} \quad (5.2)$$

where *PS* stands for power system.

For what concerns the electricity price calculation procedure, the reader may refer to chapter 3, section 3.2.4.3.

## 5.4 Local energy system model: the energy community (EC)

For the purpose of the local optimization procedure, the local energy system model is the same as the one described in chapter 3 (section 3.3). For this reason, the equations of the model are not repeated in the present chapter.

However, there is an important detail that should not be overlooked. Besides the natural gas (NG) price ( $Gas_{price}$ ), the prices of the purchased and sold electricity are also considered constant, although both models are characterized by hourly resolution and optimized for one year. This is because the Italian NES (excluding the EC) is regarded as a “perfect buffer” for the electricity exchanged with the EC. This consideration is introduced in order to simplify the LO procedure.

In this case, the moment at which an electricity flow is exchanged (between Italian NES and EC) is not important and only the total amount of electricity exchanged has to be

considered. In this approximation, the information about the hourly electricity flows cannot be used. Instead, only the levelized cost of electricity (LCOE) is introduced when electricity flows from the Italian NES to the EC. In such case, the LCOE is used as the base to calculate the electricity purchase price ( $Elec_{price}$ ) (the procedure is described in the section 5.3.2.2), which is part of the input data for the EC model. For what concerns the electricity flow from the EC to the Italian NES, an average price ( $Elec_{sold}$ ) is also introduced. The reader may refer to Figure 5.2 (B) for an illustration of the electricity flows between Italian NES and EC.

Another important detail about the EC model, is the identification of the local independent design variables. As described in chapter 3, the EC includes about ten different technologies (including thermal energy storage), which can be installed in nine different buildings (plus central unit), a considerable number of possibilities regarding electricity, heating, and cooling interconnections among the buildings, and an hourly resolution. For that reason, when it comes to the EC model, the number of independent design variables is in the order of hundreds of thousands. Examples of these variables can be the size of the boiler, the heat pump load at a given hour of the year, etc.

## **5.5 Italian NES and EC: a local optimization**

As stated in the section 5.1, the local optimization (LO) problem can be solved by performing an iterative procedure. Since both models (Italian NES model and EC model) are available, the procedure can follow the Approach 2 described in Table 5.1. For the LO under analysis, it is considered that the group of 200 ECs is the local subsystem of interest (Figure 5.2 B) (the reader may refer to section 5.2.2 to understand such number of ECs). In order to be clearer, the step-by-step to develop the iteration procedure is also described below but adapted to the LO problem under analysis. Figure 5.4 provides a big picture of the iteration procedure.

### *STEP 1 – Italian NES*

A global optimization (GO) is performed by using the Italian NES model (EnergyScopeIT – see previous section). The costs of the internal flows of the Italian NES are obtained, including the LCOE which is used to estimate the initial value of the electricity price

( $Elec_{price}$ ). The Italian NES model is optimized by using its original data (provided by the authors Borasio and Moret (2022)). The energy demands of the buildings that will make part of the future ECs are assumed to be already in the input data of the Italian NES model. The main results for the model can be seen in Figure 5.4 and Figure 5.5.

#### *STEP 2 – EC*

A LO is performed by using the EC model (by specifying initial values for key input data, including the electricity price). With this, the locally optimized independent design variables are obtained, as well as new levels of total energy required from the Italian NES (compared to the conventional solution – see section 3.4).

Moreover, the results showed that the EC purchased (or required from the Italian NES) only 24% of the total electricity demand of the buildings and sold only 0.33% of the total self-produced electricity, which indicates a high usage of self-produced electricity.

It is worth noting that step 2 represents the optimization and implementation of the ECs. The buildings go from the conventional solution mode to the EC mode. For this reason, a great amount of electricity is saved (in the Italian NES). The total NG consumption of the buildings reduced from 33.7 GWh/year (conventional solution) to 30.2 GWh/year (EC mode), highlighting even further the potential benefits of ECs deployment.

#### *STEP 3 – Italian NES*

By inputting the new levels of total energy required from the Italian NES, a second GO is performed. The costs of the internal flows of the Italian NES are recalculated, including the LCOE which is used to estimate the new value of the electricity price ( $Elec_{price}$ ).

It is important to highlight that, in this step, the new levels of total energy required from the Italian NES regards not only electricity, but also heating. In this case, as the entire heating demand of the EC is now self-produced, such heating demand has been removed from the heating demand of the Italian NES.

The main results indicated that the LCOE dropped from 95.56 to 94.89 €/MWh. Also, the total annual cost of the Italian NES and the total primary energy supply (TPES) decreased

from 109 to 102.7 billion€/year and 841 to 836.4 TWh/year, respectively. As expected, it indicates a positive effect to the Italian NES regarding the reduction in the total energy required from the Italian NES.

#### *STEP 4 – EC*

The new  $Elec_{price} = 158.14$  €/MWh is used as input to perform a LO for the second time. This step allows to obtain a second new set of locally optimized independent design variables and second new levels of total energy required from the Italian NES.

Step 4 represents a scenario where the ECs already exist and are optimized (only the operation) with the new electricity price.

The new levels of total energy required from the Italian NES should be compared with the total energy required from the Italian NES obtained in step 2 and not with the total energy required from the Italian NES of the conventional solution. In this way the energy savings are very few and the next two steps is only to confirm the convergence.

#### *STEP 5 – Italian NES*

It is similar to step 3; however, the Italian NES model is updated with the new levels of total energy required from the Italian NES.

The main results showed that the LCOE dropped from 94.89 to 94.88 €/MWh. Also, the total annual cost of the Italian NES and the total primary energy supply (TPES) decreased from 102.7 to 102.6 billion€/year and 836.4 to 836.1 TWh/year, respectively.

In the case of a convergence of the independent design variables, the optimal global solution has been achieved.

#### *STEP 6 – EC*

In a similar way as for step 4, the new  $Elec_{price} = 158.13$  €/MWh is used as input to perform a LO for the third time. This step allows to verify that the new set of locally optimized independent design variables and the new levels of total energy required from the Italian NES have converged.



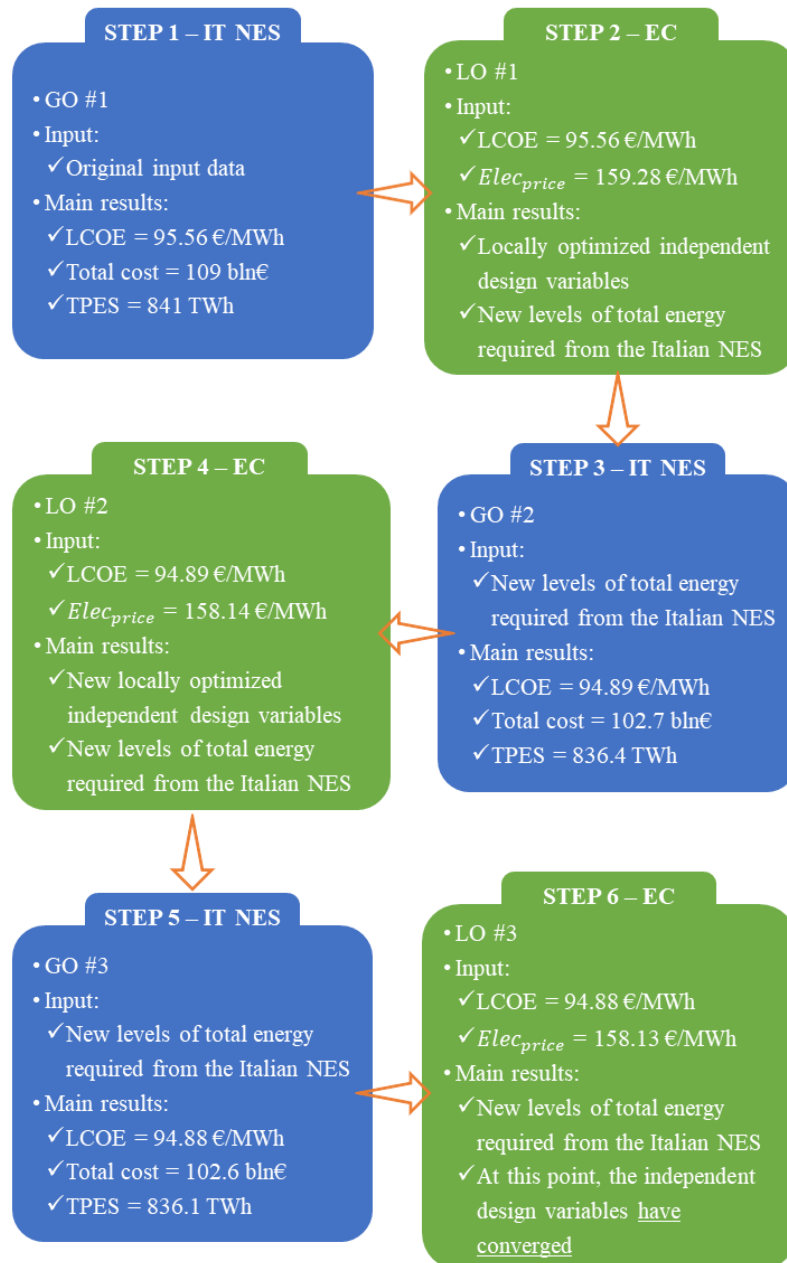


Figure 5.4 – Step-by-step of the local-global iteration procedure until the convergence of the independent design variables. Abbreviations: (GO) global optimization, (LO) local optimization, (LCOE) levelized cost of electricity, (TPES) total primary energy supply.

Figure 5.5 presents some results from the iterations regarding four parameters; two of them regard only the Italian NES (total annual Italian NES cost and TPES), the LCOE regards one of the main parameters at the frontier between the local and global system, and the last one refers to the economic objective function of the EC model (total annual

EC cost). In this way, it is possible to analyze some of the main results from both models since they can effectively reflect variations from their respective design variables.

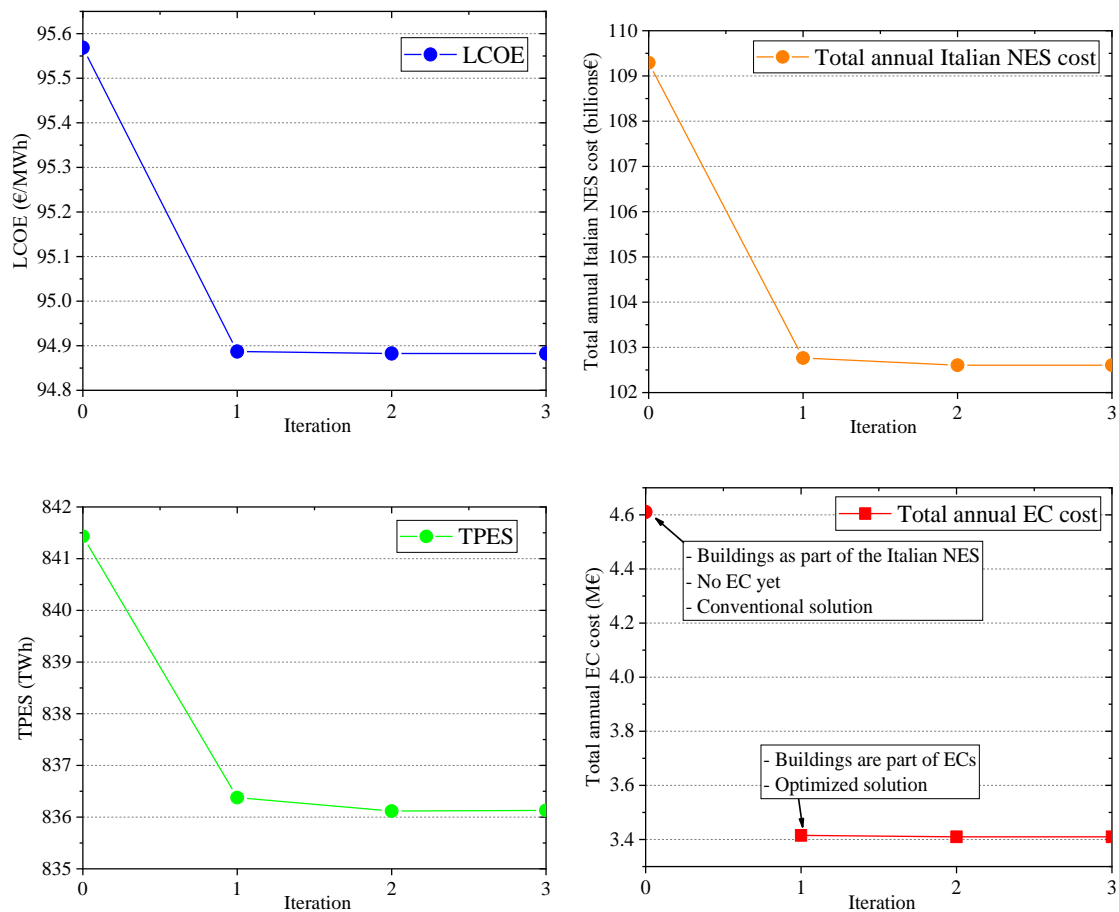


Figure 5.5 – Results from the iterations. Iteration zero regards the initial conditions while iteration 3 regards the conditions of the optimal global solution. The total annual EC cost refers to one EC only. LCOE (levelized cost of electricity), TPES (total primary energy supply).

The iteration 0 “zero” in Figure 5.5 regards the initial conditions. It means that the buildings that will make part of future ECs are connected to the Italian NES in the conventional way. That is why the graph regarding the total annual EC cost does not present a value at iteration zero (the initial total annual cost regarding the buildings in the conventional way is assumed to be part of the total annual Italian NES cost). As mentioned before, the iteration 1 represent the optimization and implementation of such ECs.

It is important to remember that the two models (global and local) are not trivial; they have a substantial number of design variables. However, the assumptions introduced in the section 5.2 could support the simplification of the analysis, which allowed the evaluation of only annual values (instead of the hourly ones).

### **5.5.1 On the role of ECs in the Italian NES**

Now it is possible to return to the research question presented in the opening section of this chapter: what the role of ECs (such as the case study of this thesis) in the economic and environmental aspects of a future Italian energy system scenario with a high level of renewable energy diffusion could be?

As the reader may infer from the analysis developed in this chapter, some thoughts are necessary to answer the question. Evidently, the defined assumptions, needed to develop the analysis, increase the uncertainty regarding the results. However, it has been possible to obtain results with an acceptable approximation given that the local (EC) and global (Italian NES) models have a considerable high level of details and can be regarded as effective representations of the actual systems.

Therefore, bearing in mind:

- that the concept of a thermoeconomically isolated subsystem is always an approximation (Reini, 1994) and that the local optimization procedure, consequently, is also a heuristic procedure,
- the assumptions to overcome the difference in size proportions between the Italian NES and one EC,
- the consideration of ECs implemented only in the north and central regions,
- the assumptions to simplify the interactions between the results obtained from the Italian NES model and EC model, and
- the fact that the Italian NES model (EnergyScopeIT) is optimized for a scenario pictured for 2050 with a high level of renewable energy deployment,

a reasonable answer can be divided into the following aspects:

1. The implementation of the ECs implies a reduction in the amount of energy required from the Italian NES since the installed polygeneration systems (in the ECs) provide a high level of processes integration, which ultimately increases the overall efficiency of the system. Such reduction in the energy required from the Italian NES resulted in lower installed capacities for different technologies. The consequence was a reduction of 6% in the total annual Italian NES cost (Figure 5.5), representing 6.6 billion€.
2. As observed in Figure 5.5, the reduction in the LCOE was much less significant. From the starting point up to the last step of the LO procedure, it reduced only 0.7% (95.56 to 94.88 €/MWh). This is because the reduced costs in the power sector was less significant, i.e., based on the optimal solution of the Italian NES model, the most significant reductions in terms of installed capacity were in the heating sector.
3. The reduction in the total primary energy supply (TPES) was also modest. It decreased from 841 to 836.1 TWh per year, representing only 0.5% of the original TPES. The reader should bear in mind that, as explained in section 5.3.2, the selected Italian NES model (EnergyScopeIT) is developed for the year 2050, which foresees a high deployment of renewable energy sources. Moreover, the results have shown that the mentioned slight reduction, derived from LO procedure, was achieved by an increasing in the usage of more efficient energy conversion technologies, such as district heating network (DHN) (mainly operated by geothermal energy) and heat pumps (HPs), which are in line with the scenario considered by the authors Borasio and Moret (2022) in EnergyScopeIT model for the year 2050.
4. Starting from iteration 1, no relevant enhancements are achieved for the ECs. This is because (i) in the mentioned iteration they are already optimized in terms of total annual cost, and (ii) the change in the electricity price is very small and, for this reason, the solutions obtained in iterations 2 and 3 are very similar to the one of iteration 1.

Therefore, a reasonable deployment of ECs (such as the case study of this thesis) throughout the Italian territory, has the potential to promote even further the usage of more efficient energy conversion technologies in the Italian NES with a trend of decreasing TPES. Moreover, the lower level of installed capacities for different technologies provided a considerable decrease in the total annual Italian NES cost, which might indicate a possible economic benefit to be passed on to society. Finally, from the environmental perspective, the impacts are certainly reduced if a lower level of installed capacities is achieved (environmental impacts due to manufacturing). However, from the operation viewpoint, the environmental impacts are dependent on the amount of consumed fossil fuels, which is already considerably low given that the selected Italian NES model (EnergyScopeIT) is optimized for a 2050 scenario with a high level of renewable energy deployment.

## 5.6 Conclusions

The present chapter was developed in order to answer a research question by using the thermo-economic methodology named local optimization (LO). Considering all the research work developed in chapters 3 and 4, in which a case study of an energy community (EC) has been the center of the investigation, a specific question has arisen: *what the role of ECs (such as the case study of this thesis) in the economic and environmental aspects of a future Italian energy system scenario with a high level of renewable energy deployment could be?*

In order to answer the question, three main elements were needed: a local subsystem, a global system, and a methodology. As stated before, the selected method was the LO approach whereas the local subsystem was set to be the EC. The global system was thought to be a smaller Italian region. However, due to some specific aspects (explained on section 5.2.1), the global system was the Italian national energy system (NES). After presenting and discussing each one of the three mentioned elements, the LO approach was developed through section 5.5.

Neither the Italian NES model nor the EC model are trivial. They have a considerable high level of details and a substantial number of design variables. For these reasons, assumptions have been made in order to simplify the interactions between both models.

The results demonstrated the potential that a reasonable deployment of ECs has to promote even further the usage of more efficient energy conversion technologies in the Italian NES with a tendency of decreasing the total primary energy supply. Moreover, the results showed that the lower level of installed capacities for different technologies provided a considerable decrease in the total annual Italian NES cost, which might indicate a possible economic benefit to be passed on to society. With this, environmental impacts due to technologies manufacturing are certainly reduce. However, further improvements in this sense will depend on the operation of the Italian NES (i.e., usage level of fossil fuels).

---

## *CHAPTER 6 – Conclusions*

---





## CHAPTER 6 – Conclusions

The conclusion of the thesis is structured as follows: section 6.1 provides a synthesis of the work developed; section 6.2 highlights the contributions made; and section 6.3 presents possible future works.

### 6.1 Synthesis

The work developed in this thesis revolved around an energy community (EC) model and was based on three main pillars: (i) the design and optimization of the EC powered by polygeneration systems and sharing not only heating and cooling among its members, but also purchased electricity (from the electric grid) and self-produced electricity, (ii) the proposal of a thermoeconomic analysis (through marginal costs) to evaluate the best operational strategy according to variations on the energy services demand with respect to the optimal solution of the energy supply system, and (iii) evaluate the role of such ECs in the economic and environmental aspects of a future Italian energy system scenario with a high level of renewable energy deployment.

Chapter 1 provided a global energy landscape background based on two main aspects: (i) the direct connection between economic development and the increase of serious environmental impacts, and (ii) the actions that governments and scientific community have taken to face energy and, hence, economic crises. The state of the art provided a review on what the scientific community has developed, from the viewpoint of energy supply systems' efficiency improvements and highlighted the lack of works analyzing ECs from the three main pillars stressed in the last paragraph. The general objective of this PhD thesis was also emphasized, which is to advance the understanding and development of a sustainable and efficient integration of polygeneration systems into ECs through a comprehensive optimization of their energy systems.

Chapter 2 discussed the methodologies used in the work through the presentation of the research framework. The chapter provided an overview about the optimization process of energy systems by discussing four main steps: (i) the importance of defining the energy supply system's superstructure by taking into account the boundaries of the problem, the type of technology, and the interactions among them, (ii) the critical role owned by the

data collection and analysis phase since the quality of data directly affects the integrity and credibility of the results, (iii) the translation of all gathered information into a mathematical model which represents the characteristics and performance of all technologies, the desired detail level, and the optimization criteria, and (iv) the calculation of an optimal solution for the energy supply system by solving the mathematical model. Moreover, thermoeconomic methodologies have also been considered. The first one is the analysis and interpretation of marginal costs derived from the optimization process, which provide critical insights for efficient system management under varying energy demands. The second one is the local optimization, which offers a simplified approach for subsystems improvements.

Chapter 3 presented the development of the multi-objective optimization model for an EC consisting in a group of nine buildings plus a central unit sharing electricity, heating, and cooling among each other. The objective functions were the total annual cost (related to maintenance, investment, and hourly operation) and total annual CO<sub>2</sub>eq emissions (related to the hourly operation). The chapter presented the superstructure for both the buildings and central unit, the gathering of the input data, the mathematical model, and the reference case scenario. In accordance with the objective function, the results from the single-objective optimization indicated the (i) optimal energy supply system structure within each building, (ii) optimal hourly operation of each technology, (iii) optimal connections between buildings in terms of DHCN pipelines, (iv) optimal distribution (among the building) of self-produced electricity and electricity purchased from the grid, and (v) optimal energy supply system structure and hourly operation for the central unit. In addition, the results from the multi-objective optimization demonstrated the importance of this kind of approach by presenting a range of trade-off solutions comprising a set of valuable pieces of information that can support decision-makers to take informed choices based on their interests.

A thermoeconomic analysis of the EC was developed through Chapter 4. Such study was developed through the analysis and interpretation of the hourly marginal costs related to the electricity, heating, and cooling demands. Such study allowed obtaining insights in the direction of determining the optimal operation of the system when the energy demand of a given building is increased. As already discussed in the literature (Pina, Lozano and Serra, 2017), the consideration of thermal energy storage (TES) decouples energy service

production from consumption, i.e., it becomes relevant knowing not only the amount of energy produced, but also the time at which it took place. On top of that, the incorporation of DHCN pipelines (provided by this thesis) added a new complexity layer, i.e., besides the necessity of knowing the amount of energy and time in which the energy production took place, it becomes also necessary to know (i) in which building such energy production took place, (ii) what is the related marginal path, and (iii) the reasons why some paths are more expensive than others.

The overall aim of Chapter 5 was to answer the research question “*what the role of ECs (such as the case study of this thesis) in the economic and environmental aspects of a future Italian energy system scenario with a high level of renewable energy deployment could be?*” by using the methodology of local optimization. Besides the methodology, two main elements were needed: a local subsystem and a global system. The local subsystem was set to be the EC whereas the global system was the Italian national energy system (NES). The results demonstrated the potential that a reasonable deployment of ECs has to promote even further the usage of more efficient energy conversion technologies in the Italian NES with a trend of decreasing the total primary energy supply. Moreover, the results showed that the lower level of installed capacities for different technologies provided a considerable decrease in the total annual Italian NES cost, which might indicate a possible economic benefit to be passed on to society.

## **6.2 Contributions**

The main contributions and results from this thesis are the following:

- Optimal synthesis and operation of polygeneration systems for ECs, characterized by complex integrated processes and dealing, at the same time, with: (i) a district heating and cooling network (DHCN) of pipelines connecting the buildings, (ii) a central unit to support the buildings’ energy demands, (iii) heat and cooling storage, (iv) management and distribution of self-produced and purchased electricity among the buildings and between the EC and the national electric grid, (v) integration of solar technologies, (vi) hourly electricity purchasing price, (vii) hourly electricity selling price, and (viii) hourly CO<sub>2</sub> emissions factors.

- Multi-objective optimization of the EC presenting a range of trade-off solutions through which it is possible to have important pieces of information about installed capacities, structure for the DHCN pipelines, total annual costs and CO<sub>2</sub> emissions, cost of moving from one solution to another, and cost of choosing a more environmentally friendly solution. The results from the EC case study showed the possibility of reducing total annual CO<sub>2</sub>eq emissions by about 20% (about 1.5 kt CO<sub>2</sub>eq/year) and total annual costs by approximately 24% (about 1.1 M€/year), when comparing to the reference case.
- The analysis and interpretation of the hourly marginal costs of a complex and highly integrated polygeneration system supported by (i) thermal energy storages, (ii) DHCN pipelines, and (iii) the sharing of purchased and self-produced electricity among the nine buildings.
- The outline of different optimal marginal paths through advanced, delayed, simultaneous, and remote energy services production types.
- Finally, another important contribution was the evaluation of the role of ECs in the economic and environmental aspects of a future Italian national energy system (NES) scenario with a high level of renewable energy deployment. From the environmental viewpoint, the implementation of the ECs does not represent a substantial positive benefit for the analyzed NES scenario. However, such implementation presented a potential of reducing the amount of energy required from the Italian NES since the installed polygeneration systems (in the ECs) provide a higher level of processes integration, which ultimately increases the overall efficiency of the energy supply systems. Such reduction in the energy required from the Italian NES resulted in lower installed capacities for different technologies. The consequence was a reduction of 6% in the total annual Italian NES cost, representing 6.6 billion€/year.

### **6.3 Future work**

The research conducted in this Ph.D. thesis has laid an important advancement for the optimization and analysis of polygeneration systems integrated into ECs, identifying key strategies for enhancing efficiency, sustainability, and cost-effectiveness within such

systems. Future works could follow several avenues for further exploration and development. The reader can find below a non-exhaustive list of suggestions.

- Subsequent research efforts could focus on incorporating financial incentives for new technologies, adapting to new policy landscapes, and exploring the social implications of energy community development.
- The start-up and shutdown effects could be incorporated into the technologies performance models in order of obtaining more-refined optimization solutions. Moreover, the incorporation of technologies such as power-to-gas (e.g. electrolyzer and methanation reactor) and power-to-power (e.g. pumped thermal energy storages and electricity storages) could also be evaluated.
- The environmental impacts associated with the life cycle of all technologies comprising the polygeneration systems integrated into the EC could be evaluated and incorporated into the multi-objective optimization. In addition, the economic objective function could consider also costs regarding carbon emissions or carbon mitigation initiatives.
- The self-produced electricity exchange among the EC buildings could be further developed by considering a rewarding for the hours in which a given building sends self-produced electricity to the DS manager, as well as a fee for receiving electricity self-produced by another EC member.



## CAPITOLO 6 – Conclusioni

La conclusione della tesi è strutturata come segue: la sezione 6.1 fornisce una sintesi del lavoro sviluppato; la sezione 6.2 evidenzia i contributi apportati; e la sezione 6.3 presenta possibili lavori futuri.

### 6.1 Sintesi

Il lavoro sviluppato in questa tesi ha ruotato attorno a un modello di comunità energetica (CE) ed è stato basato su tre pilastri principali: (i) la progettazione e l'ottimizzazione della CE alimentata da sistemi di poligenerazione e condividendo non solo riscaldamento e raffreddamento tra i suoi membri, ma anche elettricità acquistata (dalla rete elettrica) ed elettricità autoprodotta, (ii) la proposta di un'analisi termoeconomica (attraverso costi marginali) per valutare la migliore strategia operativa in base alle variazioni della domanda di servizi energetici rispetto alla soluzione ottimale del sistema di approvvigionamento energetico, e (iii) valutare il ruolo di tali CE negli aspetti economici e ambientali di uno scenario futuro del sistema energetico italiano con un alto livello di implementazione di energia rinnovabile.

Il Capitolo 1 ha fornito un contesto globale sull'energia basato su due aspetti principali: (i) la connessione diretta tra sviluppo economico e l'aumento di impatti ambientali seri, e (ii) le azioni intraprese da governi e comunità scientifica per affrontare le crisi energetiche e, di conseguenza, economiche. Lo stato dell'arte ha fornito una revisione su ciò che la comunità scientifica ha sviluppato, dal punto di vista dei miglioramenti dell'efficienza dei sistemi di approvvigionamento energetico e ha evidenziato la mancanza di lavori che analizzano le CE dai tre pilastri principali sottolineati nell'ultimo paragrafo. L'obiettivo generale di questa tesi di dottorato è stato anche sottolineato, ossia avanzare la comprensione e lo sviluppo di un'integrazione sostenibile ed efficiente di sistemi di poligenerazione nelle CE attraverso un'ottimizzazione comprensiva dei loro sistemi energetici.

Il Capitolo 2 ha discusso le metodologie utilizzate nel lavoro attraverso la presentazione del quadro di ricerca. Il capitolo ha fornito una panoramica sul processo di ottimizzazione dei sistemi energetici discutendo quattro passaggi principali: (i) l'importanza di definire

la superstruttura del sistema di approvvigionamento energetico tenendo conto dei confini del problema, del tipo di tecnologia e delle interazioni tra di loro, (ii) il ruolo critico posseduto dalla fase di raccolta e analisi dei dati poiché la qualità dei dati influenza direttamente l'integrità e la credibilità dei risultati, (iii) la traduzione di tutte le informazioni raccolte in un modello matematico che rappresenta le caratteristiche e le prestazioni di tutte le tecnologie, il livello di dettaglio desiderato e i criteri di ottimizzazione, e (iv) il calcolo di una soluzione ottimale per il sistema di approvvigionamento energetico risolvendo il modello matematico. Inoltre, sono state considerate anche metodologie termoeconomiche. La prima è l'analisi e interpretazione dei costi marginali derivanti dal processo di ottimizzazione, che forniscono intuizioni critiche per una gestione efficiente del sistema sotto variabili domande energetiche. La seconda è l'ottimizzazione locale, che offre un approccio semplificato per il miglioramento dei sottosistemi.

Il Capitolo 3 ha presentato lo sviluppo del modello di ottimizzazione multi-obiettivo per una CE costituita da un gruppo di nove edifici più un'unità centrale che condividono elettricità, riscaldamento e raffreddamento tra loro. Le funzioni obiettivo erano il costo annuale totale (relativo a manutenzione, investimento e funzionamento orario) e le emissioni totali annue di CO<sub>2</sub>eq (relative al funzionamento orario). Il capitolo ha presentato la superstruttura sia per gli edifici che per l'unità centrale, la raccolta dei dati di input, il modello matematico e lo scenario di caso di riferimento. In accordo con la funzione obiettivo, i risultati dall'ottimizzazione mono-obiettivo hanno indicato l'(i) struttura ottimale del sistema di approvvigionamento energetico all'interno di ciascun edificio, (ii) funzionamento orario ottimale di ciascuna tecnologia, (iii) connessioni ottimali tra gli edifici in termini di condotte DHCN, (iv) distribuzione ottimale (tra gli edifici) dell'elettricità autoprodotta e acquistata dalla rete, e (v) struttura del sistema di approvvigionamento energetico e funzionamento orario ottimali per l'unità centrale. Inoltre, i risultati dall'ottimizzazione multi-obiettivo hanno dimostrato l'importanza di questo tipo di approccio presentando una gamma di soluzioni di compromesso comprendenti un insieme di informazioni preziose che possono supportare i decisori nel prendere scelte informate in base ai loro interessi.

Un'analisi termoeconomica della CE è stata sviluppata attraverso il Capitolo 4. Tale studio è stato sviluppato attraverso l'analisi e interpretazione dei costi marginali orari relativi alla



domanda di elettricità, riscaldamento e raffreddamento. Tale studio ha permesso di ottenere intuizioni nella direzione di determinare il funzionamento ottimale del sistema quando la domanda energetica di un dato edificio aumenta. Come già discusso in letteratura (Pina, Lozano e Serra, 2017), la considerazione dello stoccaggio di energia termica (TES) scollega la produzione di servizi energetici dal consumo, ovvero diventa rilevante conoscere non solo la quantità di energia prodotta, ma anche il momento in cui ciò è avvenuto. Inoltre, l'incorporazione delle condotte DHCN (fornite da questa tesi) ha aggiunto un nuovo strato di complessità, ovvero, oltre alla necessità di conoscere la quantità di energia e il momento in cui la produzione energetica ha avuto luogo, diventa anche necessario sapere (i) in quale edificio tale produzione energetica ha avuto luogo, (ii) qual è il percorso marginale correlato, e (iii) le ragioni per cui alcuni percorsi sono più costosi di altri.

L'obiettivo complessivo del Capitolo 5 era rispondere alla domanda di ricerca "*qual è il ruolo delle CE (come il caso di studio di questa tesi) negli aspetti economici e ambientali di uno scenario futuro del sistema energetico italiano con un alto livello di implementazione di energia rinnovabile?*" utilizzando la metodologia dell'ottimizzazione locale. Oltre alla metodologia, erano necessari due elementi principali: un sottosistema locale e un sistema globale. Il sottosistema locale è stato impostato per essere la CE mentre il sistema globale era il sistema energetico nazionale italiano (NES). I risultati hanno dimostrato il potenziale che un ragionevole dispiegamento delle CE ha nel promuovere ulteriormente l'uso di tecnologie di conversione energetica più efficienti nel NES italiano con una tendenza alla diminuzione dell'offerta energetica primaria totale. Inoltre, i risultati hanno mostrato che il livello inferiore di capacità installate per diverse tecnologie ha fornito una notevole diminuzione del costo annuale totale del NES italiano, il che potrebbe indicare un possibile beneficio economico da trasferire alla società.

## **6.2 Contributi**

I principali contributi e risultati di questa tesi sono i seguenti:

- Sintesi e funzionamento ottimali dei sistemi di poligenerazione per le Comunità Energetiche (CE), caratterizzati da processi integrati complessi e che affrontano, contemporaneamente: (i) una rete di teleriscaldamento e teleraffrescamento (DHCN)

---

di condotte che collegano gli edifici, (ii) un'unità centrale per supportare le richieste energetiche degli edifici, (iii) stoccaggio di calore e di raffreddamento, (iv) gestione e distribuzione dell'elettricità autoprodotta e acquistata tra gli edifici e tra la CE e la rete elettrica nazionale, (v) integrazione delle tecnologie solari, (vi) prezzo di acquisto orario dell'elettricità, (vii) prezzo di vendita orario dell'elettricità, e (viii) fattori orari delle emissioni di CO<sub>2</sub>.

- Ottimizzazione multi-obiettivo della CE che presenta una gamma di soluzioni di compromesso attraverso le quali è possibile ottenere informazioni importanti sulle capacità installate, sulla struttura delle condotte DHCN, sui costi annuali totali e sulle emissioni di CO<sub>2</sub>, sul costo del passaggio da una soluzione all'altra e sul costo della scelta di una soluzione più rispettosa dell'ambiente. I risultati dello studio di caso della CE hanno mostrato la possibilità di ridurre le emissioni totali annue di CO<sub>2</sub>eq di circa il 20% (circa 1,5 kt CO<sub>2</sub>eq/anno) e i costi annuali totali di circa il 24% (circa 1,1 M€/anno), rispetto al caso di riferimento.
- L'analisi e l'interpretazione dei costi marginali orari di un sistema di poligenerazione complesso e altamente integrato supportato da (i) stoccaggi di energia termica, (ii) condotte DHCN, e (iii) la condivisione dell'elettricità acquistata e autoprodotta tra i nove edifici.
- La definizione di diversi percorsi marginali ottimali attraverso tipi di produzione di servizi energetici avanzati, ritardati, simultanei e remoti.
- Infine, un altro importante contributo è stata la valutazione del ruolo delle CE negli aspetti economici e ambientali di uno scenario futuro del sistema energetico nazionale italiano (NES) con un alto livello di implementazione delle energie rinnovabili. Dal punto di vista ambientale, l'implementazione delle CE non rappresenta un beneficio sostanziale positivo per lo scenario NES analizzato. Tuttavia, tale implementazione ha presentato un potenziale di riduzione della quantità di energia richiesta dal NES italiano poiché i sistemi di poligenerazione installati (nelle CE) forniscono un livello più elevato di integrazione dei processi, che in ultima analisi aumenta l'efficienza complessiva dei sistemi di approvvigionamento energetico. Tale riduzione dell'energia richiesta dal NES italiano ha comportato capacità installate inferiori per diverse

tecnologie. La conseguenza è stata una riduzione del 6% nel costo annuale totale del NES italiano, rappresentando 6,6 miliardi di €/anno.

### 6.3 Prospettive future

La ricerca condotta in questa tesi di dottorato ha segnato un importante progresso per l'ottimizzazione e l'analisi dei sistemi di poligenerazione integrati nelle CE, identificando strategie chiave per migliorare l'efficienza, la sostenibilità e la convenienza economica all'interno di tali sistemi. I lavori futuri potrebbero seguire diverse strade per ulteriori esplorazioni e sviluppi. Di seguito, il lettore può trovare un elenco non esaustivo di suggerimenti.

- Gli sforzi di ricerca successivi potrebbero concentrarsi sull'incorporazione di incentivi finanziari per le nuove tecnologie, adattandosi ai nuovi paesaggi politici ed esplorando le implicazioni sociali dello sviluppo delle comunità energetiche.
- Gli effetti di avviamento e arresto potrebbero essere incorporati nei modelli di prestazione delle tecnologie al fine di ottenere soluzioni di ottimizzazione più raffinate. Inoltre, potrebbe essere valutata anche l'incorporazione di tecnologie quali il power-to-gas (ad es. elettrolizzatore e reattore di metanazione) e il power-to-power (ad es. stoccaggi di energia termica pompata e stoccaggi di elettricità).
- Gli impatti ambientali associati al ciclo di vita di tutte le tecnologie che compongono i sistemi di poligenerazione integrati nella CE potrebbero essere valutati e incorporati nell'ottimizzazione multi-obiettivo. Inoltre, la funzione obiettivo economica potrebbe considerare anche i costi relativi alle emissioni di carbonio o alle iniziative di mitigazione del carbonio.
- Lo scambio di elettricità autoprodotta tra gli edifici della CE potrebbe essere ulteriormente sviluppato considerando una ricompensa per le ore in cui un dato edificio invia elettricità autoprodotta al gestore della DS, così come una tariffa per ricevere elettricità autoprodotta da un altro membro della CE.



## **CAPÍTULO 6 – Conclusiones**

Las conclusiones de la tesis están estructuradas de la siguiente manera: la sección 6.1 proporciona una síntesis del trabajo desarrollado; la sección 6.2 destaca las contribuciones realizadas; y la sección 6.3 presenta posibles trabajos futuros.

### **6.1 Síntesis**

El trabajo desarrollado en esta tesis se realizó en torno a un modelo de comunidad energética (CE) y se basó en tres pilares principales: (i) el diseño y optimización de la CE alimentada por sistemas de poligeneración, compartiendo no sólo la energía para la calefacción y la refrigeración entre sus miembros, sino también la electricidad comprada (de la red eléctrica) y la electricidad auto-producida, (ii) la propuesta de un análisis termoeconómico (a través de costos marginales) para evaluar la mejor estrategia de operación para atender las variaciones en la demanda de servicios energéticos respecto a la solución óptima del sistema de suministro de energía, y (iii) la evaluación del papel de dichas CEs en los aspectos económicos y ambientales de un futuro escenario del sistema energético italiano con un alto nivel de implementación de energías renovables.

En el Capítulo 1 se ha presentado el contexto global del panorama energético basado en dos aspectos principales: (i) la conexión directa entre el desarrollo económico y el aumento de impactos ambientales graves, y (ii) las acciones que gobiernos y la comunidad científica han tomado para enfrentar crisis energéticas y, por ende, económicas. El estado del arte ha proporcionado una revisión crítica sobre lo que la comunidad científica ha desarrollado, desde el punto de vista de mejoras en la eficiencia de los sistemas de suministro de energía y ha destacado la falta de trabajos que analicen las CEs desde los tres pilares principales enfatizados en el último párrafo. Una vez presentado el contexto global del panorama energético y analizado el estado del arte se ha definido el objetivo general de esta tesis doctoral, que es avanzar en el entendimiento y desarrollo de una integración sostenible y eficiente de sistemas de poligeneración en las CEs a través de una optimización integral de sus sistemas energéticos.

En el Capítulo 2 se han discutido las metodologías utilizadas en el trabajo mediante la presentación del marco de investigación. En este capítulo se ha presentado una visión

general sobre el proceso de optimización de sistemas energéticos al analizar cuatro pasos principales: (i) la importancia de definir la superestructura del sistema de suministro de energía teniendo en cuenta los límites del problema, el tipo de tecnología y las interacciones entre ellas, (ii) el papel crítico que tiene la fase de recolección y análisis de datos ya que la calidad de los datos afecta directamente a la integridad y credibilidad de los resultados, (iii) la traducción de toda la información recopilada en un modelo matemático que representa las características y el rendimiento de todas las tecnologías, el nivel de detalle deseado y los criterios de optimización, y (iv) el cálculo de una solución óptima para el sistema de suministro de energía mediante la resolución del modelo matemático. Además, también se han considerado metodologías termoeconómicas. La primera es el análisis e interpretación de costos marginales derivados del proceso de optimización, que proporcionan estrategias de operación óptimas para una gestión eficiente del sistema bajo demandas energéticas variables. La segunda es la optimización local, que ofrece un enfoque simplificado para mejoras en los subsistemas.

En el Capítulo 3 se presentó el desarrollo del modelo de optimización multiobjetivo para una CE que consiste en un grupo de nueve edificios más una unidad central compartiendo electricidad, calefacción y refrigeración entre sí. Las funciones objetivo fueron el costo anual total (relacionado con el mantenimiento, la inversión y la operación horaria) y las emisiones totales anuales de gases de efecto invernadero evaluadas en emisiones de CO<sub>2</sub>eq (relacionadas con la operación horaria). En este capítulo se presentó la superestructura tanto para los edificios como para la unidad central, la recopilación de los datos de entrada, el modelo matemático y el escenario de caso de referencia. De acuerdo con la función objetivo, los resultados de la optimización mono-objetivo proporcionaron el (i) óptimo estructural del sistema de suministro de energía dentro de cada edificio, (ii) óptimo funcionamiento por hora de cada tecnología, (iii) óptimas conexiones entre edificios en términos de tuberías DHCN, (iv) óptima distribución (entre el edificio) de electricidad auto-producida y electricidad comprada de la red, y (v) óptima estructura del sistema de suministro de energía y funcionamiento horario de la unidad central. Además, los resultados de la optimización multiobjetivo demostraron la importancia de este tipo de enfoque al presentar un rango de soluciones de compromiso que comprenden un conjunto de información valiosa que puede apoyar/ayudar a las personas responsables de tomar decisiones para seleccionar soluciones informadas basadas en sus intereses.

Un análisis termoeconómico de la CE se desarrolló en el Capítulo 4 mediante el análisis e interpretación de los costos marginales horarios relacionados con las demandas de electricidad, calefacción y refrigeración. Dicho estudio permitió la obtención de perspectivas orientadas a determinar la operación óptima del sistema cuando se modifica la demanda energética de un edificio dado. Tal y como ya se discutió en la literatura (Pina, Lozano y Serra, 2017), la consideración del almacenamiento de energía térmica (TES) desacopla la producción de servicios energéticos del consumo, es decir, se vuelve relevante conocer no sólo la cantidad de energía producida, sino también el momento en que tuvo lugar. Además, la incorporación de tuberías DHCN (consideradas en el modelo desarrollado en esta tesis) añadió una nueva capa de complejidad, es decir, además de la necesidad de conocer la cantidad de energía y el momento en que la producción de energía tuvo lugar, se vuelve también necesario saber (i) en qué edificio tuvo lugar dicha producción de energía, (ii) cuál es el camino marginal relacionado, y (iii) las razones por las cuales algunos caminos son más caros que otros.

El objetivo general del Capítulo 5 fue responder a la pregunta de investigación "¿cuál podría ser el papel de las CEs (como el caso de estudio de esta tesis) en los aspectos económicos y ambientales de un futuro escenario del sistema energético italiano con un alto nivel de implementación de energías renovables?". Para dar respuesta a esta pregunta se utilizó la metodología de optimización local, que requiere de la definición de dos elementos principales: un subsistema local, la CE, y un sistema global, el sistema energético nacional italiano (NES). Los resultados pusieron de manifiesto el potencial que tiene una implementación razonable de las CEs para promover aún más el uso de tecnologías de conversión energética más eficientes en el NES italiano con una tendencia a disminuir el suministro total de energía primaria. Además, los resultados mostraron que el menor nivel de capacidades instaladas para diferentes tecnologías proporcionó una disminución considerable en el costo anual total del NES italiano, lo que podría indicar un posible beneficio económico para ser trasladado a la sociedad.

## **6.2 Contribuciones**

Las principales contribuciones y resultados de esta tesis son los siguientes:

- Síntesis y operación óptima de sistemas de poligeneración para CE, caracterizada por procesos integrados complejos que consideran, al mismo tiempo: (i) una red de tuberías de calefacción y refrigeración de distrito (DHCN) que conecta los edificios, (ii) una unidad central para apoyar las demandas energéticas de los edificios, (iii) almacenamiento de calor y refrigeración, (iv) gestión y distribución de electricidad auto-producida y comprada entre los edificios y entre la CE y la red eléctrica nacional, (v) integración de tecnologías solares, (vi) precio horario de compra de electricidad, (vii) precio horario de venta de electricidad, y (viii) factores horarios de emisiones de CO<sub>2</sub>eq.
- Optimización multiobjetivo de la CE presentando un rango de soluciones de compromiso a través de las cuales es posible tener, para cada una de las soluciones alcanzadas, información relevante sobre capacidades instaladas, estructura para las tuberías DHCN, costos totales anuales y emisiones de CO<sub>2</sub>eq, comparación de costos de cada una de las soluciones obtenidas, y costo de elegir una solución más amigable con el medio ambiente. Los resultados del caso de estudio de la CE mostraron la posibilidad de reducir las emisiones totales anuales de CO<sub>2</sub>eq en torno al 20% (aproximadamente 1.5 kt CO<sub>2</sub>eq/año) y los costos anuales totales en aproximadamente un 24% (alrededor de 1.1 M€/año), al comparar con el caso de referencia.
- El análisis e interpretación de los costos marginales por hora de un sistema de poligeneración complejo y altamente integrado respaldado por (i) almacenamientos de energía térmica, (ii) tuberías DHCN, y (iii) la posibilidad de compartir electricidad comprada y auto-producida entre los nueve edificios.
- La descripción de diferentes rutas de producción marginal óptimas considerando modos de producción de servicios energéticos avanzados, retrasados, simultáneos y remotos.
- Finalmente, otra contribución importante fue la evaluación del papel de las CE en los aspectos económicos y ambientales de un futuro escenario del sistema energético nacional italiano (NES) con un alto nivel de despliegue de energías renovables. Desde el punto de vista ambiental, la implementación de las CE no representa un beneficio positivo sustancial para el escenario NES analizado, en el que se ha considerado un



despliegue masivo de las energía renovables. Sin embargo, tal implementación presentó un potencial de reducir la cantidad de energía requerida del NES italiano ya que los sistemas de poligeneración instalados (en las CE) proporcionan un mayor nivel de integración de procesos, lo que finalmente aumenta la eficiencia general de los sistemas de suministro de energía. Tal reducción en la energía requerida del NES italiano resultó en menores capacidades instaladas para diferentes tecnologías. La consecuencia fue una reducción del 6% en el costo anual total del NES italiano, representando 6.6 mil millones de €/año. Este resultado pone de manifiesto no sólo el interés actual de instalar CE, gracias a los beneficios económicos y ambientales que conlleva, sino también el interés de estos sistemas a largo plazo, incluso en escenarios con una alta contribución de energías renovables en los sistemas energéticos nacionales.

### **6.3 Trabajos futuros**

La investigación realizada en esta tesis doctoral ha marcado un avance importante para la optimización y análisis de sistemas de poligeneración integrados en las CE, identificando estrategias clave para mejorar la eficiencia, sostenibilidad y rentabilidad dentro de dichos sistemas. Los trabajos futuros podrían seguir varias vías para una exploración y desarrollo adicionales. A continuación, se puede encontrar una lista no exhaustiva de sugerencias.

- Los esfuerzos de investigación subsiguientes podrían centrarse en incorporar incentivos financieros para nuevas tecnologías, adaptándose a nuevos paisajes políticos y explorando las implicaciones sociales del desarrollo de comunidades energéticas.
- Los efectos de arranque y parada podrían incorporarse en los modelos de rendimiento de las tecnologías con el fin de obtener soluciones de optimización más refinadas. Además, la incorporación de tecnologías como el power-to-gas (por ejemplo, electrolizador y reactor de metanización) y power-to-power (por ejemplo, almacenamientos térmicos de energía bombeada y almacenamientos eléctricos) también podría evaluarse.

- Los impactos ambientales asociados con el ciclo de vida de todas las tecnologías que componen los sistemas de poligeneración integrados en la CE podrían evaluarse e incorporarse en la optimización multiobjetivo. Además, la función objetivo económica también podría considerar costos relacionados con las emisiones de carbono o iniciativas de mitigación del carbono.
- El intercambio de electricidad auto-producida entre los edificios de la CE podría desarrollarse aún más considerando una recompensa por las horas en las que un edificio determinado envía electricidad auto-producida al gestor del DS, así como una tarifa por recibir electricidad auto-producida por otro miembro de la CE.

## **CAPÍTULO 6 – Conclusões**

A conclusão da tese é estruturada da seguinte forma: a seção 6.1 oferece uma síntese do trabalho desenvolvido; a seção 6.2 destaca as contribuições realizadas; e a seção 6.3 apresenta possíveis trabalhos futuros.

### **6.1 Síntese**

O trabalho desenvolvido nesta tese girou em torno de um modelo de comunidade energética (CE) e baseou-se em três pilares principais: (i) projeto e otimização da CE alimentada por sistemas de poligeração e compartilhamento não apenas de aquecimento e resfriamento entre seus membros, mas também de eletricidade comprada (da rede elétrica) e eletricidade autoproduzida, (ii) a proposta de uma análise termoeconômica (através de custos marginais) para avaliar a melhor estratégia operacional de acordo com variações na demanda dos serviços de energia em relação à solução ótima do sistema de fornecimento de energia, e (iii) avaliação do papel de tais CEs nos aspectos econômicos e ambientais de um cenário futuro do sistema energético italiano com um alto nível de implantação de energias renováveis.

O Capítulo 1 forneceu um contexto do panorama energético global baseado em dois aspectos principais: (i) a conexão direta entre desenvolvimento econômico e o aumento de impactos ambientais graves, e (ii) as ações que governos e a comunidade científica têm tomado para enfrentar crises energéticas e, portanto, econômicas. O estado da arte forneceu uma revisão sobre o que a comunidade científica desenvolveu, do ponto de vista de melhorias na eficiência dos sistemas de fornecimento de energia e destacou a falta de trabalhos analisando CEs a partir dos três pilares principais enfatizados no último parágrafo. O objetivo geral desta tese de doutorado também foi enfatizado, que é avançar no entendimento e desenvolvimento de uma integração sustentável e eficiente de sistemas de poligeração em CEs através da otimização de seus sistemas energéticos.

O Capítulo 2 discutiu as metodologias usadas no trabalho através da apresentação da estrutura de pesquisa. O capítulo forneceu uma visão geral sobre o processo de otimização de sistemas energéticos ao discutir quatro etapas principais: (i) a importância de definir a superestrutura do sistema de fornecimento de energia levando em conta os limites do

problema, os tipos de tecnologias e as interações entre elas, (ii) o papel crítico da fase de coleta e análise de dados, uma vez que a qualidade dos dados afeta diretamente a integridade e credibilidade dos resultados, (iii) a tradução de todas as informações coletadas em um modelo matemático que representa as características e desempenho de todas as tecnologias, o nível de detalhe desejado e os critérios de otimização, e (iv) o cálculo de uma solução ótima para o sistema de fornecimento de energia resolvendo o modelo matemático. Além disso, metodologias termoeconômicas também foram consideradas. A primeira é a análise e interpretação dos custos marginais derivados do processo de otimização, que fornecem insights críticos para o gerenciamento eficiente do sistema sob demandas energéticas variáveis. A segunda é a otimização local, que oferece uma abordagem simplificada para melhorias em subsistemas.

O Capítulo 3 apresentou o desenvolvimento do modelo de otimização multiobjetivo para uma CE consistindo em um grupo de nove edifícios mais uma unidade central compartilhando eletricidade, aquecimento e resfriamento entre si. As funções objetivo foram o custo anual total (relacionado à manutenção, investimento e operação horária) e as emissões totais anuais de CO<sub>2</sub>eq (relacionadas à operação horária). O capítulo apresentou a superestrutura tanto para os edifícios quanto para a unidade central, a coleta dos dados de entrada, o modelo matemático e o caso de referência. De acordo com a função objetivo, os resultados da otimização de objetivo único indicaram (i) a estrutura ótima do sistema de fornecimento de energia dentro de cada edifício, (ii) operação horária ótima de cada tecnologia, (iii) conexões ótimas entre prédios em termos de dutos de DHCN, (iv) distribuição otimizada (entre os prédios) de eletricidade autoproduzida e eletricidade comprada da rede, e (v) estrutura otimizada do sistema de fornecimento de energia e operação horária para a unidade central. Além disso, os resultados da otimização multiobjetivo demonstraram a importância deste tipo de abordagem ao apresentar uma gama de soluções trade-off que compreendem um conjunto de informações valiosas que podem apoiar os tomadores de decisão a fazer escolhas informadas com base em seus interesses.

Uma análise termoeconômica da CE foi desenvolvida através do Capítulo 4. Tal estudo foi desenvolvido através da análise e interpretação dos custos marginais horários relacionados às demandas de eletricidade, aquecimento e resfriamento. Tal estudo permitiu a obtenção de insights na direção de determinar a operação otimizada do sistema

quando a demanda de energia de um determinado edifício é aumentada. Como já discutido na literatura (Pina, Lozano e Serra, 2017), a consideração de armazenamento de energia térmica (TES) desacopla a produção do serviço de energia do consumo, ou seja, torna-se relevante saber não apenas a quantidade de energia produzida, mas também o momento em que ocorreu. Além disso, a incorporação de dutos de DHCN (fornecidos por esta tese) adicionou uma nova camada de complexidade, ou seja, além da necessidade de saber a quantidade de energia e o momento em que a produção de energia ocorreu, torna-se também necessário saber (i) em qual edifício tal produção de energia ocorreu, (ii) qual é o trajeto marginal relacionado, e (iii) as razões pelas quais alguns trajetos são mais caros que outros.

O objetivo geral do Capítulo 5 foi responder à pergunta "*qual o papel das CEs (como o caso de estudo desta tese, por exemplo) nos aspectos econômicos e ambientais de um cenário futuro do sistema energético italiano com um alto nível de implantação de energias renováveis?*" usando a metodologia de otimização local. Além da metodologia mencionada, dois elementos principais foram necessários: um subsistema local e um sistema global. O subsistema local foi definido como sendo a CE, enquanto o sistema global foi o sistema energético nacional (NES) italiano. Os resultados demonstraram o potencial que uma implantação razoável de CEs tem para promover ainda mais o uso de tecnologias mais eficientes de conversão de energia no NES italiano com uma tendência de diminuição do fornecimento total de energia primária. Além disso, os resultados mostraram que o menor nível de capacidades instaladas para diferentes tecnologias proporcionou uma diminuição considerável no custo anual total do NES italiano, o que pode indicar um possível benefício econômico a ser repassado para a sociedade.

## **6.2 Contribuições**

As principais contribuições e resultados desta tese são os seguintes:

- Síntese e operação ótimas de sistemas de poligeração para CEs, caracterizados por processos integrados complexos e lidando, ao mesmo tempo, com: (i) uma rede de dutos de aquecimento e resfriamento em distrito (DHCN) conectando os edifícios, (ii) uma unidade central para atender às demandas energéticas dos edifícios, (iii) armazenamento de calor e resfriamento, (iv) gerenciamento e distribuição de

---

eletricidade autoproduzida e comprada entre os edifícios e entre a CE e a rede elétrica nacional, (v) integração de tecnologias solares, (vi) preço horário de compra de eletricidade, (vii) preço horário de venda de eletricidade, e (viii) fatores horários de emissões de CO<sub>2</sub>.

- Otimização multiobjetivo da CE apresentando uma gama de soluções trade-off por meio das quais é possível obter informações importantes sobre capacidades instaladas, estrutura para os dutos de DHCN, custos anuais totais e emissões de CO<sub>2</sub>, custo de transição de uma solução para outra e custo de escolha de uma solução mais ambientalmente amigável. Os resultados do estudo de caso da CE mostraram a possibilidade de redução das emissões totais anuais de CO<sub>2</sub>eq em cerca de 20% (cerca de 1,5 kt CO<sub>2</sub>eq/ano) e dos custos anuais totais em aproximadamente 24% (cerca de 1,1 M€/ano), em comparação com o caso de referência.
- A análise e interpretação dos custos marginais horários de um sistema de poligeração complexo e altamente integrado, apoiado por (i) armazenamento de energia térmica, (ii) dutos de DHCN e (iii) o compartilhamento de eletricidade comprada e autoproduzida entre os nove edifícios.
- O delineamento de diferentes trajetórias marginais otimizados por meio dos seguintes tipos de produção de serviços energéticos: advanced, delayed, simultaneous, e remote.
- Por fim, outra contribuição importante foi a avaliação do papel das CEs nos aspectos econômicos e ambientais de um cenário futuro do sistema energético nacional (NES) italiano com um alto nível de implantação de energia renovável. Do ponto de vista ambiental, a implementação das CEs não representa um benefício positivo substancial para o cenário NES analisado. No entanto, tal implementação apresentou um potencial de redução da quantidade de energia necessária do NES italiano, uma vez que os sistemas de poligeração instalados (nas CEs) proporcionam um nível mais elevado de integração de processos, o que aumenta a eficiência global dos sistemas de fornecimento de energia. Essa redução na energia necessária do NES italiano resultou em menores capacidades instaladas para diferentes tecnologias. A consequência foi uma redução de 6% no custo anual total do NES italiano, representando 6,6 bilhões de euros/ano.

### 6.3 Trabalhos Futuros

A pesquisa conduzida nesta tese de doutorado proporcionou um avanço importante para a otimização e análise de sistemas de poligeração integrados em CEs, identificando estratégias-chave para melhorar a eficiência, sustentabilidade e custo-efetividade dentro desses sistemas. Trabalhos futuros poderiam seguir várias direções para exploração e desenvolvimento adicionais. Abaixo, o leitor pode encontrar uma lista não exaustiva de sugestões.

- Esforços de pesquisa subsequentes poderiam focar na incorporação de incentivos financeiros para novas tecnologias, adaptação a novos cenários políticos e exploração das implicações sociais do desenvolvimento de CEs.
- Os efeitos de start-up e shutdown poderiam ser incorporados aos modelos de desempenho das tecnologias a fim de obter soluções de otimização mais refinadas. Além disso, a incorporação de tecnologias como power-to-gas (por exemplo, eletrolisador e reator de metanação) e power-to-power (por exemplo, PTES e baterias elétricas) também poderia ser avaliada.
- Os impactos ambientais associados ao ciclo de vida de todas as tecnologias que compõem os sistemas de poligeração integrados na CE poderiam ser avaliados e incorporados à otimização multiobjetivo. Além disso, a função objetivo econômica poderia considerar também custos relativos às emissões de carbono ou iniciativas de mitigação de carbono.
- A troca de eletricidade autoproduzida entre os edifícios da CE poderia ser desenvolvida considerando uma recompensa pelas horas em que um determinado edifício envia eletricidade autoproduzida à subestação de distribuição, bem como uma taxa por receber eletricidade autoproduzida por outro membro da CE.





---

## *REFERENCES*

---



---

## CHAPTER 7 – References

Alarcon-Rodriguez, A., Ault, G. and Galloway, S. (2010) ‘Multi-objective planning of distributed energy resources: A review of the state-of-the-art’, *Renewable and Sustainable Energy Reviews*, 14(5), pp. 1353–1366. Available at: <https://doi.org/10.1016/j.rser.2010.01.006>.

Andiappan, V. (2017) ‘State-Of-The-Art Review of Mathematical Optimisation Approaches for Synthesis of Energy Systems’, *Process Integration and Optimization for Sustainability*, 1(3), pp. 165–188. Available at: <https://doi.org/10.1007/s41660-017-0013-2>.

ARERA (2006) *ARERA - Delibera181/2006. Aggiornamento delle fasce orarie con decorrenza 1 gennaio 2007*.

ARERA (2023) *ARERA - Autorità di Regolazione per Energia, Reti e Ambiente - Dati statistici*.

Asim, M. *et al.* (2020) ‘Thermo-economic and environmental analysis of integrating renewable energy sources in a district heating and cooling network’, *Energy Efficiency*, 13(1), pp. 79–100. Available at: <https://doi.org/10.1007/s12053-019-09832-9>.

Assembayeva, M., Zhakiyev, N. and Akhmetbekov, Y. (2017) ‘Impact of storage technologies on renewable energy integration in Kazakhstan’, *Materials Today: Proceedings*, 4(3), pp. 4512–4523. Available at: <https://doi.org/10.1016/j.matpr.2017.04.024>.

Balaman, Ş.Y. (2016) ‘Investment planning and strategic management of sustainable systems for clean power generation: An  $\epsilon$ -constraint based multi objective modelling approach’, *Journal of Cleaner Production*, 137, pp. 1179–1190. Available at: <https://doi.org/10.1016/j.jclepro.2016.07.202>.

Baños, R. *et al.* (2011) ‘Optimization methods applied to renewable and sustainable energy: A review’, *Renewable and Sustainable Energy Reviews*, 15(4), pp. 1753–1766. Available at: <https://doi.org/10.1016/j.rser.2010.12.008>.

- 
- Barroco Fontes Cunha, F. *et al.* (2021) ‘Transitioning to a low carbon society through energy communities: Lessons learned from Brazil and Italy’, *Energy Research & Social Science*, 75, p. 101994. Available at: <https://doi.org/10.1016/j.erss.2021.101994>.
- Batista, A.C. and Batista, L.S. (2018) ‘Demand Side Management using a multi-criteria  $\epsilon$ -constraint based exact approach’, *Expert Systems with Applications*, 99, pp. 180–192. Available at: <https://doi.org/10.1016/j.eswa.2018.01.040>.
- Bauwens, T. *et al.* (2022) ‘Conceptualizing community in energy systems: A systematic review of 183 definitions’, *Renewable and Sustainable Energy Reviews*, 156, p. 111999. Available at: <https://doi.org/10.1016/j.rser.2021.111999>.
- Becker, H. and Maréchal, F. (2012) ‘Targeting industrial heat pump integration in multi-period problems’, in, pp. 415–419. Available at: <https://doi.org/10.1016/B978-0-444-59507-2.50075-5>.
- Bellina, R. (2012) *Progetto Ottimo di un Sistema Integrato con Impianto Trigenerativo e Rete di Teleriscaldamento per il Comune di Tolmezzo*. University of Udine.
- Bellos, E. and Tzivanidis, C. (2021) ‘Parametric Analysis of a Polygeneration System with CO<sub>2</sub> Working Fluid’, *Applied Sciences*, 11(7), p. 3215. Available at: <https://doi.org/10.3390/app11073215>.
- Biegler, L.T. and Grossmann, I.E. (2004) ‘Retrospective on optimization’, *Computers & Chemical Engineering*, 28(8), pp. 1169–1192. Available at: <https://doi.org/10.1016/j.compchemeng.2003.11.003>.
- Bogdanov, D. *et al.* (2019) ‘Radical transformation pathway towards sustainable electricity via evolutionary steps’, *Nature Communications*, 10(1), p. 1077. Available at: <https://doi.org/10.1038/s41467-019-08855-1>.
- Bogdanov, D. *et al.* (2021) ‘Full energy sector transition towards 100% renewable energy supply: Integrating power, heat, transport and industry sectors including desalination’, *Applied Energy*, 283, p. 116273. Available at: <https://doi.org/10.1016/j.apenergy.2020.116273>.

---

Bompard, E. *et al.* (2020) ‘An electricity triangle for energy transition: Application to Italy’, *Applied Energy*, 277, p. 115525. Available at: <https://doi.org/10.1016/j.apenergy.2020.115525>.

Borasio, M. and Moret, S. (2022) ‘Deep decarbonisation of regional energy systems: A novel modelling approach and its application to the Italian energy transition’, *Renewable and Sustainable Energy Reviews*, 153, p. 111730. Available at: <https://doi.org/10.1016/j.rser.2021.111730>.

Bose, A. *et al.* (2022) ‘Evaluation of a biomethane, food and biofertiliser polygeneration system in a circular economy system’, *Renewable and Sustainable Energy Reviews*, 170, p. 112960. Available at: <https://doi.org/10.1016/j.rser.2022.112960>.

Breyer, C. *et al.* (2018) ‘Solar photovoltaics demand for the global energy transition in the power sector’, *Progress in Photovoltaics: Research and Applications*, 26(8), pp. 505–523. Available at: <https://doi.org/10.1002/pip.2950>.

Brown, T.W. *et al.* (2018) ‘Response to “Burden of proof: A comprehensive review of the feasibility of 100% renewable-electricity systems”’, *Renewable and Sustainable Energy Reviews*, 92, pp. 834–847. Available at: <https://doi.org/10.1016/j.rser.2018.04.113>.

Buoro, D. *et al.* (2010) ‘Optimal Lay-Out and Operation of District Heating and Cooling Distributed Trigeneration Systems’, in *Volume 5: Industrial and Cogeneration; Microturbines and Small Turbomachinery; Oil and Gas Applications; Wind Turbine Technology*. ASME/EDC, pp. 157–166. Available at: <https://doi.org/10.1115/GT2010-23416>.

Buoro, D. *et al.* (2011) ‘Optimization of Distributed Trigeneration Systems Integrated with Heating and Cooling Micro-grids’, *Distributed Generation and Alternative Energy Journal*, 26(2), pp. 7–34. Available at: <https://doi.org/10.1080/21563306.2011.10412189>.

Buoro, D. (2013) *Development of an Environmental and Economic Optimization Model for Distributed Generation Energy Systems*. PhD Thesis. University of Udine.

---

Buoro, D. *et al.* (2013) ‘Multicriteria optimization of a distributed energy supply system for an industrial area’, *Energy*, 58, pp. 128–137. Available at: <https://doi.org/10.1016/j.energy.2012.12.003>.

Buoro, D. and Reini, M. (2010) ‘Mixed Integer Linearized Exergoeconomic (MILE) method for energy system synthesis and optimization’, in *23th International Conference on Efficiency, Cost, Optimization, Simulation and Environmental Impact of Energy Systems*. Lausanne, Switzerland: ECOS 2010.

Cabeza, L.F. *et al.* (2021) ‘Perspectives on thermal energy storage research’, *Energy*, 231, p. 120943. Available at: <https://doi.org/10.1016/j.energy.2021.120943>.

Calise, F. *et al.* (2022) ‘Optimal design of a 5th generation district heating and cooling network based on seawater heat pumps’, *Energy Conversion and Management*, 267, p. 115912. Available at: <https://doi.org/10.1016/j.enconman.2022.115912>.

Capstone (2009) *Capstone Microturbine Technical Reference*. Los Angeles, CA, USA.

Capuder, T. and Mancarella, P. (2014) ‘Techno-economic and environmental modelling and optimization of flexible distributed multi-generation options’, *Energy*, 71, pp. 516–533. Available at: <https://doi.org/10.1016/j.energy.2014.04.097>.

Carvalho, M., Lozano, M.A. and Serra, L.M. (2012) ‘Multicriteria synthesis of trigeneration systems considering economic and environmental aspects’, *Applied Energy*, 91(1), pp. 245–254. Available at: <https://doi.org/10.1016/j.apenergy.2011.09.029>.

Casisi, M. *et al.* (2008) ‘Effect of Different Economic Support Policies on the Optimal Definition and Operation of a CHP and RES Distributed Generation Systems’, in *Volume 7: Education; Industrial and Cogeneration; Marine; Oil and Gas Applications*. ASMEDC, pp. 123–130. Available at: <https://doi.org/10.1115/GT2008-50353>.

Casisi, M. *et al.* (2019) ‘A Comparison of Different District Integration for a Distributed Generation System for Heating and Cooling in an Urban Area’, *Applied Sciences*, 9(17), p. 3521. Available at: <https://doi.org/10.3390/app9173521>.

---

Casisi, M., Pinamonti, P. and Reini, M. (2007) ‘Optimal lay-out and operation of CHP distributed generation systems’, in. Available at: <https://api.semanticscholar.org/CorpusID:116525561>.

Chicco, G. and Mancarella, P. (2009) ‘Distributed multi-generation: A comprehensive view’, *Renewable and Sustainable Energy Reviews*, 13(3), pp. 535–551. Available at: <https://doi.org/10.1016/j.rser.2007.11.014>.

Chun, A. *et al.* (2021) ‘On the definition of part-load operation strategies in a complex trigeneration system with hourly-seasonal demands: Exergoeconomics and optimization’, *Energy Conversion and Management*, 246, p. 114688. Available at: <https://doi.org/10.1016/j.enconman.2021.114688>.

Cohon, J. (1978) ‘Multiobjective Programming and Planning’, *Academic Press* [Preprint]. Available at: [https://www.google.es/books/edition/Multiobjective\\_Programming\\_and\\_Planning/GFtwGswaMKYC?hl=en&gbpv=1&printsec=frontcover](https://www.google.es/books/edition/Multiobjective_Programming_and_Planning/GFtwGswaMKYC?hl=en&gbpv=1&printsec=frontcover) (Accessed: 19 September 2023).

Comodi, G. *et al.* (2019) ‘Achieving low carbon local energy communities in hot climates by exploiting networks synergies in multi energy systems’, *Applied Energy*, 256, p. 113901. Available at: <https://doi.org/10.1016/j.apenergy.2019.113901>.

Daikin (2013) *Chillers: Commercial and Technical Data*. Available at: [https://www.daikin.eu/en\\_us/products/product.html/EUWA-KBZW1.html](https://www.daikin.eu/en_us/products/product.html/EUWA-KBZW1.html) (Accessed: 6 April 2023).

DAIT (2021) *ELENCO DEI COMUNI ITALIANI VIGENTI (7.899) CON POPOLAZIONE RIFERITA AL CENSIMENTO DEL 31 Dic 2021*, Dipartimento per gli Affari Interni e Territoriali. Available at: [https://dait.interno.gov.it/territorio-e-autonomie-locali/sut/elenco\\_cens\\_var\\_comuni\\_italiani.php#top](https://dait.interno.gov.it/territorio-e-autonomie-locali/sut/elenco_cens_var_comuni_italiani.php#top) (Accessed: 21 August 2023).

Domínguez-Muñoz, F. *et al.* (2011) ‘Selection of typical demand days for CHP optimization’, *Energy and Buildings*, 43(11), pp. 3036–3043. Available at: <https://doi.org/10.1016/j.enbuild.2011.07.024>.

---

Dorfner, J. and Hamacher, T. (2014) ‘Large-Scale District Heating Network Optimization’, *IEEE Transactions on Smart Grid*, 5(4), pp. 1884–1891. Available at: <https://doi.org/10.1109/TSG.2013.2295856>.

Edtmayer, H. *et al.* (2021) ‘Investigation on sector coupling potentials of a 5th generation district heating and cooling network’, *Energy*, 230, p. 120836. Available at: <https://doi.org/10.1016/j.energy.2021.120836>.

EEA (2023) *Delivering the European Green Deal*, European Environment Agency. Available at: <https://www.eea.europa.eu/policy-documents/2030-climate-target-plan> (Accessed: 10 January 2024).

ENTSO-E (2023) *European Network of Transmission System Operators for Electricity*.

European Council (2023) *Fit for 55*. Available at: <https://www.consilium.europa.eu/en/policies/green-deal/fit-for-55-the-eu-plan-for-a-green-transition/> (Accessed: 13 March 2023).

Evans, R.B. (1980) ‘Thermoeconomic isolation and essergy analysis’, *Energy*, 5(8–9), pp. 804–821. Available at: [https://doi.org/10.1016/0360-5442\(80\)90098-5](https://doi.org/10.1016/0360-5442(80)90098-5).

Fazlollahi, S. *et al.* (2012) ‘Methods for multi-objective investment and operating optimization of complex energy systems’, *Energy*, 45(1), pp. 12–22. Available at: <https://doi.org/10.1016/j.energy.2012.02.046>.

FICO (2023) ‘Xpress software. <https://www.fico.com>.’

Floudas, C.A. (1995) *Nonlinear and Mixed-Integer Optimization: Fundamentals and Applications*, Oxford Academic. Oxford University Press.

Floudas, C.A. and Lin, X. (2005) ‘Mixed Integer Linear Programming in Process Scheduling: Modeling, Algorithms, and Applications’, *Annals of Operations Research*, 139(1), pp. 131–162. Available at: <https://doi.org/10.1007/s10479-005-3446-x>.

Frangopoulos, C.A., Von Spakovsky, M.R. and Sciubba, E. (2002) ‘A Brief Review of Methods for the Design and Synthesis Optimization of Energy Systems’, *International Journal of Thermodynamics*, 5(4), pp. 151–160.



- 
- Gaggioli, R.A. (1983) ‘Second Law Analysis for Process and Energy Engineering’, in, pp. 3–50. Available at: <https://doi.org/10.1021/bk-1983-0235.ch001>.
- Gao, L. *et al.* (2008) ‘Proposal of a natural gas-based polygeneration system for power and methanol production’, *Energy*, 33(2), pp. 206–212. Available at: <https://doi.org/10.1016/j.energy.2007.10.011>.
- GME (2019) *GME - Gestore Mercati Energetici. Prezzo medio per fasce*.
- Gong, J. and You, F. (2015) ‘Sustainable design and synthesis of energy systems’, *Current Opinion in Chemical Engineering*, 10, pp. 77–86. Available at: <https://doi.org/10.1016/j.coche.2015.09.001>.
- GSE (2008) *GSE - Gestore dei Servizi Energetici. Ritiro Dedicato*.
- GSE (2023) *GSE - Electricity selling price. Ritiro dedicato - Archivio prezzi medi mensili 2008 - 2022*.
- Haeseldonckx, D. and D’haeseleer, W. (2011) ‘Concrete transition issues towards a fully-fledged use of hydrogen as an energy carrier: Methodology and modelling’, *International Journal of Hydrogen Energy*, 36(8), pp. 4636–4652. Available at: <https://doi.org/10.1016/j.ijhydene.2011.01.113>.
- Hansen, K., Breyer, C. and Lund, H. (2019a) ‘Status and perspectives on 100% renewable energy systems’, *Energy*, 175, pp. 471–480. Available at: <https://doi.org/10.1016/j.energy.2019.03.092>.
- Hansen, K., Breyer, C. and Lund, H. (2019b) ‘Status and perspectives on 100% renewable energy systems’, *Energy*, 175, pp. 471–480. Available at: <https://doi.org/10.1016/j.energy.2019.03.092>.
- Heard, B.P. *et al.* (2017) ‘Burden of proof: A comprehensive review of the feasibility of 100% renewable-electricity systems’, *Renewable and Sustainable Energy Reviews*, 76, pp. 1122–1133. Available at: <https://doi.org/10.1016/j.rser.2017.03.114>.

---

Hoevenaars, E.J. and Crawford, C.A. (2012) ‘Implications of temporal resolution for modeling renewables-based power systems’, *Renewable Energy*, 41, pp. 285–293. Available at: <https://doi.org/10.1016/j.renene.2011.11.013>.

Hughes, T.P. *et al.* (2018) ‘Spatial and temporal patterns of mass bleaching of corals in the Anthropocene’, *Science*, 359(6371), pp. 80–83. Available at: <https://doi.org/10.1126/science.aan8048>.

IEA (2017) *World Energy Outlook*, International Energy Agency. Available at: <https://www.iea.org/reports/world-energy-outlook-2017> (Accessed: 10 January 2024).

IEA (2019) *World Energy Outlook*, International Energy Agency. Available at: <https://www.iea.org/reports/world-energy-outlook-2019> (Accessed: 10 January 2024).

IEA (2021) *Evolution of energy prices, 2020-2021*. Available at: <https://www.iea.org/data-and-statistics/charts/evolution-of-energy-prices-2020-2021> (Accessed: 17 February 2023).

IEA (2022a) *Evolution of energy prices, Oct 2020-Jan 2022*. Available at: <https://www.iea.org/data-and-statistics/charts/evolution-of-energy-prices-oct-2020-jan-2022> (Accessed: 15 February 2023).

IEA (2022b) *Evolution of key regional natural gas prices, June 2021-October 2022*, International Energy Agency. Available at: <https://www.iea.org/data-and-statistics/charts/evolution-of-key-regional-natural-gas-prices-june-2021-october-2022> (Accessed: 15 February 2023).

IEA (2022c) *How to Avoid Gas Shortages in the European Union in 2023*. Available at: <https://www.iea.org/reports/how-to-avoid-gas-shortages-in-the-european-union-in-2023> (Accessed: 20 February 2023).

IPCC (2018) *An IPCC Special Report on the Impacts of Global Warming of 1.5 °C above pre-Industrial Levels and Related Global Greenhouse Gas Emission Pathways, in the Context of Strengthening the Global Response to the Threat of Climate Change, Sustainable Development, and Efforts to Eradicate Poverty*. Available at:

---

[https://www.ipcc.ch/site/assets/uploads/sites/2/2018/07/SR15\\_SPM\\_version\\_stand\\_alone\\_LR.pdf](https://www.ipcc.ch/site/assets/uploads/sites/2/2018/07/SR15_SPM_version_stand_alone_LR.pdf) (Accessed: 10 February 2023).

IPCC (2023) *Summary for Policymakers*. Geneva, Switzerland. Available at: <https://doi.org/10.59327/IPCC/AR6-9789291691647.001>.

ISPRA (2021) *Italian Greenhouse Gas Inventory 1990-2019. National Inventory Report*.

Jacobson, M.Z. *et al.* (2017) ‘100% Clean and Renewable Wind, Water, and Sunlight All-Sector Energy Roadmaps for 139 Countries of the World’, *Joule*, 1(1), pp. 108–121. Available at: <https://doi.org/10.1016/j.joule.2017.07.005>.

Jebamalai, J.M., Marlein, K. and Laverge, J. (2022) ‘Design and cost comparison of district heating and cooling (DHC) network configurations using ring topology – A case study’, *Energy*, 258, p. 124777. Available at: <https://doi.org/10.1016/j.energy.2022.124777>.

Kantor, I. *et al.* (2020) ‘A Mixed-Integer Linear Programming Formulation for Optimizing Multi-Scale Material and Energy Integration’, *Frontiers in Energy Research*, 8. Available at: <https://doi.org/10.3389/fenrg.2020.00049>.

Kasaean, A. *et al.* (2020) ‘Solar-driven polygeneration systems: Recent progress and outlook’, *Applied Energy*, 264, p. 114764. Available at: <https://doi.org/10.1016/j.apenergy.2020.114764>.

Kayo, G., Hasan, A. and Siren, K. (2014) ‘Energy sharing and matching in different combinations of buildings, CHP capacities and operation strategy’, *Energy and Buildings*, 82, pp. 685–695. Available at: <https://doi.org/10.1016/j.enbuild.2014.07.077>.

Ke, P. *et al.* (2022) *Carbon Monitor Europe, a near-real-time and country-level monitoring of daily CO<sub>2</sub> emissions for European Union and the United Kingdom*. Available at: <https://doi.org/https://doi.org/10.6084/m9.figshare.20219024.v2>.

Ke, P. *et al.* (2023) ‘Carbon Monitor Europe near-real-time daily CO<sub>2</sub> emissions for 27 EU countries and the United Kingdom’, *Scientific Data*, 10(1), p. 374. Available at: <https://doi.org/10.1038/s41597-023-02284-y>.

- 
- Kermani, M. *et al.* (2017) ‘A novel MILP approach for simultaneous optimization of water and energy: Application to a Canadian softwood Kraft pulping mill’, *Computers & Chemical Engineering*, 102, pp. 238–257. Available at: <https://doi.org/10.1016/j.compchemeng.2016.11.043>.
- Kim, M.-H. *et al.* (2021) ‘Energy Performance Investigation of Bi-Directional Convergence Energy Prosumers for an Energy Sharing Community’, *Energies*, 14(17), p. 5544. Available at: <https://doi.org/10.3390/en14175544>.
- Klotz, E. and Newman, A.M. (2013) ‘Practical guidelines for solving difficult mixed integer linear programs’, *Surveys in Operations Research and Management Science*, 18(1–2), pp. 18–32. Available at: <https://doi.org/10.1016/j.sorms.2012.12.001>.
- Lamedica, R. *et al.* (2018) ‘A MILP methodology to optimize sizing of PV - Wind renewable energy systems’, *Energy*, 165, pp. 385–398. Available at: <https://doi.org/10.1016/j.energy.2018.09.087>.
- Lanati, F. and Gaeta, M. (2020) ‘How to achieve a complete decarbonization of the Italian energy system by 2050?’, in *2020 17th International Conference on the European Energy Market (EEM)*. IEEE, pp. 1–5. Available at: <https://doi.org/10.1109/EEM49802.2020.9221953>.
- Li, H. *et al.* (2015) ‘A review of the pricing mechanisms for district heating systems’, *Renewable and Sustainable Energy Reviews*, 42, pp. 56–65. Available at: <https://doi.org/10.1016/j.rser.2014.10.003>.
- Limpens, G. *et al.* (2019) ‘EnergyScope TD: A novel open-source model for regional energy systems’, *Applied Energy*, 255, p. 113729. Available at: <https://doi.org/10.1016/j.apenergy.2019.113729>.
- de Lira-Flores, J.A., Gutiérrez-Antonio, C. and Vázquez-Román, R. (2018) ‘A MILP approach for optimal storage vessels layout based on the quantitative risk analysis methodology’, *Process Safety and Environmental Protection*, 120, pp. 1–13. Available at: <https://doi.org/10.1016/j.psep.2018.08.028>.

---

Liu, P., Georgiadis, M.C. and Pistikopoulos, E.N. (2013) ‘An energy systems engineering approach for the design and operation of microgrids in residential applications’, *Chemical Engineering Research and Design*, 91(10), pp. 2054–2069. Available at: <https://doi.org/10.1016/j.cherd.2013.08.016>.

Lombardi, F. *et al.* (2020) ‘Policy Decision Support for Renewables Deployment through Spatially Explicit Practically Optimal Alternatives’, *Joule*, 4(10), pp. 2185–2207. Available at: <https://doi.org/10.1016/j.joule.2020.08.002>.

Lozano, M.A. *et al.* (1994) ‘Thermoeconomic Diagnosis of Energy Systems’, in *FLOWERS’94: Florence World Energy Research Symposium*. Florence.

Lozano, Miguel A. *et al.* (2009) ‘Structure optimization of energy supply systems in tertiary sector buildings’, *Energy and Buildings*, 41(10), pp. 1063–1075. Available at: <https://doi.org/10.1016/j.enbuild.2009.05.008>.

Lozano, M.A. *et al.* (2009) ‘Thermoeconomic analysis of simple trigeneration systems’, *International Journal of Thermodynamics*, 12(3), pp. 147–153.

Lozano, M.A., Carvalho, M. and Serra, L.M. (2009) ‘Operational strategy and marginal costs in simple trigeneration systems’, *Energy*, 34(11), pp. 2001–2008. Available at: <https://doi.org/10.1016/j.energy.2009.08.015>.

Lozano, M.A., Carvalho, M. and Serra, L.M. (2011) ‘Allocation of economic costs in trigeneration systems at variable load conditions’, *Energy and Buildings*, 43(10), pp. 2869–2881. Available at: <https://doi.org/10.1016/j.enbuild.2011.07.002>.

Lozano, M.A. and Valero, A. (1993) ‘Theory of the exergetic cost’, *Energy*, 18(9), pp. 939–960. Available at: [https://doi.org/10.1016/0360-5442\(93\)90006-Y](https://doi.org/10.1016/0360-5442(93)90006-Y).

Lozano, M.A., Valero, A. and Serra, L. (1996) ‘Local Optimization of Energy Systems’, in *Advanced Energy Systems*. American Society of Mechanical Engineers, pp. 241–250. Available at: <https://doi.org/10.1115/IMECE1996-0281>.

---

Lund, H. *et al.* (2010) ‘The role of district heating in future renewable energy systems’, *Energy*, 35(3), pp. 1381–1390. Available at: <https://doi.org/10.1016/j.energy.2009.11.023>.

Mencarelli, L. *et al.* (2020) ‘A review on superstructure optimization approaches in process system engineering’, *Computers & Chemical Engineering*, 136, p. 106808. Available at: <https://doi.org/10.1016/j.compchemeng.2020.106808>.

Méndez, C.A. *et al.* (2006) ‘A simultaneous optimization approach for off-line blending and scheduling of oil-refinery operations’, *Computers & Chemical Engineering*, 30(4), pp. 614–634. Available at: <https://doi.org/10.1016/j.compchemeng.2005.11.004>.

Muñoz, J.R. and Von Spakovsky, M. (2000) ‘A Decomposition Approach for the Large Scale Synthesis/Design Optimization of Highly Coupled, Highly Dynamic Energy Systems’, *International Journal of Thermodynamics*, 4(1), pp. 19–33.

Musolino, M. *et al.* (2023) ‘Three case studies to explore relevant features of emerging renewable energy communities in Italy’, *Renewable Energy*, 210, pp. 540–555. Available at: <https://doi.org/10.1016/j.renene.2023.04.094>.

Nadalon, E. *et al.* (2023) ‘Part-Load Energy Performance Assessment of a Pumped Thermal Energy Storage System for an Energy Community’, *Energies*, 16(15), p. 5720. Available at: <https://doi.org/10.3390/en16155720>.

Ng, K.S., Zhang, N. and Sadhukhan, J. (2013) ‘Techno-economic analysis of polygeneration systems with carbon capture and storage and CO<sub>2</sub> reuse’, *Chemical Engineering Journal*, 219, pp. 96–108. Available at: <https://doi.org/10.1016/j.cej.2012.12.082>.

NOAA (2023a) *Climate at a Glance: Global Time Series*. Available at: <https://www.ncei.noaa.gov/access/monitoring/climate-at-a-glance/global/time-series> (Accessed: 10 January 2024).

NOAA (2023b) *Monthly Global Climate Report for November 2023*. Available at: <https://www.ncei.noaa.gov/access/monitoring/monthly-report/global/202311> (Accessed: 10 January 2024).

---

NREL (2023) ‘System Advisor Model’. Available at: <https://sam.nrel.gov/weather-data.html> (Accessed: 5 February 2023).

Obama, B. (2017) ‘The irreversible momentum of clean energy’, *Science*, 355(6321), pp. 126–129. Available at: <https://doi.org/10.1126/science.aam6284>.

Park, H.-S. and Jun, C.-H. (2009) ‘A simple and fast algorithm for K-medoids clustering’, *Expert Systems with Applications*, 36(2), pp. 3336–3341. Available at: <https://doi.org/10.1016/j.eswa.2008.01.039>.

Pezic, M. and Cedres, V.M. (2013) ‘Unit commitment in fully renewable, hydro-wind energy systems’, in *2013 10th International Conference on the European Energy Market (EEM)*. IEEE, pp. 1–8. Available at: <https://doi.org/10.1109/EEM.2013.6607331>.

Pina, E.A. (2019) *Thermoeconomic and environmental synthesis and optimization of polygeneration systems supported with renewable energies and thermal energy storage applied to the residential-commercial sector*. University of Zaragoza. Available at: <https://zaguan.unizar.es/record/87519> (Accessed: 19 September 2023).

Pina, E.A. *et al.* (2020) ‘Tackling thermal integration in the synthesis of polygeneration systems for buildings’, *Applied Energy*, 269, p. 115115. Available at: <https://doi.org/10.1016/j.apenergy.2020.115115>.

Pina, E.A., Lozano, M.A. and Serra, L.M. (2017) ‘Optimal operation and marginal costs in simple trigeneration systems including thermal energy storage’, *Energy*, 135, pp. 788–798. Available at: <https://doi.org/10.1016/j.energy.2017.06.101>.

Pina, E.A., Lozano, M.A. and Serra, L.M. (2021) ‘Assessing the influence of legal constraints on the integration of renewable energy technologies in polygeneration systems for buildings’, *Renewable and Sustainable Energy Reviews*, 149, p. 111382. Available at: <https://doi.org/10.1016/j.rser.2021.111382>.

Pinto, E. (2021) *Thermoeconomic and environmental optimization of polygeneration systems for small-scale residential buildings integrating thermal and electric energy storage, renewable energy and legal restrictions*. Ph.D. Thesis. University of Zaragoza.

---

Pinto, E.S., Serra, L.M. and Lázaro, A. (2020) ‘Evaluation of methods to select representative days for the optimization of polygeneration systems’, *Renewable Energy*, 151, pp. 488–502. Available at: <https://doi.org/10.1016/j.renene.2019.11.048>.

Pinto, E.S., Serra, L.M. and Lázaro, A. (2022) ‘Energy communities approach applied to optimize polygeneration systems in residential buildings: Case study in Zaragoza, Spain’, *Sustainable Cities and Society*, 82, p. 103885. Available at: <https://doi.org/10.1016/j.scs.2022.103885>.

Poncelet, K. *et al.* (2017) ‘Selecting Representative Days for Capturing the Implications of Integrating Intermittent Renewables in Generation Expansion Planning Problems’, *IEEE Transactions on Power Systems*, 32(3), pp. 1936–1948. Available at: <https://doi.org/10.1109/TPWRS.2016.2596803>.

Potrč, S. *et al.* (2021) ‘Sustainable renewable energy supply networks optimization – The gradual transition to a renewable energy system within the European Union by 2050’, *Renewable and Sustainable Energy Reviews*, 146, p. 111186. Available at: <https://doi.org/10.1016/j.rser.2021.111186>.

Pursiheimo, E., Holttinen, H. and Koljonen, T. (2019) ‘Inter-sectoral effects of high renewable energy share in global energy system’, *Renewable Energy*, 136, pp. 1119–1129. Available at: <https://doi.org/10.1016/j.renene.2018.09.082>.

Ram, M., Aghahosseini, A. and Breyer, C. (2020) ‘Job creation during the global energy transition towards 100% renewable power system by 2050’, *Technological Forecasting and Social Change*, 151, p. 119682. Available at: <https://doi.org/10.1016/j.techfore.2019.06.008>.

Reini, M. (1994) *Analisi e Sviluppo dei Metodi Termoeconomici per lo Studio degli Impianti di Conversione dell’Energia*. Ph.D. Thesis. Università di Padova.

Reini, M., Lazzaretto, A. and Macor, A. (1995) ‘Average structural and marginal costs as result of a unified formulation of the thermoeconomic problem’, in *Proc. of Second Law Analysis of Energy Systems: Towards the 21-st Century*. Rome.



- 
- Reini, M. and Lozano, M. (1994a) ‘Local optimization of the energy system components - Part 1: theoretical formulation’, in *Proceeding of the National Italian Conference ATI, [in Italian]*. Perugia.
- Reini, M. and Lozano, M. (1994b) ‘Local optimization of the energy system components - Part 2: the case study of a steam power plant’, in *Proceeding of the National Italian Conference ATI, [in Italian]*.
- Rogelj, J. *et al.* (2015) ‘Energy system transformations for limiting end-of-century warming to below 1.5 °C’, *Nature Climate Change*, 5(6), pp. 519–527. Available at: <https://doi.org/10.1038/nclimate2572>.
- Rong, A. and Su, Y. (2017) ‘Polygeneration systems in buildings: A survey on optimization approaches’, *Energy and Buildings*, 151, pp. 439–454. Available at: <https://doi.org/10.1016/j.enbuild.2017.06.077>.
- Sadiqa, A., Gulagi, A. and Breyer, C. (2018) ‘Energy transition roadmap towards 100% renewable energy and role of storage technologies for Pakistan by 2050’, *Energy*, 147, pp. 518–533. Available at: <https://doi.org/10.1016/j.energy.2018.01.027>.
- Sartor, K., Quoilin, S. and Dewallef, P. (2014) ‘Simulation and optimization of a CHP biomass plant and district heating network’, *Applied Energy*, 130, pp. 474–483. Available at: <https://doi.org/10.1016/j.apenergy.2014.01.097>.
- Savic, D. (2002) ‘Single-objective vs. Multiobjective Optimisation for Integrated Decision Support’, in *1st International Congress on Environmental Modelling and Software*. Lugano, Switzerland, pp. 7–12.
- Schellnhuber, H.J., Rahmstorf, S. and Winkelmann, R. (2016) ‘Why the right climate target was agreed in Paris’, *Nature Climate Change*, 6(7), pp. 649–653. Available at: <https://doi.org/10.1038/nclimate3013>.
- Serra, L.M. (1994) *Optimización exergoeconómica de sistemas térmicos*. Ph.D. Thesis. Universidad de Zaragoza.

---

Shirizadeh, B. and Quirion, P. (2022) ‘Do multi-sector energy system optimization models need hourly temporal resolution? A case study with an investment and dispatch model applied to France’, *Applied Energy*, 305, p. 117951. Available at: <https://doi.org/10.1016/j.apenergy.2021.117951>.

De Souza, R. *et al.* (2021) ‘A Review of Small–Medium Combined Heat and Power (CHP) Technologies and Their Role within the 100% Renewable Energy Systems Scenario’, *Energies*, 14(17), p. 5338. Available at: <https://doi.org/10.3390/en14175338>.

De Souza, R. *et al.* (2022) ‘Optimal Sharing Electricity and Thermal Energy Integration for an Energy Community in the Perspective of 100% RES Scenario’, *Sustainability*, 14(16), p. 10125. Available at: <https://doi.org/10.3390/su141610125>.

De Souza, R.J. *et al.* (2023) ‘Towards a Low Carbon Future: Evaluating Scenarios for an Energy Community Through a Multi-Objective Optimisation Approach’, in *36th International Conference on Efficiency, Cost, Optimization, Simulation and Environmental Impact of Energy Systems (ECOS 2023)*. Las Palmas De Gran Canaria, Spain: ECOS 2023, pp. 2614–2625. Available at: <https://doi.org/10.52202/069564-0235>.

Steffen, W. *et al.* (2018) ‘Trajectories of the Earth System in the Anthropocene’, *Proceedings of the National Academy of Sciences*, 115(33), pp. 8252–8259. Available at: <https://doi.org/10.1073/pnas.1810141115>.

Subramanian, A.S.R. *et al.* (2020) ‘Optimal Design and Operation of Flexible Polygeneration Systems using Decomposition Algorithms’, in *Computer Aided Chemical Engineering*, pp. 919–924. Available at: <https://doi.org/10.1016/B978-0-12-823377-1.50154-3>.

Terrier, C. *et al.* (2024) ‘From Local Energy Communities towards National Energy System: A Grid-Aware Techno-Economic Analysis’, *Energies*, 17(4), p. 910. Available at: <https://doi.org/10.3390/en17040910>.

Teske, S., Morris, T. and Nagrath, K. (2020) *100% Renewable Energy: An Energy [R]evolution for Italy*. Available at: <https://www.greenpeace.org/static/planet4-italy-stateless-develop/2020/06/a7955fe1-italy-report-forgp-2020.pdf> (Accessed: 24 October 2023).

---

Trevisan, R., Ghiani, E. and Pilo, F. (2023) ‘Renewable Energy Communities in Positive Energy Districts: A Governance and Realisation Framework in Compliance with the Italian Regulation’, *Smart Cities*, 6(1), pp. 563–585. Available at: <https://doi.org/10.3390/smartcities6010026>.

Umeda, T., Hirai, A. and Ichikawa, A. (1972) ‘Synthesis of optimal processing system by an integrated approach’, *Chemical Engineering Science*, 27(4), pp. 795–804. Available at: [https://doi.org/https://doi.org/10.1016/0009-2509\(72\)85013-9](https://doi.org/https://doi.org/10.1016/0009-2509(72)85013-9).

UNFCCC (2015) ‘The Paris Agreement’. Paris: United Nations Framework Convention on Climate Change. Available at: [https://unfccc.int/sites/default/files/english\\_paris\\_agreement.pdf](https://unfccc.int/sites/default/files/english_paris_agreement.pdf) (Accessed: 20 January 2023).

Uniyal, N., Pant, S. and Kumar, A. (2020) ‘An Overview of Few Nature Inspired Optimization Techniques and Its Reliability Applications’, *International Journal of Mathematical, Engineering and Management Sciences*, 5(4), pp. 732–743. Available at: <https://doi.org/10.33889/IJMEMS.2020.5.4.058>.

Urbanucci, L., Testi, D. and Bruno, J.C. (2018) ‘An operational optimization method for a complex polygeneration plant based on real-time measurements’, *Energy Conversion and Management*, 170, pp. 50–61. Available at: <https://doi.org/10.1016/j.enconman.2018.05.076>.

Vesterlund, M., Toffolo, A. and Dahl, J. (2017) ‘Optimization of multi-source complex district heating network, a case study’, *Energy*, 126, pp. 53–63. Available at: <https://doi.org/10.1016/j.energy.2017.03.018>.

Viessmann (2020) *VITOBLOC 200: Gruppo di cogenerazione - elettricità e calore da gas metano*.

Vivian, J. *et al.* (2022) ‘Investigation on Individual and Collective PV Self-Consumption for a Fifth Generation District Heating Network’, *Energies*, 15(3), p. 1022. Available at: <https://doi.org/10.3390/en15031022>.

---

Vogel, J. *et al.* (2021) ‘Socio-economic conditions for satisfying human needs at low energy use: An international analysis of social provisioning’, *Global Environmental Change*, 69, p. 102287. Available at: <https://doi.org/10.1016/j.gloenvcha.2021.102287>.

Voll, P. *et al.* (2015) ‘The optimum is not enough: A near-optimal solution paradigm for energy systems synthesis’, *Energy*, 82, pp. 446–456. Available at: <https://doi.org/10.1016/j.energy.2015.01.055>.

Volpato, G. *et al.* (2022) ‘General guidelines for the optimal economic aggregation of prosumers in energy communities’, *Energy*, 258, p. 124800. Available at: <https://doi.org/10.1016/j.energy.2022.124800>.

Wakui, T., Kawayoshi, H. and Yokoyama, R. (2016) ‘Optimal structural design of residential power and heat supply devices in consideration of operational and capital recovery constraints’, *Applied Energy*, 163, pp. 118–133. Available at: <https://doi.org/10.1016/j.apenergy.2015.10.154>.

Waters, C.N. *et al.* (2016) ‘The Anthropocene is functionally and stratigraphically distinct from the Holocene’, *Science*, 351(6269). Available at: <https://doi.org/10.1126/science.aad2622>.

Wu, H. *et al.* (2017) ‘Low-energy-penalty principles of CO<sub>2</sub> capture in polygeneration systems’, *Applied Energy*, 203, pp. 571–581. Available at: <https://doi.org/10.1016/j.apenergy.2017.06.012>.

Wu, Y. and Wang, Y. (2017) ‘A chemical industry area-wide layout design methodology for piping implementation’, *Chemical Engineering Research and Design*, 118, pp. 81–93. Available at: <https://doi.org/10.1016/j.cherd.2016.12.005>.

Yazaki (2018) *Water Fired Absorption Chillers WFC Series*. Available at: <https://maya-airconditioning.com/assorbitori-ad-acqua/> (Accessed: 6 April 2023).

Yokoyama, R., Hasegawa, Y. and Ito, K. (2002) ‘A MILP decomposition approach to large scale optimization in structural design of energy supply systems’, *Energy Conversion and Management*, 43(6), pp. 771–790. Available at: [https://doi.org/10.1016/S0196-8904\(01\)00075-9](https://doi.org/10.1016/S0196-8904(01)00075-9).

Zare, A. *et al.* (2018) ‘A Distributionally Robust Chance-Constrained MILP Model for Multistage Distribution System Planning With Uncertain Renewables and Loads’, *IEEE Transactions on Power Systems*, 33(5), pp. 5248–5262. Available at: <https://doi.org/10.1109/TPWRS.2018.2792938>.

Zhang, B.J. and Hua, B. (2007) ‘Effective MILP model for oil refinery-wide production planning and better energy utilization’, *Journal of Cleaner Production*, 15(5), pp. 439–448. Available at: <https://doi.org/10.1016/j.jclepro.2005.08.004>.

Zhang, J.D. and Rong, G. (2008) ‘An MILP model for multi-period optimization of fuel gas system scheduling in refinery and its marginal value analysis’, *Chemical Engineering Research and Design*, 86(2), pp. 141–151. Available at: <https://doi.org/10.1016/j.cherd.2007.11.002>.



---

*APPENDIX A – Energy Demands  
and Adopted Technologies*

---





## **APPENDIX A – Additional information**

This appendix provides a more detailed information about the energy community (EC) buildings and the adopted technologies, and is organized as follows: section A.1 provides the hourly energy demands (electricity, heating, and cooling) for each building and for one winter and one summer typical day; section A.2 presents some equations that, for the sake of brevity, were not presented on section 3.3.1; finally, section A.3 provides the technical data related to the technologies selected for the superstructure of the EC.

### **A.1 Energy demand of the buildings**

The energy demands of the buildings were obtained through three types of procedures: from the literature, from pieces of information found on webpages related to the respective building, and from the owner/manager of the building.

The energy demand data related to buildings 1 to 6 were retrieved from Buoro (2013). For what concerns building 7 (hospital), the energy demand data were estimated based on the energy demand of the hospital in the work of Bellina (2012), who developed a study about a DHN in the city of Tolmezzo, within the same Italian region as Pordenone. A scale factor was calculated based on the number of beds of both hospitals (information obtained through contact with the administration of both hospitals) and, in this way, the energy demand profiles for the hospital of Pordenone was obtained.

In a similar way, the data related to building 8 (secondary school) was estimated based on the number of students (information found on the website of the school) and the energy demands of a similar school, also analyzed in the work of Bellina (2012).

The energy demand information about building 9 (swimming pool) was obtained through direct contact with the owner of the building, who kindly provided the requested information.

Table A.1, Table A.2, and Table A.3 present the hourly energy demands for each building in a January working day for electricity, heating, and cooling demands, respectively. Table A.4, Table A.5, and Table A.6 present similar data, but for a July working day.

Table A.1 – Electricity demand for each building in a January working day. Values in kW.

Hour	Building								
	1	2	3	4	5	6	7	8	9
1	0	0	0	0	50	0	686.48	10.16	18.44
2	0	0	0	0	50	0	686.48	10.16	18.44
3	0	0	0	0	50	0	686.48	10.16	18.44
4	0	0	0	0	50	0	686.48	10.16	18.44
5	0	0	0	0	50	0	801.02	10.16	18.44
6	0	0	0	0	50	0	1029.84	33.86	18.44
7	0	0	0	0	63	0	1144.13	56.48	13.23
8	189	32	110	54	63	29	1280.25	124.2	19.08
9	189	32	110	54	101	29	1577.14	199.91	19.08
10	189	32	110	54	101	29	1445.84	199.91	19.08
11	189	32	110	54	76	29	1445.84	199.91	19.08
12	122	18	110	54	76	19	1314.29	199.91	19.08
13	122	18	110	29	76	19	1445.84	199.91	19.08
14	189	270	110	54	76	29	1445.84	151.15	19.08
15	189	270	110	54	58	29	1445.84	189.62	19.08
16	189	270	110	54	58	29	1445.84	189.62	19.08
17	189	270	110	0	53	29	1577.14	189.62	19.08
18	0	238	110	0	61	20	1577.14	189.62	19.08
19	0	238	110	0	68	20	1577.14	87.09	13.23
20	0	238	110	0	68	0	1386.92	18.28	13.23
21	0	238	110	0	50	0	1173.59	18.28	13.23
22	0	238	110	0	50	0	746.92	18.28	13.23
23	0	238	0	0	50	0	640.25	18.28	18.44
24	0	0	0	0	50	0	686.48	10.16	18.44

Table A.2 – Heat demand for each building in a January working day. Values in kW.

Hour	Building								
	1	2	3	4	5	6	7	8	9
1	0	0	0	0	159	0	4307.3	0	0
2	0	0	0	0	160	0	4548.57	0	0
3	0	0	0	0	161	0	4871.11	0	0
4	0	0	0	0	161	0	5031.11	0	0
5	0	0	0	0	161	0	5353.65	0	0
6	395	93	286	569	237	230	6478.73	0	195.29
7	397	93	287	572	238	231	6156.19	1320.53	195.29
8	393	92	284	566	236	228	5914.92	2634.29	195.29
9	365	87	255	521	233	224	4388.57	2822.55	195.29
10	358	86	250	505	229	220	3344.76	2822.55	195.29
11	338	81	235	475	216	208	3263.49	2508.34	54.25
12	311	75	216	437	200	193	2699.68	2508.34	54.25
13	304	71	220	392	180	175	2298.41	2508.34	54.25
14	294	454	212	377	174	169	2138.41	1126.85	54.25
15	267	447	184	393	173	167	1737.14	2397.28	54.25
16	276	460	190	405	178	172	1897.14	2508.34	54.25
17	286	477	198	420	184	178	2940.95	2322.78	54.25
18	305	507	211	447	196	189	3263.49	1759.36	54.25
19	329	547	229	483	211	203	3263.49	0	54.25
20	0	1572	232	124	214	0	3263.49	0	54.25
21	0	491	241	129	221	0	3263.49	0	54.25
22	0	491	241	129	221	0	3664.76	0	54.25
23	0	500	0	0	153	0	3746.03	0	0
24	0	505	0	0	155	0	3987.3	0	0

Table A.3 – Cooling demand for each building in a January working day. Values in kW.

Hour	Building								
	1	2	3	4	5	6	7	8	9
1	0	0	0	0	0	0	0	0	0
2	0	0	0	0	0	0	0	0	0
3	0	0	0	0	0	0	0	0	0
4	0	0	0	0	0	0	0	0	0
5	0	0	0	0	0	0	0	0	0
6	0	0	0	0	0	0	0	0	0
7	0	0	0	0	0	0	0	0	0
8	0	0	0	0	0	0	27.53	0	0
9	0	0	0	0	0	0	55.06	0	0
10	0	0	0	0	0	0	55.06	0	0
11	0	0	0	0	0	0	55.06	0	0
12	0	0	0	0	0	0	55.06	0	0
13	0	0	0	0	0	0	55.06	0	0
14	0	0	0	0	0	0	55.06	0	0
15	0	0	0	0	0	0	55.06	0	0
16	0	0	0	0	0	0	55.06	0	0
17	0	0	0	0	0	0	55.06	0	0
18	0	0	0	0	0	0	55.06	0	0
19	0	0	0	0	0	0	55.06	0	0
20	0	0	0	0	0	0	41.3	0	0
21	0	0	0	0	0	0	27.53	0	0
22	0	0	0	0	0	0	13.77	0	0
23	0	0	0	0	0	0	0	0	0
24	0	0	0	0	0	0	0	0	0

Table A.4 – Electricity demand for each building in a July working day. Values in kW.

Hour	Building								
	1	2	3	4	5	6	7	8	9
1	0	0	0	0	30	0	756.32	4.74	17.21
2	0	0	0	0	30	0	756.32	4.74	17.21
3	0	0	0	0	30	0	756.32	4.74	17.21
4	0	0	0	0	30	0	794.41	4.74	17.21
5	0	0	0	0	30	0	952.38	4.74	17.21
6	0	0	0	0	30	0	1229.97	15.85	17.21
7	0	0	0	0	56	0	1349.84	26.28	10.74
8	99	25	89	0	56	18	1473.02	38.19	17.19
9	99	25	89	0	94	18	1645.21	49.03	17.19
10	85	20	89	0	94	18	1399.87	49.03	17.19
11	85	20	89	0	89	17	1342.48	49.03	17.19
12	76	18	89	0	89	15	1077.84	49.03	17.19
13	76	18	89	0	89	15	1170.54	49.03	17.19
14	85	246	89	0	89	18	1132.19	37.11	17.19
15	85	246	89	0	73	18	1113.14	46.59	17.19
16	85	246	89	0	73	18	1132.19	46.59	17.19
17	85	246	89	0	76	18	1339.43	46.59	17.19
18	0	235	89	0	76	8	1454.22	46.59	17.19
19	0	235	89	0	71	8	1607.11	21.4	10.74
20	0	235	89	0	71	0	1659.43	5.69	10.74
21	0	235	89	0	30	0	1439.49	5.69	10.74
22	0	235	89	0	30	0	846.48	5.69	10.74
23	0	235	0	0	30	0	698.16	5.69	17.21
24	0	0	0	0	30	0	756.32	4.74	17.21

Table A.5 – Heat demand for each building in a July working day. Values in kW.

Hour	Building								
	1	2	3	4	5	6	7	8	9
1	0	0	0	0	12	0	2478.73	0	0
2	0	0	0	0	16	0	2615.87	0	0
3	0	0	0	0	18	0	2801.27	0	0
4	0	0	0	0	22	0	2892.7	0	0
5	0	0	0	0	24	0	3078.1	0	0
6	132	31	95	190	73	77	3725.71	0	46.97
7	122	29	88	176	67	71	3540.32	0	46.97
8	93	22	67	134	49	54	3403.17	0	46.97
9	37	11	18	49	30	34	2524.44	0	46.97
10	17	6	3	12	17	22	1922.54	0	46.97
11	2	2	0	0	8	13	1876.83	0	13.05
12	0	0	0	0	0	3	1554.29	0	13.05
13	0	0	0	0	0	0	1323.17	0	13.05
14	0	0	0	0	0	0	1229.21	0	13.05
15	0	0	0	0	0	0	998.1	0	13.05
16	0	0	0	0	0	0	1092.06	0	13.05
17	0	0	0	0	0	0	1691.43	0	13.05
18	0	0	0	0	0	0	1876.83	0	13.05
19	0	13	0	6	6	11	1876.83	0	13.05
20	0	102	5	9	18	0	1876.83	0	13.05
21	0	63	17	15	29	0	1876.83	0	13.05
22	0	87	30	22	40	0	2107.94	0	13.05
23	0	102	0	0	3	0	2153.65	0	0
24	0	113	0	0	7	0	2293.33	0	0

Table A.6 – Cooling demand for each building in a July working day. Values in kW.

Hour	Building								
	1	2	3	4	5	6	7	8	9
1	0	0	0	0	31	0	512.08	0	0
2	0	0	0	0	31	0	512.08	0	0
3	0	0	0	0	31	0	512.08	0	0
4	0	0	0	0	31	0	410.21	0	0
5	0	0	0	0	31	0	410.21	0	0
6	0	0	0	0	31	0	512.08	0	0
7	150	0	115	0	31	91	616.7	0	0
8	150	0	115	0	138	91	820.43	0	0
9	120	0	102	0	138	85	1026.91	0	0
10	120	0	102	0	113	85	1230.64	0	0
11	126	0	109	0	113	85	1384.81	0	0
12	126	0	109	0	119	85	1640.85	0	0
13	120	458	102	0	119	85	1847.33	0	0
14	120	458	102	0	113	85	1949.2	0	0
15	120	413	102	0	113	85	2001.51	0	0
16	120	413	102	0	113	85	1949.2	0	0
17	120	413	102	0	113	85	1847.33	0	0
18	0	413	86	0	91	0	1538.99	0	0
19	0	413	86	0	91	0	1128.77	0	0
20	0	413	86	0	91	0	718.56	0	0
21	0	413	0	0	31	0	512.08	0	0
22	0	413	0	0	31	0	512.08	0	0
23	0	413	0	0	31	0	512.08	0	0
24	0	0	0	0	31	0	512.08	0	0

## A.2 Mathematical model (complement)

The aim of this section is to provide some equations that, for the sake of brevity, were not presented in the section 3.3.1. Such equations are the ones presented from Eq. (A.1) to Eq. (A.8), which are essential to understanding how the total annual operation cost ( $AOC_{tot}$ ), total annual maintenance cost ( $AMC_{tot}$ ), and total annual investment cost ( $AIC_{tot}$ ) have been calculated (the reader may refer to Eq. (3.2) to Eq. (3.4)).

Equation (A.1) shows the expression through which the operation cost regarding the central unit has been calculated. This cost comprises the hourly gas consumption by the

BOIc and ICEc. The price of the gas (as shown in Table 3.12) has an incentive of 25% to self-producers who adopt cogeneration devices into their own energy systems. The term  $\tau(d)$  was discussed in the sections 3.3.1.

Similarly, the operation cost regarding the buildings (Eq. (A.2)) comprises also the gas consumption by boilers and cogeneration systems. The difference is that the latter can comprise ICE and MGT.

$$OC_{central} = \sum_{m=1}^{12} \sum_{d=1}^2 \sum_{h=1}^{24} [gas_{price\_BOI} \cdot Fuel_{BOIc}(m, d, h) + gas_{price\_ICE} \cdot Fuel_{ICEc}(m, d, h)] \cdot \tau(d) \quad (A.1)$$

$$OC_{building}(B) = \sum_{m=1}^{12} \sum_{d=1}^2 \sum_{h=1}^{24} \left[ gas_{price\_BOI} \cdot Fuel_{BOI}(m, d, h) + gas_{price\_ICE} \cdot \sum_{c=1}^{component} (Fuel_{ICE}(m, d, h, B) + Fuel_{MGT}(m, d, h, B)) \right] \cdot \tau(d) \quad (A.2)$$

Equations (A.3) and (A.4) calculate the maintenance costs of the technologies installed in the central unit and in each building, respectively. From the four technologies comprising the superstructure of the central unit, only the BOIc and ICEc were assumed to produce a maintenance cost. Equation (A.4) computes the hourly maintenance cost for each building and for each one of the ten technologies (comprising the building superstructure) but the thermal storages (HST and CST), which were assumed as zero-maintenance technologies. Although foreseen in the equation, the maintenance factors for PV and ST were assumed to be zero (Table 3.10) in this work.

$$mC_{central} = m_{BOIc} \cdot Heat_{BOIc} + m_{ICEc} \cdot Elec_{ICEc} \quad (A.3)$$



$$\begin{aligned}
mC_{building}(B) = & \sum_{m=1}^{12} \sum_{d=1}^2 \sum_{h=1}^{24} \left[ m_{BOI} \cdot Heat_{BOI}(m, d, h, B) + m_{CC} \right. \\
& \cdot Cool_{CC}(m, d, h, B) + m_{PV} \cdot Elec_{PV}(m, d, h, B) + m_{ST} \\
& \cdot Heat_{ST}(m, d, h, B) + m_{MGT} \cdot \sum_{c=1}^{component} Elec_{MGT}(m, d, h, c, B) \\
& + m_{ICE} \cdot \sum_{c=1}^{component} Elec_{ICE}(m, d, h, c, B) + m_{ABS} \\
& \cdot \sum_{c=1}^{component} Cool_{ABS}(m, d, h, c, B) + m_{HP} \\
& \left. \cdot \sum_{c=1}^{component} Elec_{HP}(m, d, h, c, B) \right] \cdot \tau(d)
\end{aligned} \tag{A.4}$$

Equations (A.5) to (A.8) show how the annual investment costs were calculated. Equation (A.5) calculates the annual investment concerning the technologies in the central unit. The  $IC_{tech}$  values can be found in section 3.2.4, the capital recovery factor ( $f_{tech}$ ) can be calculated through Eq. (A.6) ( $i = 5\%$ ), and the lifetime of each technology can be found in Table A.7.

Table A.7 – Lifetime of the adopted technologies.

	<b>MGT</b>	<b>ICE</b>	<b>BOI</b>	<b>CC</b>	<b>HP</b>	<b>ABS</b>	<b>ST</b>	<b>PV</b>	<b>HST</b>	<b>CST</b>	<b>DHCN</b>
<b>Lifetime [years]</b>	15	15	10	10	15	15	20	20	20	20	30

The annual investment cost concerning the technologies installed in each building of the EC is calculated through Eq. (A.7). As observed, besides the capital recovery factor and the investment cost, the annual cost of the technologies MGT, ICE, ABS, and HP depends also on two important aspects: (i) the existence ( $X_{tech}$ ) (in the optimal solution) of the technology, and (ii) the factor  $IC_{install}(c)$  which tells the models that there is a discount on the installation of the equipment, starting from the second one (Table A.8). the remaining technologies depend only on the capital recovery factor and their optimal size.

Table A.8 – Factor to account for a cost reduction when installing more than one from the same technology.

Installed technology						
	First	Second	Third	Fourth	Fifth	Sixth
$IC_{install}(c)$	1.00	0.80	0.75	0.70	0.70	0.70

$$IC_{central} = IC_{ICEc} \cdot f_{ICE} + IC_{BOIc} \cdot f_{BOI} + IC_{STc} \cdot f_{ST} + IC_{HSTc} \cdot f_{HST} \quad (A.5)$$

$$f_{tech} = \frac{i \cdot (1 + i)^{lifetime\_tech}}{(1 + i)^{lifetime\_tech} - 1} \quad (A.6)$$

$$\begin{aligned}
IC_{building}(B) = & f_{MGT} \cdot \sum_{c=1}^{component} (X_{MGT}(c, B) \cdot IC_{MGT}(B) \cdot IC_{install}(c)) + f_{ICE} \\
& \cdot \sum_{c=1}^{component} (X_{ICE}(c, B) \cdot IC_{ICE}(B) \cdot IC_{install}(c)) + f_{ABS} \\
& \cdot \sum_{c=1}^{component} (X_{ABS}(c, B) \cdot IC_{ABS}(B) \cdot IC_{install}(c)) + f_{HP} \\
& \cdot \sum_{c=1}^{component} (X_{HP}(c, B) \cdot IC_{HP}(B) \cdot IC_{install}(c)) + f_{BOI} \\
& \cdot Size_{BOI}(B) \cdot IC_{BOI} + f_{CC} \cdot Size_{CC}(B) \cdot IC_{CC} + f_{PV} \cdot Size_{PV}(B) \\
& \cdot IC_{PV} + f_{ST} \cdot Size_{ST}(B) \cdot IC_{ST} + f_{HST} \cdot Size_{HST}(B) \cdot IC_{HST} + f_{CST} \\
& \cdot Size_{CST}(B) \cdot IC_{CST}
\end{aligned} \quad (A.7)$$

Equation (A.8) computes the annual investment cost regarding the DHCN pipelines. The equation is composed essentially by two parts: the first one for the pipes connecting the buildings and the second one for the pipe connecting the central unit and the buildings. The two parts are dependent on the length of the pipes and the variable and fixed investment costs. The variable costs are linked to the optimal sizes of the pipes whereas the fixed cost is related to the existence of a given pipeline connection.

$$\begin{aligned}
IC_{pipes} = & \left[ \sum_{k,B | k \neq B} \left[ L_{pipe}(k, B) \cdot \left( Size_{pipe_c}(k, B) + Size_{pipe_h}(k, B) \right) \cdot IC_{pipes_v} \right. \right. \\
& + \left. \left. \left( X_{pipe_c}(k, B) + X_{pipe_h}(k, B) \right) \cdot IC_{pipes_f} \right] + L_{central} \right. \\
& \cdot \left. \left( Size_{pipe_{central}} \cdot IC_{pipes_{central_v}} + X_{pipe_{central}} \right. \right. \\
& \left. \left. \cdot IC_{pipes_{central_f}} \right) \right] \cdot f_{pipes}
\end{aligned} \tag{A.8}$$

### A.3 Technical data

This section presents the main technical data regarding some of the technologies considered for the superstructure of each EC building. The technologies not presented in this section, are fully described in section 3.2.

#### A.3.1 Internal combustion engine (ICE)

The considered ICE technical input data is based on real technology available on the market. As specified on chapter CHAPTER 3 –, and according to the energy demand level, the buildings are allowed to install up to six engines of one of the four ICE sizes: EM-50/81, EM-70/115, EM-140/207, or EM-199/263. These ICE units are similar to the one shown in Figure A.1 and are manufactured by Viessmann (2020).



Figure A.1 – Internal combustion engine. Vitobloc 200 (EM-50/81) (Viessmann, 2020).

Table A.9 shows the technical data obtained from the Viessmann catalogues of the four ICE models. As observed, the data correspond to the equipment working at full load, as well as at partial load (30%, 50%, and 75%). Then, Table A.10 provides the linear coefficients obtained from the data shown in Table A.9.

Table A.9 – Technical data regarding the four ICE models from Viessmann (2020).

ICE model	Power (kW)	Heat (kW)	Fuel (kW)	Power efficiency	Total CHP efficiency
EM-50/81	15.00	30.82	62.81	0.24	0.73
	25.00	46.00	86.00	0.29	0.83
	38.00	64.00	118.00	0.32	0.86
	50.00	83.00	145.00	0.34	0.92
EM-70/115	21.00	43.32	87.56	0.24	0.73
	35.00	66.00	122.00	0.29	0.83
	53.00	85.00	159.00	0.33	0.87
	70.00	117.00	204.00	0.34	0.92
EM-140/207	42.00	98.90	165.70	0.25	0.85
	70.00	130.00	227.00	0.31	0.88
	105.00	171.00	310.00	0.34	0.89
	140.00	209.00	384.00	0.36	0.91
EM-199/263	57.00	142.59	214.46	0.27	0.93
	95.00	180.00	301.00	0.32	0.91
	143.00	235.00	408.00	0.35	0.93
	190.00	278.00	516.00	0.37	0.91

Table A.10 – Linear coefficients for the linearized equations derived from the ICE performance data (Table A.9).

ICE model	Fuel x Power		Heat x Power	
	$kf_{ICE}(t, B, 1)$	$kf_{ICE}(t, B, 2)$	$kh_{ICE}(t, B, 1)$	$kh_{ICE}(t, B, 2)$
EM-50/81	2.362	27.379	1.479	8.637
EM-70/115	2.340	38.423	1.453	12.798
EM-140/207	2.243	71.502	1.129	51.501
EM-199/263	2.263	85.471	1.032	83.771

### A.3.2 Micro gas turbine (MGT)

The MGT technical input data is also based on real technology available on the market. As specified on chapter CHAPTER 3 –, and according to the energy demand level, the

buildings are allowed to install up to six turbines of one of the four MGT sizes: C30, C65, T100, or C200. These MGT units are similar to the one shown in Figure A.2 and are manufactured by Capstone (2009).

Table A.11 shows the technical data obtained from the Capstone catalogues of the four MGT models. Then, Table A.12 provides the linear coefficients obtained from the data shown in Table A.11.

Table A.11 – Technical data regarding the four MGT models from Capstone (2009).

Capstone	Power [kW]	Heat [kW]	Fuel [kW]	Power efficiency	Total CHP efficiency
<b>C30</b>	9.23	27.79	47.89	0.19	0.77
	13.85	35.69	64.08	0.22	0.77
	18.46	42.06	78.30	0.24	0.77
	23.08	48.24	92.26	0.25	0.77
	27.69	54.92	106.88	0.26	0.77
	30.00	59.19	115.38	0.26	0.77
<b>C65</b>	20.00	52.37	93.02	0.22	0.78
	30.00	66.85	124.48	0.24	0.78
	40.00	78.33	152.09	0.26	0.78
	50.00	89.43	179.21	0.28	0.78
	60.00	101.52	207.61	0.29	0.78
	65.00	109.38	224.14	0.29	0.78
<b>T100</b>	30.77	73.92	138.34	0.22	0.76
	46.15	93.94	185.13	0.25	0.76
	61.54	109.63	226.19	0.27	0.76
	76.92	124.76	266.52	0.29	0.76
	92.31	141.34	308.76	0.30	0.76
	100.00	152.25	333.33	0.30	0.76
<b>C200</b>	61.54	113.53	251.53	0.24	0.70
	92.31	141.96	336.59	0.27	0.70
	123.08	163.15	411.25	0.30	0.70
	153.85	183.42	484.58	0.32	0.70
	184.62	206.10	561.38	0.33	0.70
	200.00	221.82	606.06	0.33	0.70



Figure A.2 – Micro gas turbine Capstone C65 (Capstone, 2009).

Table A.12 – Linear coefficients for the linearized equations derived from the MGT performance data (Table A.11 shows the technical data obtained from the Capstone catalogues of the four MGT models. Then, Table A.12 provides the linear coefficients obtained from the data shown in Table A.11.

Table A.11).

ICE model	Fuel x Power		Heat x Power	
	$kf_{ICE}(t, B, 1)$	$kf_{ICE}(t, B, 2)$	$kh_{ICE}(t, B, 1)$	$kh_{ICE}(t, B, 2)$
<b>EM-50/81</b>	2.362	27.379	1.479	8.637
<b>EM-70/115</b>	2.340	38.423	1.453	12.798
<b>EM-140/207</b>	2.243	71.502	1.129	51.501
<b>EM-199/263</b>	2.263	85.471	1.032	83.771

### A.3.3 Absorption chiller (ABS)

According to the manufacturer's datasheet (Yazaki, 2018), the equipment can be used for several applications including cogeneration, solar cooling, and district heating. The selected models were WFC-SC10, WFC-SC20, and WFC-SC30, which have a nominal cooling capacity (NCC) of 35 kW, 70 kW, and 105 kW, respectively. The single-effect absorption cycle works with the working fluid pair lithium bromide/water, is fed by hot water ranging from 70 °C to 95 °C, and the condenser circuit is cooled by water from a cooling tower. The mentioned models are similar to the one shown in Figure A.3.



Figure A.3 – Water fired Absorption Chiller WFC series (Yazaki, 2018).

Table A.13 to Table A.15 present the technical data regarding the adopted ABS models. Such data represent the performance characteristics for a cooling power supply at the temperature of 7 °C. As observed in the tables, the ABS performance depends on the Cooling Water Temperature (CWT), which is the water circuit coming from the cooling tower to remove heat from the absorber and condenser. As expected, the higher this temperature the lower the ABS COP, although there is not a substantial variation. The equipment is designed to provide the nominal cooling capacity when the cooling capacity factor (CCF) is equal to 1. As the CWT increases, the heat medium inlet temperature (HMIT) should be higher in order for the ABS achieve the nominal cooling capacity. A variation in the HMIT results a corresponding variation on the cooling capacity of the ABS. Therefore, it was assumed that the ABS operation range is  $ABS_{max} = NCC$  and  $ABS_{min} = (1/3) NCC$ , while the COP are the ones presented in Table 3.4.

Table A.13 – Technical data from the ABS manufacturer (Yazaki, 2018) for the model WFC-SC10. Nominal cooling capacity: 35.2 kW; Heat input: 50.2 kW. Abbreviations: Heat Medium Inlet Temperature (HMIT), Cooling Capacity Factor (CCF), Heat Input Factor (HIF).

<b>WFC-SC10</b>					
<b>HMIT [°C]</b>	<b>CCF</b>	<b>HIF</b>	<b>Cooling [kW]</b>	<b>Heat input [kW]</b>	<b>COP</b>
<b>Cooling Water Temperature at 27 °C</b>					
<b>72.50</b>	0.68	0.65	23.94	32.63	0.73
<b>75.00</b>	0.80	0.73	28.16	36.65	0.77
<b>77.50</b>	0.90	0.82	31.68	41.16	0.77
<b>80.00</b>	1.00	0.95	35.20	47.69	0.74
<b>82.50</b>	1.10	1.07	38.72	53.71	0.72
<b>85.00</b>	1.20	1.18	42.24	59.24	0.71
<b>87.50</b>	1.29	1.28	45.41	64.26	0.71
<b>90.00</b>	1.34	1.36	47.17	68.27	0.69
<b>92.50</b>	1.38	1.44	48.58	72.29	0.67
<b>95.00</b>	1.40	1.49	49.28	74.80	0.66
<b>Cooling Water Temperature at 29.5 °C</b>					
<b>72.50</b>	0.40	0.44	14.08	22.09	0.64
<b>75.00</b>	0.52	0.53	18.30	26.61	0.69
<b>77.50</b>	0.65	0.63	22.88	31.63	0.72
<b>80.00</b>	0.77	0.73	27.10	36.65	0.74
<b>82.50</b>	0.89	0.87	31.33	43.67	0.72
<b>85.00</b>	1.00	0.98	35.20	49.20	0.72
<b>87.50</b>	1.10	1.10	38.72	55.22	0.70
<b>90.00</b>	1.19	1.19	41.89	59.74	0.70
<b>92.50</b>	1.23	1.27	43.30	63.75	0.68
<b>95.00</b>	1.25	1.32	44.00	66.26	0.66
<b>Cooling Water Temperature at 31 °C</b>					
<b>72.50</b>	0.33	0.32	11.62	16.06	0.72
<b>75.00</b>	0.45	0.41	15.84	20.58	0.77
<b>77.50</b>	0.60	0.51	21.12	25.60	0.82
<b>80.00</b>	0.70	0.64	24.64	32.13	0.77
<b>82.50</b>	0.82	0.78	28.86	39.16	0.74
<b>85.00</b>	0.92	0.89	32.38	44.68	0.72
<b>87.50</b>	1.00	1.00	35.20	50.20	0.70
<b>90.00</b>	1.05	1.10	36.96	55.22	0.67
<b>92.50</b>	1.08	1.20	38.02	60.24	0.63
<b>95.00</b>	1.10	1.25	38.72	62.75	0.62



Table A.14 – Technical data from the ABS manufacturer (Yazaki, 2018) for the model WFC-SC20. Nominal cooling capacity: 70.3 kW; Heat input: 100 kW. Abbreviations: Heat Medium Inlet Temperature (HMIT), Cooling Capacity Factor (CCF), Heat Input Factor (HIF).

<b>WFC-SC20</b>					
<b>HMIT [°C]</b>	<b>CCF</b>	<b>HIF</b>	<b>Cabs [kW]</b>	<b>Habs [kW]</b>	<b>COP</b>
<b>Cooling Water Temperature at 27 °C</b>					
<b>72.50</b>	0.66	0.60	46.40	60.00	0.77
<b>75.00</b>	0.75	0.69	52.73	69.00	0.76
<b>77.50</b>	0.84	0.77	59.05	77.00	0.77
<b>80.00</b>	0.95	0.87	66.79	87.00	0.77
<b>82.50</b>	1.04	0.95	73.11	95.00	0.77
<b>85.00</b>	1.12	1.07	78.74	107.00	0.74
<b>87.50</b>	1.18	1.19	82.95	119.00	0.70
<b>90.00</b>	1.20	1.27	84.36	127.00	0.66
<b>92.50</b>	1.21	1.33	85.06	133.00	0.64
<b>95.00</b>	1.22	1.38	85.77	138.00	0.62
<b>Cooling Water Temperature at 29.5 °C</b>					
<b>72.50</b>	0.46	0.42	32.34	42.00	0.77
<b>75.00</b>	0.60	0.51	42.18	51.00	0.83
<b>77.50</b>	0.73	0.61	51.32	61.00	0.84
<b>80.00</b>	0.82	0.71	57.65	71.00	0.81
<b>82.50</b>	0.91	0.84	63.97	84.00	0.76
<b>85.00</b>	1.00	0.96	70.30	96.00	0.73
<b>87.50</b>	1.07	1.06	75.22	106.00	0.71
<b>90.00</b>	1.10	1.14	77.33	114.00	0.68
<b>92.50</b>	1.12	1.21	78.74	121.00	0.65
<b>95.00</b>	1.14	1.26	80.14	126.00	0.64
<b>Cooling Water Temperature at 31 °C</b>					
<b>72.50</b>	0.35	0.31	24.61	31.00	0.79
<b>75.00</b>	0.49	0.41	34.45	41.00	0.84
<b>77.50</b>	0.60	0.51	42.18	51.00	0.83
<b>80.00</b>	0.71	0.63	49.91	63.00	0.79
<b>82.50</b>	0.81	0.75	56.94	75.00	0.76
<b>85.00</b>	0.91	0.88	63.97	88.00	0.73
<b>87.50</b>	1.00	0.99	70.30	99.00	0.71
<b>90.00</b>	1.05	1.09	73.82	109.00	0.68
<b>92.50</b>	1.08	1.16	75.92	116.00	0.65
<b>95.00</b>	1.09	1.20	76.63	120.00	0.64

Table A.15 – Technical data from the ABS manufacturer (Yazaki, 2018) for the model WFC-SC30. Nominal cooling capacity: 105.6 kW; Heat input: 151 kW. Abbreviations: Heat Medium Inlet Temperature (HMIT), Cooling Capacity Factor (CCF), Heat Input Factor (HIF).

<b>WFC-SC30</b>					
<b>HMIT [°C]</b>	<b>CCF</b>	<b>HIF</b>	<b>Cabs [kW]</b>	<b>Habs [kW]</b>	<b>COP</b>
<b>Cooling Water Temperature at 27 °C</b>					
<b>72.50</b>	0.70	0.62	73.92	93.62	0.79
<b>75.00</b>	0.80	0.75	84.48	113.25	0.75
<b>77.50</b>	0.89	0.88	93.98	132.88	0.71
<b>80.00</b>	0.97	0.97	102.43	146.47	0.70
<b>82.50</b>	1.05	1.07	110.88	161.57	0.69
<b>85.00</b>	1.13	1.16	119.33	175.16	0.68
<b>87.50</b>	1.20	1.25	126.72	188.75	0.67
<b>90.00</b>	1.26	1.33	133.06	200.83	0.66
<b>92.50</b>	1.30	1.40	137.28	211.40	0.65
<b>95.00</b>	1.34	1.45	141.50	218.95	0.65
<b>Cooling Water Temperature at 29.5 °C</b>					
<b>72.50</b>	0.41	0.42	43.30	63.42	0.68
<b>75.00</b>	0.54	0.54	57.02	81.54	0.70
<b>77.50</b>	0.66	0.65	69.70	98.15	0.71
<b>80.00</b>	0.78	0.77	82.37	116.27	0.71
<b>82.50</b>	0.90	0.87	95.04	131.37	0.72
<b>85.00</b>	0.99	0.98	104.54	147.98	0.71
<b>87.50</b>	1.07	1.09	112.99	164.59	0.69
<b>90.00</b>	1.13	1.20	119.33	181.20	0.66
<b>92.50</b>	1.18	1.30	124.61	196.30	0.63
<b>95.00</b>	1.21	1.34	127.78	202.34	0.63
<b>Cooling Water Temperature at 31 °C</b>					
<b>72.50</b>	0.26	0.31	27.46	46.81	0.59
<b>75.00</b>	0.40	0.42	42.24	63.42	0.67
<b>77.50</b>	0.55	0.55	58.08	83.05	0.70
<b>80.00</b>	0.69	0.68	72.86	102.68	0.71
<b>82.50</b>	0.81	0.79	85.54	119.29	0.72
<b>85.00</b>	0.92	0.90	97.15	135.90	0.71
<b>87.50</b>	1.00	1.00	105.60	151.00	0.70
<b>90.00</b>	1.06	1.10	111.94	166.10	0.67
<b>92.50</b>	1.10	1.19	116.16	179.69	0.65
<b>95.00</b>	1.13	1.25	119.33	188.75	0.63

### A.3.4 Heat pump (HP)

The adopted HP technologies are manufactured by Daikin (2013) and similar to the one shown in Figure A.4. They are air cooled multiple scroll chillers that, according to the manufacturer, provide a better partial load efficiency. The adopted models are EUWY-KBZW1, EWYQ-DAYNN080, and EWYQ-DAYNN100 with cooling/heating capacities of 35 kW, 80 kW, and 100 kW, respectively.



Figure A.4 – Heat pump EWYQ-DAYN (Daikin, 2013).

Table A.16 shows the COP values for each adopted HP model and for different values of ambient temperature. As observed, the performance of the equipment is considerably affected by the ambient temperature and whether it is working under heating or cooling mode.

It should be noted that, in the case of heating mode, the HP works to overcome a  $\Delta T$  between 30 °C (when the ambient temperature is 20 °C) and 50 °C (when the ambient temperature is 0 °C). For this reason, the COP values tend to be lower when compared to a scenario where the same HP (still in heating mode) works to overcome a  $\Delta T$  around 20 °C. When it comes to the cooling mode, the HP should overcome a  $\Delta T$  between 10 °C and 25 °C, which results in higher levels of cooling production with a lower level of power input. As a consequence, this operation mode provides higher levels of COP.

Table A.16 – Technical data regarding the three adopted HP models (Daikin, 2013).

Operation mode	Ambient temperature [°C]	Nominal capacity [kW]	COP
Heating	0	35	2.17
		80	2.26
		100	2.30
	4	35	2.31
		80	2.45
		100	2.51
	10	35	2.61
		80	2.72
		100	2.77
	15	35	2.90
		80	2.96
		100	2.99
	21	35	3.10
		80	3.21
		100	3.27
Cooling	20	35	4.90
		80	4.63
		100	4.51
	25	35	4.40
		80	4.09
		100	3.95
	30	35	4.00
		80	3.59
		100	3.40
35	35	3.50	
	80	3.12	
	100	2.94	

### A.3.5 Solar technologies

The solar technologies regard photovoltaic (PV) panels and solar thermal (ST) panels. The energy production from both types of technologies was obtained by using the System Advisor Model (SAM) software (NREL, 2023). The production for both PV and ST were calculated per square meter of the installed technology. Table A.17 and Table A.18 provide the hourly energy production by PV and ST, respectively.

Table A.17 – Hourly photovoltaic (PV) specific energy production ( $k_{PV}(t)$ ), in W/m<sup>2</sup>.

Hour	Jan	Feb	Mar	Apr	May	Jun	Jul	Aug	Sep	Oct	Nov	Dec
1	0.00	0.00	0.00	0.00	0.00	0.00	0.00	0.00	0.00	0.00	0.00	0.00
2	0.00	0.00	0.00	0.00	0.00	0.00	0.00	0.00	0.00	0.00	0.00	0.00
3	0.00	0.00	0.00	0.00	0.00	0.00	0.00	0.00	0.00	0.00	0.00	0.00
4	0.00	0.00	0.00	0.00	0.00	0.00	0.00	0.00	0.00	0.00	0.00	0.00
5	0.00	0.00	0.00	0.00	0.00	0.00	0.00	0.00	0.00	0.00	0.00	0.00
6	0.00	0.00	0.00	0.18	1.35	4.87	3.25	0.93	0.00	0.00	0.00	0.00
7	0.00	0.00	1.01	4.32	3.89	16.66	11.75	10.39	5.28	0.26	0.00	0.00
8	0.00	3.77	17.78	14.52	16.01	42.37	36.96	30.35	23.34	11.38	2.00	0.00
9	17.13	29.73	41.93	31.62	30.12	67.62	61.41	59.78	46.56	20.85	13.55	16.96
10	32.00	36.83	68.61	49.92	48.59	84.97	83.06	81.46	61.47	36.06	18.72	35.39
11	40.36	63.53	90.79	58.77	55.48	98.96	90.94	96.61	81.89	46.52	26.47	38.64
12	56.96	72.78	97.96	73.11	67.91	111.20	97.49	105.84	88.21	55.30	27.62	40.90
13	65.52	88.75	97.98	76.41	59.09	114.59	95.68	114.38	85.58	61.49	28.58	44.48
14	48.54	79.01	88.67	68.67	57.62	107.64	89.54	102.41	70.57	52.14	27.95	36.82
15	40.23	69.15	71.41	60.88	46.12	95.52	71.68	91.08	64.52	42.28	20.12	33.63
16	25.77	46.74	58.76	42.67	39.97	75.53	57.56	60.10	44.56	23.50	6.34	15.60
17	3.68	22.52	32.54	30.46	27.60	53.91	42.48	40.42	29.74	10.20	0.20	0.00
18	0.00	0.76	8.41	10.99	13.29	27.04	19.80	16.48	7.26	0.10	0.00	0.00
19	0.00	0.00	0.00	1.20	3.55	7.11	5.59	3.31	0.00	0.00	0.00	0.00
20	0.00	0.00	0.00	0.00	0.00	1.07	0.46	0.00	0.00	0.00	0.00	0.00
21	0.00	0.00	0.00	0.00	0.00	0.00	0.00	0.00	0.00	0.00	0.00	0.00
22	0.00	0.00	0.00	0.00	0.00	0.00	0.00	0.00	0.00	0.00	0.00	0.00
23	0.00	0.00	0.00	0.00	0.00	0.00	0.00	0.00	0.00	0.00	0.00	0.00
24	0.00	0.00	0.00	0.00	0.00	0.00	0.00	0.00	0.00	0.00	0.00	0.00

Table A.18 – Hourly solar thermal (ST) specific energy production ( $k_{ST}(t)$ ), in W/m<sup>2</sup>.

Hour	Jan	Feb	Mar	Apr	May	Jun	Jul	Aug	Sep	Oct	Nov	Dec
1	0.00	0.00	0.00	0.00	0.00	0.00	0.00	0.00	0.00	0.00	0.00	0.00
2	0.00	0.00	0.00	0.00	0.00	0.00	0.00	0.00	0.00	0.00	0.00	0.00
3	0.00	0.00	0.00	0.00	0.00	0.00	0.00	0.00	0.00	0.00	0.00	0.00
4	0.00	0.00	0.00	0.00	0.00	0.00	0.00	0.00	0.00	0.00	0.00	0.00
5	0.00	0.00	0.00	0.00	0.00	2.83	0.00	0.00	0.00	0.00	0.00	0.00
6	0.00	0.00	0.00	3.26	11.87	37.52	26.19	11.62	0.00	0.00	0.00	0.00
7	0.00	0.00	6.93	20.58	22.29	64.78	52.07	49.39	24.12	2.95	0.00	0.00
8	0.00	9.48	30.34	41.47	64.14	104.62	96.39	92.54	51.97	23.08	5.88	0.00
9	15.87	32.77	183.68	171.67	169.77	393.24	353.78	334.20	252.10	107.29	44.05	15.11
10	161.79	198.65	383.53	290.23	284.16	532.85	517.61	488.25	366.18	203.44	98.83	177.43
11	219.46	371.15	539.13	354.08	334.65	651.38	589.34	605.78	521.11	273.45	149.43	210.76
12	318.77	434.80	602.05	448.14	416.25	745.92	643.17	684.82	570.57	329.50	156.81	228.22
13	372.24	549.49	604.67	465.20	359.06	766.61	634.63	739.79	549.32	360.57	158.27	249.16
14	267.12	472.04	531.66	413.14	344.28	706.95	582.86	651.97	445.06	301.23	155.66	200.06
15	214.67	397.03	412.50	357.38	268.39	605.24	447.25	563.60	386.95	233.95	103.83	173.46
16	94.08	243.98	315.13	237.16	226.82	452.24	343.32	348.65	247.09	105.35	15.95	16.84
17	8.71	34.53	48.88	83.86	88.57	118.40	119.62	109.33	61.93	26.87	2.04	0.00
18	0.00	4.05	24.00	42.74	57.77	89.00	74.36	64.98	27.43	1.32	0.00	0.00
19	0.00	0.00	0.00	12.33	25.47	49.80	38.69	26.67	1.48	0.00	0.00	0.00
20	0.00	0.00	0.00	0.00	1.89	14.93	8.74	0.00	0.00	0.00	0.00	0.00
21	0.00	0.00	0.00	0.00	0.00	0.00	0.00	0.00	0.00	0.00	0.00	0.00
22	0.00	0.00	0.00	0.00	0.00	0.00	0.00	0.00	0.00	0.00	0.00	0.00
23	0.00	0.00	0.00	0.00	0.00	0.00	0.00	0.00	0.00	0.00	0.00	0.00
24	0.00	0.00	0.00	0.00	0.00	0.00	0.00	0.00	0.00	0.00	0.00	0.00

Table A.19 provides the main input parameters specified in the SAM simulations for calculating the hourly energy productions by PV and ST panels. Most of the data are automatically updated when the location is specified. For what concerns ST panels, the input parameters as well as the hourly energy productions were considered the same for ST panels installed on the buildings or in the central unit.

Table A.19 – Main input parameters (to SAM software (NREL, 2023)) to simulate the hourly energy production from PV and ST panels. Abbreviations: Annual average (AA), Collector heat removal factor ( $F_R$ ), Transmittance and Absorptance ( $\tau\alpha$ ), Heat loss coefficient ( $U_L$ ), Incidence Angle Modifier (IAM).

Parameter	Value	Unit
<b>Shared parameters (PV and ST)</b>		
Location	Pordenone	-
Latitude	45.97	degrees
Longitude	12.66	degrees
AA global horizontal	3.77	kWh/m <sup>2</sup> /day
AA direct normal (beam)	4.02	kWh/m <sup>2</sup> /day
AA diffuse horizontal	1.52	kWh/m <sup>2</sup> /day
AA temperature	14.6	°C
Array type	Fixed roof mount	-
Tilt	30	degrees
Azimuth	180	degrees
<b>PV</b>		
Total loss	14	%
DC to AC ratio	1.15	-
Inverter efficiency	96	%
<b>ST</b>		
Working fluid	Water	-
$F_R(\tau\alpha)$	0.689	-
$F_R U_L$	3.85	W/m <sup>2</sup> .°C
IAM coefficient	0.2	-
Water flow rate	0.046	kg/s